2007

Molecular Regulation of Hair Follicle Morphogenesis

Horace Rhee

MOLECULAR REGULATION OF HAIR FOLLICLE MORPHOGENESIS

A Thesis Presented to the Faculty of

The Rockefeller University

in Partial Fulfillment of the Requirements for

the degree of Doctor of Philosophy

by

Horace Rhee

June 2007

MOLECULAR REGULATION OF HAIR FOLLICLE MORPHOGENESIS

Horace Rhee
The Rockefeller University 2007

The skin epidermis develops from a single uniform layer of multipotent cells during embryogenesis. Morphogenesis of hair follicles is initiated when a series of reciprocal interactions between this undifferentiated ectoderm and its underlying mesenchyme leads to a localized invagination of epithelial cells. As hair follicle development proceeds, stem cells are specified and set aside to fuel the postnatal hair cycle and repair the epidermis after injury. Although many signaling pathways have been identified by genetic studies to be essential for the induction of hair follicle morphogenesis and differentiation, little is known about the downstream genetic targets and molecular mechanisms in specifying a hair cell fate and establishing the stem cell niche. To define how the embryonic epithelium is able to integrate signals to direct, maintain, and regulate the hair cell lineage, I developed a strategy to isolate and transcriptionally profile embryonic hair progenitors and interfollicular epidermis in mice. This screen not only substantiated genes previously implicated in hair and epidermal development, but also uncovered genes that could be important in orchestrating lineage specification of multipotent skin progenitors. Many of these uncharacterized genes were also differentially expressed in the stem cells of postnatal hair follicles, suggesting that

embryonic hair progenitors may directly give rise to and reflect functional attributes of adult stem cells. To test this premise, I evaluated the role of transcription factor Lhx2 in skin development. Expressed specifically by both embryonic hair progenitors and postnatal follicle stem cells, Lhx2 functions to establish hair follicle stem cells and maintain their undifferentiated, quiescent state. Loss of Lhx2 reduces hair follicle number and causes stem cells to precociously differentiate, whereas gain of Lhx2 inhibits differentiation and promotes a hair follicle stem cell fate. Thus, Lhx2 appears to be a molecular link between the specification of embryonic hair progenitors and adult multipotent stem cells. Further characterization into genes that regulate hair follicle morphogenesis is expected to expand our understanding of how stem cells are established and maintained, and the potential mechanisms by which they are disrupted in skin disease.

To my ever supportive family

ACKNOWLEDGMENTS

Foremost, I extend my deepest gratitude to my thesis research advisor, Elaine Fuchs, without whom this work would not have been possible. Thank you for giving me the latitude to develop my interest in this project and having confidence in me at times when I doubted myself. You have provided great leadership and a wonderful environment to learn science and do research.

A special appreciation also goes out to Brad Merrill, Colin Jamora, Cedric Blanpain, and Bill Lowry, who have contributed invaluable mentorship and advice along the way. Many thanks to Michael Rendl for teaching me a number of experimental techniques and sharing your unpublished data, to Lisa Polak for performing skin grafts even on weekends, to Nicole Stokes for generating transgenic mice, to June Dela Cruz for in situ hybridizations, to Ram DasGupta for getting me started in the lab, and to all members of the Fuchs Lab, both past and present, for your willingness to share ideas, reagents, protocols, and in general putting up with me for the last 5 years. I consider you all not only my colleagues, but also my friends.

In the materials and methods, I cite the many colleagues for their generous contributions of mice and reagents. In particular, I would like to thank Masatoshi Takeichi for the P-cadherin hybridoma cells, Thomas Jessell for the Lhx2 antibody, Junji Hirota for the Lhx2 cDNA, and Heiner Westphal for the Lhx2 null

mice. I am also grateful for the technical expertise of several people in core resource facilities: Svetlana Mazel and Tamara Shengelia (flow cytometry); Francisco Berguido (monoclonal antibody); Agnes Viale and Juan Li (genomics core).

Thank you to members of my thesis committee, Ali Brivanlou, Markus Stoffel, and Angela Christiano for your time and thoughtful insights.

And finally to the support I have received through the Graduate Program at The Rockefeller University and the Medical Scientist Training Program of The University of Chicago and The Pritzker School of Medicine.

TABLE OF CONTENTS

Acknowledgments.....(iv)

List of Figures.....(viii)

List of Tables.....(ix)

Chapter 1: Introduction.....1
- Architecture of skin.....2
- Hair follicle morphogenesis.....4
- Hair follicle stem cells.....7
- Signaling during hair follicle morphogenesis.....10
  - Wnt signaling.....11
  - Shh signaling.....14
  - Bmp signaling.....17
  - Other signaling pathways.....20
- Specific aims.....21

Chapter 2: Isolation and Analysis of Embryonic Hair Follicle Progenitors....24
- Results.....25
  - Isolation of embryonic hair progenitors.....25
  - Transcriptional differences during hair morphogenesis.....35
  - PCAD– interfollicular epidermal cells.....39
  - PCAD+ hair progenitor cells.....44
  - Comparisons with other cell populations.....51
  - Label retaining cells during hair morphogenesis.....55
- Discussion.....57
  - Justification of strategy to isolate hair progenitors.....57
  - Insights into hair follicle morphogenesis.....58
  - Insights into hair follicle stem cells.....64
- Materials and Methods.....65
  - Mice.....65
  - Histology and immunofluorescence.....66
  - Isolation of hair progenitors and flow cytometry.....67
  - β-galactosidase activity assay.....69
  - RNA isolation and semi-quantitative RT-PCR.....69
  - Microarray analysis.....71
  - BrdU label retaining experiments.....72

Chapter 3: Characterization of Lhx2 in Hair Follicles..... 73
Results.....75
Lhx2 expression during hair morphogenesis.....75
Lhx2 expression in genetic mutants..... 76
Lhx2 inhibits differentiation.....80
Lhx2 promotes hair follicle stem cell fate..... 84
Lhx2 maintains follicle stem cells in a quiescent state.....89
Discussion.....97
Materials and Methods..... 103
Mice.....103
Histology, immunofluorescence, and in situ hybridizations..... 104
Engraftment and BrdU experiments..... 105
Flow cytometry analysis.....106
Barrier function assay.....107
RNA isolation and semi-quantitative RT-PCR..... 107
Transient transfections and western blots..... 108

Chapter 4: Summary and Perspectives.....110
Origins of hair follicle stem cells.....110
Regulation of hair follicle stem cells..... 114
Implications beyond hair follicles.....118

Appendix: Complete Microarray Data.....120

References.....140

LIST OF FIGURES

1.1 Skin and its appendages....3
1.2 Key signals regulating hair morphogenesis....5
1.3 Hair follicle morphogenesis and cycling....8
1.4 Wnt signaling during hair morphogenesis....12
1.5 Shh signaling during hair morphogenesis....15
1.6 Bmp signaling during hair morphogenesis....19

2.1 P-cadherin expression in embryonic hair follicle progenitors....27
2.2 Expression of molecules used to isolate hair follicle progenitors....29
2.3 FACS strategy to isolate hair follicle progenitors....30
2.4 P-cadherin is resistant to EDTA in isolating epidermal cells....31
2.5 FACS analysis on mutant embryos....32
2.6 Expression of marker genes in sorted cell populations....34
2.7 Cytospin analysis of sorted cell populations....35
2.8 Verification of differentially expressed genes in the microarrays....38
2.9 Comparisons to other epithelial cell lineages....52
2.10 Comparison to the postnatal hair follicle bulge....53
2.11 Label retaining cells during hair follicle morphogenesis....56

3.1 Differential expression of Lhx2 in embryonic hair progenitors....75
3.2 Lhx2 expression during hair morphogenesis and in postnatal stem cells....77
3.3 Lhx2 expression in genetic mutants of hair morphogenesis....79
3.4 Design and expression of the Lhx2 transgene....81
3.5 Gross phenotype of Lhx2 transgenic mice....82
3.6 Lhx2 inhibits terminal differentiation in skin....83
3.7 Lhx2 inhibits terminal differentiation in tongue....84
3.8 Expression of Lhx2 induces hair follicle stem cell markers....85
3.9 Loss of Lhx2 reduces hair follicle morphogenesis....87
3.10 Development and differentiation of Lhx2 null hair follicles....88
3.11 Hair cycle of Lhx2 null hair follicles....90
3.12 Precocious anagen entry of Lhx2 null hair follicles....91
3.13 Diminished expression of CD34 in Lhx2 null hair follicles....92
3.14 Expression of bulge markers in Lhx2 null hair follicles....93
3.15 Loss of BrdU label retention in Lhx2 null follicle stem cells....95
3.16 Increased BrdU incorporation in Lhx2 null follicle stem cells....96
3.17 Model for Lhx2 during hair follicle development....98

LIST OF TABLES

2.1 Microarray hybridization statistics..... 36
2.2 Fold changes of known hair placode markers..... 37
2.3 Selected genes in PCAD– fraction..... 40
2.4 Selected genes in PCAD+ fraction..... 45
2.5 Differentially expressed transcription factors..... 54

CHAPTER 1
INTRODUCTION

Mechanisms to regulate cell lineage occur throughout the life of multicellular organisms. Beginning in the early embryo, pluripotent cells of the inner cell mass must restrict their lineage and differentiate into the myriad of cell types that make up an organism. Lineage restriction continues in adult life as somatic stem cells balance cell proliferation and differentiation to maintain homeostasis and repair tissues after injury. Control of these processes relies on extrinsic cues from the environment which ultimately direct intrinsic genetic programs within cells (Fuchs et al., 2004; Li and Xie, 2005). Disruption of these regulatory mechanisms not only causes developmental defects, but also the pathogenesis of diseases such as cancer (Reya et al., 2001). Although progress has been made towards understanding the external signals that control cell fate decisions, questions still remain regarding the downstream molecular factors that integrate these signals to modulate cell specification.

As a continuously self-renewing tissue composed of multiple cell types, the skin is an excellent model system to address the mechanisms of cell lineage determination. Epithelial stem cells have been identified and their progeny follow well defined spatial and temporal programs of differentiation to replenish aged or damaged cells (Niemann and Watt, 2002; Gambardella and Barrandon, 2003). The

accessibility of the skin and the existence of molecular markers to identify specific cell lineages allows for tractable manipulation and phenotypic analysis of function.

Architecture of skin

Mammalian skin consists of a stratified squamous epidermis and an underlying dermis of connective tissue, separated by a basement membrane of extracellular matrix (Figure 1.1). Although there is variation between body sites, the major appendage of the skin is the hair follicle. Skin epithelial cells are also referred to as keratinocytes, named for the keratin intermediate filaments that are abundantly expressed in each cell.

Epithelial cells between hair follicles, also known as the interfollicular epidermis, is comprised of four distinct layers which function to provide a protective barrier against dehydration, infection, and mechanical stress. Attached to the basement membrane are mitotically active cells known as the basal layer. Cells of the basal layer give rise to differentiating spinous cells by withdrawing from the cell cycle through oriented cell divisions and detaching from the basement membrane (Lechler and Fuchs, 2005). Moving outwards towards the skin surface and altering their gene expression, the spinous layer becomes the granular layer by expressing structural proteins necessary to produce the final

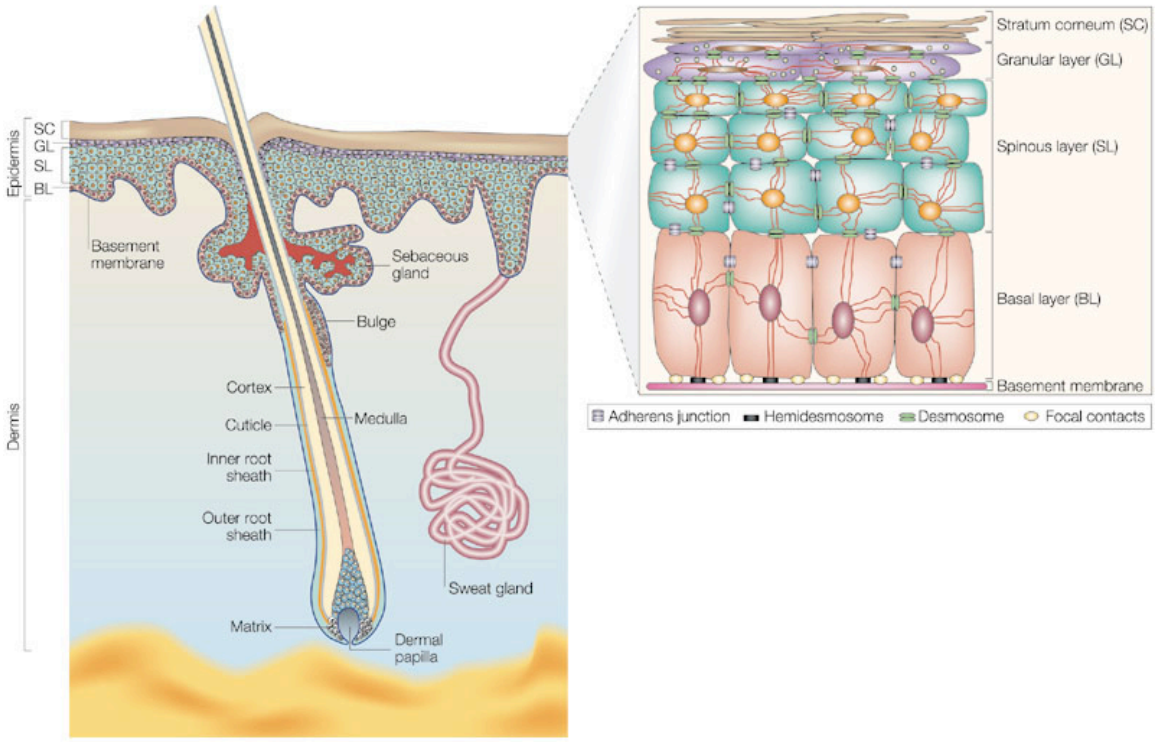

Figure 1.1 Skin and its appendages. Mammalian skin consists of the epidermis and its appendages, hair follicles and sweat glands, separated from the underlying dermis by a basement membrane of extracellular matrix. The interfollicular epidermis is a stratified squamous epithelium composed of four cell layers. Attached to the basement membrane is the proliferative basal layer. Cells committed to epidermal differentiation detach from the basement membrane, move outwards towards the skin surface, and undergo an ordered progression of molecular and metabolic changes to form the spinous layer, granular layer, and stratum corneum. The hair follicle is composed of concentric rings of cell layers. The outermost layer of the hair follicle, the outer root sheath, is contiguous with the basal layer of epidermis. At the base of the follicle are highly proliferative matrix cells associated with the dermal papilla. Cells committed to hair differentiation leave the matrix compartment, move upwards towards the skin surface, and acquire a specific hair lineage, including the inner root sheath and hair shaft (medulla, cortex, cuticle). Figure from Fuchs and Raghavan, 2002.

terminally differentiated layer, the stratum corneum, consisting of highly cross-linked proteins and extruded lipids (Fuchs and Raghavan, 2002; Dai and Segre, 2004).

An analogous differentiation program takes place in the hair follicle. Contiguous with the interfollicular basal layer is the outer root sheath which extends down to the base of the follicle, where highly proliferative cells known as the matrix reside closely associated with the dermal papilla. Specific hair lineages with unique biochemical and molecular properties arise from matrix cells as they move upward in concentric rings of cells to differentiate and form the different layers of the hair follicle, including from outside in, the three layers of the inner root sheath (Henle, Huxley, cuticle) and the three layers of the hair shaft (cuticle, cortex, medulla). The hair shaft which penetrates the skin is the visible part of the hair follicle.

Hair follicle morphogenesis

The skin epidermis develops during embryogenesis from a single uniform layer of multipotent ectoderm through interactions with the mesenchymally derived dermis. Cells of this proliferative basal layer can differentiate into one of two major lineages: epidermal or hair (Figure 1.2). To serve its function as a protective barrier, cells directed towards the epidermal lineage begin a program of

terminal differentiation by detaching from the basement membrane, moving outward toward the skin surface, and undergoing molecular and metabolic changes to create a keratinized, stratified squamous cell layer (Fuchs and Raghavan, 2002; Dai and Segre, 2004).

Undifferentiated cells of the basal layer not only undergo epidermal stratification, but upon a mesenchymal cue, they can give rise to hair follicles

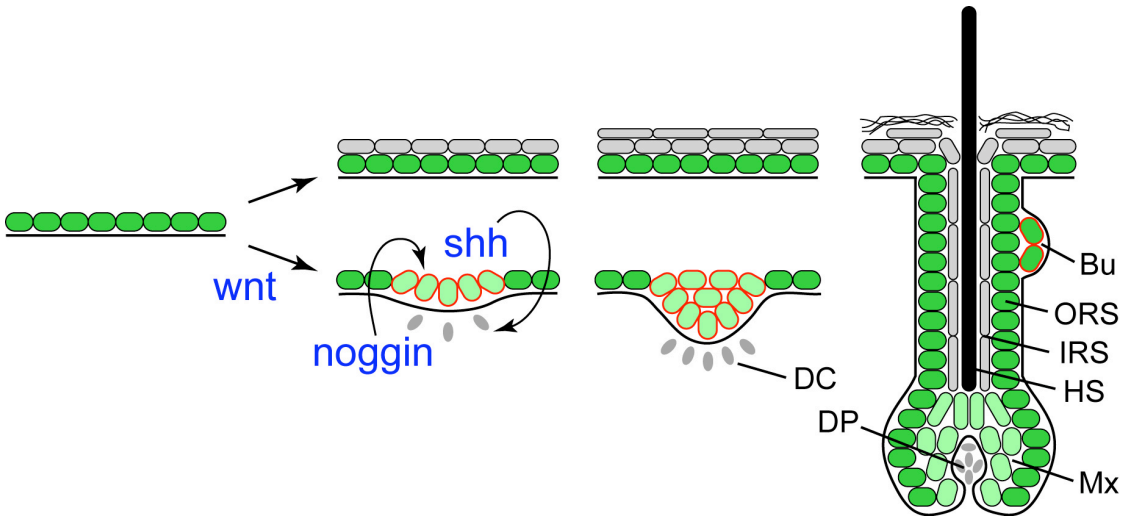

Figure 1.2 Key signals regulating hair morphogenesis. During embryogenesis, cells from a single uniform layer of ectoderm differentiate into two main cell lineages. They can either divide and stratify to form an epithelial barrier, or upon receiving a Wnt signal, they can invaginate into the dermis to form a hair follicle. Following placode induction, reciprocal signaling between the ectoderm and the underlying mesenchyme through Noggin and Shh is necessary for proper hair follicle organization and development. The hair follicle continues to grow downwards and progenitor cells of the matrix differentiate into various lineages that constitute a mature follicle. During this morphogenetic process, stem cells residing in the bulge are specified and set aside for postnatal hair cycles and epidermal repair. Abbreviations: Bu, bulge; ORS, outer root sheath; IRS, inner root sheath; HS, hair shaft; Mx, matrix; DC, dermal condensate; DP, dermal papilla.

(Hardy, 1992). In response to this inductive signal, embryonic hair morphogenesis begins with a localized thickening of epidermal cells in the basal layer and a subsequent bud-like invagination into the dermis. Known as a hair placode or hair germ, these progenitor cells send a reciprocal signal back to the underlying mesenchymal cells to organize into a dermal condensate, a tight cluster of precursor cells of the dermal papilla. As the hair follicle continues to develop by growing further down into the dermis, a group of rapidly proliferating follicular cells called the matrix surrounds the dermal papilla, forming the hair bulb. Cells losing contact with the hair bulb become the outer root sheath, contiguous with the interfollicular epidermis. The close association between the matrix and dermal papilla within the hair bulb likely results in another exchange of epithelial-mesenchymal signals to begin terminal hair differentiation. Matrix cells move upward and adopt specific hair lineages through changes in gene expression to form the concentric layers of the hair follicle, including the inner root sheath and hair shaft. (Paus et al., 1999)

This period of active hair growth and differentiation known as anagen continues until the proliferative capacity of matrix cells is exhausted. A regressive period of catagen ensues where the lower portion of the hair follicle undergoes apoptosis and the dermal papilla is brought upwards towards a region of the hair follicle known as the bulge. The hair follicle then enters a resting period of

telogen, until an inductive signal, possibly from the dermal papilla, instructs cells of the bulge to proliferate and differentiate into a new anagen hair follicle. Hair growth continues in this cyclical fashion throughout life, and many of the same mechanisms of embryonic hair morphogenesis are reiterated with each initiation of anagen from the bulge cells (Figure 1.3). (Muller-Rover et al., 2001; Stenn and Paus, 2001)

Hair follicle stem cells

Several lines of evidence indicate that the hair follicle bulge is the niche and reservoir of epithelial stem cells (Cotsarelis, 2006). Located at the base of the permanent portion of the adult hair follicle, cells of the bulge are generally slow cycling and quiescent, imparting them with "label-retaining" attributes after a short nucleotide analog pulse and extended chase period (Cotsarelis et al., 1990; Morris and Potten, 1999). When isolated and placed in culture, bulge cells become highly clonogenic, suggesting that they possess the ability to self-renew (Kobayashi et al., 1993; Rochat et al., 1994).

The label retaining cells of the bulge also give rise to all the epithelial lineages of the skin, including the interfollicular epidermis. Using two different labeling techniques, cells of the bulge were found to contribute to hair follicles during anagen induction and to epidermis during wound healing (Taylor et al.,

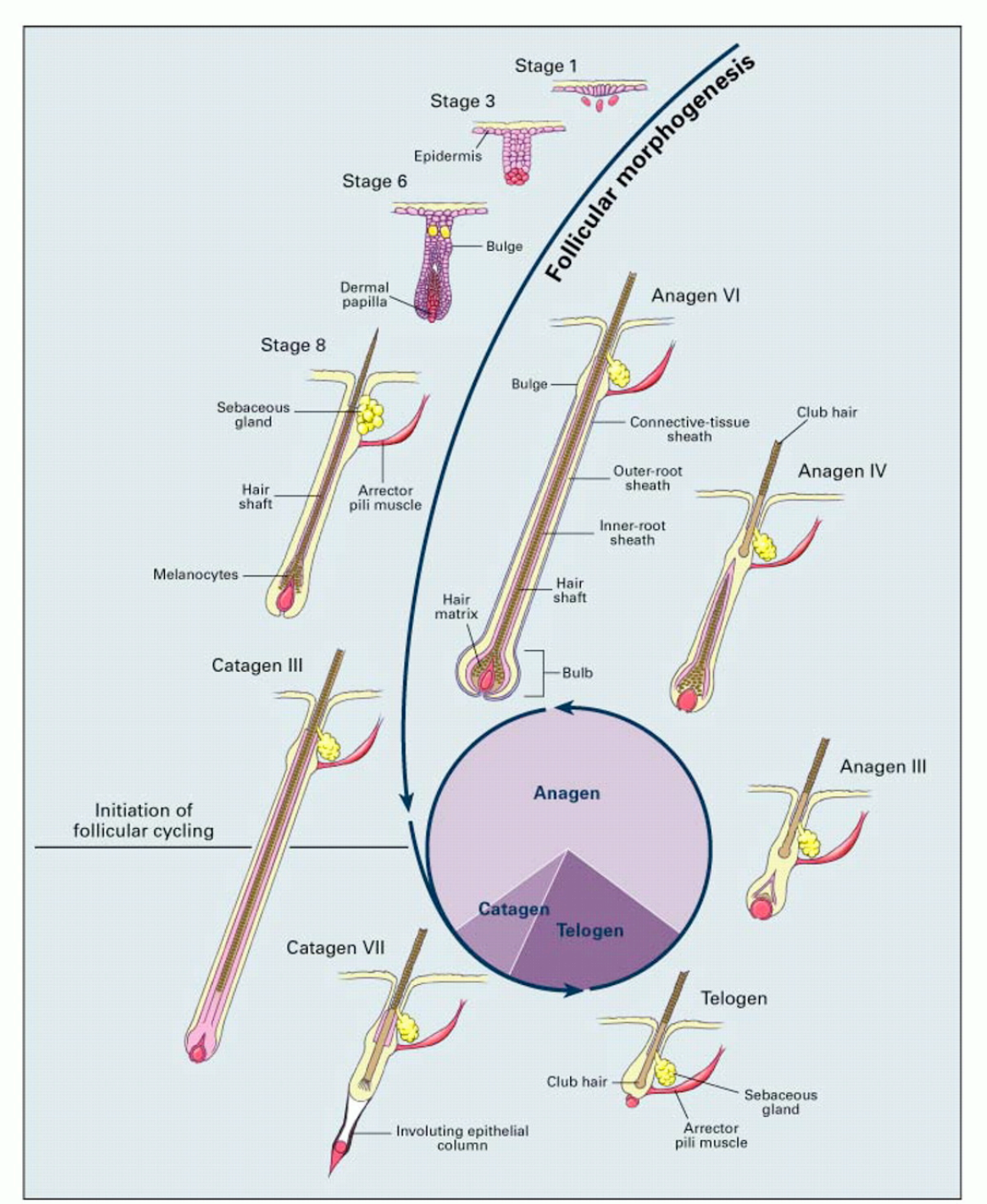

Figure 1.3 Hair follicle morphogenesis and cycling. Schematic diagram of different stages of follicular morphogenesis and the hair cycle. Hair follicles are specified from the epidermis only during embryogenesis and enter the postnatal hair cycle, where follicles go through stages of growth (anagen), regression (catagen) and rest (telogen). Note that only the lower portion of the hair follicle below the bulge is regenerated with each hair cycle. Figure from Paus and Cotsarelis, 2004.

2000; Tumbar et al., 2004). Transplantation experiments in which a labeled bulge was grafted onto an unlabeled hair follicle also revealed the bulge's ability to differentiate into multiple cell lineages (Oshima et al., 2001). The recent identification of bulge specific markers have enabled the isolation and purification of bulge cells, providing the means to definitively demonstrate through clonal analysis that bulge cells exhibit the two fundamental properties of all stem cells: self-renewal and multipotency (Trempus et al., 2003; Morris et al., 2004; Blanpain et al., 2004; Claudinot et al., 2005). In sum, epithelial stem cells reside in the hair follicle bulge and are endowed with the proliferative capacity and potency to fuel the hair cycle and regenerate damaged epidermis.

The bulge acquires its distinctive morphology and expresses specific molecular markers after the initial morphogenetic cycle of hair development. As a consequence, the existence of epidermal stem cells prior to the first postnatal telogen is uncertain and awaits the identification of markers which can label these putative cells during hair follicle morphogenesis. Thus, the origin of epidermal stem cells and establishment of the bulge niche during development remains to be determined.

Clues into the origin of adult bulge stem cells may lie within the embryonic hair placode, which possesses many salient features in common with these cells. Although committed to a follicular cell fate, the hair placode remains

undifferentiated, yet capable of differentiating into all the lineages of the hair follicle (Levy et al., 2005). Likewise, under normal homeostatic conditions, bulge cells contribute primarily to hair follicle lineages and not the interfollicular epidermis (Ito et al., 2005). The morphologic features of hair renewal during anagen induction from postnatal bulge cells also mirrors the induction of hair placodes from embryonic ectoderm during development, where reciprocal epithelial-mesenchymal signaling leads to downgrowth, proliferation, and differentiation (Fuchs et al., 2001). Thus, mechanisms regulating hair morphogenesis serve as a paradigm for studying stem cell activation and cell lineage determination.

Signaling during hair follicle morphogenesis

Studies using genetically engineered mice implicate several key signals in the induction of hair follicle morphogenesis (Nakamura et al., 2001; Millar, 2002; Botchkarev and Paus, 2003; Schmidt-Ullrich and Paus, 2005). Reflecting the morphological and functional similarities between embryonic hair placodes and bulge stem cells, many of these signaling pathways also direct and specify a hair fate during postnatal anagen induction. Misregulation or disruption of these pathways leads to abnormal hair development and pathogenesis of skin disease.

Wnt signaling

Of the different signaling pathways involved in hair follicle morphogenesis, Wnt/β-catenin signaling is absolutely essential for the specification and maintenance of the hair cell lineage (Alonso and Fuchs, 2003). Initially identified as a component of adherens junctions, excess β-catenin is normally targeted for proteosome-mediated degradation. Upon receipt of a Wnt signal through Frizzled receptors, the degradation of β-catenin is inhibited, resulting in its cytoplasmic accumulation and nuclear translocation where it can partner with members of the Lef/Tcf family of DNA binding proteins to function as a transcription factor complex (Logan and Nusse, 2004). Mutations in different components of the Wnt/β-catenin signaling pathway can result in constitutive activation and the pathogenesis of various epithelial malignancies (Polakis, 2000).

Genetic studies demonstrate the importance of Wnt/β-catenin signaling in hair morphogenesis. By following the activation of this pathway using transgenic mice that express a β-catenin/Lef1 responsive β-galactosidase reporter (TOPGAL), hair placodes were positively marked coinciding with nuclear β-catenin and Lef1 expression (Figure 1.4A-C; DasGupta and Fuchs, 1999). Conditional loss of *β-catenin* or transgenic expression of a Wnt signaling inhibitor within the epidermis completely abrogates all signs of hair morphogenesis (Figure 1.4D; Huelsken et al., 2001; Andl, et al., 2002), and mice mutant for *Lef1* exhibit a

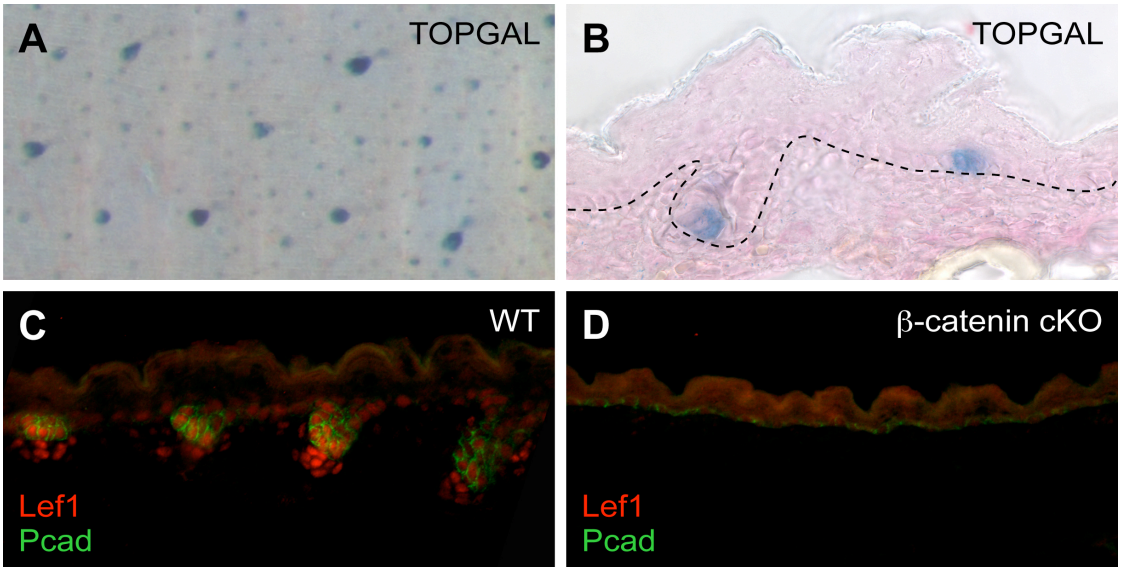

Figure 1.4 Wnt signaling during hair morphogenesis. (A-B) Back skin from E17.5 TOPGAL embryos were stained for β-galactosidase activity and sectioned (DasGupta and Fuchs, 1999). Hair placodes and a few cells at the leading front of invaginating hair germs express the TOPGAL reporter, indicative of active Wnt signaling. The positive staining of larger hair follicles in (A) is from differentiating precortical cells of more mature guard hairs. **(C-D)** Early hair progenitors express P-cadherin and Lef1, the nuclear partner of stabilized β-catenin. In the absence of epithelial β-catenin, hair follicles are not induced as evident by the lack of P-cadherin staining (Huelsken et al., 2001). *K14-Cre* was used to ablate *β-catenin* from the skin epithelium (Vasioukhin et al., 1999). Thus, Wnt signaling is absolutely necessary to initiate hair follicle morphogenesis. Immunofluorescence images are color-coded according to secondary antibodies used.

marked reduction in the number of hair follicles (van Genderen et al., 1994). Conversely, overexpression of a constitutively active form of β-catenin in the epidermis induces de novo hair follicles in postnatal epithelia, suggesting that activated β-catenin is sufficient to direct a hair cell fate (Gat et al., 1998). Since hair follicles are specified entirely during embryogenesis, the presence of *de novo*

follicles further suggests that β-catenin may impart multipotency to interfollicular epidermal cells.

Active β-catenin complexes are also found in precortex cells as they differentiate to form the hair shaft. Consistent with this role in terminal hair differentiation, Lef1 binding sites are present in several hair specific keratin genes and the hair shafts Lef1 knockout mice are poorly keratinized (Zhou et al., 1995; Kratochwil et al., 1996).

Wnt signaling is also active in the bulge stem cells particularly at the onset of a new hair cycle. Transient expression of a stabilized β-catenin in the epidermis can initiate a new anagen follicle (van Mater et al., 2003; Lo Celso et al., 2004), whereas sustained expression leads to precocious stem cell activation (Lowry et al., 2005) and eventually pilomatricomas, hair follicle tumors composed of undifferentiated matrix cells (Gat et al., 1998; Chan et al., 1999). Finally, postnatal loss of *β-catenin* in the bulge results in the formation of epithelial cysts instead of the normal induction of new hair cycles, suggesting that in the absence of β-catenin, stem cells are directed toward an epidermal cell fate rather than a hair cell fate (Huelsken et al., 2001; Lowry et al., 2005).

Although the source of the Wnt signal remains elusive, Wnt/β-catenin signaling is clearly necessary to induce the hair cell lineage during morphogenesis and activate bulge stem cells during postnatal hair cycles.

Shh signaling

Absent in *β-catenin* null epidermis, sonic hedgehog (Shh) lies downstream of Wnt signaling during hair follicle morphogenesis (Callahan and Oro, 2001). Shh signals by binding to its receptor Patched (Ptch) thereby antagonizing its inhibition of Smoothened (Smo). This allows Smo to activate downstream target genes through the Gli family of transcription factors (Lum and Beachy, 2004).

Expressed in the hair placodes and germs during morphogenesis, Shh is required to promote epidermal proliferation and subsequent downgrowth once hair follicles are induced (Figure 1.5A-B; St-Jacques et al., 1998; Chiang et al., 1999). In the absence of *Shh*, developing follicles are arrested as hair germs and the underlying mesenchyme fails to aggregate and organize into a dermal condensate (Figure 1.5C-D). Among the Gli family members, only *Gli2* null mice exhibit the same phenotype as *Shh* nulls, but transgenic expression of *Gli2* in the epidermis of *Shh* knockouts is unable to completely rescue the arrested hair germs (Mill et al., 2003), suggesting that Shh has Gli2 independent effects and/or a cell non-autonomous role within the dermis. In line with this possibility, loss of Shh is unable to properly organize mesenchymal cells expressing a platelet derived growth factor (PDGF) receptor, which could prevent hair germs that express a PDGF ligand from signaling back to the mesenchyme for further development

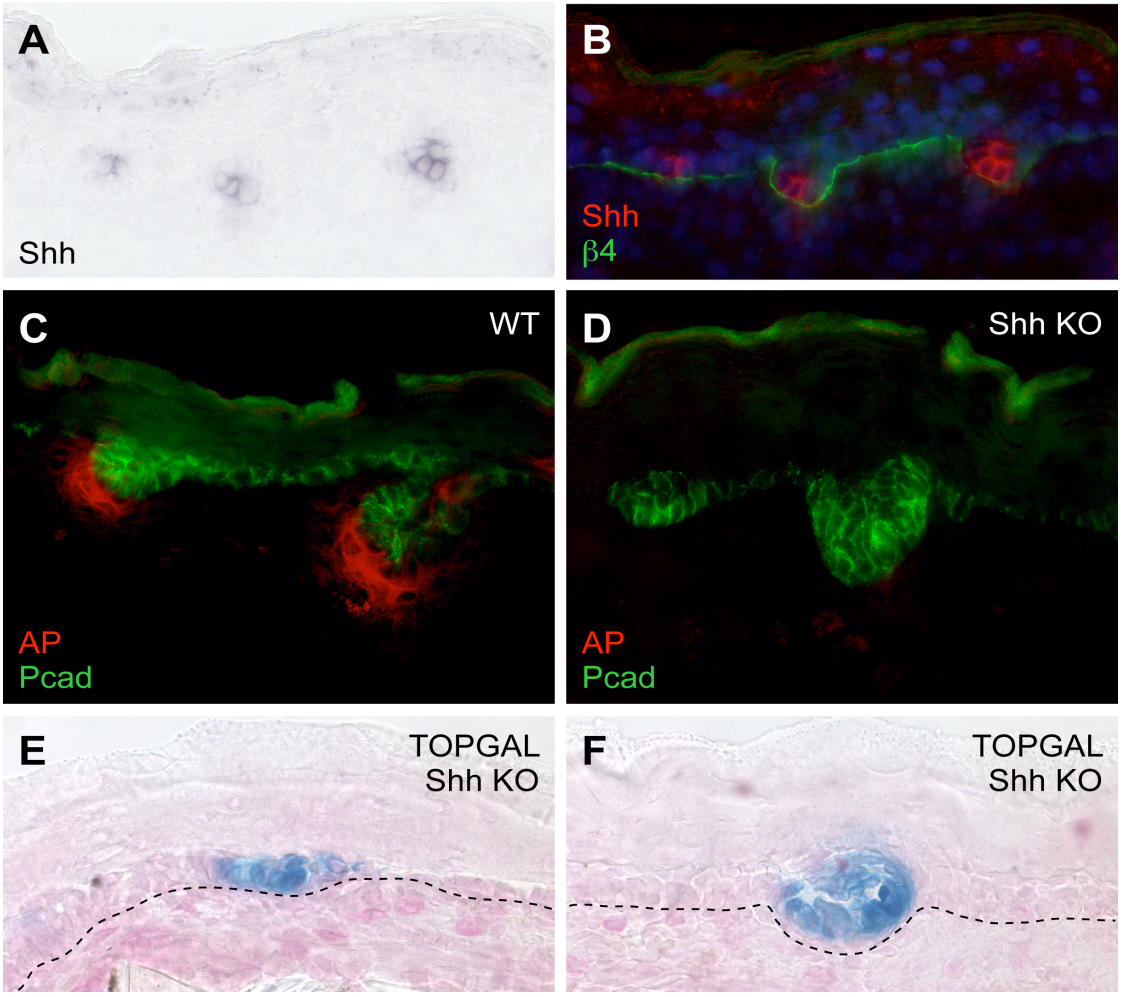

Figure 1.5 Shh signaling during hair morphogenesis. (A-B) Shh is expressed in hair placodes and germs. Back skin sections from E17.5 embryos were probed with *Shh* cRNA, then immunostained for β4-integrin. The Shh *in situ* hybridization signal in (A) was pseudo-colored and overlayed with the β4-integrin image (B). **(C-D)** Although hair follicles are induced in Shh null embryos, they fail to develop a dermal condensate and are unable to develop beyond the hair germ stage (St-Jacques et al., 1998; Chiang et al., 1999). Alkaline phosphatase (AP) is a marker of the dermal condensate. **(E-F)** The arrested hair germs of Shh knockout embryos continue to exhibit activated Wnt signaling as determined by TOPGAL reporter expression. Thus, Wnt signaling lies upstream of Shh to initiate hair follicle morphogenesis, but Shh signaling is subsequently required to organize the dermal condensate and promote hair downgrowth.

(Karlsson et al., 1999). Since Shh signaling effectors are expressed in both the epidermis and dermal condensates of hair follicles, it is still unclear which compartment is responsive to and requires Shh signaling.

Shh signaling also regulates the adult hair cycle. During the telogen to anagen transition, Shh target genes are expressed in the both the developing hair follicle and dermal papilla (Oro and Higgins, 2003). Exogenous Shh or a small molecule agonist can trigger this transition, while mice treated with antibodies against Shh or a known antagonist cyclopamine can block this transition (Paladini et al., 2005; Sato et al., 1999; Wang et al., 2000; Silva-Vargas et al., 2005). Interestingly, anagen does appear to initiate despite blocking Shh, but like embryonic hair germs, the follicles do not progress beyond small bulb-like structures (Wang et al., 2000).

Consistent with a role in promoting proliferation during development, activating mutations in the Shh signaling pathway lead to hair derived tumorigenesis, particularly basal cell carcinoma (BCC) (Daya-Grosjean and Couve-Privat, 2005). Germline mutations in *Ptch1* cause basal cell nevus syndrome, an autosomal dominant predisposition to multiple cancers especially BCC (Hahn et al., 1996; Johnson et al., 1996). Spontaneous BCC also has inactivating patched and activating smoothened mutations (Gailani et al., 1996; Xie et al., 1998). In addition, mouse models overexpressing Shh, Smo, Gli1 and

Gli2 lend further support that misregulation of Shh signaling is sufficient to induce tumors (Oro et al., 1997; Fan et al., 1997; Xie et al., 1998; Nilsson et al., 2000; Grachtchouk et al., 2000). Tumors arising from constitutive Shh signaling also express hair follicle bulge markers, suggesting that they result from an inappropriate expansion of undifferentiated hair progenitor cells (Jih et al., 1999). Recently, a study showed that BCC cells isolated from regressing tumors could completely reconstitute a new hair follicle when combined with inductive dermal cells, providing evidence that BCC represents "an aberrant form of hair follicle organogenesis" (Hutchin et al., 2005).

Bmp signaling

In contrast to Wnt and Shh, bone morphogenetic protein (Bmp) signaling appears to inhibit hair follicle morphogenesis (Botchkarev and Sharov, 2004). Belonging to the transforming growth factor-β (Tgf-β) superfamily, Bmp ligands signal by binding two serine/threonine kinase receptors which result in the activation of the Smad family of intracellular messengers. Specifically, Bmps signal through Smad-1/5/8 while Tgf-βs signal though Smad-2/3. These activated Smad proteins then associate with Smad4, translocate into the nucleus, and mediate gene transcription (Shi and Massague, 2003).

Bmp signaling in skin development begins as early as gastrulation when prospective ectoderm cells are specified to be epidermal, rather than neural (Hemmati-Brivanlou and Melton, 1997). As evident by phosphorylated Smad-1/5/8, active Bmp signaling continues within the epidermis as it differentiates. However, these activated Smad complexes are not present in the developing hair follicles despite the strong expression of Bmp ligands and receptors (Figure 1.6A-C). Similar to neural induction, Bmp signaling must be inhibited by antagonists such as Noggin for proper specification of hair follicles during embryogenesis.

Noggin is expressed in the dermal condensates beneath developing hair placodes and likely exerts its effects on the epithelium (Figure 1.6D). Mutant mice lacking *Noggin* have fewer hair follicles and retarded hair development (Botchkarev et al., 1999). Although Bmp signaling is dispensable for hair follicle induction, it is required later for proper hair shaft and inner root sheath differentiation (Figure 1.6E-F). Inhibition of Bmp signaling during hair differentiation leads to reduced expression of several molecular factors required for lineage commitment and terminal differentiation (Kulessa et al., 2000; Kobielak et al., 2003; Andl et al., 2004; Yuhki et al., 2004). Interestingly, Lef1 and Shh were enhanced in these mutant follicles lacking Bmp signaling. Likewise, expression of Lef1 in the embryonic hair germ is dependent on

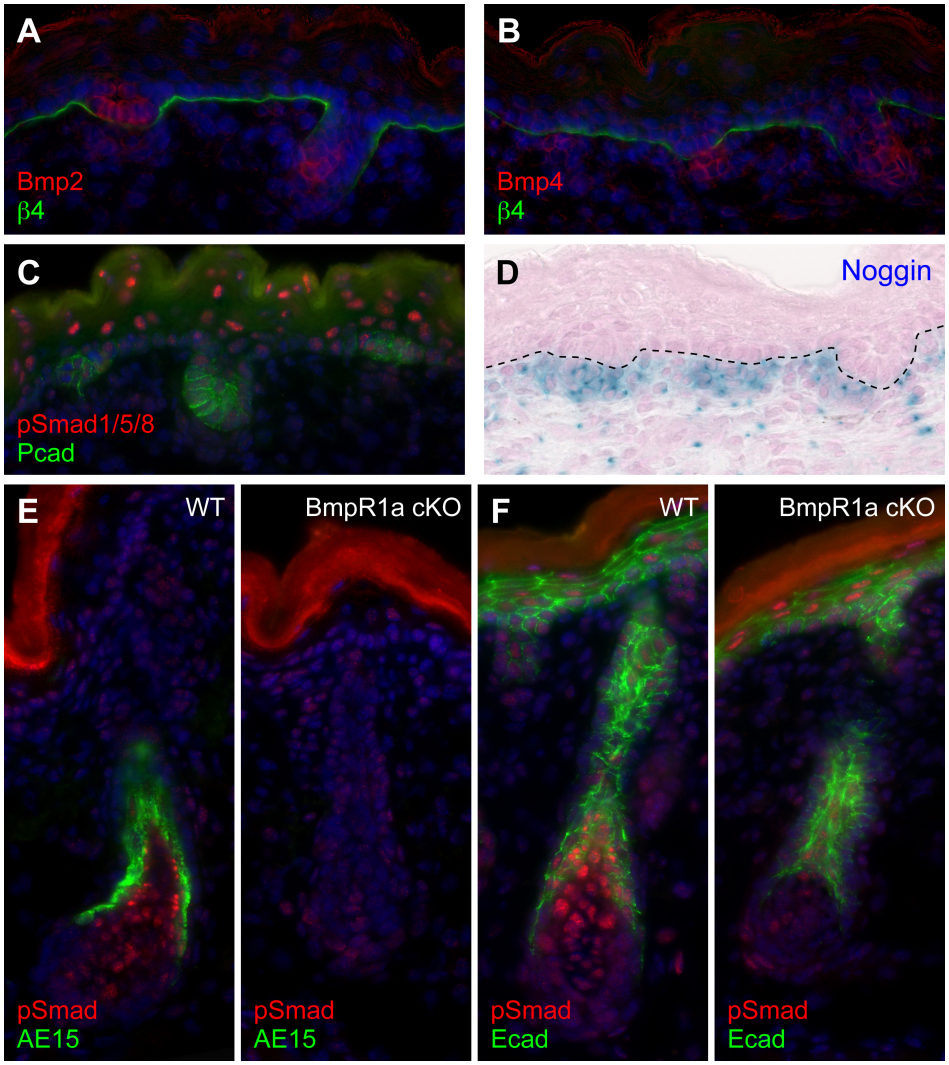

Figure 1.6 Bmp signaling during hair morphogenesis. **(A-B)** Bmp ligands are expressed at sites of hair follicle morphogenesis. By *in situ* hybridization, Bmp2 is primarily localized in hair placodes, while Bmp4 is present in both the placodes and underlying dermal condensates. **(C)** However, Bmp signaling is not active in early hair progenitors. Phosphorylated Smad1/5/8 (pSmad) is excluded from hair placodes and germs, but is prominent in the differentiating epidermis. **(D)** Bmp inhibition during hair morphogenesis is likely mediated by Noggin. Heterozygous *noggin* embryos were stained for β-galactosidase activity to detect endogenous Noggin expression in dermal condensates (Botchkarev et al., 1999). **(E-F)** Bmp signaling is required for terminal hair differentiation. Active Bmp signaling is present in precursors of the inner root sheath and hair shaft. Absence of Bmp signaling, as exemplified by the Bmp receptor-1a (BmpR1a) conditional null, results in the loss of AE15 immunoreactivity, which marks the inner root sheath trichohyalin. Thus, inhibition of Bmp signaling is necessary to initiate hair morphogenesis, but active signaling is required for terminal hair differentiation.

inhibition of Bmp signaling by Noggin (Botchkarev et al., 1999; Jamora et al., 2003), and studies on feather induction in chick embryos support the notion that Bmps downregulate Shh to mediate lateral inhibition of epithelial placode fate (Jung et al., 1998; Noramly and Morgan, 1998).

Similar to its role in hair morphogenesis, inhibition of Bmp signaling is necessary for the activation of anagen during the postnatal hair cycle. The telogen to anagen transition is associated with an upregulation of Noggin expression and can be stimulated by exogenous Noggin, while Bmp treatment blocks anagen entry (Botchkarev et al., 2001). In line with this observation, transgenic expression of Noggin results in faster anagen entry (Plikus et al., 2004). Noggin also increases Shh expression during postnatal hair induction (Botchkarev et al., 2001).

In short, Bmp signaling inhibits the specification and/or activation of hair follicle progenitors during both embryogenesis and postnatal hair renewal, but promotes their terminal differentiation into various cell lineages. Bmp signaling also appears to intersect with both the Wnt and Shh signaling pathways to control hair follicle morphogenesis.

Other signaling pathways

Several other signaling factors are expressed in early hair germs, including members of the transforming growth factor-β (Tgf-β), fibroblast growth factor

(Fgf), and ectodysplasin (Eda) family. Through mouse and human genetics, all are implicated in different aspects of hair follicle induction and differentiation (Foitzik et al., 1999; Petiot et al., 2003; Laurikkala et al., 2002).

Specific aims

With the simultaneous expression of multiple extrinsic factors, the hair placode can be considered a signaling center that must integrate and translate both stimulatory and inhibitory inputs into a program of gene expression that specifies a hair cell fate from embryonic ectoderm. However, little is known about the molecular machinery that coordinates these signaling pathways to orchestrate hair follicle induction and morphogenesis. Reflecting their morphological similarities, these same signals direct the activation of adult stem cells to initiate new rounds of hair growth. When altered, these normal developmental processes can lead to diseases such as cancer. Thus identifying and characterizing genes involved in early hair placode development will extend our understanding of the downstream intrinsic mechanisms that regulate cell lineage commitment of multipotent progenitors during morphogenesis and postnatally. It will also shed light into potential avenues of development that can be disrupted during the pathogenesis of skin disease.

The study of hair morphogenesis is also anticipated to have broader implications that extend beyond the hair follicle. Many organs such as teeth, mammary glands, lungs, and kidneys develop like hair follicles, utilizing a process of "budding morphogenesis" (Hogan 1999; Pispa and Thesleff, 2003). Despite their diversity in final form and function, the same signaling pathways used in hair morphogenesis modulate the epithelial-mesenchymal inductive interactions in the initial development of these organs. Thus, analyzing the gene expression profile during hair morphogenesis can reveal how organs utilize basic cellular functions such as proliferation, cell fate determination, differentiation, and migration involving changes in shape, polarity, and adhesion to coordinate placode development. At the same time, unique factors which lie downstream of these evolutionary conserved pathways may be uncovered that lend specificity to hair follicle determination and morphogenesis.

To define the molecular mechanisms regulating hair follicle morphogenesis, I initially developed a strategy to isolate and transcriptionally profile embryonic hair placodes and interfollicular epidermis in mice. By comparing the gene expression profiles of these two cell populations, genetic changes that occur when the hair follicle lineage is specified from the undifferentiated ectoderm were unveiled. In addition to substantiating genes previously documented in hair and epidermal development, this screen revealed insights into the embryonic origins of

the adult hair follicle stem cell niche. To validate this approach to identify genes that specify hair follicle progenitors and regulate their functional properties during development, I characterized the transcription factor Lhx2. I demonstrate that Lhx2 is expressed specifically in both embryonic hair progenitors and adult stem cells, and appears to link the induction of hair follicle morphogenesis to the establishment and maintenance of stem cells.

CHAPTER 2
ISOLATION AND ANALYSIS OF EMBRYONIC HAIR PROGENITORS

Hair follicle morphogenesis involves a temporal series of reciprocal interactions between the ectoderm and its underlying mesenchyme (Figure 1.2). In response to an inductive Wnt and an inhibitory Bmp signal (Noggin), small hair placodes bud from the epithelium, giving rise to larger hair germs. In the presence of the mitogen Shh, these hair germs develop further and grow downward to form a mature follicle that actively produces hair. Although the molecular details of bud formation are still poorly defined, the general features of this process are repeated at the start of each postnatal hair cycle when multipotent stem cells in the hair follicle bulge become activated to initiate a new round of hair growth. In addition, the early epithelial remodeling to form the hair germ shares many features with the development of other epithelial tissues and organs, including feathers, teeth, and mammary glands. Understanding how tissues form buds that then progress along different lineages is predicated on elucidating the molecular mechanisms that funnel these early signaling pathways into a transcriptional program that drives morphogenesis.

To examine the genetic changes that occur during epithelial bud formation, I developed a method to isolate and purify embryonic hair progenitors along with interfollicular epidermal cells. The gene expression profiles of these two cell

populations were compared and analyzed to reveal transcriptional differences that occur as ectodermal cells commit to a hair follicle lineage and undergo morphogenesis. Apart from a number of genes with previously documented roles in hair development, the embryonic hair progenitors differentially expressed several genes in common with the postnatal hair follicle bulge, suggesting functional similarities to those of adult stem cells. Interestingly, a presumptive bulge was identified in developing follicles by the presence of label retaining cells which were initially labeled during embryonic hair induction. As the morphogenetic hair cycle completed, these slow cycling cells persisted as bulge stem cells in adult hair follicles.

Results

Isolation of embryonic hair progenitors

The murine hair coat is composed of several different hair types that are initiated during embryonic development at different times (Mann, 1962). The largest hair follicles known as tylotrich, guard, or primary hairs begin morphogenesis at embryonic day E13.5. Relatively few in number, these follicles eventually from the hair overcoat and can be recognized during embryogenesis by a raised area of epidermis. The undercoat is composed of the awl, auchene, and

zigzag hair follicles, otherwise known as nontylotrich or secondary hair follicles. These hair types comprise the vast majority, between 90-95%, of total hair follicles and are indistinguishable from each other during early morphogenesis. Initiation of nontylotrich hair follicles begins around embryonic day E15.5 and continues in waves until a few days postnatal. Although the initial timing of morphogenesis in all hair follicles is not synchronous, each follicle follows the same program of development in approximately the same length of time.

To determine an ideal stage of development to isolate early hair progenitors, the dorsal skin of mouse embryos at various ages was evaluated for P-cadherin expression, a calcium dependent cell adhesion molecule upregulated at sites of hair follicle morphogenesis (Hardy and Vielkind, 1996; Jamora et al., 2003). At E13.5, P-cadherin was expressed uniformly throughout the single layer of epidermis as detected by immunofluorescence. Large thickenings of the epidermis, corresponding to guard hair placodes, would occasionally be morphologically visible. By E15.5, hair placodes were spaced throughout the dorsal epidermis and expressed elevated levels of P-cadherin relative to the basal layer of keratinocytes. Many more P-cadherin positive hair placodes were induced a day later at E16.5, with some forming dermal condensates. Although P-cadherin was still found along the basal layer, its expression was diminished relative to the developing hair follicles. By E17.5, larger hair downgrowths were evident,

however recently induced hair placodes and germs strongly positive for P-cadherin were also present (Figure 2.1).

Since P-cadherin is a cell surface molecule, its differential expression in hair placodes and germs was exploited to selectively isolate early hair progenitor cells from other epidermal cells with the use of fluorescence activated cell sorting (FACS). To eliminate other cell types in the epidermis which might express P-cadherin, transgenic embryos for *Keratin 14-ActinGFP* were utilized (Vaezi et al., 2002). Keratin 14 (K14) is specifically expressed in the keratinocytes of the basal layer of epidermis (Vassar et al., 1989), but the stability of actin causes all cells derived from the basal layer, including hair placodes and suprabasal keratinocytes, to express GFP. To restrict analysis to the basal epidermal cells, α6-integrin or β4-

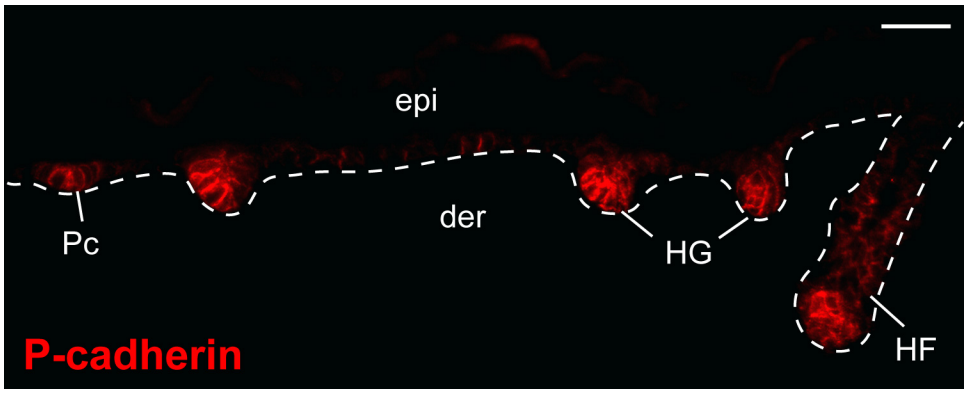

Figure 2.1 P-cadherin expression in embryonic hair follicle progenitors. Skin sections from E17.5 embryos were stained for P-cadherin and found to be up-regulated at sites of hair follicle morphogenesis (Hardy and Vielkind, 1996). This differential expression was used to isolate PCAD+ hair progenitors and PCAD– interfollicular basal cells by FACS. Abbreviations: epi, epidermis; der, dermis; Pc, placode; HG, hair germ; HF, hair follicle. Scale bar, 40μm.

integrin, transmembrane proteins involved in basement membrane assembly and adhesion, was also used as a surface marker to isolate hair follicle progenitors and interfollicular basal keratinocytes.

To create of suspension of epidermal cells for FACS, embryonic skin from E17.5 *K14-ActinGFP* embryos was dissected and treated with dispase to separate the epidermis, including hair placodes and germs, from the underlying dermis, which harbored more mature hair pegs and follicles (Figure 2.2). After dissociating the epidermal fraction with the divalent ion chelator EDTA, the embryonic "PCAD+" hair progenitors (K14-GFP+, α6-integrin+, P-cadherin+) were then separated from the "PCAD–" interfollicular epidermis (K14-GFP+, α6-integrin+, P-cadherin–) on the basis of their differential surface P-cadherin expression (Figure 2.3). Although P-cadherin is a calcium dependent cell adhesion molecule, it is resistant to EDTA treatment in the absence of trypsin (Figure 2.4).

The specificity of P-cadherin to label hair placodes was tested using epidermal cells isolated from mutant embryos (Figure 2.5). As expected, P-cadherin did not stain cells isolated from *P-cadherin* null mice which undergo normal hair morphogenesis. Epidermal cells isolated from the *β-catenin* conditional knockout, which lack all hair follicles and thus P-cadherin expression by immunohistochemistry, were also negative for P-cadherin by FACS analysis

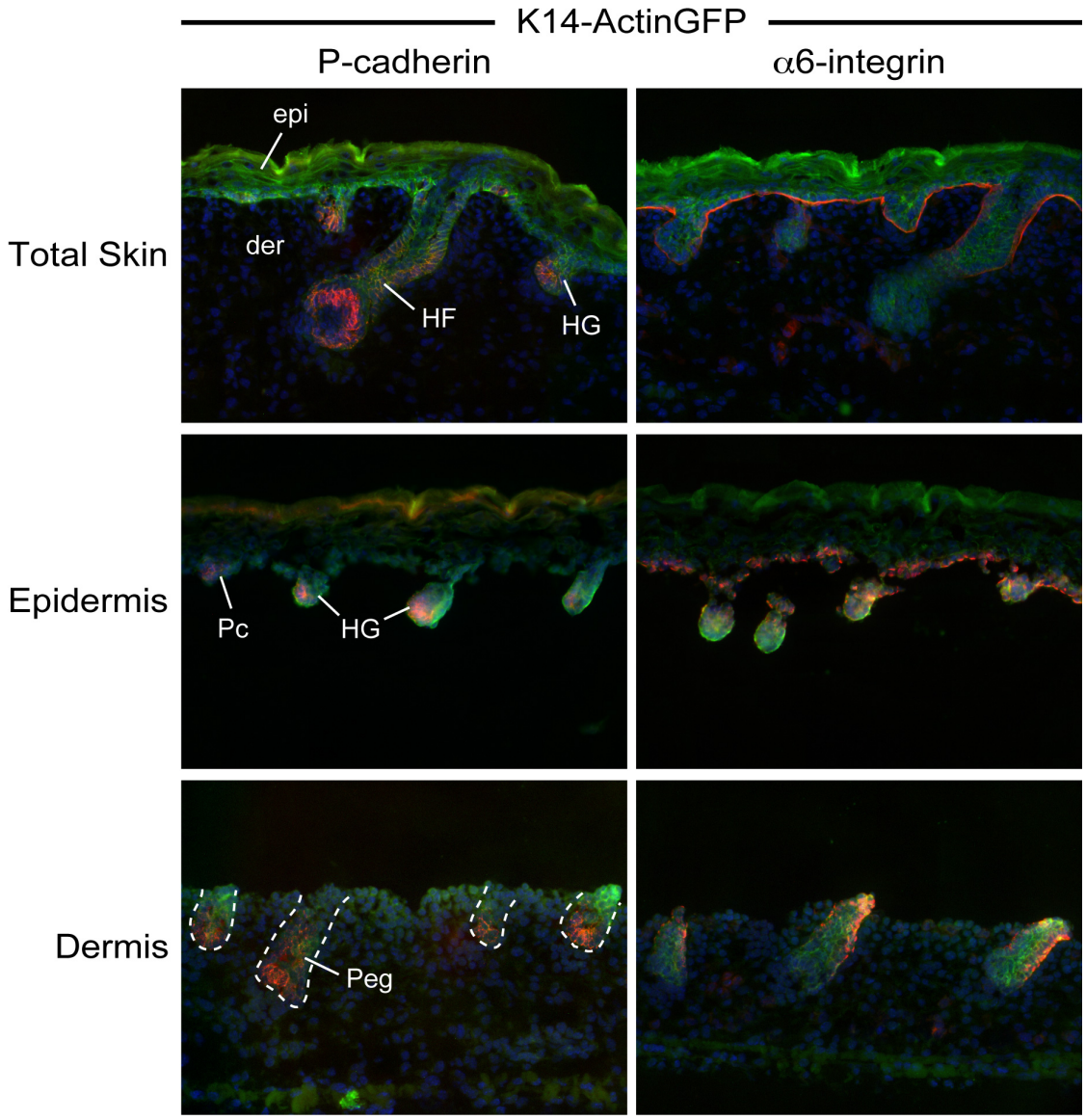

Figure 2.2 Expression of molecules used to isolate hair follicle progenitors. Skin from E17.5 *K14-ActinGFP* embryos was dissected and treated overnight with dispase at 4°C. Dispase treatment separates the hair germs, marked by P-cadherin expression, and the interfollicular epidermis from more mature hair follicles which remain in the dermis. α6-integrin marks the epidermal cells of the basal cell layer, including the early hair follicle progenitors. Abbreviations: epi, epidermis; der, dermis; Pc, hair placode; HG, hair germ; Peg, hair peg; HF, hair follicle.

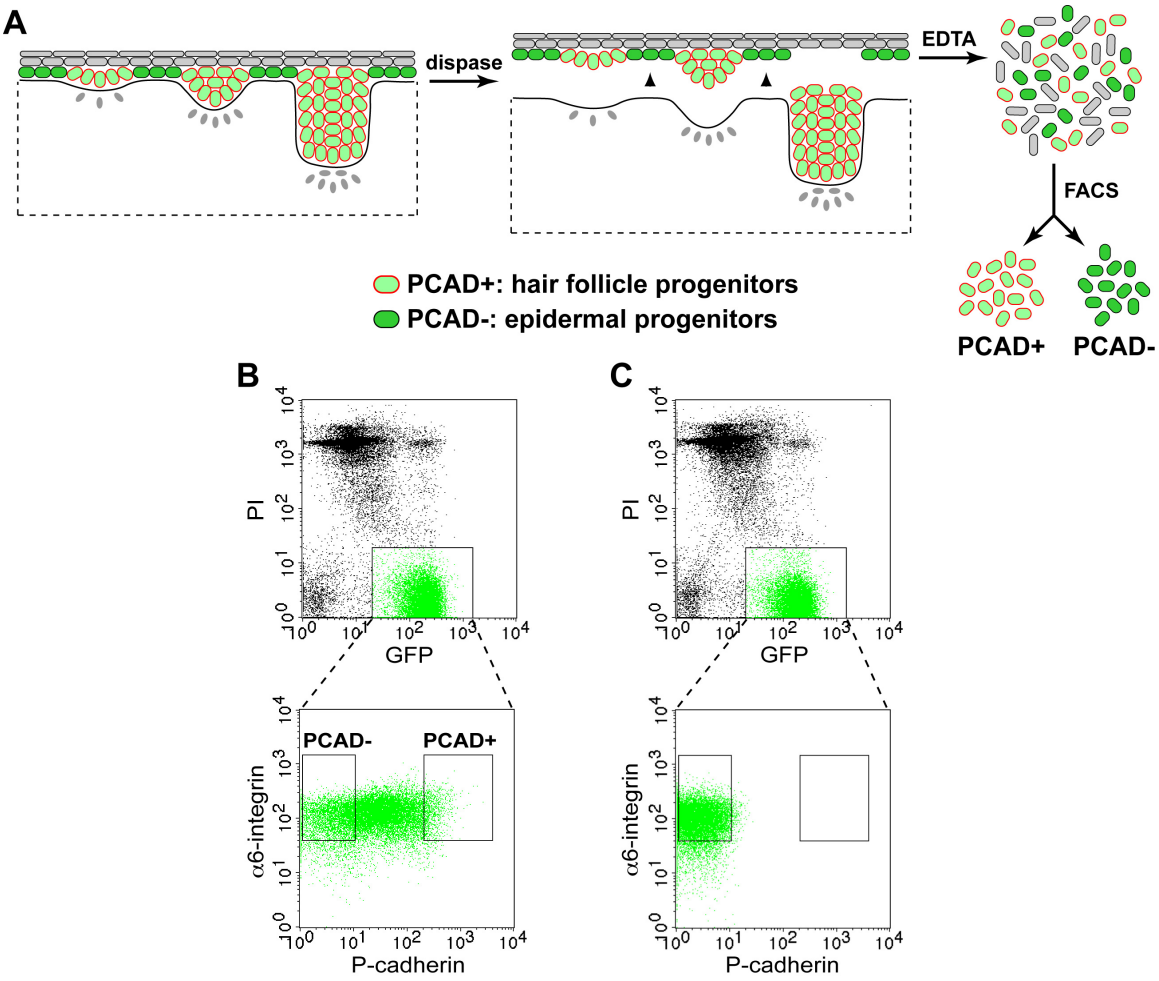

Figure 2.3 FACS strategy to isolate hair follicle progenitors. Differential expression of P-cadherin was used to FACS isolate PCAD+ hair progenitors and PCAD– interfollicular basal cells from the epidermal fraction of dispase treated E17.5 *K14-ActinGFP* transgenic skin. **(A)** Schematic to generate epidermal cell suspensions for flow cytometry. **(B-C)** Single cell suspensions were gated for propidium iodide (PI) exclusion, keratinocyte GFP expression, and the basal cell marker α6-integrin. These live basal keratinocytes were then sorted based on their P-cadherin expression. Thus, the "PCAD+" hair progenitors (K14-GFP+, α6-integrin+, P-cadherin+) can be separated from the "PCAD–" interfollicular epidermis (K14-GFP+, α6-integrin+, P-cadherin–). The secondary only control for P-cadherin is shown in (C).

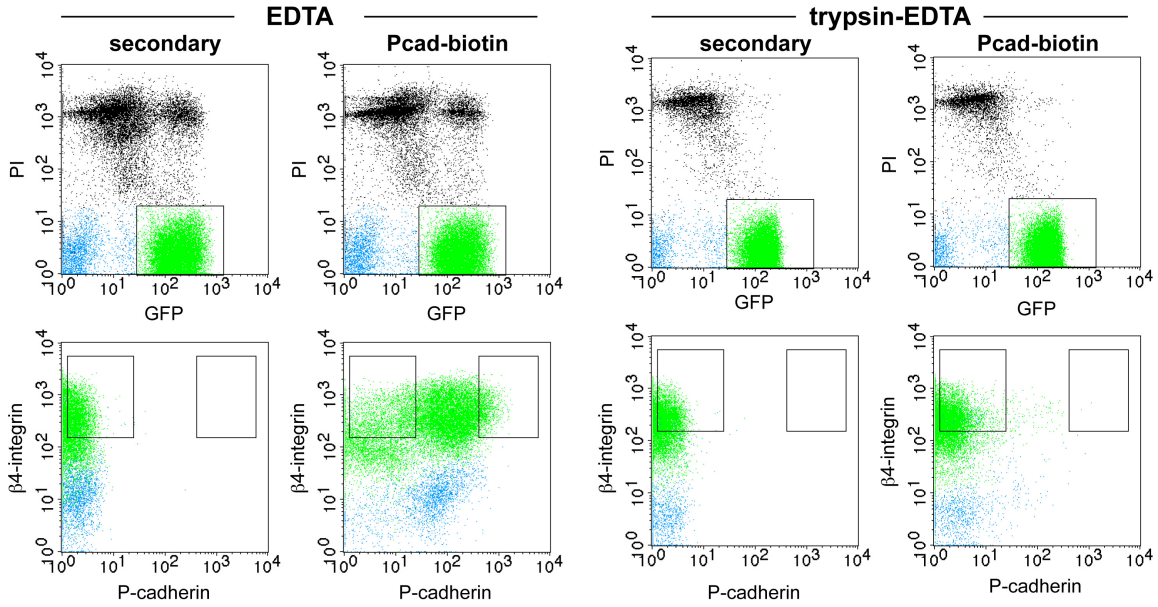

Figure 2.4 P-cadherin is resistant to EDTA in isolating epidermal cells. After dispase treatment of E17.5 *K14-ActinGFP* skin, the epidermal fraction was treated either with EDTA or trypsin plus EDTA. Cell suspensions were then stained with P-cadherin and β4-integrin before analyzed by flow cytometry. As a calcium dependent adhesion molecule, P-cadherin is destabilized without calcium, but in the absence of trypsin, P-cadherin remains present on the cell surface. However, P-cadherin is lost when cells are treated with trypsin in the presence of divalent ion chelator EDTA which destabilizes and digests intercellular adhesive contacts. Although the presence of calcium during trypsinization can preserve P-cadherin expression, epidermal cells are not readily dissociated, creating cell clumps. Thus, EDTA alone was used after dispase to create single cell suspensions of keratinocytes that maintain P-cadherin expression for FACS. Surface integrins are not affected by either treatment.

verifying that P-cadherin can specifically label hair placode cells.

Finally, the purity of the PCAD+ and PCAD− sorted cell populations was evaluated with various molecular markers. Reflecting their basal character, nearly all sorted cells in both populations stained positively for K5, the keratin partner of

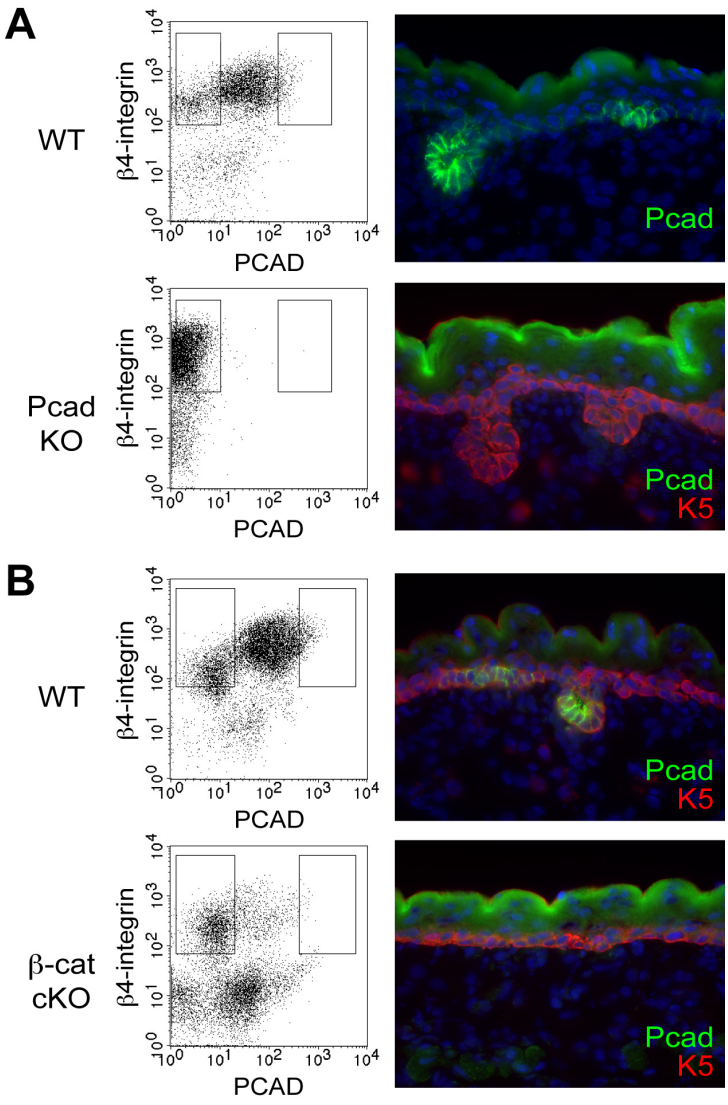

Figure 2.5 FACS analysis on mutant embryos. The specificity of P-cadherin to label hair follicle progenitors was tested using epidermal cells isolated from mutant embryos at E17.5. **(A)** P-cadherin does not stain cells isolated from *P-cadherin* knockout (Pcad KO) mice which undergo normal hair morphogenesis. **(B)** *β-catenin* conditional knockout mice (β-cat cKO) lack all hair follicles and expression for P-cadherin. Weak positive staining is due to the slightly mosaic expression of *K14-Cre* recombinase, resulting in the induction of sporadic hair follicles. Immunofluorescence images are color-coded according to the secondary antibodies used.

K14, and for β4-integrin, a partner of α6-integrin (Figure 2.6A). A very small percentage of cells in the PCAD– fraction stained positive for K1, a keratin expressed in the suprabasal layers of the epidermis, but this could represent cells at a transitional stage of differentiation since they displayed a small and round morphology and often co-stained with K5 (Figure 2.7).

Semi-quantitative reverse transcription polymerase chain reaction (RT-PCR) for known placode markers confirmed the distinction between the two sorted cell populations (Figure 2.6C). Previously demonstrated to be transcriptionally upregulated in hair placodes, mRNAs for *P-cadherin*, *Bmp2*, *Bmp4*, *Shh*, *Wnt10b*, and *Msx2* were elevated in the PCAD+ relative to the PCAD– cells. Keratin 5 was slightly repressed in PCAD+ cells by RT-PCR, similar to its expression pattern in skin at sites of hair follicle induction (Byrne et al., 1994). Cells were also sorted from *TOPGAL* transgenic embryos and the specific activity of β-galactosidase, indicating active Wnt signaling, in PCAD+ embryonic hair progenitors was verified (Figure 2.6B). Thus, the purity and inherent differences between the two isolated cell populations distinguished by surface P-cadherin expression was validated through analysis of known molecular markers.

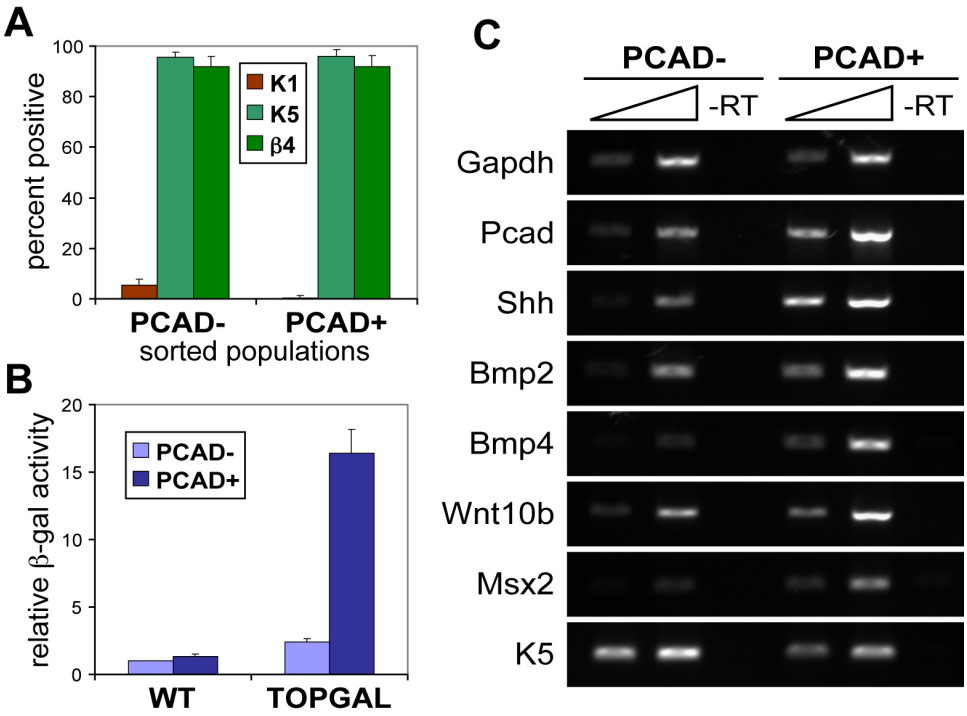

Figure 2.6 Expression of marker genes in sorted cell populations. The sorted PCAD+ cells express known markers of hair placodes. **(A)** Sorted cells were cytospun and stained for epidermal markers K1, K5, and β4-integrin. A summary of cell counts from three independent sorts is shown. Reflecting their basal character, both PCAD– and PCAD+ cells express basal layer markers. **(B)** Cells were sorted from *TOPGAL* positive and negative embryos, and β-galactosidase activity was assessed by chemiluminescence. Relative activity was measured against wild-type PCAD– cells, which was arbitrarily set at 1. An average of three independent sorts is shown. Reflecting their active Wnt signaling, only PCAD+ cells from transgenic mice exhibit strong reporter activity. **(C)** RNA was extracted from sorted cell populations and semi-quantitative RT-PCR was performed for known genes differentially expressed in hair placodes. PCAD+ cells express higher levels of these placode genes relative to PCAD– cells. K5 and K14 are known to be down-regulated, but still expressed in hair germs.

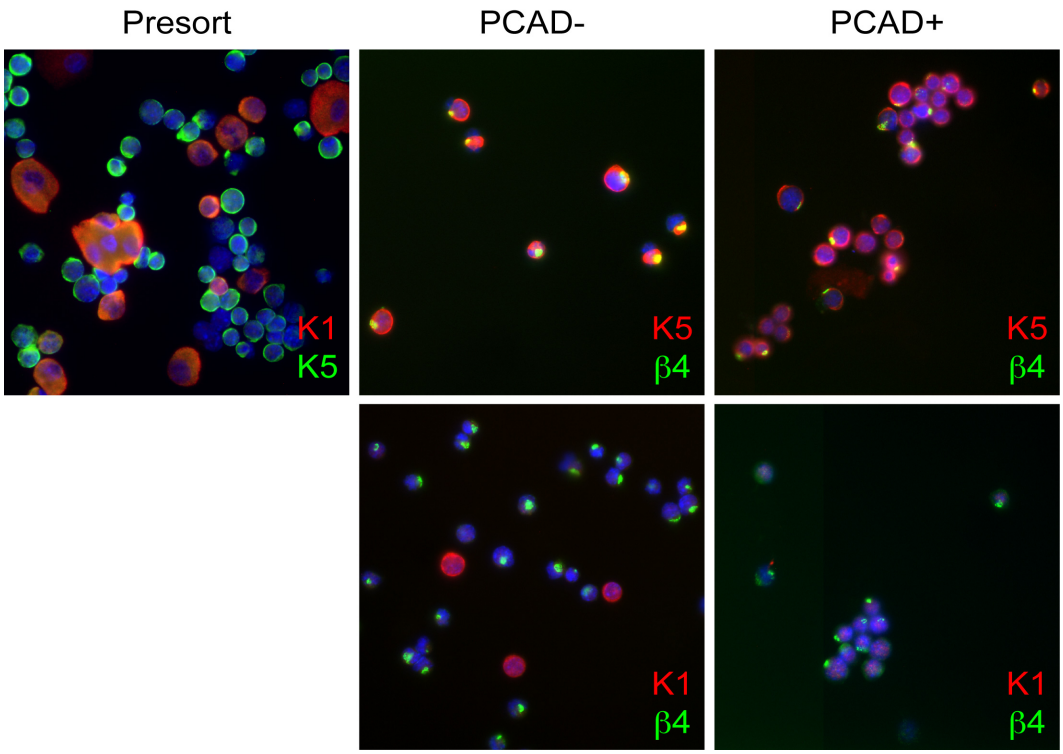

Figure 2.7 Cytospin analysis of sorted cell populations. Unsorted and sorted cells were cytospun and immunostained for epidermal markers, K1, K5, and β4-integrin. Quantitation of three independent cell sorts is provided in Figure 2.6A. Although the PCAD– cell fraction had a minor contamination of K1 positive cells, these cells were small and round, unlike the large and flat, squamous-like K1 positive cells in the unsorted total epidermal cell population. Often co-staining with antibodies against K5, these cells may represent an early transitional stage of epidermal differentiation. Images are color-coded according to the secondary antibodies used.

Transcriptional differences during hair morphogenesis

The gene expression profiles of purified PCAD+ hair progenitors and PCAD– interfollicular basal keratinocytes were further analyzed using oligonucleotide microarrays to identify transcriptional changes that occur as epithelial cells commit to a hair cell lineage. Two entirely independent samples

were initially assessed for overall hybridization quality using various parameters (Table 2.1). All arrays showed similar scaling factors and percent present calls, indicating that equivalent amounts of labeled RNA was hybridized. Although there was some 3' bias in the labeled RNA samples, it was also comparable across the hybridizations. This consistency allowed us to make comparisons between the two sorted populations and cross-comparisons across replicates to generate transcriptional differences.

Table 2.1. Microarray hybridization statistics. Arrays were scaled to a target signal of 500 using default parameters in Affymetrix GeneChip Operating Software. See materials and methods for details on analysis.

ARRAY	SCALE FACTOR	% PRESENT	β-ACTIN 3'/5'	GAPDH 3'/5'
PCAD−_1	1.530	49.2	2.74	4.60
PCAD+_1	1.541	49.1	2.70	4.71
PCAD−_2	1.649	48.5	2.89	5.20
PCAD+_2	1.709	48.5	2.94	4.91

To determine the capability and fidelity of the array data to reflect significant genetic differences that occur during hair morphogenesis, the presence of known hair placode markers in the PCAD+ samples relative to PCAD− samples was examined. In general, the comparative analysis faithfully reflected a number of these changes, sometimes with multiple probe sets (Table 2.2). Using fold

differences of these hair placode markers as a sensitivity gauge, a two-fold cutoff was assigned as a genuine difference between the two cell populations. As a result, a total of 1394 probes (660 in PCAD+ and 724 in PCAD–) were preferentially expressed in one population relative to the other (see Appendix for complete list). Semi-quantitative RT-PCR on a independent sorted sample further verified a set of transcriptional differences between the PCAD+ hair progenitors and PCAD– interfollicular epidermis identified in the microarray (Figure 2.8).

Table 2.2 Fold changes of known hair placode markers. Mean fold changes of genes were determined by comparing the PCAD+ array replicates to the PCAD– array replicates. Multiple values represent independent probe sets in the microarray. See materials and methods for details on analysis.

GENE	↑/↓	FOLD CHANGE	REFERENCE
P-cadherin	↑	1.3, 1.2	Hardy & Vielkind, 1996
E-cadherin	↓	-1.7, -1.6	Jamora et al., 2003
Shh	↑	14.8	St-Jacques et al., 1998
Bmp2	↑	2.5	Botchkarev et al., 1999
Bmp4	↑	4.6	Botchkarev et al., 1999
Tgf-β2	↑	11.5, 10.6, 8.8, 5.7	Foitzik et al., 1999
EdaR	↑	5.4	Laurikkala et al., 2002
Wnt10b	↑	-	Reddy et al., 2001
β-catenin	↑	1.8, 1.3	Huelsken et al., 2001
Lef1	↑	no change	Zhou et al., 1995
Msx2	↑	-	Satokata et al., 2000
K5	↓	-2.4	Byrne et al., 1994

Recapitulating their *in vivo* genetic programs, a number of these differentially expressed genes have documented roles in either hair morphogenesis (PCAD+) or epidermal differentiation (PCAD–).

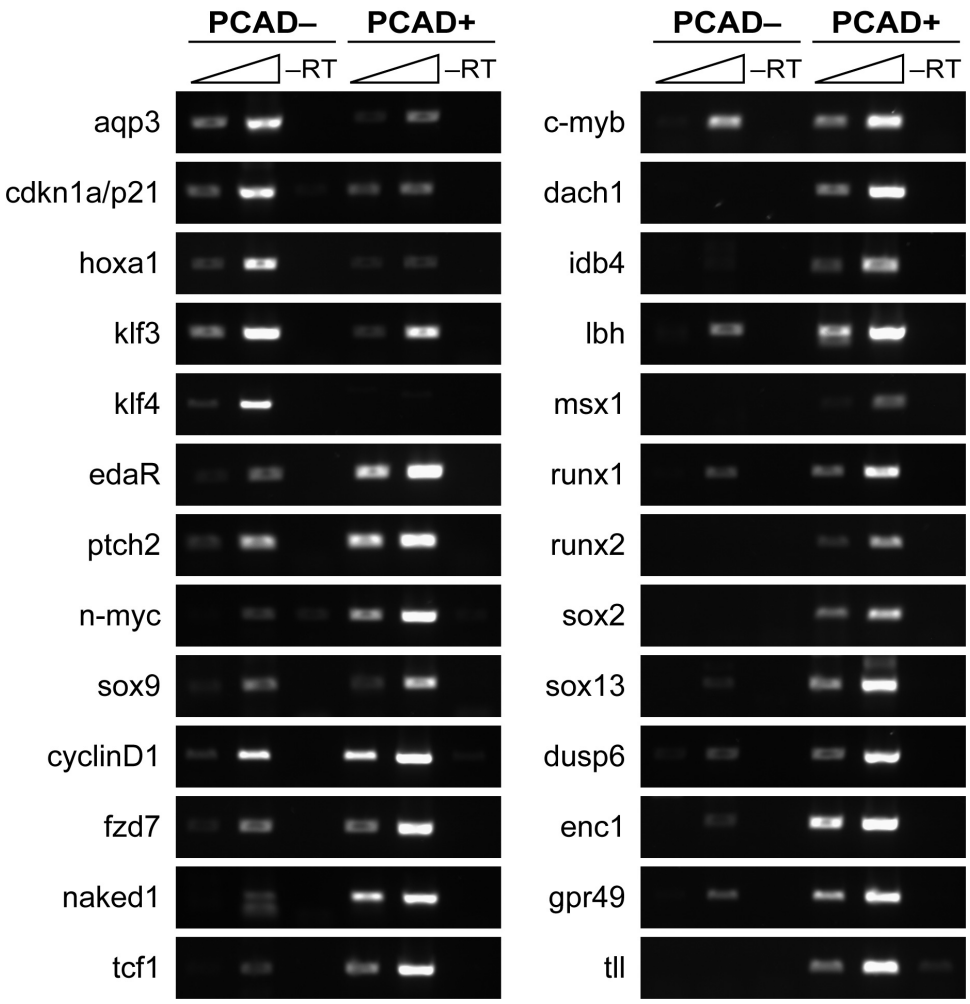

Figure 2.8 Verification of differentially expressed genes in the microarrays. RNA was extracted from sorted cell populations of an independent sample and semi-quantitative RT-PCR was performed on a set of differentially expressed genes identified by the array data. All genes tested recapitulated the expression changes in the microarrays. See appendix for raw values and fold changes.

PCAD– interfollicular epidermal cells

The PCAD– interfollicular epidermal population was typified by adhesive and cytoskeletal components and molecular factors implicated in differentiation (Table 2.3). In particular, keratin intermediate filaments and components of the desmosome were prominently present. Desmosomes are adhesive intercellular junctions that link keratin filaments to the cell surface and ultimately to adjacent cells. At the core of the desmosome are desmocollins and desmogleins, desmosomal cadherins which mediate cell-cell contact through their extracellular domains. The cytoplasmic tails of these proteins associate with plakoglobin, plakophilins, and members of the plakin family, which anchor desmosomes to the keratin cytoskeletal network. Although more prominent in the suprabasal cell layers, desmosomes are also present in basal cells and function to maintain tissue integrity and strength amid the constant mechanical stress that the epidermis endures. Disruption of these junctions or their associated keratins leads to skin fragility and blistering diseases such as pemphigus, palmoplantar keratoderma, epidermolysis bullosa, and epidermolytic hyperkeratosis (Kottke et al., 2006; Garrod et al., 2002; Leung et al., 2002; Lane and McLean, 2004; Rugg and Leigh, 2004).

The PCAD– cells also expressed higher levels of other junctional proteins such as Col17a1 (BPAG2), a component of hemidesmosomes which mediates

Table 2.3 Selected genes in PCAD– fraction. Genes upregulated ≥2-fold in the PCAD– cell population relative to the PCAD+ cell population with established roles in epidermal development are listed. See appendix for raw values.

ADHESION/STRUCTURAL		DIFFERENTIATION	
Cldn1	Furuse et al., 2002	BmpR1b	Botchkarev & Sharov, 2004
Col17a1	McGrath et al., 1995	Dll1	
Dsc2	Garrod et al., 2002	Dtx2	
Dsg1a	Garrod et al., 2002	Jag1	
Evpl	Maatta et al., 2001	Krtdap	Oomizu et al., 2000
Eppk1	Fujiwara et al., 2001	Notch3	
Jup	Bierkamp et al., 1996	Sprr2a	Cabral et al., 2001
Krt1-10	Cheng et al., 1992	Sfn	Herron/Li et al., 2005
Krt1-14	Coulombe et al., 1991	Sbsn	Park et al., 2002
Krt1-15	Lloyd et al., 1995		
Krt1-16	McLean et al., 1995	**TRANSCRIPTION FACTORS**	
Krt2-1	Chipev et al., 1992	Esr1	Thornton, 2002
Krt2-5	Lane et al., 1992	Foxn1	Brissette et al., 1996
Krt2-6a	Wong et al., 2000	Grhl1	Tao et al., 2005
Krt2-6b	Wong et al., 2000	Grhl3	Ting et al., 2005
Ocln	Saitou et al., 2000	Klf4	Segre et al., 1999
Ppl	Aho et al., 2004	Klf5	Ohnishi et al., 2000
Pkp1	McGrath et al., 1997	Myc	Arnold & Watt, 2001
		Ovol1	Nair et al., 2006
		Pou3f1	Andersen et al., 1997
		Stat1	
		Tcfap2e	Tummala et al., 2003

attachment of basal keratinocytes to its underlying basement membrane. BPAG2 is a target of the autoimmune disease bullous pemphigoid, a blistering disease similar to junctional epidermolysis bullosa (McGrath et al., 1995). Tight junction proteins, claudin and occludin, were also upregulated in the PCAD– cells. Tight junctions were initially thought not to play a major role in stratified epithelia, but *claudin-1* null mice are born with an epidermal barrier defect resulting in progressive water loss and dehydration (Furuse et al., 2002).

Components of two signaling pathways implicated in epidermal differentiation, Notch and Bmp, were also preferentially expressed in the PCAD– cells. In human epidermis, the receptor Notch3 and ligands Delta1 and Jagged1 are expressed throughout the basal layer, with Delta1 enriched in epidermal stem cells (Thelu et al., 2002; Lowell et al., 2000). Although these specific components have not been functionally characterized, Notch signaling has been demonstrated to affect the proliferative and differentiation status of epidermal keratinocytes. Loss of *Notch1* results in epidermal hyperplasia, inhibition of early differentiation markers, and increased susceptibility to skin tumorigenesis (Rangarajan et al., 2001; Nicolas et al., 2003).

Bmp signaling also plays a critical role in interfollicular epidermal differentiation. Bmps and their antagonists are expressed spatiotemporally throughout epidermal development (Botchkarev, 2003). Beginning in gastrulation,

Bmps induce the epidermal lineage by inhibiting neural cell fate (Hemmati-Brivanlou and Melton, 1997). Several studies have demonstrated using cultured keratinocytes that Bmp signaling also inhibits proliferation and promotes differentiation. However, conditional ablation of the BmpR1A receptor *in vivo* has no effect on the interfollicular epidermis. Notably, the PCAD– cells expressed higher levels of BmpR1B. Thus confirmation of Bmp signaling in epidermal differentiation awaits further genetic studies.

Lending support to a role for Bmps in epidermal differentiation are the evolutionary conserved grainyhead family of transcription factors, of which Grhl1 and Grhl3 are enriched in the PCAD– cells. Originally identified in Drosophila to modulate cuticle formation, grainyheads are expressed in an epithelial-restricted pattern across species. In Xenopus, Grhl1 expression in the epidermis is Bmp4 dependent and loss of *Grhl1* inhibits key epidermal structural genes resulting in severe terminal differentiation defects (Tao et al., 2005). Similarly, *Grhl3* null mice exhibit defective skin barrier function accompanied by reduced expression of transglutaminase, an enzyme that crosslinks structural components to form the water-impermeable cornified layer of epidermis (Ting et al., 2005).

Other transcription factors that regulate epidermal differentiation were also increased in the PCAD– interfollicular cell population. Expressed in proliferative basal cells as they transition into terminal differentiation, inactivation or

misregulation of these factors leads to abnormal programs of epidermal differentiation. Consistent with its expression pattern and oncogenic role, c-Myc overexpression drives proliferation and promotes epidermal cell fate at the expense of hair follicles (Waikel et al., 2001; Arnold and Watt, 2001). c-Myc expression is regulated in part by Ovol1 which represses c-Myc to restrict the proliferative potential of differentiating epidermal progenitor cells (Nair et al., 2006). Pou3f1, also known as Tst1/Oct6/SCIP, also appears to function at the transition to differentiation since loss of *Pou3f1* fails to suppress basal keratin genes in the suprabasal cell layers (Andersen et al., 1997). Likewise, keratinocytes lacking *Foxn1* retain basal markers, but have a greater propensity to differentiate, suggesting a role at the initiation of differentiation (Brissette et al., 1996; Baxter and Brissette, 2002). Finally, acquisition of a functional barrier during epidermal differentiation requires Klf4 (Segre et al., 1999).

Additional factors linked to epidermal stratification were also differentially expressed in the PCAD– cells. Stratifin, also known as 14-3-3σ, mediates cell cycle arrest and terminal differentiation in epidermis. Mutations in stratifin found in the repeated-epilation (*Er*) mouse mutant results in a hyperplastic epidermis and a failure of terminal differentiation (Herron et al., 2005; Li et al., 2005). Although not completely characterized, suprabasin and Sprr2 are implicated as cornified

envelope precursor proteins and potential substrates of transglutaminase activity (Park et al., 2002; Cabral et al., 2001).

PCAD+ hair progenitor cells

The PCAD+ hair progenitor population featured several signaling morphogens and transcription factors involved in hair morphogenesis (Table 2.4). Hair placode markers such as Bmp2, Bmp4, Edar, Shh, and Tgf-β2 were differentially expressed as previously described. Despite the importance of Wnt signaling in hair morphogenesis, only one wnt ligand, Wnt5a, and one frizzled receptor, Fzd7, was identified in the PCAD+ hair progenitors. Fzd7 expression has been reported to be upregulated in hair placodes (Reddy et al., 2004), but finding Wnt5a is perplexing in light of a study that found Wnt5a expression downstream of Shh in dermal condensates (Reddy et al., 2001). In fact, the PCAD + cells expressed several Wnt inhibitory genes such as Wif1, which binds and sequesters Wnt ligands, and members of the dickkopf family, which inhibit the Wnt coreceptor Lrp6 (Mao et al., 2002). The function of these negative regulators during hair development remains to be determined, but there appears to be a competitive balance between stimulatory and inhibitory signals to control hair morphogenesis.

Table 2.4 Selected genes in PCAD+ fraction. Genes upregulated ≥2-fold in the PCAD+ cell population relative to the PCAD− cell population with established roles in hair follicle development are listed. See appendix for raw values.

MORPHOGENS/SIGNALING		TRANSCRIPTION FACTORS	
Bmp2	Botchkarev et al., 1999	Cutl1	Ellis et al., 2001
Bmp4	Botchkarev et al., 1999	Gli1	St-Jacques et al., 1998
Dkk3		Hoxc13	Godwin & Capecchi, 1998
Dkk4		Nmyc1	Mill et al., 2005
Edar	Laurikkala et al., 2002	Prdm1	Horsley et al., 2006
Fgfr1	Peters et al., 1992	Sox9	Vidal et al., 2005
Fzd7	Reddy et al., 2004	Trps1	Malik et al., 2002
Hhip		Vdr	Li/Yoshizawa et al., 1997
Inhbb			
Ptch2	St-Jacques et al., 1998	Bnc1	Weiner & Green, 1998
Pdgfa	Karlsson et al., 1999	Bnc2	Romano et al., 2004
Pdgfrl		Egr2	Gambardella et al., 2000
Sgk		Myb	Ess et al., 1999
Shh	St-Jacques et al., 1998	Sox13	Roose et al., 1998
Tgfa	Luetteke/Mann et al., 1993	Tbx1	Zoupa et al., 2006
Tgfb2	Foitzik et al., 1999		
Tgfb3	Foitzik et al., 1999		
Wnt5a	Reddy et al., 2001		
Wif1			

Indicating active sonic hedgehog signaling in hair placodes, Shh ligand and its downstream transcriptional targets Ptch2, Gli1, and Hhip were expressed in the PCAD+ cells. However, Ptch2 and Hhip are also negative regulators of Shh signaling, suggesting that feedback mechanisms might exist to restrict the level, location, and timing of Shh signaling during hair morphogenesis.

Several members of the transforming growth factor-β (Tgf-β) family of signaling molecules were also preferentially expressed in the PCAD+ hair progenitor cells. Among the three Tgf-β isoforms, only Tgf-β2 has been demonstrated to regulate proliferation in hair germs and mice lacking *Tgf-β2* have fewer follicles and a delay in development (Foitzik et al., 1999; Jamora et al., 2005). This block in morphogenesis at the germ stage, similar to the *Shh* null, could also be secondary to defects in the dermal condensate since Tgf-β2 is sufficient to induce dermal condensations during feather bud development (Ting-Berreth and Chuong, 1996). Related family members Bmp2 and Bmp4 are also known to be expressed in the hair placodes, but unlike Tgf-β2, inhibition of their activity by Noggin is essential for proper hair morphogenesis (Botchkarev et al., 1999; Jamora et al., 2003). Inhbb is a subunit of the dimeric activins and inhibins. Loss of *Inhbb* does not affect development, but *Inhba* null mice have whisker and tooth defects (Schrewe et al., 1994; Matzuk et al., 1995).

Another positive regulator of hair morphogenesis, ectodysplasin receptor Edar, was upregulated in the PCAD+ cells. A member of the tumor necrosis factor receptor family, Edar is mutated in humans with autosomal hypohidrotic ectodermal dysplasia who present with decreased hair follicles and abnormal teeth and sweat glands. A similar phenotype is manifested in X-linked anhidrotic ectodermal dysplasia where mutations are found in the Edar ligand, Eda. Identical phenotypes also exist in the corresponding Edar and Eda mouse mutants, *downless* and *tabby*, which lack particular hair follicle types and exhibit tooth and sweat gland defects (Headon and Overbeek, 1999; Laurikkala et al., 2002). Components downstream of Edar, particularly the NF-κB pathway, have also been identified to affect the development of ectodermal appendages (Botchkarev and Fessing, 2005; Schmidt-Ullrich, et al., 2006).

The PCAD+ hair progenitor genes also contained components of tyrosine kinase receptor signaling pathways. Transforming growth factor-α (Tgf-α) signals through the receptor Egfr to mediate proliferation and survival via activation of the Mapk or Akt pathway. In the hair follicle, Tgf-α may function in regulating orientation and shape because the Tgf-α mutation in the *waved-1* mouse is characterized by curly whiskers and a wavy hair coat (Luetteke et al., 1993; Mann et al., 1993). Similarly, loss of *Fgfr2-IIIb*, a fibroblast growth factor receptor also known as keratinocyte growth factor receptor, results not only in fewer but also

misaligned hair follicles (Li et al., 2001; Petiot et al., 2003). Fgfr2 is expressed throughout the basal layer of the epidermis during development, but a role for Fgfr1 found to be upregulated in the PCAD+ hair progenitors and the underlying dermal condensates remains to be established (Peters et al., 1992). A function for Sgk1, an intracellular kinase similar to Akt, in hair morphogenesis is also unknown, but *Sgk3* knockout mice display abnormal hair structures possibly due to reduced proliferation of hair progenitor cells and subsequently a shorter hair cycle (Alonso et al., 2005). Misshapen and sparse hair along with reduced proliferation is also seen in *Pdgfa* null mice (Karlsson et al., 1999), which signals through the platelet-derived growth factor receptor tyrosine kinase Pdgfr.

Transcription factors associated with genetic hair disorders were also differentially expressed in the PCAD+ hair progenitor cells. Trps1 is mutated patients with trichorhinophalangeal syndrome, a dominantly inherited disorder characterized by sparse scalp hair and craniofacial abnormalities (Momeni et al., 2000). Mutant mice lacking the Gata domain of Trps1 display similar facial features, no whisker follicles, and reduced pelage hair follicles (Malik et al., 2002). Vitamin D receptor (Vdr) mutations cause vitamin D-dependent rickets type II. Along with hypocalcemia, hyperparathyroidism, osteomalacia, and rickets, some patients exhibit alopecia. In mouse *Vdr* mutants, hair loss after the initial morphogenetic hair cycle is completely penetrant (Yoshizawa et al., 1997;

Li et al., 1997). Unlike the metabolic disorders, alopecia is not found in vitamin D deficiency, suggesting that the effects of Vdr within the hair follicle are ligand independent (Sakai et al., 2001; Skorija et al., 2005). As a nuclear hormone receptor, Vdr heterodimerizes with other nuclear receptors such as retinoid X receptor (Rxr) and the corepressor hairless (Hr) on target genes (Hsieh et al., 2003). Interestingly, inactivation Rxr-α and Hr phenocopy loss of Vdr, histologically developing utricles and dermal cysts in lieu of initiating postnatal hair cycles (Li et al., 2001; Zarach et al., 2004).

Although not implicated in human disease, mutations in *Hoxc13* and *Cutl1* also cause postnatal hair follicle defects. Hoxc13 is strongly expressed in the hair shaft and mutant mice lack external hairs attributable to brittle hair follicles (Godwin and Capecchi, 1998). Reflecting its expression pattern in the inner root sheath progenitors, Cutl1 deficient hair follicles are structurally abnormal due to diminished inner root sheath differentiation (Ellis et al., 2001). Since the hair follicle defects in these mutants are manifested postnatally, the expression of these genes has not been analyzed in embryonic skin during hair morphogenesis.

Other transcription factors of the PCAD+ cell population have been demonstrated to be expressed in the hair placode during morphogenesis. Sox9 is activated in the epithelium upon hair induction and its expression persists throughout the outer root sheath as development proceeds. Mice with disrupted

Sox9 also exhibit hair fragility because of defects in the outer root sheath which acquire more epidermal characteristics. Furthermore, *Sox9* null hair follicles lack expression of several bulge markers, suggesting a role in maintaining the stem cell compartment (Vidal et al., 2005). N-myc is also induced in the hair placode, coinciding with Shh expression (Mill et al., 2005). A functional role for N-myc within early hair progenitors, as well as its intriguing inverse correlation to c-Myc's preferential expression in the interfollicular epidermis, awaits further investigation. Similarly, expression of an assortment of additional transcription factors enriched in the PCAD+ cells have already been described in the developing hair follicle, but they have not been directly implicated in specifying hair progenitor cell fates, including basonuclin, Egr2/Krox20, c-Myb, Sox13, and Tbx1 (Weiner and Green, 1998; Gambardella et al., 2000; Ess et al., 1999; Roose et al., 1998; Zoupa et al., 2006). Although genetic mouse mutants have been developed for *Krox20* (Schneider-Maunoury et al., 1993; Swiatek and Gridley, 1993), *c-Myb* (Mucenski et al., 1991), and *Tbx1* (Lindsay et al., 2001; Merscher et al., 2001; Jerome and Papaioannou, 2001), their embryonic or perinatal lethality has precluded any analysis of hair morphogenesis.

Recently, Prdm1/Blimp1 was determined using conditional gene targeting to regulate the development of sebaceous glands, another lineage within the hair follicle. Initially found to be expressed in the differentiated epidermis, inner root

sheath, and dermal papilla (Chang et al., 2002), Blimp1 is also expressed in a progenitor population that gives rise to mature sebocytes (Horsley et al., 2006). Since germline loss of *Blimp1* is embryonic lethal before hair morphogenesis is induced (Vincent et al., 2005), utilizing conditional alleles to generate tissue-specific mutants was essential in this case to evaluate the function of genes expressed in the hair follicle.

Comparisons with other cell populations

The presence of physiologically significant genes within the PCAD– interfollicular and PCAD+ hair progenitor cell populations validated the functional importance of the differentially expressed genes in regulating epidermal cell fates. To gain further insights into the attributes of these cells, comparisons were made to the "molecular signatures" of other cell populations from mature hair follicles and epidermis (Rendl et al, 2005 and unpublished data). Approximately 40% of the 1394 differentially expressed embryonic genes were in common with either the interfollicular epidermis, outer root sheath, or matrix signature genes (Figure 2.9). Notably, the PCAD– genes composed of over 96% of the overlap with the interfollicular epidermis whereas the PCAD+ genes composed of around 84% and 76% of the overlap with the outer root sheath and matrix, respectively. Thus, the degree of overlap revealed similarities of the embryonic cell populations to

postnatal hair follicle compartments and further confirmed their intrinsic differences. This comparative analysis was also extended to a transcriptional profile of the postnatal hair follicle bulge (Blanpain et al., 2004). Of the approximately 36% shared genes in the hair germ, nearly 75% exhibited a similar

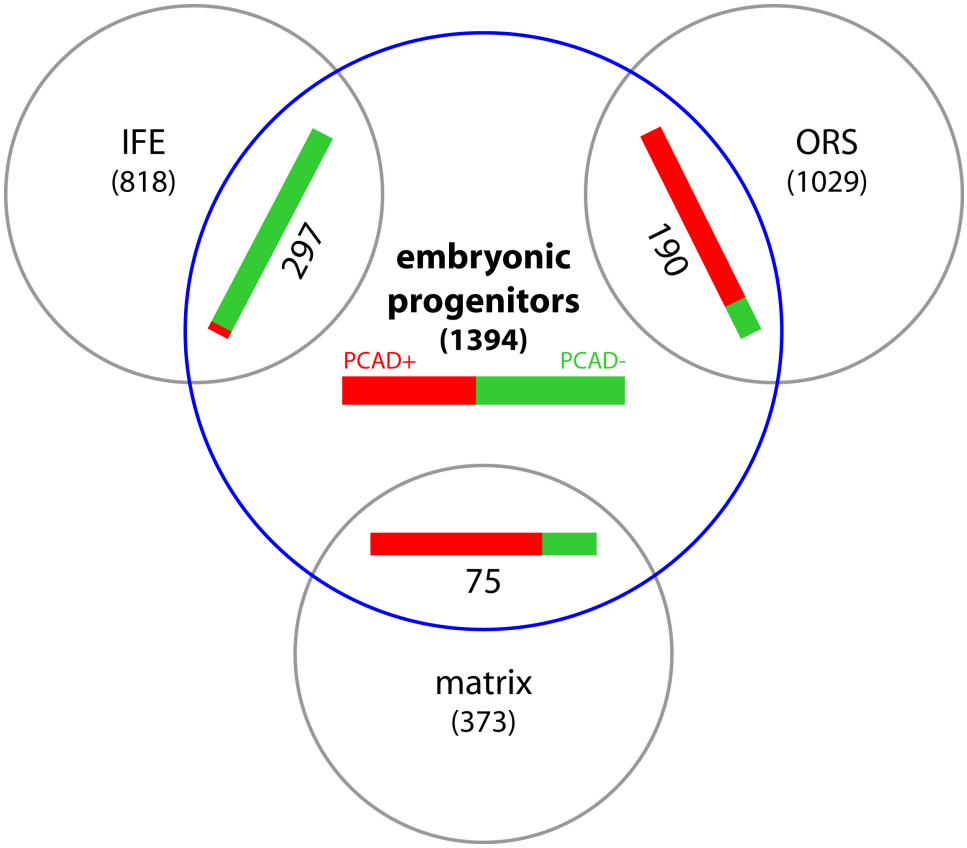

Figure 2.9 Comparisons to other epithelial cell lineages. The differentially expressed genes in the embryonic PCAD+ and PCAD– cell populations were compared to the "molecular signatures" of the interfollicular epidermis (IFE), outer root sheath (ORS), and matrix isolated from postnatal day 5 skin (Rendl et al., 2005 and unpublished data). Of the genes overlapping with each epithelial cell lineage, the proportion represented by the PCAD+ and PCAD– cell populations are color-coded in red and green, respectively. Values in parentheses represent the total number of genes in each set.

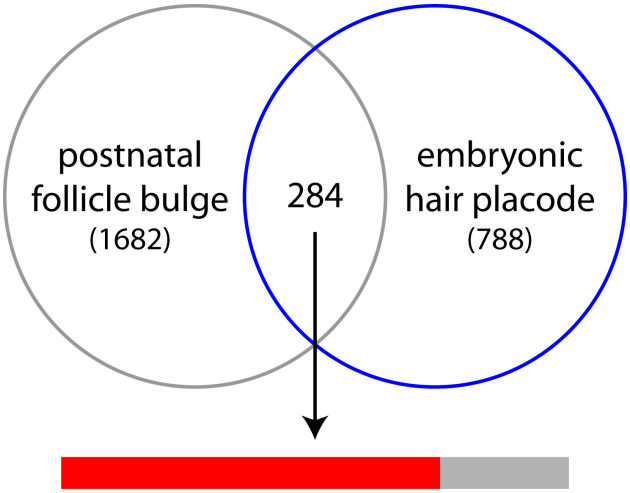

Figure 2.10 Comparison to the postnatal hair follicle bulge. The differentially expressed genes in the embryonic hair progenitors were compared to the differentially expressed genes in the postnatal hair follicle bulge during anagen (Blanpain et al., 2004). Of the genes in common, the proportion of genes which showed the same trend in expression (up or down in the hair germ and bulge relative to their respective reference) is represented in red. Values in parentheses represent the total number of genes in each set.

differential expression pattern in the bulge (Figure 2.10), suggesting that the embryonic hair progenitors exhibit molecular and thus functional properties similar to those of adult stem cells.

Given the importance of gene regulation in determining cell lineages not only in skin but throughout development, a list of all transcription factors differentially expressed in the PCAD+ and PCAD– cell populations was generated (Table 2.5). A strong correlation also existed with these genes and the bulge stem cells. Since a smaller array was used to profile the bulge, the overlap is likely an

under-representation of the actual similarities between the embryonic hair progenitors and the adult stem cells.

Table 2.5 Differentially expressed transcription factors. All regulators of gene expression upregulated ≥2-fold in either the PCAD+ (hair progenitors) or PCAD− (interfollicular basal keratinocytes) relative to the other are listed. Highlighted in red are genes upregulated and in blue are genes downregulated within the bulge of postnatal hair follicles compared against the total skin epithelial cell population. The gene overlap is likely underrepresented since a smaller array was used to profile the bulge stem cells (Blanpain et al., 2004). See appendix for raw values.

PCAD+			PCAD−		
Bach2	Id4	Runx1	Aff1	Mafb	Sox6
Bcl6	Isl1	Runx2	Ankrd22	Mef2c	Sox7
Bnc1	Lhx2	Scmh1	Ascl2	Mllt2h	Stat1
Bnc2	Lbh	Six4	Ell2	Mrg1	Tcfap2e
Cutl1	Lass4	Sox2	Esr1	Msl2	Tcfcp2l1
Dach1	Mitf	Sox9	Foxn1	Myc	
Dlx2	Myb	Sox13	Ghr	Nfia	
Egr2	Nap1l5	Sox21	Grhl1	Nr2f2	
Egr3	Nfatc1	Sp5	Grhl3	Nrip3	
Foxc1	Nfe2l3	Tbx1	Hoxa1	Ovol1	
Gli1	Nmyc1	Tcf7	Irx3	Pou3f1	
Gtf2ird1	Nr4a1	Tcfl5	Klf3	Ror1	
Hmga2	Prdm1	Trps1	Klf4	Rora	
Hoxc13	Prdm5	Vdr	Klf5	Satb1	
Id2	Rai14	Zfp566	Klf12	Spib	

Label retaining cells during hair morphogenesis

The molecular similarities of the embryonic hair progenitors to bulge stem cells suggest that they might also share functional attributes. One of more salient features of bulge stem cells is their relative quiescence, thereby gaining an ability to retain nucleotide label (Cotsarelis et al., 1990; Morris and Potten, 1999). However these studies labeled mice throughout the neonatal period as the hair follicle fully develops into an anagen follicle and focused on periods after the initial morphogenetic hair cycle. To determine if label retaining cells exist within hair follicles during morphogenesis, embryos were pulsed with the nucleotide analog bromodeoxyuridine (BrdU) at days E16.5 and E17.5 when the majority of hair induction occurs, and chased for various lengths of time (Figure 2.11). After two days of chase, nearly every cell throughout the epidermal basal layer including early hair germs retained BrdU, confirming the completeness of labeling. As hair morphogenesis was followed during subsequent days, the BrdU label diluted out particularly in the highly proliferative matrix cells. However, a group of cells located in the upper outer root sheath beneath the developing sebaceous gland characteristically retained BrdU. Seen in almost every hair follicle, these label retaining cells persisted throughout the initial hair cycle and eventually resided in the adult hair follicle bulge, expressing the specific marker CD34 (Figure 2.11F). Thus, this location within the upper outer root sheath of

developing hair follicles can be considered the presumptive bulge and likely originates from the embryonic hair placode.

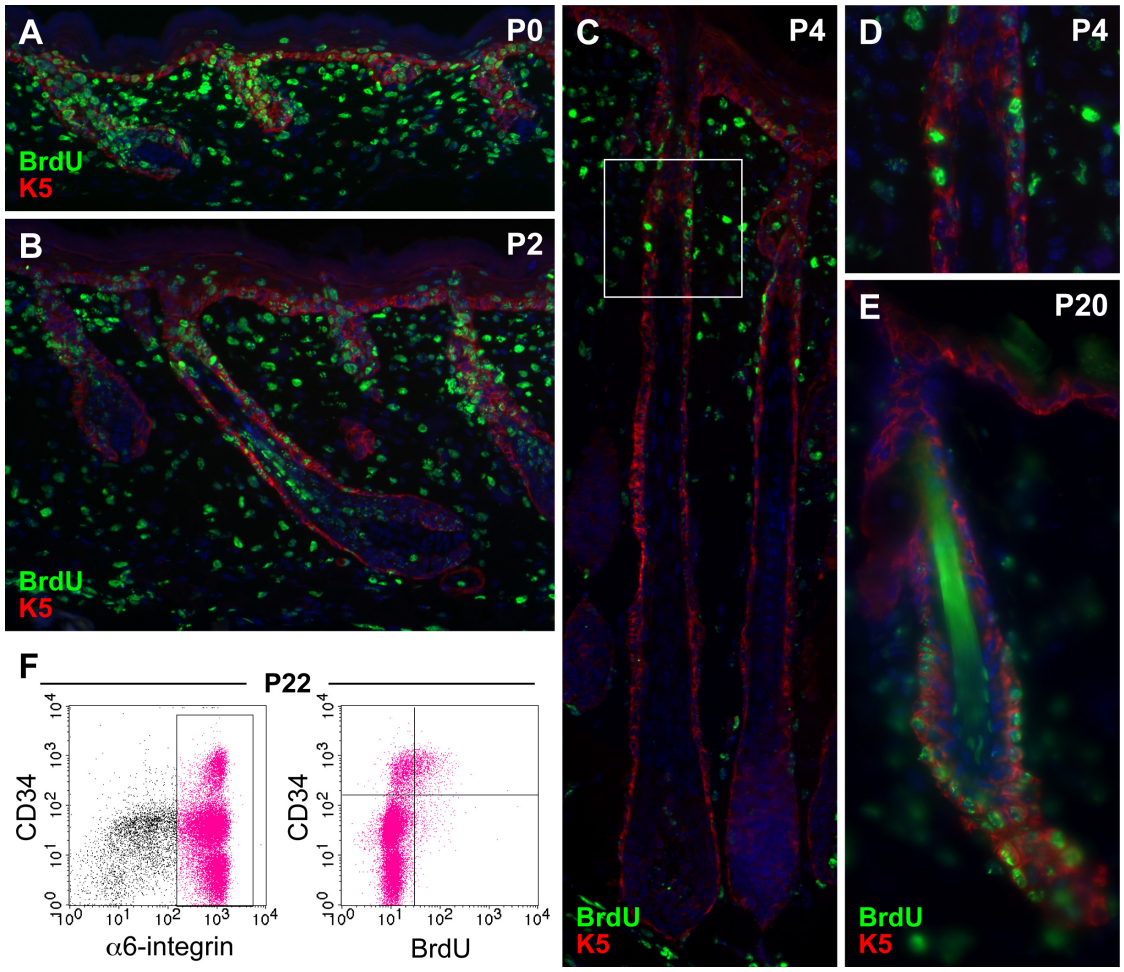

Figure 2.11 Label retaining cells during hair follicle morphogenesis. Pregnant dams were injected with BrdU twice a day between E16.5 and E17.5, and their pups were analyzed for BrdU incorporation at indicated ages. **(A-E)** Skin sections immunostained for BrdU show retention of the BrdU label in the upper outer root sheath beneath the sebaceous gland, which remains at the base of the postnatal telogen hair follicle (E). Boxed area in (C) is magnified in (D). **(F)** Epidermal cells were isolated from back skins of BrdU pulse-chased mice and analyzed by flow cytometry. BrdU positive cells express CD34 and α6-integrin, markers of adult bulge stem cells (Trempus et al., 2003; Blanpain et al., 2004). Images are color-coded according to the secondary antibodies used.

Discussion

Hair follicle morphogenesis requires the interplay of several signaling pathways, but the molecular mechanisms that coordinate these signals into a transcriptional program of lineage commitment and differentiation have remained elusive. To investigate changes that occur as hair follicles are induced from the epithelium, a strategy was developed to isolate and profile the gene expression of hair placodes and germs. By comparing these cells to the interfollicular epidermis and other cell populations, new insights were revealed into the characteristics of embryonic hair progenitors.

Justification of strategy to isolate hair progenitors

Although hair follicle induction occurs over several days during embryogenesis, utilizing differential P-cadherin expression at E17.5 to isolate early hair progenitor cells has distinct advantages. Although the hair follicles at E17.5 are heterogeneous in their morphological development, dispase treatment separates early hair germs and interfollicular epidermis from more mature follicles, which have grown down and remain stuck within the dermis. Since this enzymatic process is difficult to manipulate at earlier embryonic ages, a cell suspension derived from total skin (epidermis and dermis) prior to E17.5 would

include these more developed follicles, which also express P-cadherin, and hence be more heterogeneous. The uniform expression of P-cadherin throughout the basal layer of the epidermis at even earlier ages when hair specification first begins precludes using this marker to selectively isolate hair progenitors. Also considering that the majority of hair follicle induction occurs around E17.5, skin from this age is the most feasible to specifically isolate early hair progenitor cells from interfollicular epidermis.

Substantiating this approach is the enriched expression of various hair placode markers in the sorted PCAD+ cells relative to the PCAD– cells, which is further supported by the microarray analysis. In particular, a number of genes differentially expressed in the two cell populations are associated with diseases of either the hair follicle or epidermis. Implicated in diverse cellular processes, these documented genes expand our current understanding of how ectoderm cells become committed to a hair lineage and undergo follicular morphogenesis. Furthermore, they lend biological significance to the expression profiles and point to possible functions of the many uncharacterized genes in hair morphogenesis.

Insights into hair follicle morphogenesis

Upholding the concept as a signal integrator, the PCAD+ hair placode simultaneously expresses several critical morphogens, including components of

the Wnt, Shh, Bmp, Tgf-β, Edar and receptor tyrosine kinase signaling pathways. Disruption of each these pathways in genetically modified or mutant mice has elucidated their essential roles in various aspects of hair follicle morphogenesis.

Initiation of hair follicle morphogenesis requires Wnt signaling, but the origin and specific ligand necessary to direct activation remains elusive. Confirming a previous study on Wnt gene expression in hair placodes, *Wnt10b* is upregulated in isolated PCAD+ cells by RT-PCR (Reddy et al., 2001). However this difference is not reflected in the microarray due to probe design. This technical issue aside, other Wnt ligands are preferentially expressed in either the PCAD+ hair progenitors (*Wnt5a*) or the PCAD– interfollicular epidermis (*Wnt3a, -4, -10a, -16*). Although not all of these ligands may act through the canonical signaling pathway to stabilize β-catenin, the broad expression of Wnts suggests the need to spatially restrict their activity to initiate hair follicle induction. Interestingly, only the PCAD+ cells differentially express several Wnt inhibitory genes. Although expression of these inhibitory factors may indicate feedback mechanisms to regulate the level and timing of Wnt activation within the hair placode, they could also as secreted inhibitors laterally restrict the extent of Wnt activity, thereby localizing it to sites of hair follicle induction.

Lateral inhibition may also be the role of Bmp signaling in specifying the hair cell lineage and regulating placode size. Although *Bmp2* and *Bmp4* are highly

expressed in the PCAD+ hair placode, their local inhibition by Noggin derived from the dermal condensates is necessary for proper hair follicle induction (Botchkarev et al., 1999; Jamora et al., 2003). In contrast, excess Bmp signaling suppresses epidermal appendage development in a variety of systems (Botchkarev et al., 1999; Jung et al., 1998; Noramly and Morgan, 1998). Thus, Bmps could prevent surrounding cells from adopting a hair follicle fate, and by establishing a morphogen gradient also regulate the spacing of hair placodes from each other.

Other positive regulators of hair follicle induction are strongly expressed in the PCAD+ hair progenitors. Edar is necessary for guard hair induction and also regulates aspects of zigzag hairs (Laurikkala et al., 2002). Tgf-β2 is necessary for induction and subsequent growth of a majority of hair follicles (Foitzik et al., 1999). Since absence of either of these signals does not completely abrogate hair follicle induction, specifying hair placodes from embryonic ectoderm likely results from a competition between activators and repressors in which negative regulators must be counteracted for hair morphogenesis to initiate and proceed.

The PCAD+ hair placode also expresses several signals required for morphogenetic events downstream of induction. Not necessary for specifying hair follicles, *Shh* is expressed in hair placodes to promote epidermal proliferation and to organize the underlying mesenchyme into dermal condensates upon induction (St-Jacques et al., 1998; Chiang et al., 1999). Pdgfa also promotes the

development of the dermal condensate (Karlsson et al., 1999). Both Shh and Pdgfa may also have a role in determining the polarity and shape of the hair placode, because grafted skin from mutant mice null for *Shh* or *Pdgfa* have abnormally angled hair follicles. Although this could be attributable to defects in the dermal papilla, the lack of overall orientation in *Shh* null hair germs and the asymmetric localization of *Shh* expression in mature hair follicles suggest that these signals may govern the normal anterior to posterior direction of hair growth.

Regulation of polarity and orientation within the hair placode is further supported by the expression of components of receptor tyrosine kinase signaling pathways in the PCAD+ cells. Although the curly and misshapen hair phenotypes of mutant mice with defects in genes such as *Tgf-α* are manifested in adult follicles, the expression of these factors in hair placodes suggests that polarity cues are received and set up early in morphogenesis. Since receptor tyrosine kinases are better known in growth and cell survival programs, links between proliferation and cell polarity in hair morphogenesis are intriguing, but remain to be determined.

Changes in polarity and shape during morphogenesis is also dependent on rearrangements of cell adhesion and cytoskeletal dynamics (Jamora and Fuchs, 2002). Evidence of these changes occurring in the hair placode is found in the downregulation of intercellular and substratum adhesion molecules in the PCAD+

cells relative to the PCAD– interfollicular basal keratinocytes. Various components adherens junctions, desmosomes, tight junctions, and hemidesmosomes are all repressed in the hair placode. This breakdown in cell-cell and cell-matrix contacts probably allows hair progenitors to alter their shape and motility to transform into a three-dimensional structure that buds from a sheet of epithelial cells (Hogan, 1999). Keratinocytes with mutations in these components often display weakened adhesion and increased migration upon culture (Tasanen et al., 2004; Yin et al., 2005; Matter et al., 2005). On the other hand, forced expression of E-cadherin, normally downregulated upon hair follicle induction, blocks invagination and hair follicle formation (Jamora et al., 2003), but complete loss of adhesion also prevents hair morphogenesis (Vasioukhin et al., 2001). Thus, a proper balance of adhesion and motility is necessary to modulate the changes in polarity and shape during morphogenesis. Since regulation of adhesion and cytoskeletal dynamics typically occurs at the post-transcriptional level, the observation of transcriptional differences in these molecules within the hair placode suggest that acquisition of a hair cell fate is accompanied by a different set of structural components which can facilitate the unique morphological properties of hair follicles.

The best illustration that the hair placode adopts a distinct set of molecules upon induction is the differential expression of transcription factors which regulate

the defined genetic program for subsequent morphogenesis. Specification of a hair cell lineage from the embryonic ectoderm entails a repression of epidermal differentiation regulators and an activation of regulators associated with hair follicle development. Among the transcription factors expressed in the hair placode, several are implicated in hair follicle disorders. Unexpectedly, these disorders are manifested later in development as specific lineages of the hair follicle are affected: outer root sheath (*Sox9*); inner root sheath (*Cutl1*); hair shaft (*Hoxc13*); sebaceous gland (*Prdm1*). These lineage specific differentiation defects reflect the postnatal expression pattern of these genes, but their expression in the PCAD+ embryonic hair placode indicates that lineage determination may occur earlier in morphogenesis. Two possibilities can be considered as to how these lineage specific regulators are simultaneously expressed in the hair placode. Consisting of early multipotent progenitor cells capable of differentiating into all the lineages of the hair follicle, the hair placode could co-express these critical factors of more committed downstream progenitors and then modulate their expression for specific follicular compartments to develop. Alternatively, the hair placode may be a heterogeneous population of progenitor cells already committed to different lineages of the hair follicle, which become partitioned as specific follicular compartments develop. Analysis of the expression pattern of these regulators at the cellular level and how they are controlled by environmental cues

during hair follicle induction and subsequent morphogenesis will be necessary to distinguish between these possibilities. Nonetheless, the defined functions of these genes in determining cell fates will guide studies into the many uncharacterized transcription factors differentially expressed in the hair placode.

Insights into hair follicle stem cells

In line with the multi-lineage potential of the hair placode, the gene expression profile of PCAD+ cells exhibits a strong similarity to the "molecular signatures" of both the outer root sheath and hair matrix. Even more striking is the molecular resemblance between the embryonic hair placode and the adult bulge stem cells, indicating that they might also share functional attributes. Both the hair placode and bulge stem cells are undifferentiated, but possess the potential to differentiate into the diverse cell types of the entire hair follicle. In theory, the hair placode also has self-renewal character by giving rise to the bulge which supplies cells for multiple rounds of hair growth throughout life. However, whether the embryonic hair placode is composed of stem cells which persist as adult bulge stem cells is presently unknown.

The presence of label retaining cells in a region of the upper outer root sheath of developing hair follicles is compelling evidence that a stem cell compartment exists prior to completion of the initial morphogenetic hair cycle.

Precisely located where the future bulge will develop, these label retaining cells remain as CD34 positive stem cells in the adult hair follicle. In contrast to other studies which labeled the developing follicle once this presumptive bulge formed a few days postnatal, embryonic hair placodes and germs were pulsed and chased. This allowed the fate of labeled progenitor cells to be traced during morphogenesis from hair follicle induction to the presumptive bulge.

More functional studies are necessary to demonstrate that initiation of hair follicle morphogenesis entails the specification of stem cells, but the persistence of label retaining cells clearly suggests that the hair placode contains slow cycling cells, a hallmark of adult bulge stem cells. Identifying the hair placode as the embryonic origin of the bulge is also supported by the molecular similarities between them. Further characterization into these shared genes will shed light into the mechanisms by which this important somatic stem cell niche is established and regulated during development.

Materials and Methods

Mice

The following mice were generous gifts: P-cadherin$^{-/-}$ (G. Radice, University of Pennsylvania); β-catenin$^{fl/fl}$ (R. Kemler, Max Plank, Freiburg).

TOPGAL and K14-ActinGFP were previously generated (DasGupta and Fuchs, 1999; Vaezi et al., 2002). For timed pregnancies, the morning of a vaginal plug was considered embryonic day E0.5.

Histology and immunofluorescence

Tissues were embedded in OCT (Tissue-Tek) and immediately frozen on dry ice. Sections of 10μm were cut with a cryostat onto glass slides, fixed in 4% paraformaldehyde for 8 minutes, and subjected to immunofluorescence microscopy. When applicable, the MOM Basic Kit (Vector Labs) was used to prevent non-specific binding of mouse monoclonal antibodies. Otherwise, stainings were performed in phosphate buffered saline (PBS) with 0.1% Triton X-100, 2.5% normal donkey serum, and 2.5% normal goat serum. BrdU unmasking involved treatment with 1M HCl at 37°C for 45 minutes prior to blocking. Primary antibodies were incubated overnight at 4°C and secondary antibodies at room temperature for 1 hour. Slides were washed after antibody incubations with PBS for 5 minutes, three times. Antibodies and dilutions used: P-cadherin (rat, 1:100; M. Takeichi, Riken, Kobe); α6-integrin (rat, 1:100; Pharmingen); β4-integrin (rat, 1:100; Pharmingen); K5 (rabbit, 1:500; Fuchs lab); K1 (rabbit, 1:500; Fuchs lab); BrdU (rat, 1:500; Abcam); FITC (1:100; Jackson) or Alexa594 (1:1000; Molecular Probes) conjugated secondary antibodies. Nuclei

were stained with 4'6'-diamidino-2-phenylindole (DAPI; 1:10000) in a single wash step after staining. Slides were mounted with antifade. Imaging was performed using Zeiss Axioskop and Axiophot microscopes equipped with Spot RT (Diagnostic Instruments) and Axiocam (Zeiss) digital cameras, respectively.

Isolation of hair progenitors and flow cytometry

Back skins from E17.5 K14-ActinGFP transgenic or other genetic embryos were dissected using the shoulders and hips as landmarks, and treated overnight with dispase (Gibco, 0.4mg/mL) at 4°C, which selectively removed the epidermis, hair placodes, and hair germs from the rest of the skin upon mechanical manipulation. The epidermal fraction was treated with versene, a solution of 0.5mM ethylenediaminetetraacetic acid (EDTA) in phosphate buffered saline (PBS) with 0.1% glucose, and cell suspensions were neutralized with culture media (E high calcium) and strained (40μM pores; BD Biosciences). Single cells were washed once and resuspended in PBS containing $CaCl_2$ and $MgCl_2$ (Gibco) with 5% fetal bovine serum at a concentration of 10^7 cells/mL. Approximately 10^6 cells can be obtained per embryonic back skin and typically between 5-15 embryos were used per isolation and sort. Cells were incubated with primary antibodies coupled to biotin for 30 minutes on ice, and after washing once with PBS, cells were stained with streptavidin and antibodies directly conjugated to

specific fluorophores for 30 minutes on ice. Cells were washed once in PBS and resuspended in 300ng/mL propidium iodide for dead cell exclusion. All centrifugation steps were performed at 300xg for 5 minutes at 4°C. Cell sorts were performed on a FACSVantage SE system equipped with FACS DiVa software (BD Biosciences). Epidermal cells were gated for single events and viability, then sorted according to their expression of K14-ActinGFP, α6-integrin, and P-cadherin. Typically after gating for GFP and α6-integrin expression, the brightest ~5% P-cadherin positive and negative cells were sorted as PCAD+ and PCAD– respectively. Cells collected for RNA were directly sorted into lysis buffer, otherwise cells were collected into PBS with 5% serum. Purity of sorted cells was determined by post-sort FACS analysis and typically exceeded 95%. Flow cytometry analysis was performed on a FACSort equipped with CellQuest (BD Biosciences). Antibodies and dilutions used for FACS: P-cadherin conjugated to biotin (1:100, Fuchs lab); α6-integrin coupled to APC or PE (1:100, Pharmingen); β4-integrin (1:100, Pharmingen) coupled to APC; CD34 conjugated to biotin (1:50, Pharmingen); streptavidin-PE (1:1000, Pharmingen); streptavidin-APC (1:200, Pharmingen). Cytospin analysis was performed with a Cytospin4 unit (Thermo/Shandon) onto glass slides, and stained as described above.

β-galactosidase activity assay

FACS sorted cells from TOPGAL/K14-ActinGFP double transgenic and K14-ActinGFP single transgenic E17.5 embryos were counted and equal numbers of cells were analyzed using Galacto-Light (Applied Biosystems) per manufacturer's directions. Between 15,000-20,000 cells were lysed in 20μL and the relative activity of β-galactosidase was measured against wild-type PCAD–cells.

RNA isolation and semi-quantitative RT-PCR

Total RNA from FACS sorted cells was isolated using the Absolutely RNA Microprep kit (Stratagene) and quantified using Ribogreen (Molecular Probes). Approximately 10^5 sorted cells yielded 1μg of total RNA. Normalized RNA quantities were reverse transcribed with Superscript III using oligo-dT primers (Invitrogen). Typically, 30ng of total RNA was reverse transcribed into a 20μL volume of cDNA, which was then diluted 12-fold. One microliter of this working stock was used as template for PCR reactions: 2.5μL of 10X PCR buffer with $MgCl_2$, 0.5μL of 10mM dNTPs, 0.25μL of AmpliTaq DNA polymerase (Applied Biosystems), 0.5μL each of forward and reverse primers at 20mM, 1μL of template DNA, and 19.75μL of H_2O. PCR amplification of selected genes of interest was performed using primers designed to produce a product spanning

exon/intron boundaries. Primers were designed using PrimerSelect of Lasergene (DNAStar) to work at the following settings: initial denaturing at 94°C for 3 minutes; 27-36 cycles of 20 seconds at 94°C denaturing, 30 seconds at 60°C annealing, and 45 seconds at 72°C extension. Primers used:

gapdh: 5'-cgtagacaaaatggtgaaggtcgg-3'; 5'-aagcagttggtggtgcaggatg-3'
pcad: 5'-tgccatggtcagacaaagaaagat-3'; 5'-gcttgggtgcctgagaacgaa-3'
shh: 5'-aaagcgcacggaaggagactt-3'; 5'-acccccatggagcaggtttt-3'
bmp2: 5'-gaagtggcccatttagaggagaac-3'; 5'-cccggaggtgccacgat-3'
bmp4: 5'-agtccagctatagggaagcagtttg-3'; 5'-tccactggctgatcacctcaac-3'
wnt10b: 5'-tgccctctgtccttttccaacc-3'; 5'-tgtaaatgaaggtgagcctcgc-3'
msx2: 5'-tcaagtggccctgtcgcttag-3'; 5'-tatgctgccctcaggcttcag-3'
keratin5: 5'-aacattttggggtctgggtcac-3'; 5'-ggcccacagagactgcttcttt-3'
aqp3: 5'-gctggcccacatgaaacaca-3'; 5'-tcagcccctcccaatgtctatc-3'
cdkn1a: 5'-agcagttgcgccgtgattg-3'; 5'-aggccgaagatggggaagag-3'
c-myb: 5'-aaccctctaggagctcatttgtgg-3'; 5'-ctaagctctattgccccctgaca-3'
cyclinD1: 5'-gctaccgcacaacgcactttcttt-3'; 5'-gcacccccctggctccctactctc-3'
dach1: 5'-gcggcagcacaagttcagagt-3'; 5'-agatggaaagccgggaggtagt-3'
dusp6: 5'-ccccgggtgtcaaaagtgtc-3'; 5'-ccacgaaaatgccgtcagaat-3'
edar: 5'-gtttagaaggcggttgggttttt-3'; 5'-aggggaatcgcagcgtcat-3'
enc1: 5'-ctgcctgctccgcttacaaat-3'; 5'-cccccacccctccttca-3'
fzd7: 5'-tggctcccctcctaatttgtatc-3'; 5'-gctggcattaaaaactgctctgag-3'
gpr49: 5'-actcgcgtgttttgatctcatcc-3'; 5'-ccccttgctaggaggcagtaagt-3'
hoxa1: 5'-tcacccccctaacttagctggtttc-3'; 5'-cattgtgcgacatgcagaagacta-3'
idb4: 5'-gctgagctgcgatggatgg-3'; 5'-ggttggattcacgattgctcttct-3'
klf3: 5'-cacgggtcagacctaaagaatgtg-3'; 5'-agcaggtgagccaggtcaaca-3'
klf4: 5'-caccggccctttcagtgc-3'; 5'-cccccgtttggtacctttagg-3'
lbh: 5'-tggaatagcgggttagaggacag-3'; 5'-cacggcaagaccaagacagataac-3'
msx1: 5'-ctccccagccacctctttga-3'; 5'-tcttggcctctgcatccttagtt-3'
naked1: 5'-tagacctggcggggatagagaa-3'; 5'-agatgggcagagggggagac-3'
n-myc: 5'-ggcgaggcagcagcagtt-3'; 5'-gttcccaggggcatcaaatg-3'
ptch2: 5'-caccctgccccagagttttg-3'; 5'-acccattgcgtcccagtgac-3'
runx1: 5'-gccccaaggcctcctcat-3'; 5'-ccagcggttaggcttcatacg-3'
runx2: 5'-tcggaggaaaggcactgactg-3'; 5'-gaaagcaaatcttgggcaatagc-3'
sox2: 5'-ctcggcagcctgattccaata-3'; 5-tactggcaagaccgttttcgtg-3'
sox9: 5'-cggcggaggaagtcggtgaagaac-3'; 5'-ggtgggtgcggtgctgctgatg-3'
sox13: 5'-ggtgtgggccaaggatgaacg-3'; 5'-tcccggagactgcaggtattgatg-3'

tcf1: 5'-caccctccccatgccaatac-3'; 5'-gcagccccacagagaaactga-3'
tll: 5'-atgccgaccctccctcaga-3'; 5'-tacgtccccagatcttggaaaagt-3'

Microarray analysis

Two rounds of amplification/labeling of 200ng total RNA was performed to obtain biotinylated cRNA for hybridization onto Affymetrix GeneChip Mouse Genome MOE430 2.0 oligonucleotide microarrays at the Genomics Core Laboratory of Memorial Sloan-Kettering Cancer Center (New York, USA). Two entirely independent samples were used for data analyses. Scanned microarray images were imported into GeneChip Operating Software (GCOS, Affymetrix) to generate signal values and present/absent calls for each probe set using the MAS 5.0 statistical expression algorithm. Assuming equal levels of total signal in each of the hybridizations, arrays were scaled to a target signal of 500 using default analysis parameters. Data files were imported into GeneTraffic 3.8 (Iobion Informatics), and replicate hybridizations were grouped and compared using the Robust Multi-chip Analysis algorithm. Genes represented with probe sets ≥2-fold increased in one population over the other and called present in both replicates were considered significant.

For comparative analysis, the overlap of probe sets from the "molecular signatures" of P5 epidermal cell lineages (Rendl, unpublished data) and from the

adult hair follicle bulge (Blanpain et al., 2004) with the differentially expressed genes in the PCAD+ and PCAD− sorted cells was determined.

BrdU label retaining experiments

Pregnant CD-1 females were intra-peritoneally injected with 50μg/g of 5'-bromo-2'-deoxyuridine (BrdU, Sigma) twice a day for 2 days at E16.5 and E17.5 and analyzed for BrdU incorporation postnatally. Back skins were processed for immunofluorescence as described. For flow cytometry, back skin was dissected and the subcutaneous fat was scraped using a scalpel. After treatment with trypsin plus EDTA (Gibco, 0.25%) at 4°C overnight, the epidermal cells were scraped and neutralized cell suspensions were sequentially strained (70μM, then 40μM pores; BD Biosciences). Single cells were resuspended in PBS with 5% fetal bovine serum and stained with primary and secondary antibodies as described above. BrdU detection was subsequently performed using BrdU Flow Kit (Pharmingen) and analyzed by flow cytometry.

CHAPTER 3
CHARACTERIZATION OF LHX2 IN HAIR FOLLICLES

Multiple signaling pathways converge to initiate hair follicle morphogenesis from embryonic ectoderm and activate bulge stem cells to regenerate the hair follicle. However, the molecular mechanisms that mediate the response to these signals and direct the transcription of effector genes are largely unknown. By isolating and profiling the gene expression of hair placodes and interfollicular epidermis, a number of transcriptional regulators were identified that could orchestrate lineage determination of multipotent skin progenitors. An indication of their functional similarities and possible developmental origin, the adult hair follicle bulge expressed several transcription factors in common with the embryonic hair placode. To explore the possibility that these shared transcription factors govern fundamental characteristics of both embryonic hair progenitors and adult stem cells, I focused on one of these factors, Lhx2.

Lhx2 belongs to the LIM-homeodomain (LIM-HD) family of transcription factors, which regulate patterning and cell specificity during the development of a variety of tissues and organs, particularly the central nervous system (Hobert and Westphal, 2000; Hunter and Rhodes, 2005). Initially cloned in a screen for markers of early B-lymphocyte differentiation, Lhx2 is also expressed in the developing brain, retina, olfactory organs, liver, and limbs (Xu et al., 1993;

Rincon-Limas et al., 1999). Exhibiting a functional role in these tissues, *Lhx2* null mutant embryos lack forebrain structures, are anophthalmic, have no mature olfactory sensory neurons, develop liver fibrosis, and die in utero between E15.5 and E16.5 due to impaired definitive erythropoiesis (Porter et al., 1997; Hirota and Mombaerts, 2004; Kolterud et al., 2004; Wandzioch et al., 2004). On the other hand, forced expression of Lhx2 can immortalize multipotent hematopoietic progenitor cells *in vitro* and is associated with chronic myelogenous leukemia (Pinto do O et al, 1998; –2002; Richter et al., 2003; Wu et al., 1996). Although *Lhx2* null mice have no limb abnormalities, Lhx2 is the mammalian ortholog of Drosophila *apterous*, best known in wing imaginal discs as a selector gene for dorsal identity and in regulating wing outgrowth (Cohen et al., 1992). Lhx2 therefore appears to control the status of progenitor cells in several developmental contexts, particularly during organ expansion, but a possible role for Lhx2 in skin has not been examined.

In this study, I assessed whether Lhx2 can regulate lineage determination in the skin as it does in other tissues. Expressed in embryonic hair progenitors upon induction of hair morphogenesis, Lhx2 became restricted to the stem cell compartment as hair follicle development progressed. By analyzing its expression in genetic mutant embryos defective in aspects of hair morphogenesis, Lhx2 was positioned downstream of signals necessary to specify hair follicle stem cells, but

upstream from signals required to drive stem cells to terminally differentiate. Finally using gain- and loss-of-function studies, Lhx2 was demonstrated to maintain stem cells in a undifferentiated, quiescent state.

Results

Lhx2 expression during hair morphogenesis

Lhx2 was upregulated 18-fold in the PCAD+ population relative to the PCAD– population, as determined by microarray analysis. Semi-quantitative RT-PCR of an independent sorted sample and *in situ* hybridization of E17.5 embryos confirmed this marked differential expression in early hair progenitors (Figure

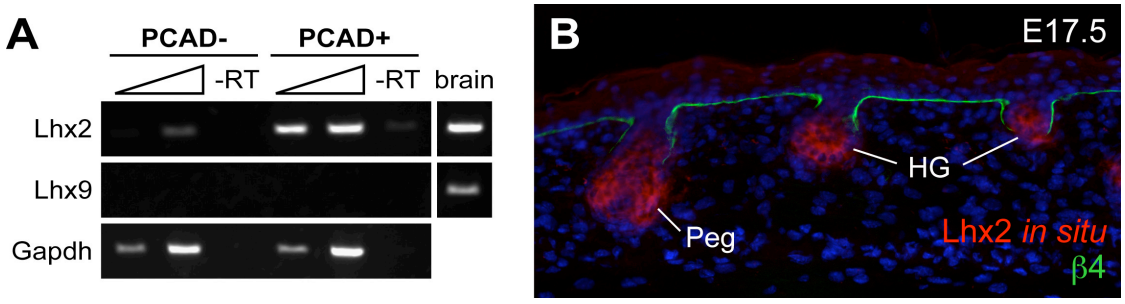

Figure 3.1 Differential expression of Lhx2 in embryonic hair progenitors. **(A)** Semi-quantitative RT-PCR on sorted cell populations of an independent sample confirms the up-regulated expression of Lhx2 in the E17.5 PCAD+ hair progenitors. Closely related family member Lhx9 is not expressed in skin. Total brain mRNA was used as a positive control. **(B)** *In situ* hybridization of digoxigenin-labeled *Lhx2* cRNA probe in E17.5 skin verifies the localization of Lhx2 in early developing hair follicles. Lhx2 images were pseudo-colored and overlayed onto an immunofluorescence image of β4-integrin.

3.1). When examined by immunofluorescence, Lhx2 first appeared in early hair placodes, and as morphogenesis progressed, became prominent at the leading front of invaginating hair germs and pegs (Figure 3.2A). As downgrowth neared completion and hair differentiation began, Lhx2 concentrated in the upper outer root sheath at the presumptive site of the developing postnatal follicle stem cell compartment (Figure 3.2A). Concomitantly, expression diminished at the base of the follicle, where highly proliferative matrix cells give rise to the differentiating inner root sheath and hair shaft (Figure 3.2B). In adult hair follicles, Lhx2 concentrated in the bulge, and as the new hair cycle began, Lhx2 extended to the emerging secondary hair germs (Figures 3.2C-D). Based on these patterns, Lhx2 appears to function in specifying embryonic hair follicle progenitor cells that then persist as bulge stem cells in adult follicles. Although the antibody used recognizes both Lhx2 and its closely related family member Lhx9, the latter is not expressed in the skin epithelia as determined by RT-PCR and microarray analysis (Figure 3.1).

Lhx2 expression in genetic mutants

To more precisely define the role of Lhx2 in hair follicle stem cell specification and/or maintenance, its status was examined in various genetic mutant embryos that are defective in different aspects of hair morphogenesis. In

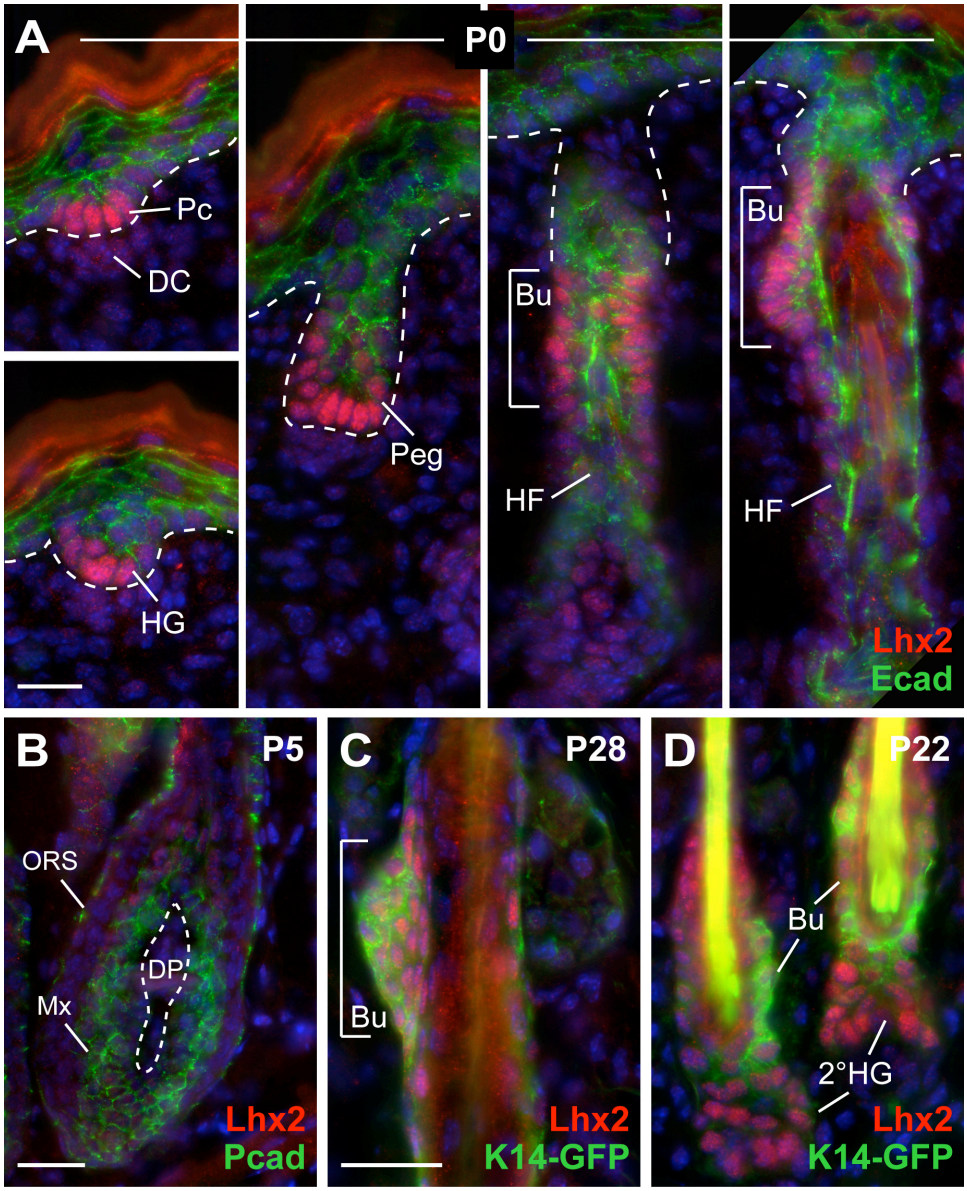

Figure 3.2 Lhx2 expression during hair morphogenesis and in postnatal stem cells. **(A-D)** Back skin sections from mice at indicated ages were stained with antibodies as color-coded and counterstained with DAPI in blue. Upon induction of hair morphogenesis, Lhx2 is expressed in epithelial cells at the leading front of invaginating follicles and in the postnatal bulge compartment, but is diminished in mature proliferative hair progenitors (Mx). Abbreviations: Pc, placode; HG, hair germ; Peg, hair peg; HF, hair follicle; Bu, (presumptive) bulge; ORS, outer root sheath; Mx, matrix; DC, dermal condensate; DP, dermal papilla; 2°HG, secondary hair germ emerging at the start of the postnatal hair cycle. Scale bars, 20μm.

the complete absence of hair follicle induction or bulge maintenance, as reflected in *β-catenin* conditionally null (cKO) skin, Lhx2 was not expressed (Figure 3.3A). In *Shh* knockout embryos where hair follicles are specified but unable to progress beyond the germ stage, Lhx2 expression was dramatically reduced (Figure 3.3B). This positioned Lhx2 downstream of Wnt and Shh, where it could play a role in establishing or expanding the early progenitors necessary for hair follicle morphogenesis.

Bmp signaling is not required for hair follicle induction, even though Bmp ligands and receptors are expressed in embryonic hair germs and in postnatal follicle stem cells. Correspondingly, in *BmpR1a* cKO skin where a Bmp receptor is ablated in the epidermis, Lhx2 was normally expressed in both embryonic hair germs and the presumptive bulge of developing follicles (Figure 3.3C-D). However, Bmp signaling is required for hair differentiation and in the absence of *BmpR1a*, proliferating undifferentiated hair progenitor cells accumulate at the follicle base (Andl et al., 2004; Kobielak et al., 2003). Lhx2 was noticeably enhanced in these follicles, with strong staining throughout the outer root sheath and matrix (Figure 3.3D-E). These cells were also positive for *Shh* and Lef1. Thus, in the absence of terminal hair differentiation, cells accumulating in postnatal *BmpR1a* null follicles resembled early embryonic hair follicle progenitors.

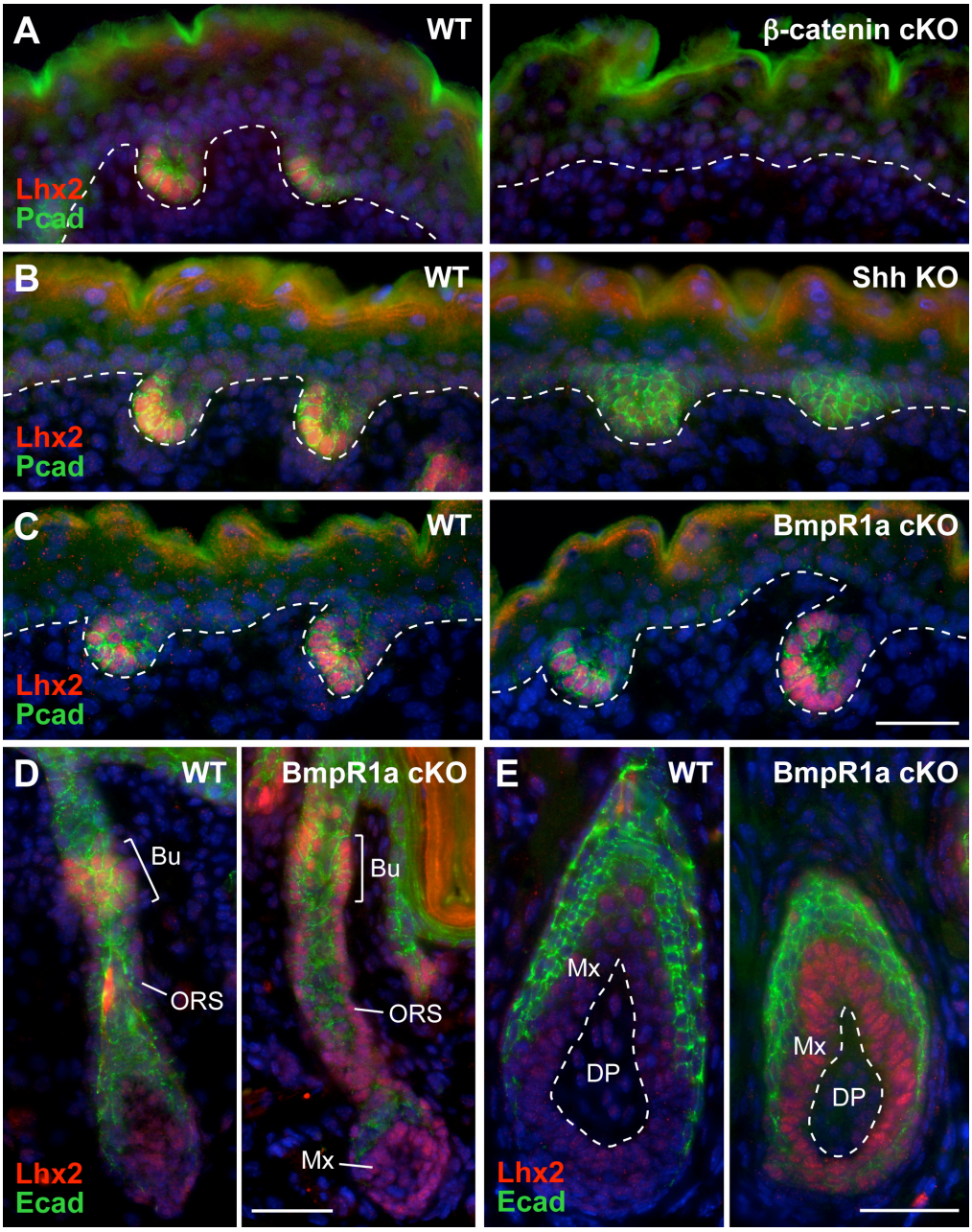

Figure 3.3 Lhx2 expression in genetic mutants of hair morphogenesis. Skin sections from indicated genetic mutant mice and their wild-type littermates were stained with antibodies as color-coded and counterstained with DAPI in blue. **(A)** Lhx2 is not expressed in the absence of hair follicle induction, as reflected in the *β-catenin* conditional null. **(B)** Lhx2 is reduced in *Shh* null hair germs, where follicles are specified but unable to progress further. **(C-E)** Lhx2 is expressed normally in *BmpR1a* conditional null hair germs and presumptive bulges, but persists in the lower ORS and Mx of neonatal and adult follicles. Unable to undergo terminal differentiation, these Lhx2 expressing cells in the *BmpR1a* null follicles appear to be undifferentiated stem cells. Scale bars, 40μm.

Lhx2 inhibits differentiation

If Lhx2 governs the gene expression program of undifferentiated hair follicle stem cells or their early progenitors, then misexpression of Lhx2 in the interfollicular epidermis might result in an induction of hair follicle progenitor genes. To test this possibility, *K14-Lhx2* transgenic mice were engineered and two independent founder lines with and without a protein tag were analyzed (Figure 3.4). Transgenic pups from both founders failed to thrive and died at birth with open eyes, kinky whiskers, and some displayed a patch of erythematous skin beneath the chin (Figure 3.5). Although more hair follicles were not induced, Lhx2 expression markedly suppressed morphological and biochemical signs of epidermal differentiation, and the skin failed to produce a functional lipid barrier (Figure 3.6). The suprabasal keratin K1 and filaggrin, expressed in keratohyalin granules of terminally differentiating cells, were completely absent from transgenic epidermis. Coinciding with the absence of these differentiation markers, the transgenic could not exclude a substrate from permeabilizing into the skin and converting into a blue precipitate.

Similarly, transgenic expression of Lhx2 suppressed differentiation in the tongue epithelium. Not normally expressed in the basal cells of tongue epithelia, ectopic Lhx2 inhibited the development and differentiation of filiform papillae

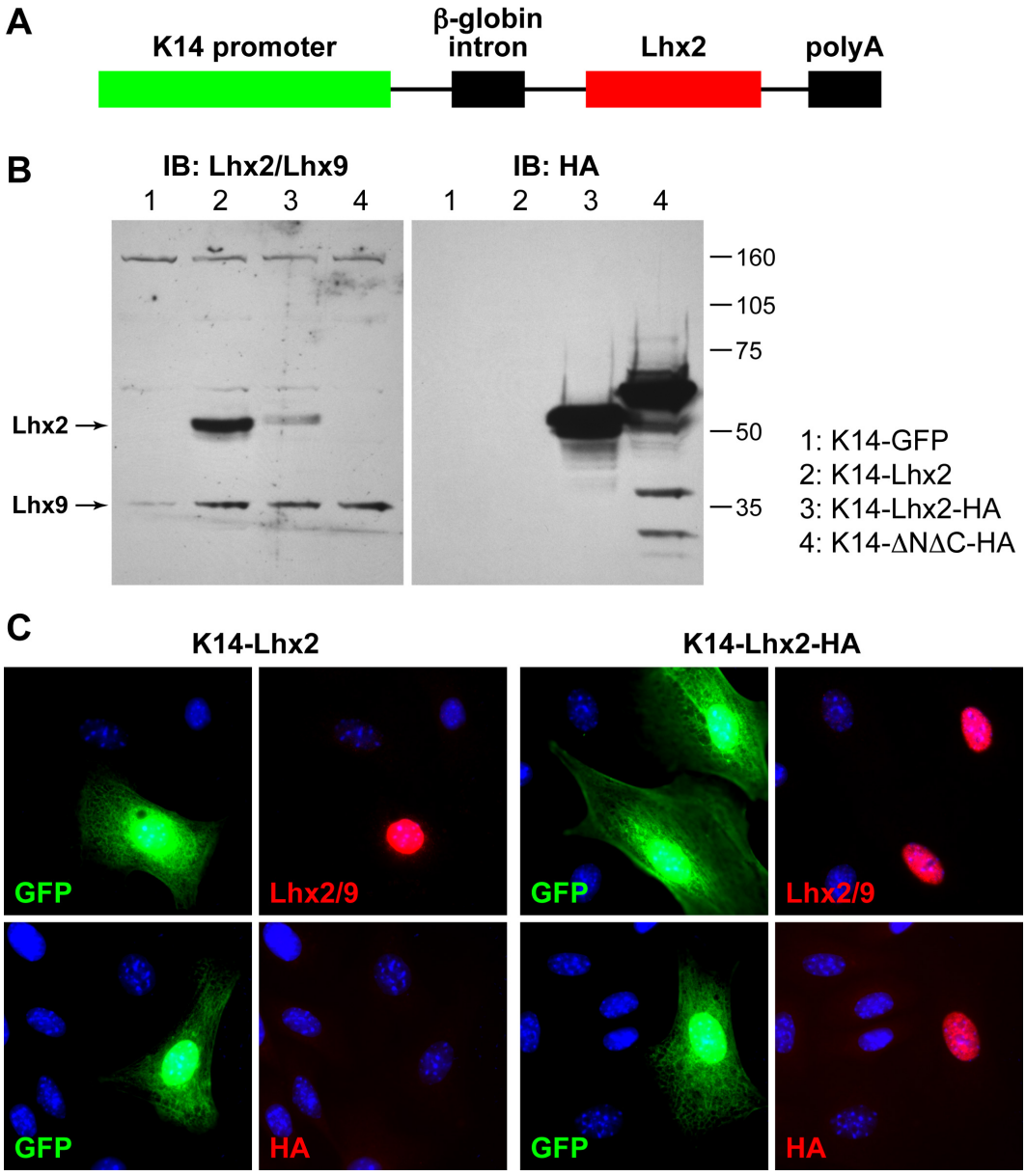

Figure 3.4 Design and expression of the Lhx2 transgene. **(A)** Diagram of the K14-Lhx2 construct. Full length murine *Lhx2* cDNA with and without a C-terminal HA epitope tag was cloned into the ~2 kB human *keratin 14* promoter (Vasioukhin et al., 1999). **(B)** Western blot of keratinocytes transfected with indicated constructs. The same blot was probed with anti-Lhx2/9 and anti-HA antibodies. Note the presence of endogenous Lhx9 in cultured keratinocytes. K14-ΔNΔCβ-catenin-HA served as a positive control for HA detection. **(C)** Immunofluorescence analysis of transfected keratinocytes. Cells were co-transfected with K14-GFP and indicated Lhx2 transgenic constructs. GFP expression identified transfected cells and antibodies used are color-coded in red. Nuclei are stained with DAPI in blue.

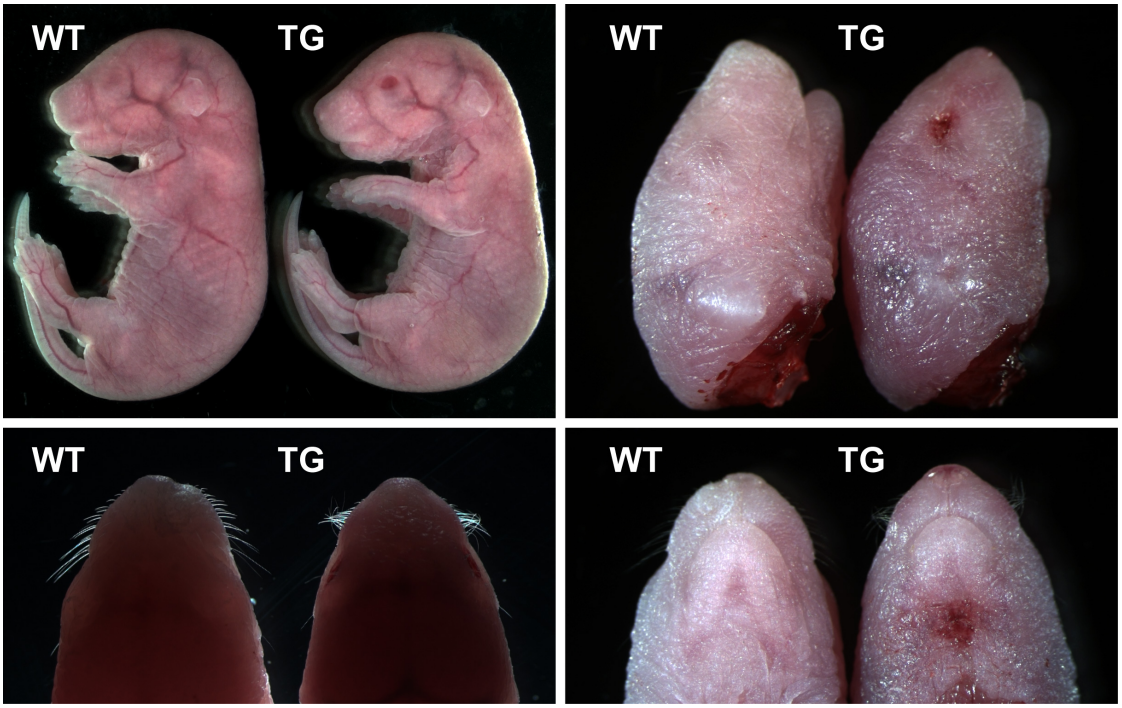

Figure 3.5 Gross phenotype of Lhx2 transgenic mice. K14-Lhx2 transgenic (TG) mice are born, but fail to thrive with open eyes, abnormal whiskers, missing ear lobes, and a patch of erythematous skin beneath the chin. The red skin is likely an area of suppressed epidermal differentiation manifested neonatally (see Figure 3.6). All pictures are of newborn pups, except for the upper left of E17.5 embryos.

(Figure 3.7). Of note, the differentiation defect in the tongue was evident at birth, but at this time the skin was morphologically and biochemically normal despite the robust expression of Lhx2 throughout the basal layer. Abnormalities in the skin became evident a few days after grafting. However, the redness seen beneath the chin of newborn transgenic pups (Figure 3.6) is reminiscent of the gross phenotype of grafted skin and is likely an area of suppressed epidermal

differentiation. Collectively, these findings suggest that Lhx2 can maintain epithelial cells in an undifferentiated state.

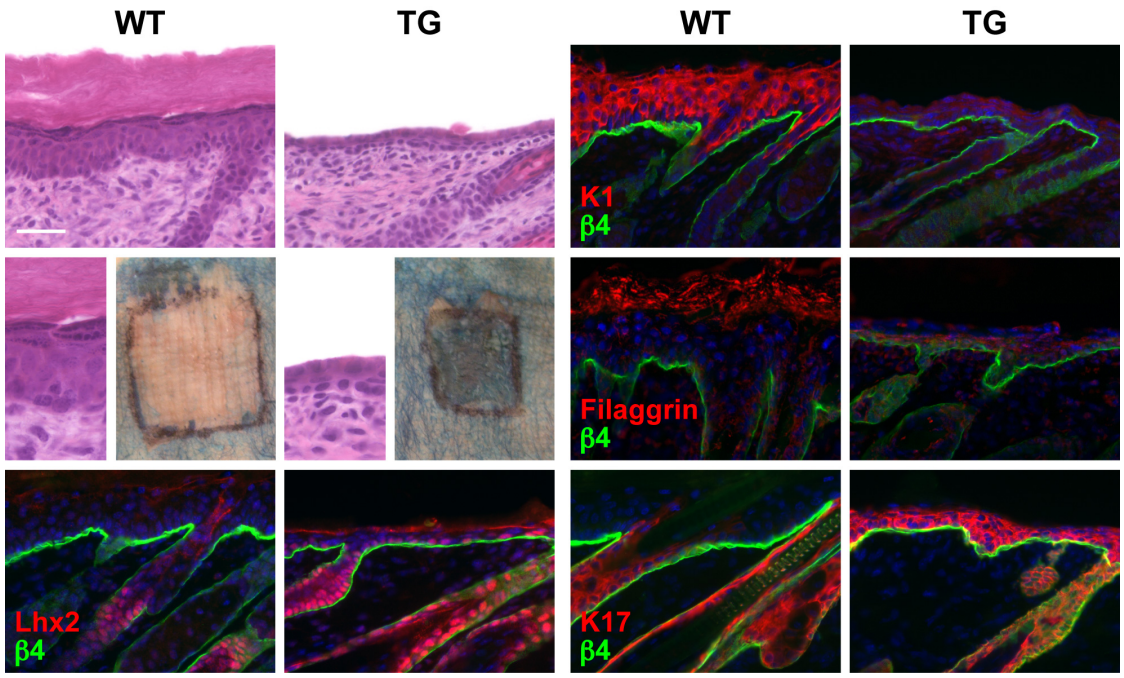

Figure 3.6 Lhx2 inhibits terminal differentiation in skin. Transgenic expression of Lhx2 in the interfollicular epidermis suppresses morphological and biochemical features of spinous, granular, and stratum corneum stages of epidermal differentiation. Newborn skin sections from *K14-Lhx2* transgenic (TG) and wild-type (WT) littermates were grafted for 8 days and processed for hematoxylin/eosin staining or immunofluorescence with antibodies as color-coded and counterstained with DAPI in blue. Patches outlined in black denote skins grafted onto *nude* mice and subjected to a β-galactosidase substrate exclusion assay to test for an intact epidermal barrier. The lack of a functional epidermal barrier in transgenic skin is evident by the penetration and conversion of the substrate into a blue precipitate. The background absorption in the surrounding *nude* skin arises from defective hair follicle orifices. Scale bar, 40μm.

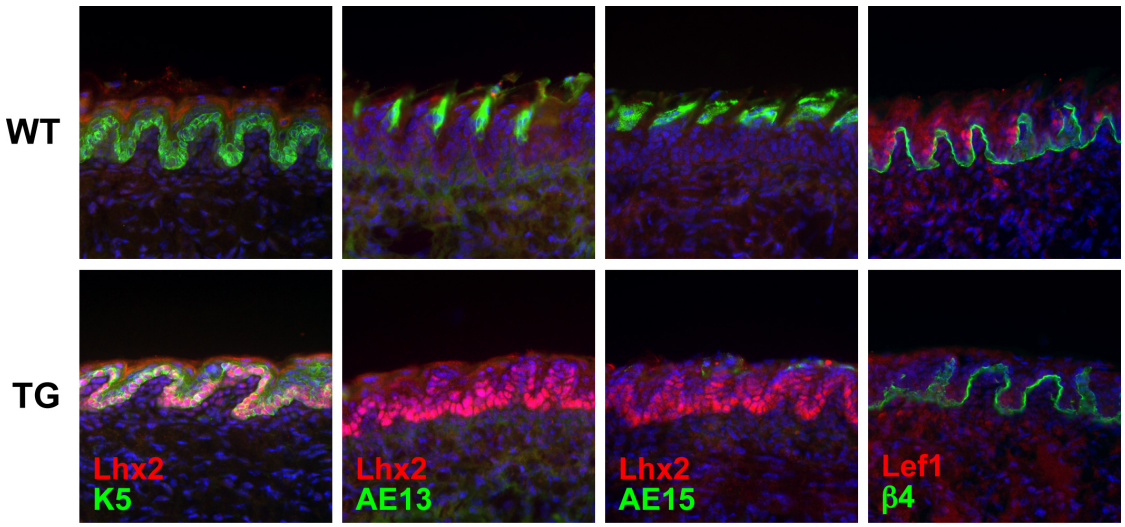

Figure 3.7 Lhx2 inhibits terminal differentiation in tongue. Transgenic expression of Lhx2 in the tongue epithelium suppresses the development of filiform papillae as evidenced by the loss of differentiation markers. Newborn tongue sections from *K14-Lhx2* transgenic (TG) and wild-type (WT) littermates were immunofluorescence stained with antibodies as color-coded and counterstained with DAPI in blue.

Lhx2 promotes hair follicle stem cell fate

In lieu of epidermal differentiation markers, the Lhx2 transgenic epidermis expressed genes associated with the hair follicle outer root sheath. For example, keratin 17 (K17) expression, normally restricted to the outer root sheath, was expanded into the interfollicular epidermis (Figure 3.6). Although K17 is also associated with hyperproliferative states, enhanced proliferation was not evident in the transgenic epithelium by Ki67 staining. Instead, induction of Tcf3 and Sox9, two key transcription factors of adult hair follicle stem cells (Merrill et al., 2001; Vidal et al., 2005), was noticeably present in the transgenic epidermis before any

overt changes in epidermal differentiation (Figure 3.8). Nfatc1, an uncharacterized bulge transcription factor, was also ectopically expressed in the interfollicular epidermis. Thus, Lhx2 alters the fate of epidermal cells and promotes the acquisition hair follicle stem cell characteristics.

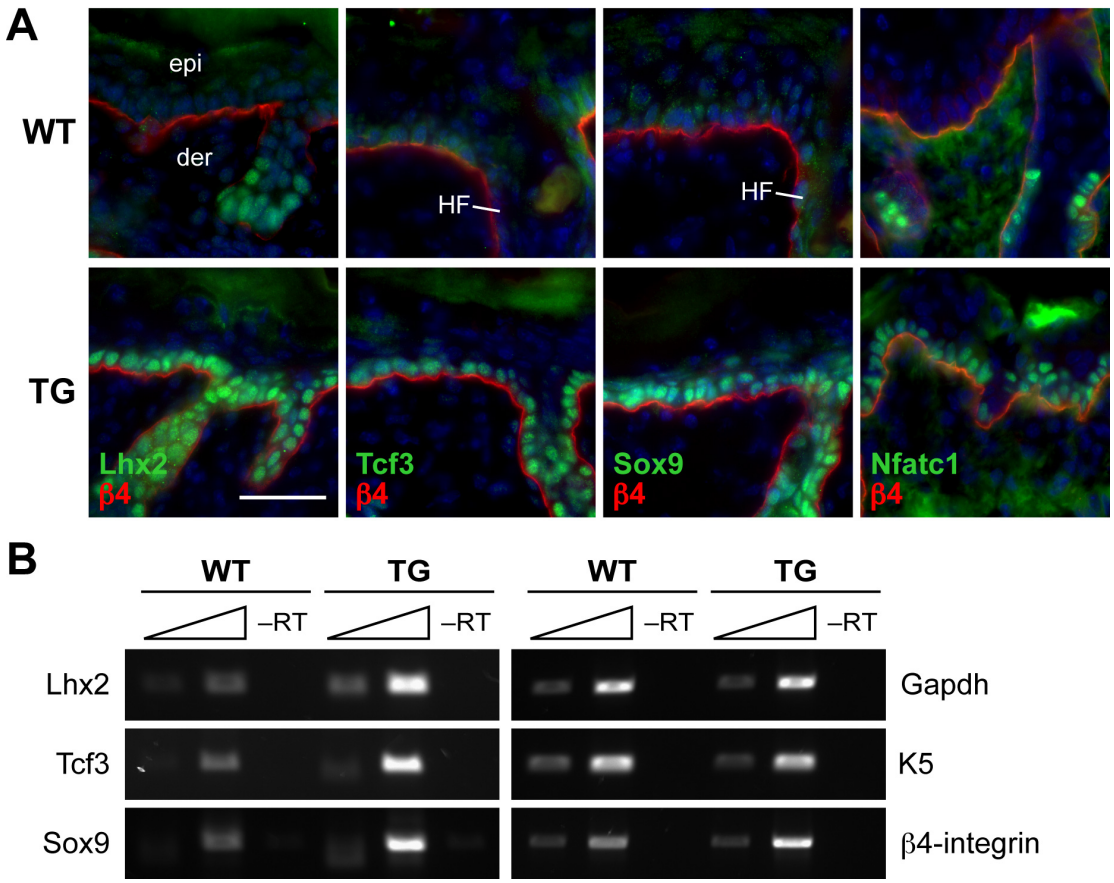

Figure 3.8 Expression of Lhx2 induces hair follicle stem cell markers. Prior to overt changes in epidermal differentiation, transgenic expression of Lhx2 in the skin epithelium induces the interfollicular expression of transcription factors normally restricted to the hair follicle bulge. **(A)** Newborn skin sections from *K14-Lhx2* transgenic (TG) and wild-type (WT) littermates were grafted for 4 days and immunofluorescence stained with antibodies as color-coded and counterstained with DAPI in blue. Scale bar, 40μm. **(B)** Semi-quantitative RT-PCR on mRNA isolated from epidermal cells of day 4 post-graft skin confirms the increased expression of bulge stem cell markers in the transgenic epidermis.

If Lhx2 is required for hair follicle stem cell maintenance, then its absence could alter the ability of follicles to form. In support of this notion, E16 *Lhx2* null embryos displayed an ~40% reduction in the overall density of P-cadherin positive hair follicles, with no noticeable defect in the epidermis or embryo size (Figure 3.9). A marked reduction in follicle density is a feature of other mouse mutants in key hair follicle morphogenetic genes (Botchkarev et al., 1999; Foitzik et al., 1999; van Genderen et al., 1994). Although *Lhx2* knockout follicle density was reduced, *Shh*, *Wnt10b*, *Bmp2*, *Bmp4* and Lef1 expression appeared unaffected in those hair placodes and germs that developed independently of Lhx2 (Figure 3.10A). To follow hair follicle development beyond E16 in the *Lhx2* null mutants, skin engraftments were performed. Hair follicles from *Lhx2* null grafts appeared morphologically and biochemically indistinguishable from their wild-type counterparts as judged by various markers of the companion layer, inner root sheath and hair shaft (Figure 3.10B). Taken together, the gain- and loss-of-function studies suggest that Lhx2, reflecting its expression pattern, functions to specify and maintain hair follicle stem cells, but does not function in their differentiation.

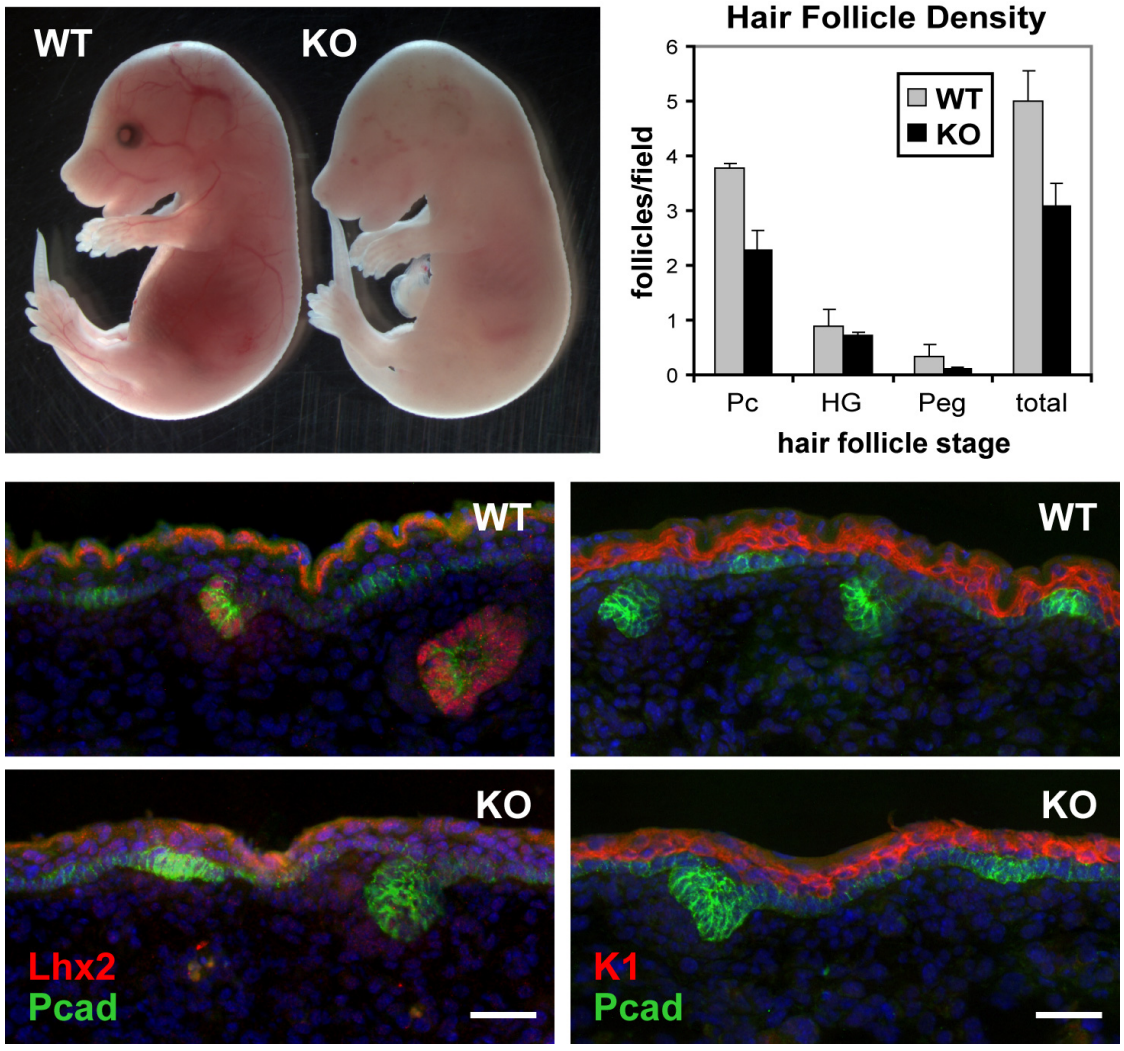

Figure 3.9 Loss of Lhx2 reduces hair follicle morphogenesis. As reported, Lhx2 knockout (KO) embryos are noticeably paler than wild-type (WT) littermates, lack eyes, and have a slightly flattened forehead by gross morphology (Porter et al., 1997). Pictured embryos are at E15.5. Representative back skin sections from E16 Lhx2 KO and WT littermates show comparable epidermal differentiation but fewer follicles at all stages of development in Lhx2 null embryos. The graph provides quantification from multiple sections of three embryos. Abbreviations: Pc, placode; HG, hair germ; Peg, hair peg. Scale bar, 40μm.

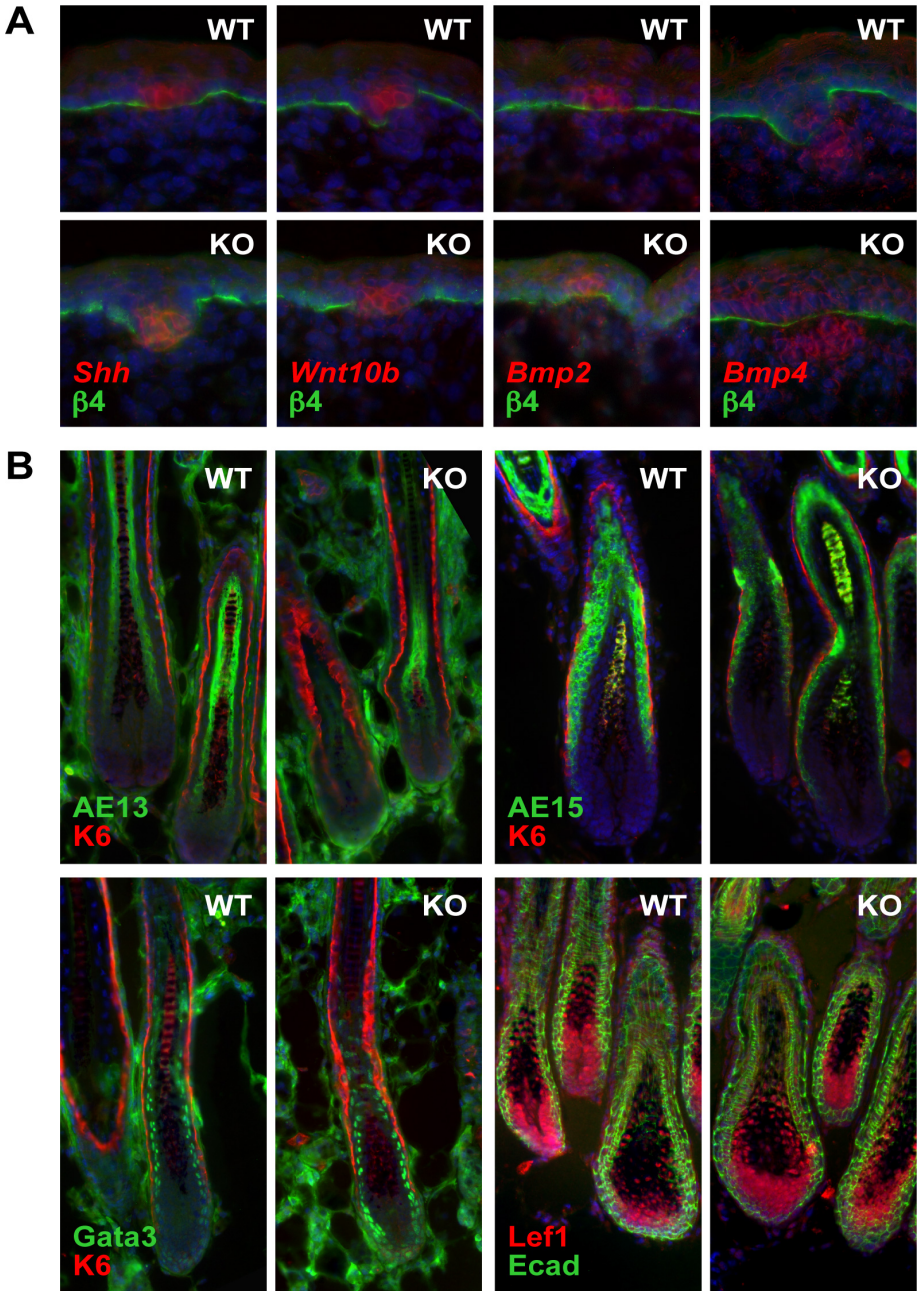

Figure 3.10 Development and differentiation of Lhx2 null hair follicles. (A) Key signals regulating hair morphogenesis are expressed normally in follicles induced independently of Lhx2. *In situ* hybridizations of E16 Lhx2 knockout (KO) and wild-type (WT) littermates were pseudo-colored and overlayed with an immunofluorescence image of β4-integrin. **(B)** Hair differentiation is normal in Lhx2 null follicles. Immunofluorescence staining with indicated antibodies of Lhx2 KO and WT skin grafts at mid-anagen show typical expression patterns of K6 (companion layer), AE15 (inner root sheath and medulla), AE13 (hair cortex), Gata3 (precursors of IRS), and Lef1 (precursors of cortex).

Lhx2 maintains follicle stem cells in a quiescent state

If Lhx2 maintains the undifferentiated state of embryonic and adult follicle stem cells, then *Lhx2* null follicles might exhibit alterations in the transition of stem cells from the resting (telogen) to the growing (anagen) phase of the postnatal hair cycle. Using skin grafts taken from E15.5 embryos, the hair cycles of wild-type and *Lhx2* knockout follicles were compared. The initial morphogenetic and first postnatal *Lhx2* knockout hair cycles progressed similarly to those in the wild-type and by 8 weeks, knockout follicles had returned to telogen (Figure 3.11). By contrast, at 11 weeks when most wild-type follicles were still in this extended telogen, knockout follicles had precociously entered the next hair cycle (Figure 3.12A). Moreover, when follicles were shaved at 8 weeks, most wild-type hairs remained in telogen whereas knockout hairs consistently and uniformly grew back within 3 weeks, confirming their shortened resting phase (Figure 3.12B-C). Relative to non-grafted skin, there was an approximately one week delay in the overall hair cycle of wild-type grafts, but this was anticipated considering that embryonic skin was grafted and allowing for a few days of healing. The length of the hair cycle and the timing of anagen initiation remained the same. Thus, follicles in the skin grafts follow an intrinsic hair cycle clock and the defects in the *Lhx2* null follicles are likely autonomous and not secondary to

grafting. Furthermore, all grafts analyzed from wild-type and knockout littermates were placed on the same recipient to control for any systemic effects.

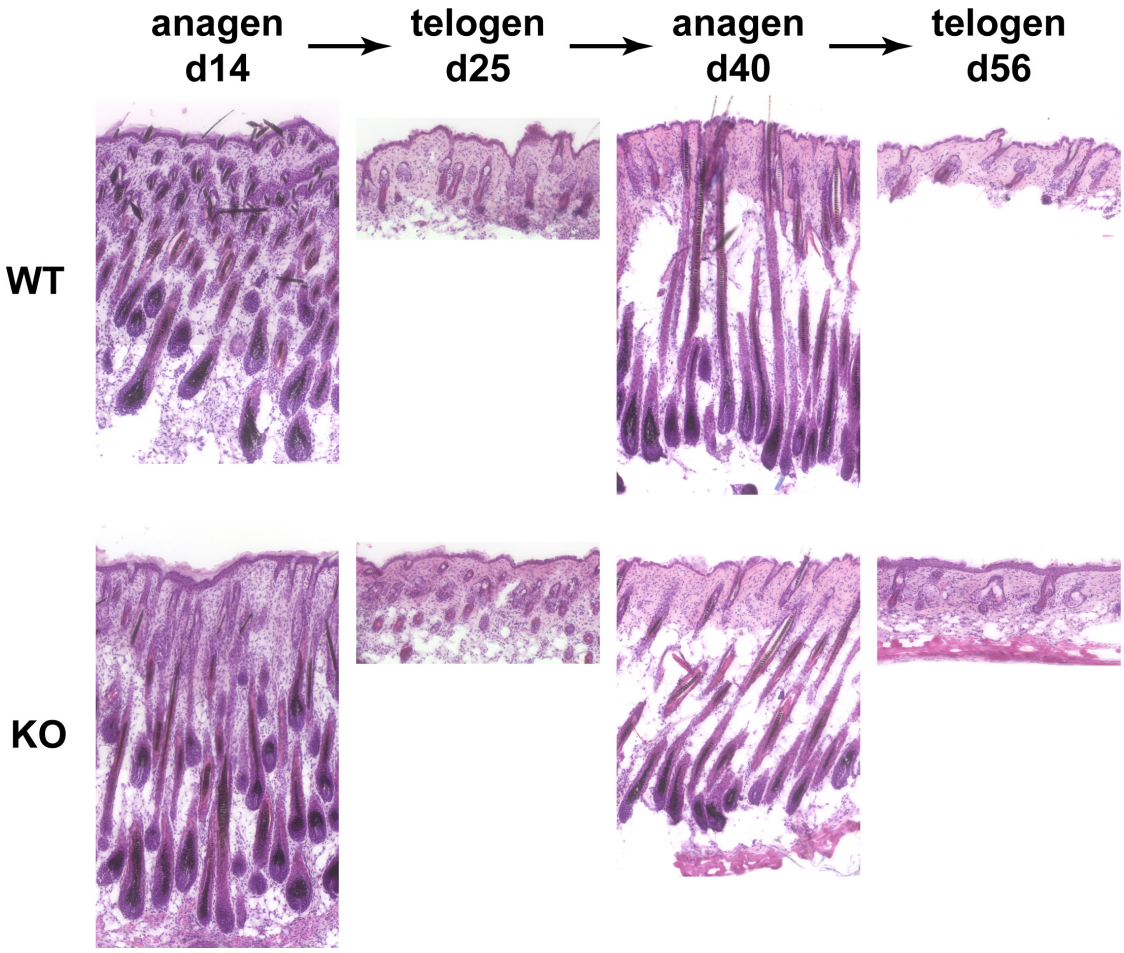

Figure 3.11 Hair cycle of Lhx2 null hair follicles. Histological analysis of Lhx2 knockout (KO) and wild-type (WT) hair follicles at various ages post-engraftment. During the initial morphogenetic and first postnatal hair cycles, follicles behave largely synchronously and proceed with similar kinetics in WT and KO skin grafts. After 8 weeks, WT hair follicles are in their second telogen stage, which in contrast to the short (1-2 days) first telogen, is prolonged for well over 3 weeks (Muller-Rover et al., 2001). Lhx2 KO follicles are unable to hold this resting phase and precociously enter anagen by 11 weeks (Figure 3.12).

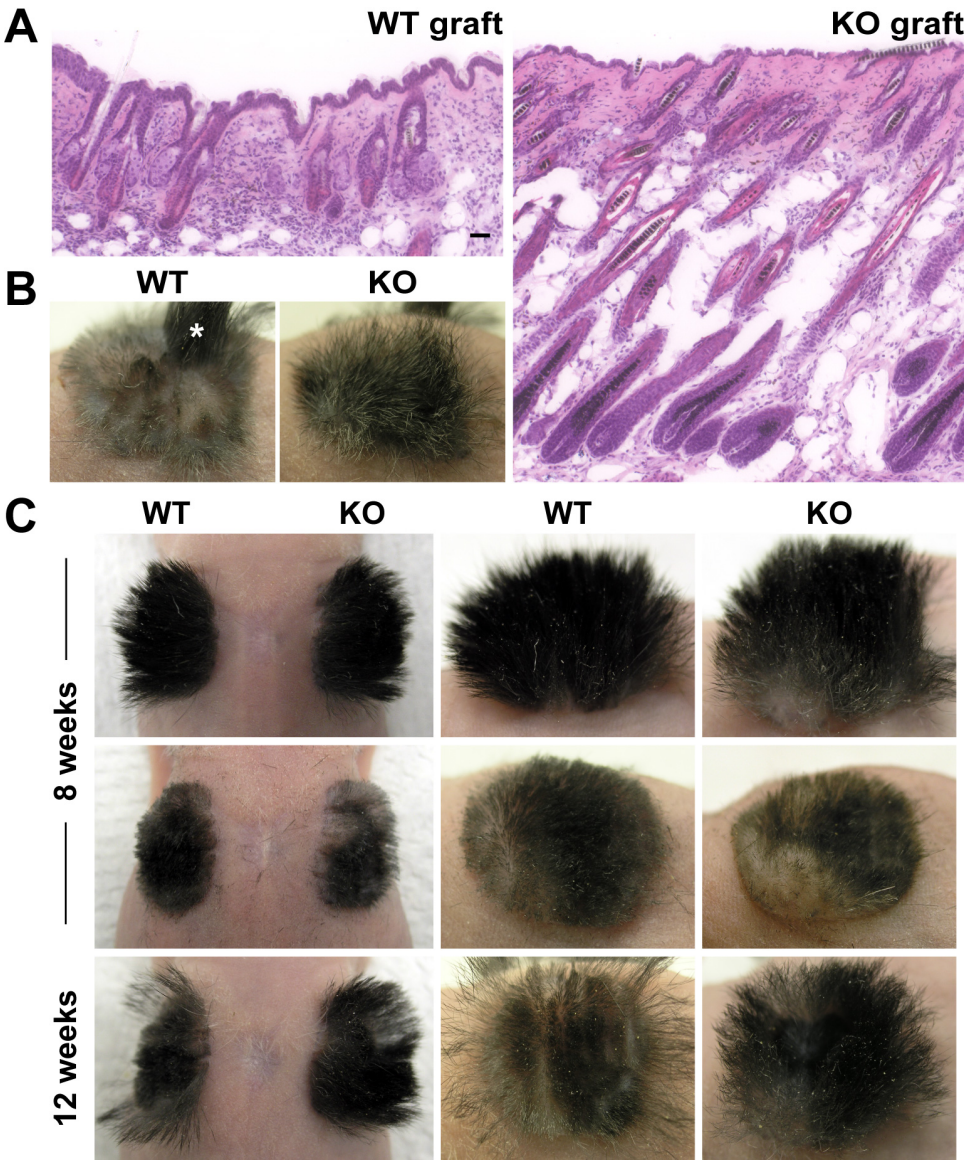

Figure 3.12 Precocious anagen entry of Lhx2 null hair follicles. **(A)** Histology of wild-type (WT) and Lhx2 knockout (KO) skins at 11 weeks post-engraftment. WT follicles are still in telogen, but KO follicles have prematurely entered anagen. Scale bar, 80μm. **(B)** Upon shaving the grafted hair follicles at 8 weeks, WT hairs do not grow back, confirming their resting state, while hair growth is evident in the KO graft. A small portion (*) of the WT graft grew hairs due to a wound response. **(C)** Another example of a shaving experiment demonstrating the regrowth of hair follicles in the KO graft after shaving while the WT graft remained at rest. The edges of the WT graft adjacent to the nude skin grew back hairs probably due to a non-autonomous effect.

The precocious activation of anagen in *Lhx2* knockout hair follicles suggested a defect in the bulge stem cells. Immunofluorescence and flow cytometry analyses revealed that knockout follicles exhibited diminished expression of CD34, a surface marker of bulge stem cells (Figure 3.13) (Trempus et al., 2003; Blanpain et al., 2004). This reduction in CD34 was observed irrespective of hair cycle number or stage. On the other hand, other stem cell markers examined were comparably expressed in wild-type and knockout hair follicle bulges (Figure 3.14).

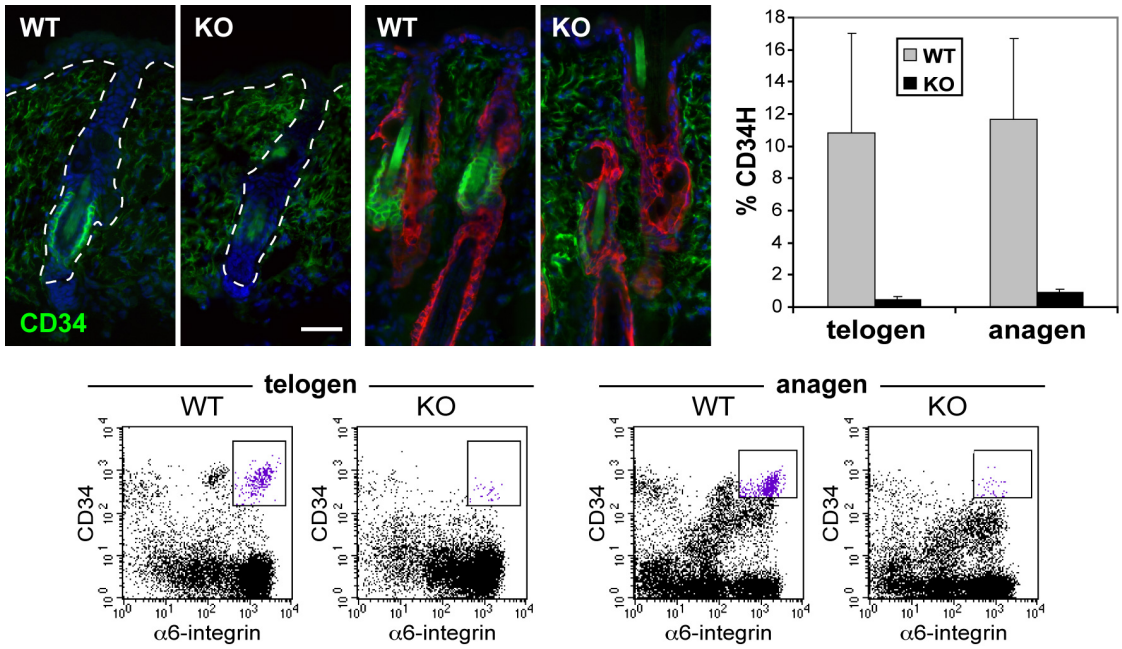

Figure 3.13 Diminished expression of CD34 in Lhx2 null hair follicles. Irrespective of the hair cycle stage, CD34 expression is dramatically reduced in Lhx2 knockout (KO) follicle bulges relative to wild-type (WT). Shown are representative immunofluorescence images and flow cytometry profiles of telogen follicles at 8 weeks and anagen follicles at 40 days post-engraftment. A summary of the percentage of α6-integrin positive cells that are also CD34 positive in each of the hair follicle stages was determined by flow cytometry. Scale bar, 40μm.

Although CD34 marks the normally quiescent adult stem cells, it is not found in the more proliferative embryonic skin progenitors, suggesting that its reduction could be an indication of enhanced proliferative activity within *Lhx2* knockout hair follicle stem cells. This hypothesis was supported by

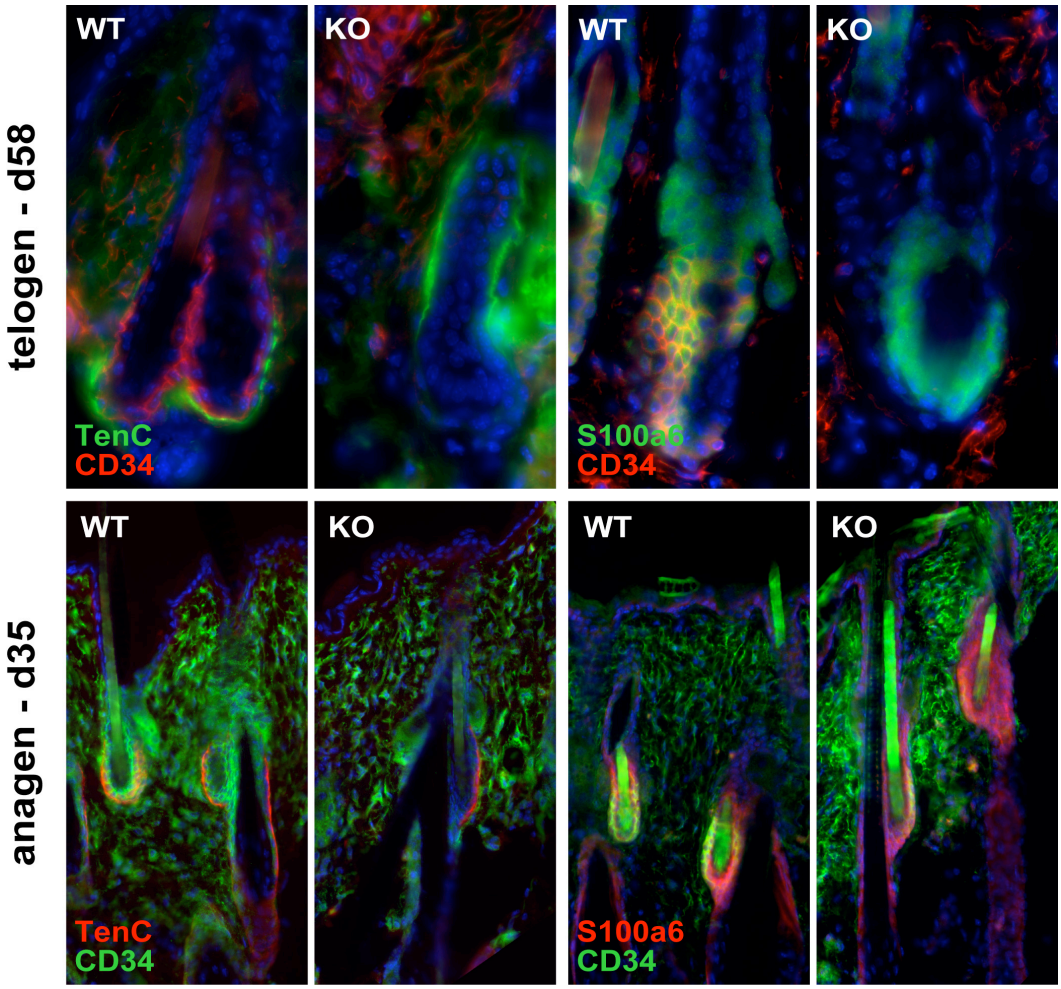

Figure 3.14 Expression of bulge markers in Lhx2 null hair follicles. Although CD34 expression is dramatically reduced in Lhx2 null hair follicles, the expression of other bulge markers, Tenascin C and S100A6, appear to be normal in both telogen and anagen hair follicles. Skin sections from Lhx2 knockout (KO) and wild-type (WT) grafts were immunofluorescence stained with antibodies as color-coded and counterstained with DAPI in blue.

bromodeoxyuridine (BrdU) pulse-chase experiments conducted prior to marked deviations in hair cycling (Figure 3.15). After a three day pulse period at the onset of anagen, both the wild-type and knockout hair follicles were equally labeled with BrdU, but only the wild-type follicle bulge retained appreciable label after a 4 week chase (Blanpain et al., 2004; Taylor et al., 2000). By contrast, knockout hair follicles displayed very few label retaining cells (LRCs), as confirmed and quantified by flow cytometry.

The reduction in label retention was accompanied by enhanced proliferation within the *Lhx2* null bulge. After a 4-hour BrdU pulse during full anagen, the percentage of S-phase labeled bulge cells was twice as high as normal (Figure 3.16). By contrast, the number of S-phase cells in the interfollicular epidermis and outer root sheath of wild-type and knockout skins was comparable, underscoring the specificity of this hyperproliferation. A similar result was observed in telogen follicles. The elevated proliferative activity of the knockout bulge did not appear to alter the overall size of the stem cell niche. Therefore without Lhx2, follicle stem cells are more readily activated to proliferate and differentiate along the hair lineage. On the other hand, Lhx2 is not sufficient to induce quiescence, because transgenic expression did not suppress proliferation or induce CD34 expression in the skin epithelium.

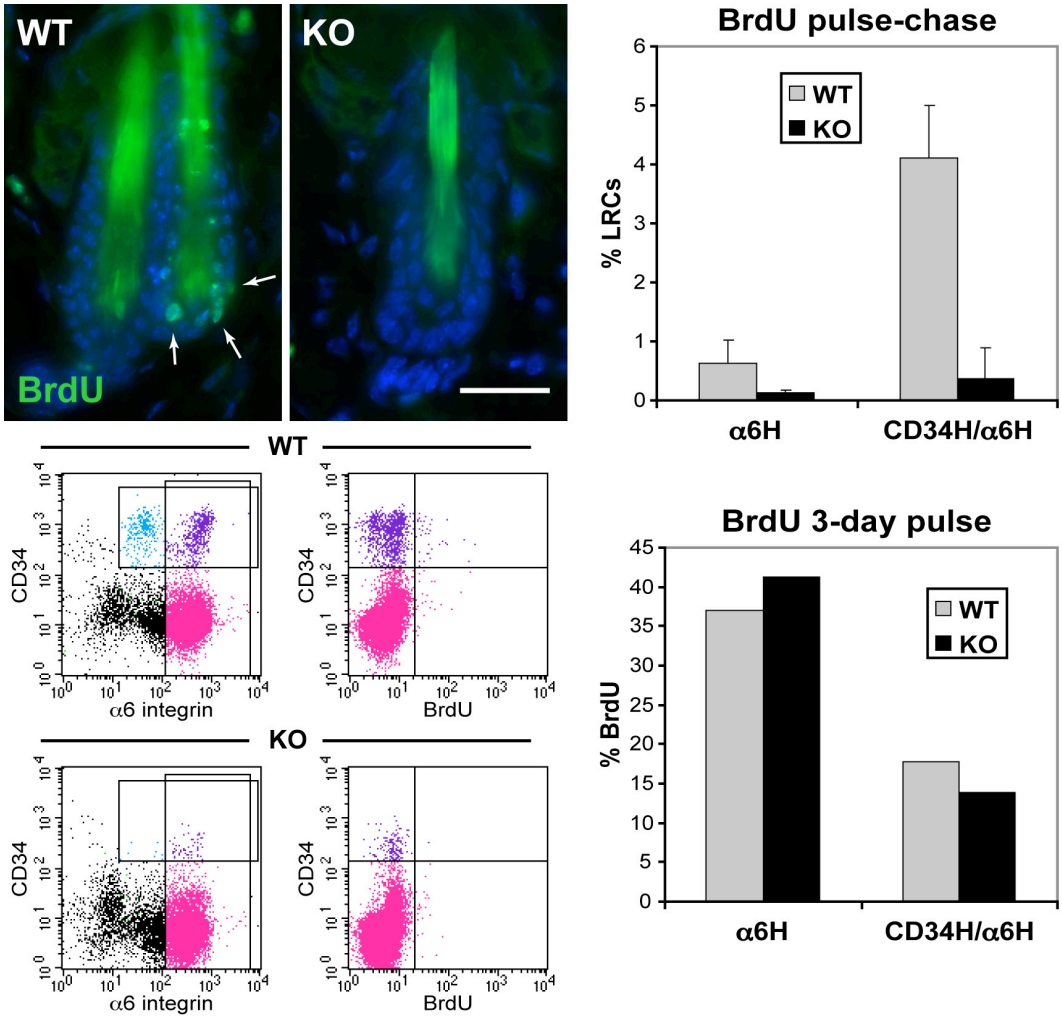

Figure 3.15 Loss of BrdU label retention in Lhx2 null follicle stem cells. Lhx2 knockout (KO) and wild-type (WT) skin grafts were pulsed with BrdU for 3 days at the onset of anagen between days 26 to 28, then chased for 4 weeks when hair follicles reentered telogen. Analysis of BrdU staining indicates that label retaining cells (LRCs) concentrated in the infrequently dividing bulge stem cells of WT follicles, but were diminished in Lhx2 KO follicles. Shown are representative skin sections stained with antibodies to BrdU and flow cytometry profiles of BrdU incorporation in the α6-integrin, CD34 positive bulge cells. Results of quantification by flow cytometry is provided. BrdU incorporation after the 3 day pulse period was also analyzed by flow cytometry and shows equivalent labeling in both WT and KO grafts. Scale bar, 20μm.

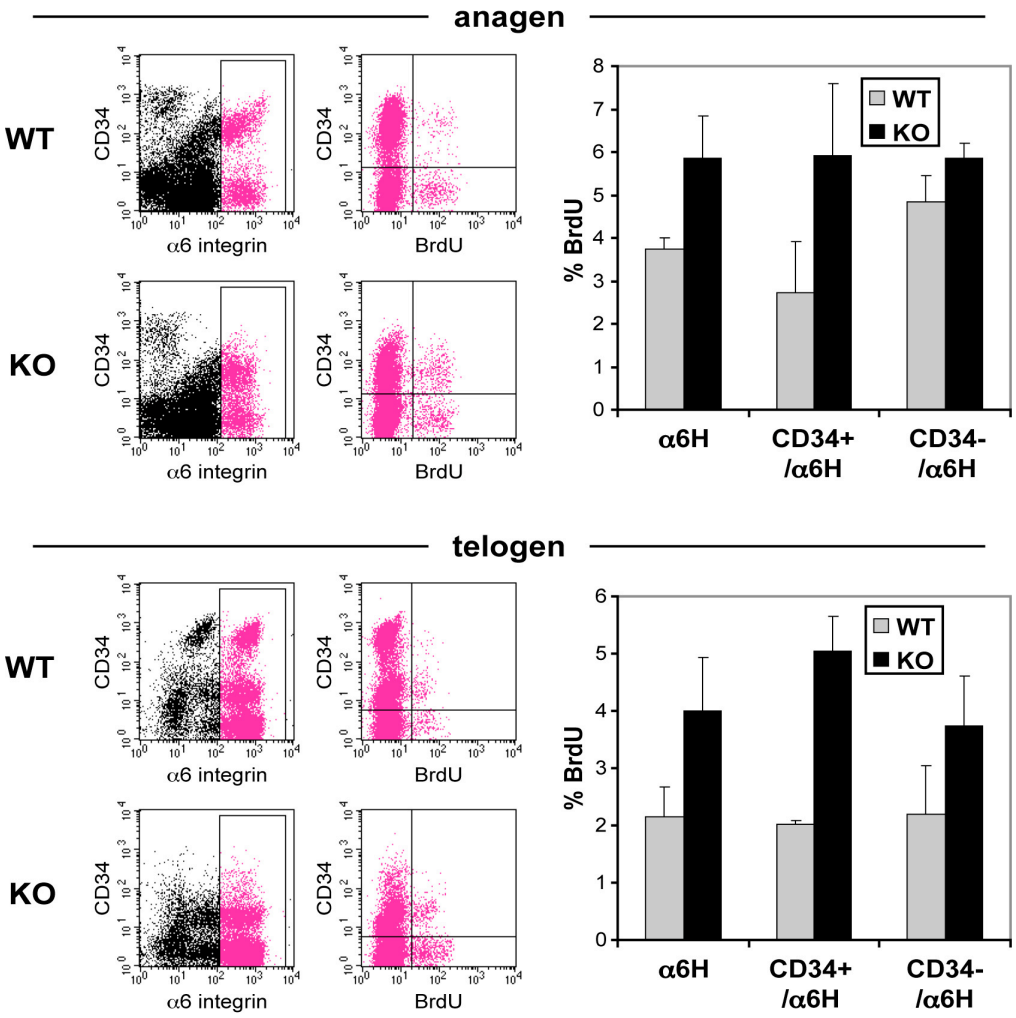

Figure 3.16 Increased BrdU incorporation in Lhx2 null follicle stem cells. Lhx2 knockout (KO) and wild-type (WT) skin grafts were pulsed with BrdU for 4 hours at day 40 (anagen) or at 8 weeks (telogen) before cells were isolated and analyzed for BrdU incorporation by flow cytometry. Proliferation was enhanced in Lhx2 KO hair follicle bulges relative to WT. Shown are representative profiles of cells gated on α6-integrin (red) and analyzed for CD34 expression and BrdU incorporation. Results of quantification by flow cytometry is provided.

Discussion

Characterization of Lhx2 in hair follicles has revealed its role in regulating the status of progenitor cells in the skin (Figure 3.17). Initially expressed in the embryonic hair placode, Lhx2 contributes to the specification and possible expansion of these early hair follicle progenitors. Lhx2 is not expressed in the absence of hair follicle induction and is dramatically diminished in arrested hair follicles that are unable to proliferate and undergo further morphogenesis. In addition, targeted loss of *Lhx2* reduces the overall number of initiated hair follicles. Although hair morphogenesis can proceed without Lhx2, null follicles that do form are unable to hold a resting state and precociously enter new hair growth cycles. This is a result of Lhx2 expression in the hair follicle bulge where it functions to maintain stem cells in a quiescent and undifferentiated state. The precocious activation of bulge stem cells is accompanied by enhanced proliferation and loss of label retaining cells in *Lhx2* null hair follicles. Once committed, cells exiting the bulge no longer require or express Lhx2 and proceed along a normal program of terminal differentiation by receiving additional signaling cues and altering gene expression. Progenitor cells incapable of responding to these cues continue to express Lhx2 and remain undifferentiated. The sufficiency of Lhx2 to maintain the undifferentiated state of epithelial cells is supported by the forced expression of Lhx2 in the epidermis and tongue, where it

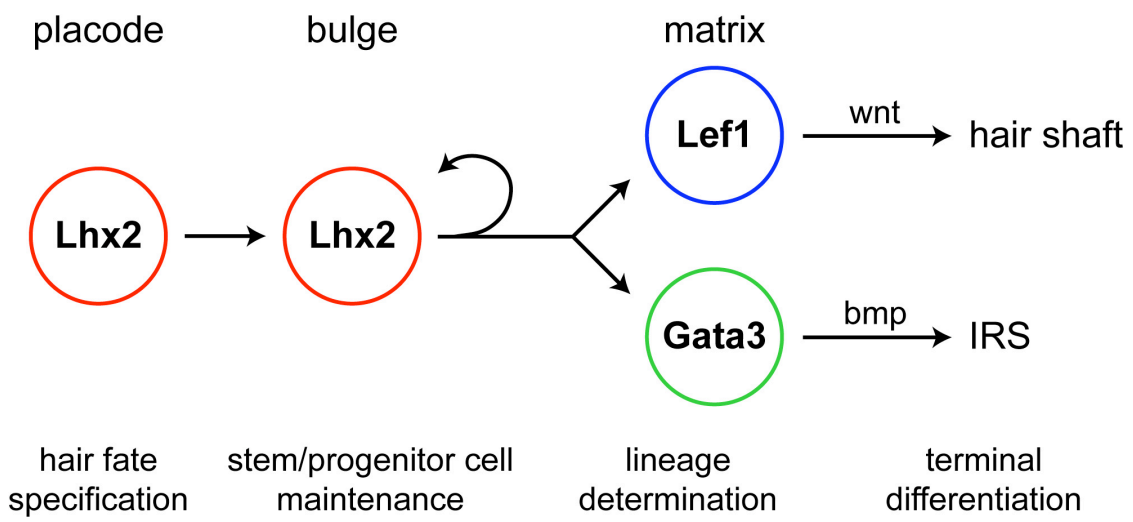

Figure 3.17 Model for Lhx2 during hair follicle development. Lhx2 is present in the early embryonic hair progenitors of the placode where it contributes to the specification of hair follicles. As morphogenesis proceeds, Lhx2 becomes restricted to the presumptive bulge cells, and postnatally it remains as a faithful bulge stem cell marker, where it functions to maintain cells in an undifferentiated, quiescent state. As stem cells become activated and embark upon different follicle lineages within the hair matrix, they down-regulate Lhx2 expression and induce expression of other transcription factors required for cell fate determination. In response to external signaling cues, the precursors become further committed to terminally differentiate.

can inhibit all signs of differentiation. Thus, Lhx2 appears to function as a molecular brake in regulating the switch between hair follicle stem cell maintenance and their activation to terminally differentiate.

Although not sufficient to induce *de novo* hair morphogenesis, Lhx2 can also change the fate of epidermal cells and induce the expression of key hair follicle stem cell genes. Two of these genes, Tcf3 and Sox9, have been described to functionally regulate hair follicle stem cell lineages (Merrill et al, 2001; Vidal et

al., 2005). Interestingly, several lines of evidence suggest that Lhx2 may function upstream of these factors in orchestrating hair follicle development. Similar to Lhx2, transgenic expression of Tcf3 also suppresses terminal epidermal differentiation and promotes features of the outer root sheath and bulge (Merrill et al., 2001). However unlike transgenic expression of Lhx2, early suprabasal markers of differentiation are normal and stratification of the epidermis seems to occur in Tcf3 transgenics. Although this discrepancy could be attributable to developmental differences in the timing of when the skins are analyzed, a recent study which conditionally induces Tcf3 for extended periods of time at various ages corroborates the initial findings in the Tcf3 transgenic mice (Nguyen et al., 2006). In addition, induction of Tcf3 did not give rise to Lhx2 expression in the epidermis (data not shown). Thus the greater severity of the Lhx2 transgenic phenotype which induces Tcf3 combined with the lack of Lhx2 induction in the Tcf3 transgenic suggests that Lhx2 can promote Tcf3 activity, but not vice versa. Furthermore, while the endogenous expression pattern of Lhx2 is largely restricted to the bulge, Tcf3 expression extends throughout the lower outer root sheath, considered to be the immediate progeny of bulge stem cells. Although sustaining Tcf3 expression in the outer root sheath is likely independent of Lhx2, it is fascinating to speculate that Lhx2 may induce Tcf3 expression in the bulge to regulate the outer root sheath lineage during hair growth.

Similarly, the expression of Sox9 is also broader than Lhx2 in the hair follicle. Along with its expression in the bulge, Sox9 is present throughout the outer root sheath like Tcf3. However during early hair morphogenesis, Sox9 expression appears to trail Lhx2 expression at the leading edge of invaginating hair follicles, and while Lhx2 becomes concentrated at the presumptive bulge, Sox9 continues to be expressed in the lower outer root sheath (data not shown). This difference in expression pattern is reflected in the distinct hair follicle phenotypes of the *Lhx2* null and *Sox9* conditional null mice. Although both mutant mice lack expression of the bulge specific marker CD34, the basis for this loss are completely different. In the *Lhx2* null, loss of CD34 is likely a consequence of the enhanced proliferative state of follicle stem cells. However in the absence of *Sox9*, the outer root sheath, and with it the bulge and entire hair structure, completely degenerates around the time developing follicles begin to penetrate the skin surface (Vidal et al., 2005). Thus reflecting their different expression patterns, Lhx2 and Sox9 regulate distinct cell types in the hair follicle, with Sox9 affecting the differentiation of a more downstream lineage than Lhx2. Although these genes seem to co-localize within the bulge, further studies are necessary to address if Lhx2 can directly regulate the transcription of Sox9 and Tcf3. Assessment of their expression in *Lhx2* null bulges has been difficult in the absence of a definitive stem cell marker like CD34, but both Sox9 and Tcf3 appear

to be normally expressed in the outer root sheath of Lhx2 independent hair follicles (data not shown). This suggests that their induction by Lhx2 is likely indirect even though the promoter regions of both Sox9 and Tcf3 contain putative homeodomain regulatory elements.

Precedence for Lhx2 functioning in an indirect or cell non-autonomous mechanism to govern progenitor status is found in several developmental contexts, particularly in the hematopoietic system. Absence of *Lhx2* impairs definitive erythropoiesis and consistent with this phenotype, colony forming assays of cells isolated from mutant fetal livers demonstrate a dramatic reduction in the number of progenitor cells of the erythroid lineage (Porter et al., 1997). However *Lhx2* null cells are still able to contribute significantly to erythrocytes in chimeric mice as well as engraft lethally irradiated mice. Thus a defective hepatic environment, mediated by Lhx2 target genes, is responsible for the loss and abnormal development of progenitor cells. Similarly, hematopoietic stem cells immortalized by expressing Lhx2 in embryonic stem cells are only able to self-renew either in high density cultures with the presence of steel factor (also known as stem cell factor or c-kit ligand) or on stromal feeder cell layers (Pinto do O et al., 2001). Growth and renewal of these cells is strictly contingent on Lhx2 expression, but their dependency on extrinsic elements further suggests that Lhx2 regulates

soluble factors involved in stem cell maintenance. The specific identity of these factors is presently unknown.

Lhx2 also regulates progenitor cells during neural development. Without functional Lhx2, progenitors of the cerebral cortex are unable to proliferate leading to cortical hypoplasia (Porter et al., 1997). Accompanying this defect is an expansion of the cortical hem, a signaling-rich band of tissue that guides dorsal neural development adjacent to the Lhx2 expressing ventricular zone. Since Lhx2 is not expressed in the cortical hem, a cell non-autonomous mechanism must exist to restrict this region for the forebrain to develop. Notably, the cortical hem is marked by the expression of several Wnt and Bmp ligands, suggesting that Lhx2 may regulate the specification and growth of cortical progenitors by limiting the extent of these key ligands (Bulchand et al., 2001; Monuki et al., 2001).

Interestingly, loss of Lhx2 in hair follicles is reminiscent of enhanced epithelial Wnt signaling, whereby bulge stem cells prematurely activate and enter new hair cycles. Similar to *Lhx2* null hair follicles, constitutive expression of a stabilized form of β-catenin in the skin epithelium results in precocious anagen entry upon reaching the extended telogen phase after the first postnatal hair cycle (Lowry et al., 2005). This parallel suggests the possibility that Lhx2 can negatively regulate Wnt activity in hair follicle progenitors, but further studies are necessary to determine if Wnt signaling is indeed elevated in Lhx2 null hair

follicles. Recently, another LIM-HD factor Lhx5 was found to promote forebrain development by activating the transcription of secreted Wnt antagonists (Peng and Westerfield, 2006). Whether Lhx2 can also modulate a Wnt-inhibited microenvironment in the hair follicle bulge to maintain the undifferentiated and quiescent state of stem cells awaits the identification of target genes regulated by Lhx2. Nonetheless, expression of Lhx2 appears to underlie a conserved means of mediating the self-renewal and maintenance of stem cells within different tissues and organs.

Materials and Methods

Mice

The following mice were generous gifts: $Lhx2^{-/-}$ (H. Westphal, NIH); β-$catenin^{fl/fl}$ (R. Kemler, Max Plank, Freiburg); $Shh^{-/-}$ (A. McMahon, Harvard); $BmpR1a^{fl/fl}$ (Y. Mishina, NIH). Lhx2 transgenic mice were generated by cloning full length murine *Lhx2* cDNA (gift from J. Hirota, Rockefeller) into a vector driving expression from a human *keratin 14* promoter faithfully expressed in the interfollicular epidermis and outer root sheath of hair follicles (Vasioukhin et al., 1999). For timed pregnancies, the morning of a vaginal plug was considered embryonic day E0.5.

Histology, immunofluorescence, and in situ hybridizations

Tissues were embedded in OCT (Tissue-Tek) and immediately frozen on dry ice. Sections of 10μm were cut with a cryostat onto glass slides, fixed in 4% paraformaldehyde for 8 minutes, and subjected to immunofluorescence microscopy or hematoxylin/eosin staining. When applicable, the MOM Basic Kit (Vector Labs) was used to prevent non-specific binding of mouse monoclonal antibodies. Otherwise, stainings were performed in phosphate buffered saline (PBS) with 0.1% Triton X-100, 2.5% normal donkey serum, and 2.5% normal goat serum. BrdU unmasking involved treatment with 1M HCl at 37°C for 45 minutes prior to blocking. Primary antibodies were incubated overnight at 4°C and secondary antibodies at room temperature for 1 hour. Slides were washed after antibody incubations with PBS for 5 minutes, three times. Antibodies and dilutions used: Lhx2 (rabbit, 1:2500; T. Jessell, Columbia); P- and E-cadherins (rat, 1:100; M. Takeichi, Riken, Kobe); α6-integrin (rat, 1:100; Pharmingen); K5 (rabbit, 1:500; Fuchs lab); K1 (rabbit, 1:500; Fuchs lab); K17 (rabbit, 1:5000; P. Coulombe, Johns Hopkins); Filaggrin (rabbit, 1:500; Covance); β4-integrin (rat, 1:100; Pharmingen); CD34 (rat, 1:100; Pharmingen); Tenascin C (mouse, 1:500; IBL); S100A6 (rabbit, 1:100; Lab Vision); BrdU (rat, 1:500; Abcam); Tcf3 (guinea pig, 1:300; Fuchs lab); Sox9 (rabbit, 1:100; Santa Cruz); Nfatc1 (mouse, 1:100;

Santa Cruz); Lef1 (rabbit, 1:250; Fuchs lab); Gata3 (mouse, 1:100; Santa Cruz); K6 (rabbit, 1:500; Fuchs lab); AE13 and AE15 (mouse, 1:50; T.T. Sun, NYU); HA (rat, 1:100; Roche); FITC (1:100; Jackson) or Alexa594 (1:1000; Molecular Probes) conjugated secondary antibodies. Nuclei were stained with 4'6'-diamidino-2-phenylindole (DAPI; 1:10000) in a single wash step after staining. Slides were mounted with antifade. Imaging was performed using Zeiss Axioskop and Axiophot microscopes equipped with Spot RT (Diagnostic Instruments) and Axiocam (Zeiss) digital cameras, respectively.

Engraftment and BrdU experiments

Full thickness skins were removed from the torsos of sex-matched wild type and *Lhx2* null E15.5 embryos, and placed onto the backs of anesthetized female *nude* recipient mice, with each recipient receiving a wild-type and knockout graft. Grafts were secured by sterile gauze and cloth bandages, which were removed after healing (12-13 days). Hairs typically appeared within 1 week after grafting. A total of forty grafts were placed (20 wild-type and 20 knockout) and each showed a consistent phenotype dependent on the presence or absence of Lhx2 in the donor skin. Newborn back skins were similarly grafted for the *K14-Lhx2* transgenic mice. The day of engraftment was considered day 0.

5'-bromo-2'-deoxyuridine (BrdU, Sigma) pulse-chase experiments were performed as described. For BrdU pulse-chase experiments, intra-peritoneal injections of 50μg/g BrdU were carried out twice a day for 3 days at day 26 to 28 post-graft and analyzed 4 weeks later for label retention. For cell cycle analysis, mice were injected once with 50μg/g BrdU at day 40 or 8 weeks post-graft and analyzed 4 hours later for BrdU incorporation. A minimum of 4 grafts (two wild-type and two knockout) were used for each BrdU experiment.

Flow cytometry analysis

For grafted skin, single cell suspensions of total skin were prepared by dissecting the graft, removing subcutaneous fat, mincing into small pieces, and sequential treatment with collagenase (Sigma, 2.5mg/mL) in Hanks' balanced salt solution (Cambrex) for 1 hour and trypsin with EDTA (Gibco, 0.25%) for 15 minutes at 37°C. Between treatments, the tissue was triturated with PBS using a pipet and spun down. Cells were neutralized with culture media (E high calcium) and strained (40μM pores; BD Biosciences). Single cells were resuspended in PBS containing 5% fetal bovine serum at a maximum concentration of 10^7 cells/mL and minimum volume of 100μL, and stained with primary antibodies coupled to biotin for 30 minutes on ice. After washing once with PBS, cells were stained with streptavidin and antibodies directly conjugated to specific fluorophores for 30

minutes on ice. Cells were washed once in PBS and resuspended in 300ng/mL propidium iodide for dead cell exclusion. All centrifugation steps were performed at 300xg for 5 minutes at 4°C. BrdU detection was subsequently performed using BrdU Flow Kit (Pharmingen). Flow cytometry analysis was performed on a FACSort equipped with CellQuest (BD Biosciences). Antibodies used for FACS: CD34 conjugated to biotin (1:50, Pharmingen), α6-integrin coupled to PE (1:100, Pharmingen); streptavidin-APC (1:200, Pharmingen).

Barrier function assay

After dissection, the grafted skin exterior was exposed for 4 hours at 37°C in a solution of 100mM $NaPO_4$, 1.3mM $MgCl_2$, 3mM $K_3Fe(CN)_6$, 3mM $K_4Fe(CN)_6$, 0.01% sodium deoxycholate, 0.01% sodium dodecyl sulfate, and 1mg/mL X-gal (Eppendorf), which was adjusted to a pH of 4.5 with HCl. At this pH in the absence of an epidermal barrier, the solution will penetrate the epidermis causing endogenous β-galactosidase activity to catalyze X-gal into a blue precipitate. The dermal interior was placed on PBS to prevent drying out.

RNA isolation and semi-quantitative RT-PCR

Total RNA from FACS sorted cells was isolated using the Absolutely RNA Microprep kit (Stratagene) and quantified using Ribogreen (Molecular Probes).

Normalized RNA quantities were reverse transcribed with Superscript III using oligo-dT primers (Invitrogen). Typically, 30ng of total RNA was reverse transcribed into a 20μL volume of cDNA, which was then diluted 12-fold. One microliter of this working stock was used as template for PCR reactions: 2.5μL of 10X PCR buffer with $MgCl_2$, 0.5μL of 10mM dNTPs, 0.25μL of AmpliTaq DNA polymerase (Applied Biosystems), 0.5μL each of forward and reverse primers at 20mM, 1μL of template DNA, and 19.75μL of H_2O. PCR amplification of selected genes of interest was performed using primers designed to produce a product spanning exon/intron boundaries. Primers were designed using PrimerSelect of Lasergene (DNAStar) to work at the following settings: initial denaturing at 94°C for 3 minutes; 27-36 cycles of 20 seconds at 94°C denaturing, 30 seconds at 60°C annealing, and 45 seconds at 72°C extension. Primers used:

gapdh: 5'-cgtagacaaaatggtgaaggtcgg-3'; 5'-aagcagttggtggtgcaggatg-3'
lhx2: 5'-gcccgggccaagttcag-3'; 5'-gggggtggcgagtcattaga-3'
lhx9: 5'-ctccggaccatgaaatcctacttt-3'; 5'-ctcgctcttttgttaaaccacacg-3'
tcf3: 5'-tctcaagccggttcccacac-3'; 5'-tttccgggcaagctcatagtattt-3'
sox9: 5'-cggcggaggaagtcggtgaagaac-3'; 5'-ggtgggtgcggtgctgctgatg-3'
K5: 5'-aacattttggggtctgggtcac-3'; 5'-ggcccacagagactgcttcttt-3'
β4: 5'-tcgtgggtagagcagcagaggaa-3'; ccactggtgttcactgccctaagc-3'

Transient transfections and western blots

Murine keratinoctyes were cultured in E low calcium media. At approximately 40% confluence, cells were transfected with FuGene 6 reagent (Roche) at a 3:1 FuGene:DNA ratio and harvested after two days. For

immunofluorescence, cells in a 24-well plate on glass coverslips were transfected with 0.3μg of total DNA and processed as described above. For immunoblotting, cells in a 6-well plate were transfected with 1.5μg of total DNA. Cells were directly lysed in 2X sample buffer (250mM Tris pH 6.8, 4% sodium dodecyl sulfate, 10% glycerol, 0.1% bromophenol blue, 2% β-mercaptoethanol), scraped, and boiled for 5 minutes. Proteins were resolved using SDS-polyacrylamide gel electrophoresis, semi-dry transferred onto nitrocellulose membrane, probed with antibodies in 5% non-fat dry milk, and detected by ECL (Amersham Biosciences). Primary antibodies were incubated overnight at 4°C and secondary antibodies at room temperature for 1 hour. Blots were washed after antibody incubations with PBS-T (0.1% Tween-20 in PBS) for 10 minutes, three times. Antibodies and dilutions used: Lhx2/Lhx9 (rabbit, 1:8000; T. Jessell, Columbia); anti-HA (rat, 1:1000; Roche); HRP conjugated secondary antibodies (1:5000; Jackson).

CHAPTER 4
SUMMARY AND PERSPECTIVES

During development, genetically identical cells acquire specific characteristics unique to its function through the activation and repression of genes. To investigate the molecular regulation of hair follicle morphogenesis, early hair progenitors and basal epidermal keratinocytes were selectively isolated from embryonic skin using cell surface markers by exploiting their differential expression of P-cadherin. Comparing the gene expression profiles of these isolated cell populations revealed transcriptional differences that occur as hair follicles are specified from the epithelium and undergo subsequent development. In addition to expressing signaling molecules already implicated in hair morphogenesis, embryonic hair progenitors adopted a distinct set of transcriptional regulators and repressed other regulators of epidermal differentiation. These functionally significant genes validate and lay the foundation to probe into the roles of the many other uncharacterized genes in hair follicle and epidermal development.

Origins of hair follicle stem cells

Most notably, the embryonic hair progenitors displayed a strong molecular resemblance to adult follicle stem cells, indicating functional similarities between

the two cell types. This is not too surprising considering that embryonic hair progenitors and adult stem cells share many common features with each other. Both cell types are undifferentiated, yet capable of differentiating into lineages of the entire follicle. The induction of hair morphogenesis from embryonic ectoderm also parallels the activation of adult stem cells during initiation of hair renewal. Both processes rely on a dermal component and utilize the same signaling pathways to mediate their epithelial-mesenchymal interactions. These similarities suggest the possibility that embryonic hair progenitors are counterparts to adult follicle stem cells, and that the commonly expressed genes regulate attributes shared by both cell types. However, the best characterized and most specific marker of hair follicle stem cells, CD34, only becomes apparent upon completion of the initial morphogenetic hair cycle at approximately three weeks of age in mice. Stem cells should theoretically exist prior to this time to supply the growing hair and contribute to epidermal wound healing, but the lack of molecular markers to identify these putative cells has precluded studies to trace the origins of the hair follicle stem cell niche. Thus, questions have remained as to when and how, if at all, stem cells are specified and set aside during development.

This study provides two lines of direct evidence, in addition to their similarities in gene expression, that demonstrate that stem cells exist during hair follicle morphogenesis and are likely specified upon embryonic hair induction.

First, label retaining cells were identified in a presumptive bulge compartment of developing hair follicles which later became CD34 positive stem cells in adult follicles. Since embryonic skin was pulse-labeled before this compartment formed, the label retaining cells, a hallmark of adult stem cells, probably originated from early hair progenitors. Second, expression of Lhx2, which was identified in the PCAD+ cells of the microarray screen, was also localized to the same presumptive bulge compartment. Present in both embryonic hair progenitors and adult stem cells, Lhx2 expression is lost in the absence of hair induction but is expanded when stem cells are unable to differentiate. Thus Lhx2's initial expression in hair placodes, concentration to the presumptive bulges of developing follicles, and final localization in adult follicle bulges, lend support to the specification of stem cells upon embryonic hair induction and the existence of a stem cell niche during hair morphogenesis.

Furthermore, Lhx2 was functionally demonstrated to regulate characteristics of hair follicle stem cells. Without Lhx2, fewer hair follicles are induced during embryogenesis and those that do form prematurely activate bulge stem cells and differentiate when hair follicles normally should be at rest. Leading up to this stem cell defect, *Lhx2* null hair follicles have diminished CD34 expression and lose label retaining abilities. Thus, loss of Lhx2 results in loss of stem cell character, whereby fewer stem cells are specified to initiate hair

morphogenesis and become more susceptible to differentiate. On the other hand, gain of Lhx2 expression inhibits terminal differentiation and promotes the acquisition of hair stem cell markers. Lhx2 therefore maintains hair follicle stem cell character by keeping them in a undifferentiated, quiescent state.

Although Lhx2 appears to link the specification of embryonic hair progenitors to the maintenance of adult follicle stem cells, more functional studies are needed to conclusively show that stem cells directly arise from the induction of hair follicle morphogenesis. With the ability to isolate and purify embryonic hair progenitors, many of the assays used to establish the proliferative potential and multipotency of adult bulge stem cells can now be applied to hair placode cells. For example, isolated embryonic hair progenitors can be cultured *in vitro* to assess their clonogenicity and self-renewal capacity through serial passage. Although lineage analysis from the *Shh* promoter clearly indicates that the entire hair follicle and bulge are derived from the hair placode (Levy et al., 2005), the multipotency of embryonic hair progenitors can be evaluated at the single cell level through transplantation experiments of isolated cells. These experiments will not only demonstrate that embryonic hair progenitors possess fundamental stem cell characteristics, but also support the notion for the hair placode as the embryonic origin of bulge stem cells.

Regulation of hair follicle stem cells

Elucidating molecular details by which Lhx2 acquires and maintains stem cell character will also further our understanding into the specification and development of the stem cell niche. Identifying genes directly regulated by Lhx2 will be important in this regard. The ability of transgenic Lhx2 expression to alter the genetic program of epidermal cells into a hair follicle stem cell lineage supports the possibility that Lhx2 could act as a master regulator of hair follicle determination through target genes. Additionally, identifying interacting proteins with Lhx2 will also be useful in analyzing its regulatory mechanisms. Through their LIM domains, LIM-HD transcription factors are well known to interact with a variety of transcriptional regulators to direct the fate of progenitor cells during development, especially of the nervous system (Curtiss and Heilig, 1998; Bach, 2000). In this combinatorial manner, distinct complexes of LIM-HD factors determine the unique identity of cells through the activation of transcriptional targets. Interestingly, Lhx2 is the only LIM-HD family member expressed at significant levels in the skin by microarray analysis. This suggests that Lhx2 may play a primary role in specifying the hair follicle stem cell lineage and distinguishing it from the surrounding embryonic ectoderm during induction of hair morphogenesis.

However, Lhx2 also functions in postnatal stem cells by maintaining their quiescence during the resting phase of the hair cycle. Although the specification of stem cells during embryogenesis appears to be distinct from the maintenance of adult stem cell quiescence, both functions of Lhx2 can be reconciled considering the co-localization of label retaining cells and Lhx2 expression in the developing stem cell niche. Nucleotide label retention is an indication of slow-cycling cells and the correlation of these cells with Lhx2 expression in both developing and mature hair follicle bulges suggests that maintaining quiescence and hence stem cell character may be a fundamental function of Lhx2 in hair follicles. Unfortunately, testing the label retaining ability of developing bulges in *Lhx2* null hair follicles was difficult given the need to graft the skin, and preliminary results were inconclusive. Additional studies are also needed to evaluate the long-term consequences of Lhx2 loss in hair follicles. Although stem cells precociously activate new rounds of hair growth even beyond the second telogen stage, it remains unknown if *Lhx2* null stem cells have defects in self-renewal resulting in niche depletion and progressive loss of hair follicles. Currently, the oldest skin graft is approximately one year old and the *Lhx2* knockout shows a thinner hair coat relative to wild-type. Despite the need for more conclusive studies, the embryonic and postnatal phenotypes of the *Lhx2* null mice can be explained by a loss in hair follicle stem cell character, particularly in their quiescent properties.

Identifying Lhx2 interacting proteins and their transcriptional targets within the embryonic hair progenitors and adult stem cells will determine how Lhx2 can modulate this critical function to maintain the stem cell niche. An attractive hypothesis is whether Lhx2 can sustain a Wnt-inhibited microenvironment in the bulge, since increased Wnt signaling also leads to precocious stem cell activation. Interestingly, both embryonic hair progenitors and adult bulge stem cells express several secreted Wnt antagonists, including at least two in common, Dkk3 and Wif1.

Characterizing other signature genes shared by embryonic hair progenitors and adult bulge stem cells will undoubtedly reveal additional insights into fundamental features of hair follicle stem cells. Together these genes may cooperatively regulate the specification and maintenance of hair follicle stem cells during development. Along with their similarities, there obviously are molecular differences between embryonic hair progenitors and adult stem cells, which could be a reflection of the distinct morphological environment in which these two cell types function. For instance, embryonic hair progenitors are specified from a layer of ectoderm lacking a defined niche, while adult stem cells are in contact with mature dermal papillae cells in a well innervated and vascularized niche. In some respect, embryonic hair progenitors may actually be a more primitive cell since they must organize into a functional stem cell niche before differentiating into

more mature hair lineages. Thus, the genes shared in common such as Lhx2 are most likely to be directly involved in the specification and maintenance of hair follicle stem cells throughout morphogenesis and postnatal life.

Aside from their similarities in gene expression, the same signaling pathways also regulate the specification of embryonic hair progenitors and the activation of follicle stem cells. Determining how these signals affect the expression and activity of intrinsic factors required for the maintenance of stem cells like Lhx2 is essential in understanding their mechanisms to govern stem cell behavior. One goal of this study was to discover genetic targets of the multiple signals that converge to regulate hair follicle morphogenesis, but their co-expression in the transcriptional profile of embryonic hair progenitors makes it difficult to discern any candidate genes without secondary screens. However the molecular mechanisms of these pathways can begin to be dissected by applying the techniques developed here on various genetic mutants of signaling pathways that affect hair morphogenesis. By isolating and transcriptionally profiling embryonic hair progenitors of *Shh*, *Noggin*, and *Tgf-β2* null mice, one can evaluate genes regulated by specific signaling pathways and their impact on hair follicle development. Combining this expression data with genome-wide chromatin immunoprecipitation using antibodies against transcriptional mediators of these pathways will be powerful in determining genes directly regulated by

these signals during hair follicle morphogenesis. Furthermore, the hierarchy of signaling events can be organized to analyze the sequential or convergent molecular controls during induction and morphogenesis of hair follicles.

Implications beyond hair follicles

In addition to the hair follicle, a variety of other stem cell systems utilize the same signaling pathways to regulate self-renewal and lineage commitment (Fuchs et al., 2004; Moore and Lemischka, 2006). Even more remarkable is the recurrence of these signals in guiding the development of tissues and organs which employ the formation of placodes. From as early as neural induction to the formation of nearly every ectodermally derived appendage, these conserved developmental pathways drive analogous cellular processes during morphogenesis (Hogan, 1999; Pispa and Thesleff, 2003). This begs the question of when and how unique cell fates are determined to favor the formation of one structure instead of another. The answer may lie in the local balance of competing transcriptional regulators which integrate spatial and temporal cues to direct a distinct genetic program for different lineages. This appears to be the case in the induction and differentiation of cranial sensory placodes where gene regulatory networks composed of transcription factors activate sets of "placode-specific" enhancers (Baker and Bronner-Fraser, 2001; Bhattacharyya and Bronner-Fraser, 2004).

Isolating the placodes of these other organs, particularly of appendages of the skin such as sweat and mammary glands, and comparing their expression profiles to those of the hair follicle placode will discern both common themes and unique aspects of individual morphogenetic processes downstream of shared signaling pathways.

A complete understanding of the molecular events in the development of these tissues and organs have therapeutic implications, particularly if they involve the specification of stem cells. Knowledge of normal morphogenesis and stem cell function will also aid in diagnosis and treatment when this process goes awry in disease. Much more work lies ahead, but the hope of manipulating stem cells to control regeneration and repair in the clinic is promising.

APPENDIX
COMPLETE MICROARRAY DATA

The following is a comprehensive list of the 1394 differentially expressed genes in the sorted cell populations. Signal values of Affymetrix probe sets and their annotated genes upregulated ≥2-fold in either the PCAD+ hair progenitors or PCAD– interfollicular keratinocytes relative to the other is provided. The Mean Log2 Ratio is calculated for PCAD+ with respect to PCAD– mean signal values.

Probe Set ID	UniGene Name	UniGene Symbol	Mean Log2 Ratio	PCAD+ Signal		PCAD- Signal	
				1	2	1	2
1425425_a_at	Wnt inhibitory factor 1	Wif1	**6.02**	2731	2330	51	27
1455280_at	Fras1 related extracellular matrix protein 1	Frem1	**5.15**	1325	1213	40	32
1416846_a_at	PDZ domain containing RING finger 3	Pdzrn3	**4.91**	9934	7866	361	227
1427053_at	RIKEN cDNA 5033411B22 gene	5033411B22Rik	**4.79**	473	473	18	17
1449530_at	trichorhinophalangeal syndrome I (human)	Trps1	**4.39**	1266	1344	70	54
1427054_s_at	RIKEN cDNA 5033411B22 gene	5033411B22Rik	**4.36**	2064	2325	103	111
1416561_at	glutamic acid decarboxylase 1	Gad1	**4.32**	397	288	19	14
1434286_at	trichorhinophalangeal syndrome I (human)	Trps1	**4.27**	608	597	39	23
1418317_at	LIM homeobox protein 2	Lhx2	**4.18**	7738	5952	450	300
1435349_at	neuropilin 2	Nrp2	**4.10**	7272	5570	456	284
1446929_at	BTB and CNC homology 2 (Bach2), mRNA	Bach2	**4.05**	3820	2920	204	198
1437667_a_at	BTB and CNC homology 2	Bach2	**4.03**	8000	5534	411	401
1434195_at	protease, serine, 35	Prss35	**3.96**	2667	2887	233	124
1457445_at	trichorhinophalangeal syndrome I (human)	Trps1	**3.90**	2800	3173	249	151
1436869_at	sonic hedgehog	Shh	**3.89**	13860	12748	1084	707
1440304_at	RIKEN cDNA E030004N02 gene	E030004N02Rik	**3.80**	4028	3243	267	250
1450065_at	adenylate cyclase 7	Adcy7	**3.79**	1727	1276	132	83
1427168_a_at	procollagen, type XIV, alpha 1	Col14a1	**3.79**	8956	7752	763	438
1436515_at	RIKEN cDNA E030004N02 gene	E030004N02Rik	**3.74**	9455	6722	619	576
1448870_at	latent transforming growth factor beta binding p	Ltbp1	**3.73**	556	432	41	33
1438214_at	trichorhinophalangeal syndrome I (human)	Trps1	**3.73**	3737	3386	362	174
1447343_at	neuropilin 2	Nrp2	**3.72**	1214	987	96	71
1420753_at	tolloid-like	Tll	**3.70**	1560	1563	149	91
1456307_s_at	adenylate cyclase 7	Adcy7	**3.69**	9337	6953	840	406
1426528_at	neuropilin 2	Nrp2	**3.68**	9358	8642	808	597
1455961_at	membrane metallo endopeptidase	Mme	**3.64**	1849	1346	133	121
1443161_at	Trichorhinophalangeal syndrome I (human)	Trps1	**3.62**	2186	1934	245	91
1442605_at	BTB and CNC homology 2 (Bach2), mRNA	Bach2	**3.60**	1923	1725	173	128
1438532_at	Similar to hemicentin; fibulin 6 (LOC240793), m	NA	**3.59**	744	709	73	47
1440339_at	RIKEN cDNA 4833416E15 gene	4833416E15Rik	**3.55**	3635	4031	273	378
1440026_at	Trichorhinophalangeal syndrome I (human)	Trps1	**3.55**	1705	1858	190	115
1450922_a_at	transforming growth factor, beta 2	Tgfb2	**3.52**	928	750	95	51
1441657_at	BTB and CNC homology 2 (Bach2), mRNA	Bach2	**3.51**	745	563	61	53
1456778_at	neuropilin 2	Nrp2	**3.50**	2668	2498	267	191
1426640_s_at	tribbles homolog 2 (Drosophila)	Trib2	**3.49**	4357	5099	560	278
1428347_at	cytoplasmic FMR1 interacting protein 2	Cyfip2	**3.41**	404	338	34	35
1450923_at	transforming growth factor, beta 2	Tgfb2	**3.41**	4148	3313	433	263
1416967_at	SRY-box containing gene 2	Sox2	**3.36**	258	216	28	18
1436002_at	RIKEN cDNA C230013L11 gene	C230013L11Rik	**3.34**	2083	1526	170	183
1417155_at	neuroblastoma myc-related oncogene 1	Nmyc1	**3.32**	5929	4936	614	469
1426766_at	RIKEN cDNA 6330403K07 gene	6330403K07Rik	**3.30**	1930	1940	238	154
1447174_at	Dachshund 1 (Drosophila)	Dach1	**3.28**	632	742	86	56
1455865_at	insulinoma-associated 1	Insm1	**3.28**	253	137	18	20
1434881_s_at	potassium channel tetramerisation domain cont	Kctd12	**3.28**	1536	1697	174	158
1435399_at	RIKEN cDNA 2310068J10 gene	2310068J10Rik	**3.27**	859	845	104	72
1436555_at	expressed sequence AI158848	AI158848	**3.23**	6564	7114	772	688
1433743_at	dachshund 1 (Drosophila)	Dach1	**3.22**	1037	703	122	62
1455277_at	Hedgehog-interacting protein	Hhip	**3.17**	317	430	43	39
1417336_a_at	synaptotagmin-like 4	Sytl4	**3.15**	812	906	90	103
1423250_a_at	transforming growth factor, beta 2	Tgfb2	**3.14**	1030	770	108	94
1454613_at	Dihydropyrimidinase-like 3	Dpysl3	**3.11**	1836	2828	303	227
1436173_at	deleted in liver cancer 1	Dlc1	**3.06**	2681	2534	326	299
1440177_at	hypothetical protein 9630027E11	9.63E+17	**3.02**	140	94	12	16
1425874_at	homeo box C13	Hoxc13	**2.95**	1027	857	130	113
1460602_at	deleted in liver cancer 1	Dlc1	**2.94**	2334	1762	290	238
1447227_at	Solute carrier family 40 (iron-regulated transpor	Slc40a1	**2.94**	890	766	133	82
1424683_at	RIKEN cDNA 1810015C04 gene	1810015C04Rik	**2.91**	3977	3785	552	482
1450988_at	G protein-coupled receptor 49	Gpr49	**2.86**	1064	1260	174	146
1437218_at	fibronectin 1	Fn1	**2.84**	741	662	103	93
1435396_at	expressed sequence C85317	C85317	**2.81**	2237	2387	351	309
1437360_at	Protocadherin 19	Pcdh19	**2.81**	435	464	62	66
1457042_at	Transcribed sequences	NA	**2.81**	293	258	33	45
1436329_at	early growth response 3	Egr3	**2.79**	4346	3845	718	464
1456901_at	A disintegrin-like and metalloprotease (reprolysi	Adamts20	**2.78**	196	140	22	26
1429088_at	limb-bud and heart	Lbh	**2.76**	677	545	105	74
1450770_at	RIKEN cDNA 3632451O06 gene	3632451O06Rik	**2.72**	776	680	118	102
1436759_x_at	calponin 3, acidic	Cnn3	**2.71**	2928	3178	535	398
1456611_at	RIKEN cDNA D430015B01 gene	D430015B01Rik	**2.69**	2088	1979	322	306
1443263_at	BTB and CNC homology 2 (Bach2), mRNA	Bach2	**2.69**	1530	1052	221	172
1447831_s_at	myotubularin related protein 7	Mtmr7	**2.66**	163	109	20	22
1441956_s_at	Cut-like 1 (Drosophila), transcript variant 2, mR	Cutl1	**2.65**	1100	797	141	156
1424704_at	runt related transcription factor 2	Runx2	**2.65**	1095	1177	170	191

1458220_at	deleted in liver cancer 1	Dlc1	**2.63**	1151	662	157	126
1423259_at	inhibitor of DNA binding 4	Idb4	**2.61**	1195	1271	190	214
1446141_at	Transforming growth factor, beta 2	Tgfb2	**2.60**	1670	1023	251	182
1436836_x_at	calponin 3, acidic	Cnn3	**2.58**	2657	3000	564	380
1428572_at	brain abundant, membrane attached signal prot	Basp1	**2.56**	9068	8067	1426	1479
1443044_at	hypothetical A830091E24	A830091E24	**2.54**	257	181	38	36
1425749_at	syntaxin binding protein 6 (amisyn)	Stxbp6	**2.54**	1370	1419	260	219
1426642_at	fibronectin 1	Fn1	**2.53**	10050	9975	1833	1630
1437385_at	Transcribed sequences	NA	**2.53**	830	458	105	109
1419276_at	ectonucleotide pyrophosphatase/phosphodieste	Enpp1	**2.52**	344	367	58	65
1458739_at	Latent transforming growth factor beta binding p	Ltbp1	**2.51**	1254	646	176	140
1438303_at	transforming growth factor, beta 2	Tgfb2	**2.51**	302	253	60	37
1460578_at	FYVE, RhoGEF and PH domain containing 5	Fgd5	**2.50**	308	448	69	62
1436218_at	leucine-rich repeat-containing G protein-couple	Lgr6	**2.49**	3471	3647	692	577
1454830_at	fibrillin 2	Fbn2	**2.48**	335	235	56	44
1455570_x_at	calponin 3, acidic	Cnn3	**2.47**	2850	3066	616	450
1429549_at	procollagen, type XXVII, alpha 1	Col27a1	**2.47**	3756	3479	651	656
1429506_at	naked cuticle 1 homolog (Drosophila)	Nkd1	**2.46**	514	544	77	116
1450627_at	progressive ankylosis	ank	**2.46**	5382	4562	1191	614
1420425_at	PR domain containing 1, with ZNF domain	Prdm1	**2.45**	1034	1068	246	138
1419724_at	ectodysplasin-A receptor	Edar	**2.44**	3788	3830	763	636
1456380_x_at	calponin 3, acidic	Cnn3	**2.42**	1253	1417	273	225
1433490_s_at	erythrocyte protein band 4.1-like 2	Epb4.1l2	**2.42**	2222	2427	454	415
1428896_at	platelet-derived growth factor receptor-like	Pdgfrl	**2.42**	225	174	34	40
1428209_at	brain expressed X-linked 4	Bex4	**2.42**	548	335	94	66
1440465_at	Cut-like 1 (Drosophila), transcript variant 2, mR	Cutl1	**2.42**	465	561	84	106
1419485_at	forkhead box C1	Foxc1	**2.41**	271	292	62	44
1456211_at	NACHT, leucine rich repeat and PYD containing	Nalp10	**2.41**	254	249	52	43
1456292_a_at	vimentin	Vim	**2.39**	113	160	21	30
1455145_at	14, 17 days embryo head cDNA, RIKEN full-len	NA	**2.38**	671	710	135	131
1450928_at	inhibitor of DNA binding 4	Idb4	**2.38**	6461	6145	1307	1115
1454890_at	angiomotin	Amot	**2.37**	741	748	164	123
1459546_s_at	ectonucleotide pyrophosphatase/phosphodieste	Enpp1	**2.37**	368	383	56	89
1423260_at	inhibitor of DNA binding 4	Idb4	**2.37**	882	924	153	198
1444780_at	RIKEN cDNA 5330421F07 gene	5330421F07Rik	**2.37**	701	528	124	112
1434909_at	Ras-related GTP binding D	Rragd	**2.36**	3334	3492	747	587
1422869_at	c-mer proto-oncogene tyrosine kinase	Mertk	**2.35**	547	401	113	71
1455256_at	TRAF2 and NCK interacting kinase	Tnik	**2.34**	1048	1026	257	152
1456111_at	hypothetical protein C130036J11	C130036J11	**2.33**	1287	1224	269	229
1423607_at	lumican	Lum	**2.27**	366	299	83	55
1434325_x_at	protein kinase, cAMP dependent regulatory, typ	Prkar1b	**2.27**	411	315	78	71
1454742_at	RasGEF domain family, member 1B	Rasgef1b	**2.27**	919	983	178	216
1439852_at	Transcribed sequences	NA	**2.27**	2154	1808	368	450
1433583_at	zinc finger protein 365	Zfp365	**2.26**	470	511	101	104
1416776_at	crystallin, mu	Crym	**2.25**	138	135	30	27
1417061_at	solute carrier family 40 (iron-regulated transport	Slc40a1	**2.25**	5078	4173	1130	802
1443544_at	Transcribed sequences	NA	**2.25**	347	316	58	81
1416221_at	follistatin-like 1	Fstl1	**2.24**	1843	1895	429	359
1417359_at	microfibrillar-associated protein 2	Mfap2	**2.24**	1855	1644	412	327
1440593_at	12 days embryo eyeball cDNA, RIKEN full-lengt	NA	**2.23**	4632	4444	1035	901
1438354_x_at	calponin 3, acidic	Cnn3	**2.23**	205	199	53	33
1438894_at	Transcribed sequences	NA	**2.23**	260	259	72	39
1457859_at	ADP-ribosylation factor related protein 2	Arfrp2	**2.22**	869	689	177	155
1434172_at	cannabinoid receptor 1 (brain)	Cnr1	**2.22**	363	212	54	65
1450505_a_at	RIKEN cDNA 1810015C04 gene	1810015C04Rik	**2.22**	405	277	81	63
1439468_at	BTB and CNC homology 2 (Bach2), mRNA	Bach2	**2.22**	1008	730	179	188
1418028_at	dopachrome tautomerase	Dct	**2.20**	704	1011	122	244
1418723_at	endothelial differentiation, lysophosphatidic acid	Edg7	**2.20**	458	548	127	91
1448259_at	follistatin-like 1	Fstl1	**2.20**	3740	3911	900	767
1438306_at	ring finger protein 180	Rnf180	**2.20**	2510	2007	509	469
1422912_at	bone morphogenetic protein 4	Bmp4	**2.19**	880	661	158	177
1422643_at	monooxygenase, DBH-like 1	Moxd1	**2.18**	5488	5646	1396	1069
1446525_at	Glypican 3, mRNA (cDNA clone MGC:35964 IM	Gpc3	**2.17**	694	570	154	126
1439766_x_at	vascular endothelial growth factor C	Vegfc	**2.17**	85	109	21	21
1459619_at	erythrocyte protein band 4.1-like 2	Epb4.1l2	**2.16**	1170	1263	248	296
1417111_at	mannosidase 1, alpha	Man1a	**2.16**	3026	2592	655	601
1438118_x_at	vimentin	Vim	**2.16**	165	239	37	52
1428455_at	procollagen, type XIV, alpha 1	Col14a1	**2.15**	724	606	140	158
1449822_at	atonal homolog 1 (Drosophila)	Atoh1	**2.14**	339	234	75	52
1422655_at	patched homolog 2	Ptch2	**2.14**	4094	4103	942	921
1434136_at	RIKEN cDNA 6332401O19 gene	6332401O19Rik	**2.14**	88	62	17	17
1441539_at	0 day neonate lung cDNA, RIKEN full-length en	NA	**2.12**	659	645	152	148
1460604_at	cytochrome b reductase 1	Cybrd1	**2.12**	132	89	22	28
1417377_at	immunoglobulin superfamily, member 4A	Igsf4a	**2.12**	5125	4096	1076	1026

1429178_at	odd Oz/ten-m homolog 3 (Drosophila)	Odz3	**2.12**	2293	2463	573	524
1434683_at	Cut-like 1 (Drosophila), transcript variant 2, mR	Cutl1	**2.12**	1134	1005	244	249
1443240_at	Glypican 3, mRNA (cDNA clone MGC:35964 IM	Gpc3	**2.12**	3607	4188	879	908
1437347_at	endothelin receptor type B	Ednrb	**2.11**	387	726	72	175
1458205_at	Mannosidase 1, alpha, mRNA (cDNA clone MG	Man1a	**2.10**	522	477	128	105
1452309_at	cingulin-like 1	Cgnl1	**2.10**	2572	2532	602	592
1438441_at	Inhibitor of DNA binding 4	Idb4	**2.10**	137	175	33	39
1422592_at	catenin delta 2	Catnd2	**2.09**	274	314	68	70
1455180_at	expressed sequence AA407270	AA407270	**2.09**	187	180	40	46
1425447_at	dickkopf homolog 4 (Xenopus laevis)	Dkk4	**2.08**	267	517	98	78
1427025_at	myotubularin related protein 7	Mtmr7	**2.08**	425	405	106	91
1455262_at	Transcribed sequences	NA	**2.08**	408	385	113	74
1453851_a_at	growth arrest and DNA-damage-inducible 45 ga	Gadd45g	**2.07**	1080	912	283	189
1446088_at	RIKEN cDNA 9430081I23 gene	9430081I23Rik	**2.07**	1665	1433	475	261
1423274_at	DEAD/H (Asp-Glu-Ala-Asp/His) box polypeptide	Ddx26	**2.06**	1887	1836	449	446
1423278_at	protein tyrosine phosphatase, receptor type, K	Ptprk	**2.05**	2663	2570	681	583
1439060_s_at	DNA segment, Chr 11, ERATO Doi 498, expres	D11Ertd498e	**2.04**	480	413	107	109
1422864_at	runt related transcription factor 1	Runx1	**2.04**	608	447	145	110
1418176_at	vitamin D receptor	Vdr	**2.04**	802	732	193	179
1427086_at	CDNA clone IMAGE:5028619, partial cds	NA	**2.03**	399	323	89	86
1435280_at	expressed sequence AI452195	AI452195	**2.03**	1261	1100	268	306
1441779_at	RIKEN cDNA 9530006C21 gene	9530006C21Rik	**2.03**	295	474	85	98
1433471_at	transcription factor 7, T-cell specific	Tcf7	**2.03**	541	565	138	133
1455843_at	fucosyltransferase 4	Fut4	**2.02**	194	139	40	41
1429870_at	RIKEN cDNA C630040K21 gene	C630040K21Rik	**2.02**	211	193	57	43
1459136_at	BTB and CNC homology 2 (Bach2), mRNA	Bach2	**2.01**	75	29	10	13
1424098_at	ELOVL family member 7, elongation of long cha	Elovl7	**2.00**	1708	1503	501	301
1417411_at	nucleosome assembly protein 1-like 5	Nap1l5	**2.00**	310	252	71	69
1417600_at	solute carrier family 15 (H+/peptide transporter)	Slc15a2	**2.00**	5339	5490	1534	1182
1435720_at	Potassium voltage-gated channel, Shal-related	Kcnd3	**2.00**	161	245	45	54
1438619_x_at	zinc finger, DHHC domain containing 14	Zdhhc14	**2.00**	359	348	84	93
1446720_at	Activated leukocyte cell adhesion molecule	Alcam	**1.99**	1793	1577	491	355
1415949_at	carboxypeptidase E	Cpe	**1.99**	538	544	157	116
1436076_at	discs, large (Drosophila) homolog-associated pr	Dlgap1	**1.99**	142	387	60	58
1447567_at	Odd Oz/ten-m homolog 3 (Drosophila)	Odz3	**1.99**	213	157	50	42
1444432_at	RIKEN cDNA D330040H18 gene	D330040H18Rik	**1.99**	338	302	94	67
1452583_s_at	galactose mutarotase	Galm	**1.98**	447	715	136	151
1423091_a_at	glycoprotein m6b	Gpm6b	**1.98**	4945	5300	1555	1048
1450723_at	ISL1 transcription factor, LIM/homeodomain (isl	Isl1	**1.98**	239	181	59	46
1415834_at	dual specificity phosphatase 6	Dusp6	**1.97**	4312	4387	1235	986
1436551_at	fibroblast growth factor receptor 1	Fgfr1	**1.97**	860	1015	262	213
1460431_at	glucosaminyl (N-acetyl) transferase 1, core 2	Gcnt1	**1.97**	360	348	94	87
1422648_at	solute carrier family 7 (cationic amino acid trans	Slc7a2	**1.97**	245	256	63	65
1436791_at	wingless-related MMTV integration site 5A	Wnt5a	**1.97**	242	100	45	34
1440372_at	ADP-ribosylation factor related protein 2	Arfrp2	**1.96**	5712	5079	1601	1176
1425779_a_at	T-box 1	Tbx1	**1.96**	143	231	44	50
1416632_at	malic enzyme, supernatant	Mod1	**1.95**	2176	2295	636	524
1458249_at	Transcribed sequence with weak similarity to p	NA	**1.95**	158	174	46	40
1445711_at	expressed sequence BB163080	BB163080	**1.94**	137	132	38	32
1424050_s_at	fibroblast growth factor receptor 1	Fgfr1	**1.94**	489	653	152	143
1442740_at	PR domain containing 5	Prdm5	**1.93**	249	217	67	54
1446247_at	a disintegrin-like and metalloprotease (reprolysi	Adamts18	**1.92**	727	879	221	202
1458605_at	ADP-ribosylation factor related protein 2	Arfrp2	**1.92**	1005	880	275	223
1417376_a_at	immunoglobulin superfamily, member 4A	Igsf4a	**1.92**	1864	1726	473	473
1417400_at	retinoic acid induced 14	Rai14	**1.92**	2729	2775	779	671
1448502_at	solute carrier family 16 (monocarboxylic acid tra	Slc16a7	**1.92**	482	451	134	112
1437466_at	activated leukocyte cell adhesion molecule	Alcam	**1.91**	4667	4243	1312	1054
1439554_at	sex comb on midleg homolog 1	Scmh1	**1.91**	898	707	227	198
1430264_at	RIKEN cDNA 2610030P05 gene	2610030P05Rik	**1.91**	5092	4606	1356	1220
1446609_at	Transcribed sequences	NA	**1.91**	675	562	201	127
1442504_at	0 day neonate thymus cDNA, RIKEN full-length	NA	**1.90**	129	220	46	44
1448765_at	Fyn proto-oncogene	Fyn	**1.90**	202	192	56	49
1439753_x_at	sine oculis-related homeobox 4 homolog (Drosc	Six4	**1.89**	39	38	11	10
1426724_at	calponin 3, acidic	Cnn3	**1.88**	579	733	163	191
1449273_at	cytoplasmic FMR1 interacting protein 2	Cyfip2	**1.88**	415	269	91	91
1431118_at	RIKEN cDNA 6720427H10 gene	6720427H10Rik	**1.88**	993	939	284	243
1444646_at	RIKEN cDNA 8430420F16 gene	8430420F16Rik	**1.88**	831	774	239	197
1423584_at	insulin-like growth factor binding protein 7	Igfbp7	**1.87**	872	847	227	244
1456621_at	RIKEN cDNA D430015B01 gene	D430015B01Rik	**1.86**	220	168	57	49
1437614_x_at	zinc finger, DHHC domain containing 14	Zdhhc14	**1.86**	370	348	96	102
1438861_at	basonuclin 2	Bnc2	**1.85**	4881	4243	1191	1329
1441972_at	RIKEN cDNA 6230424C14 gene	6230424C14Rik	**1.85**	122	70	28	24
1420965_a_at	ectodermal-neural cortex 1	Enc1	**1.84**	2745	2245	630	760
1417378_at	immunoglobulin superfamily, member 4A	Igsf4a	**1.84**	9455	8839	2666	2442

1437431_at	Cut-like 1 (Drosophila), transcript variant 2, mR	Cutl1	**1.84**	672	577	181	166
1440878_at	runt related transcription factor 1	Runx1	**1.84**	610	504	177	134
1416688_at	synaptosomal-associated protein 91	Snap91	**1.84**	137	147	45	34
1440312_at	ELOVL family member 7, elongation of long cha	Elovl7	**1.83**	1827	1779	654	357
1440586_at	RIKEN cDNA B430203I24 gene	B430203I24Rik	**1.83**	2036	2093	605	553
1448415_a_at	sema domain, immunoglobulin domain (Ig), sho	Sema3b	**1.83**	336	389	102	102
1417455_at	transforming growth factor, beta 3	Tgfb3	**1.82**	2397	2805	766	706
1449315_at	odd Oz/ten-m homolog 3 (Drosophila)	Odz3	**1.81**	872	938	297	220
1455447_at	RIKEN cDNA D430019H16 gene	D430019H16Rik	**1.81**	516	473	143	139
1443158_at	Sex comb on midleg homolog 1	Scmh1	**1.81**	600	658	185	174
1441206_at	synaptopodin 2	Synpo2	**1.81**	166	98	36	37
1443222_at	Thymoma viral proto-oncogene 3	Akt3	**1.81**	395	402	100	127
1435832_at	leucine rich repeat containing 4	Lrrc4	**1.80**	743	901	201	269
1428902_at	carbohydrate sulfotransferase 11	Chst11	**1.80**	1465	1354	387	423
1436864_at	ADP-ribosylation factor related protein 2	Arfrp2	**1.79**	771	714	239	191
1428479_at	nuclear factor of activated T-cells, cytoplasmic,	Nfatc1	**1.79**	293	324	91	87
1429359_s_at	RNA binding protein gene with multiple splicing	Rbpms	**1.79**	110	121	33	34
1444992_at	expressed sequence AI120166	AI120166	**1.78**	1850	1773	469	588
1436223_at	PREDICTED: integrin beta 8 [Mus musculus], n	Itgb8	**1.77**	1055	1174	404	248
1447040_at	Activated leukocyte cell adhesion molecule	Alcam	**1.77**	964	818	324	197
1438896_at	DnaJ (Hsp40) homolog, subfamily C, member 6	Dnajc6	**1.77**	148	116	43	34
1439895_at	expressed sequence AU021025	AU021025	**1.77**	4635	4341	1359	1277
1434073_at	G protein-coupled receptor associated sorting p	Gprasp2	**1.77**	527	551	159	157
1439556_at	neural cell adhesion molecule 1	Ncam1	**1.77**	1112	964	370	238
1434180_at	pleckstrin homology domain containing, family C	Plekhc1	**1.77**	862	993	284	258
1441644_at	Protein tyrosine phosphatase, receptor type, K	Ptprk	**1.76**	204	183	64	51
1423341_at	chondroitin sulfate proteoglycan 4	Cspg4	**1.75**	2352	2353	695	703
1420667_at	double C2, beta	Doc2b	**1.75**	315	300	92	91
1417110_at	mannosidase 1, alpha	Man1a	**1.75**	835	861	256	249
1422552_at	reprimo, TP53 dependant G2 arrest mediator ca	Reprimo	**1.75**	189	260	73	59
1436279_at	solute carrier family 26, member 7	Slc26a7	**1.75**	86	207	32	48
1453003_at	sortilin-related receptor, LDLR class A repeats-c	Sorl1	**1.75**	2992	2132	847	660
1440770_at	B-cell leukemia/lymphoma 2	Bcl2	**1.74**	4115	3926	1266	1134
1455333_at	tensin 3	Tns3	**1.74**	2795	2704	897	747
1420731_a_at	cysteine and glycine-rich protein 2	Csrp2	**1.74**	337	253	92	83
1420589_at	hyaluronan synthase 3	Has3	**1.73**	8226	8337	2524	2479
1450191_a_at	SRY-box containing gene 13	Sox13	**1.73**	848	890	256	269
1421694_a_at	chondroitin sulfate proteoglycan 2	Cspg2	**1.72**	988	1271	316	362
1422824_s_at	epidermal growth factor receptor pathway subst	Eps8	**1.72**	827	875	267	248
1419486_at	forkhead box C1	Foxc1	**1.72**	462	417	137	130
1456862_at	sine oculis-related homeobox 4 homolog (Drosc	Six4	**1.72**	39	47	13	13
1438473_at	ADP-ribosylation factor related protein 2	Arfrp2	**1.71**	306	393	104	108
1417307_at	dystrophin, muscular dystrophy	Dmd	**1.71**	1785	1806	589	509
1441891_x_at	ELOVL family member 7, elongation of long cha	Elovl7	**1.71**	2190	2294	879	487
1421598_at	per-hexamer repeat gene 3	Phxr3	**1.71**	657	538	187	177
1429671_at	RIKEN cDNA 2410018M08 gene	2410018M08Rik	**1.71**	513	486	153	152
1455535_at	RIKEN cDNA A730017D01 gene	A730017D01Rik	**1.71**	233	190	52	77
1447204_at	Fibronectin leucine rich transmembrane protein	Flrt2	**1.70**	3666	3905	1073	1252
1419700_a_at	prominin 1	Prom1	**1.70**	1976	2187	704	577
1416165_at	RAB31, member RAS oncogene family	Rab31	**1.70**	771	578	230	180
1440840_at	RIKEN cDNA D630004K10 gene	D630004K10Rik	**1.70**	1849	1505	547	478
1416617_at	acetyl-Coenzyme A synthetase 2 (AMP forming	Acas2l	**1.69**	770	728	234	231
1424097_at	ELOVL family member 7, elongation of long cha	Elovl7	**1.69**	1977	2227	807	496
1422831_at	fibrillin 2	Fbn2	**1.69**	261	337	81	102
1442467_at	RIKEN cDNA 5330421F07 gene	5330421F07Rik	**1.69**	483	405	135	140
1441573_at	sex comb on midleg homolog 1	Scmh1	**1.69**	1887	1625	618	471
1423858_a_at	3-hydroxy-3-methylglutaryl-Coenzyme A syntha	Hmgcs2	**1.68**	389	389	125	117
1418847_at	arginase type II	Arg2	**1.68**	496	350	140	119
1434557_at	huntingtin interacting protein 1	Hip1	**1.68**	729	692	222	223
1417585_at	nucleoporin 210	Nup210	**1.68**	2193	1948	622	668
1449033_at	tumor necrosis factor receptor superfamily, mer	Tnfrsf11b	**1.68**	39	27	11	9
1438975_x_at	zinc finger, DHHC domain containing 14	Zdhhc14	**1.68**	346	327	98	111
1458324_x_at	16 days embryo head cDNA, RIKEN full-length	NA	**1.67**	422	336	136	100
1439191_at	follistatin-like 1	Fstl1	**1.67**	718	511	217	164
1435941_at	rhomboid, veinlet-like 4 (Drosophila)	Rhbdl4	**1.67**	997	1024	297	338
1441091_at	Transcribed sequences	NA	**1.67**	635	653	234	170
1433699_at	tumor necrosis factor, alpha-induced protein 3	Tnfaip3	**1.67**	1548	1457	539	405
1433642_at	ADP-ribosylation factor related protein 2	Arfrp2	**1.66**	1876	2861	686	779
1423407_a_at	fibulin 2	Fbln2	**1.66**	575	738	201	212
1454799_at	Transcribed sequences	NA	**1.65**	515	456	161	149
1427256_at	chondroitin sulfate proteoglycan 2	Cspg2	**1.64**	8514	8533	2892	2594
1453514_at	glycoprotein m6b	Gpm6b	**1.64**	203	293	77	79
1446196_at	high mobility group AT-hook 2	Hmga2	**1.64**	332	216	106	66
1452366_at	RIKEN cDNA 4732435N03 gene	4732435N03Rik	**1.64**	1732	1706	583	519

1420377_at	sialyltransferase 8 (alpha-2, 8-sialyltransferase)	Siat8b	**1.64**	1021	954	301	334
1437967_at	Titin	Ttn	**1.64**	192	66	42	30
1418210_at	profilin 2	Pfn2	**1.63**	7565	9001	3149	2194
1443086_at	activated leukocyte cell adhesion molecule	Alcam	**1.63**	2251	1778	783	508
1438841_s_at	arginase type II	Arg2	**1.62**	218	173	77	49
1427257_at	chondroitin sulfate proteoglycan 2	Cspg2	**1.62**	1208	1548	483	406
1440354_at	ELOVL family member 7, elongation of long cha	Elovl7	**1.62**	415	428	162	113
1422823_at	epidermal growth factor receptor pathway subst	Eps8	**1.62**	663	623	208	211
1440678_at	Latent transforming growth factor beta binding p	Ltbp1	**1.62**	292	216	81	83
1430307_a_at	malic enzyme, supernatant	Mod1	**1.62**	1013	1193	368	350
1442680_at	Neural cell adhesion molecule 1	Ncam1	**1.62**	290	299	116	75
1453041_at	Trp53 inducible protein 5	Trp53i5	**1.62**	645	628	228	187
1443837_x_at	B-cell leukemia/lymphoma 2	Bcl2	**1.61**	1182	1375	370	468
1423277_at	protein tyrosine phosphatase, receptor type, K	Ptprk	**1.61**	674	769	255	217
1448566_at	solute carrier family 40 (iron-regulated transport	Slc40a1	**1.61**	1002	789	323	261
1440758_at	7 days neonate cerebellum cDNA, RIKEN full-le	NA	**1.60**	359	344	115	117
1457275_at	desmuslin	Dmn	**1.60**	122	86	38	29
1447491_at	Leucine rich repeat containing 5	Lrrc5	**1.60**	2338	1952	785	624
1426865_a_at	neural cell adhesion molecule 1	Ncam1	**1.60**	893	1015	348	280
1429893_at	RIKEN cDNA 2810004A10 gene	2810004A10Rik	**1.60**	812	821	274	267
1433776_at	lipoma HMGIC fusion partner	Lhfp	**1.60**	138	119	38	47
1443394_at	RIKEN cDNA 9230105E05 gene	9230105E05Rik	**1.60**	889	859	312	263
1450061_at	ectodermal-neural cortex 1	Enc1	**1.59**	1985	1975	649	665
1453102_at	fibronectin leucine rich transmembrane protein	Flrt3	**1.59**	3583	3475	1265	1079
1417505_s_at	interleukin 11 receptor, alpha chain 1	Il11ra1	**1.59**	1243	1032	376	377
1443018_at	Neural cell adhesion molecule 1	Ncam1	**1.59**	1199	1122	498	275
1453191_at	procollagen, type XXVII, alpha 1	Col27a1	**1.59**	720	592	193	239
1416041_at	serum/glucocorticoid regulated kinase	Sgk	**1.59**	1011	1211	467	268
1426301_at	activated leukocyte cell adhesion molecule	Alcam	**1.58**	5975	5097	1967	1712
1419044_at	contactin associated protein 4	Cntnap4	**1.58**	269	305	103	89
1427182_s_at	DNA segment, Chr 18, ERATO Doi 653, expres	D18Ertd653e	**1.58**	91	77	33	23
1442174_at	tetraspanin 18	Tspan18	**1.58**	581	631	203	202
1450781_at	high mobility group AT-hook 2	Hmga2	**1.57**	2443	2222	715	850
1452287_at	Musashi homolog 1(Drosophila)	Msi1h	**1.57**	1289	1071	407	386
1417621_at	nuclear factor of activated T-cells, cytoplasmic,	Nfatc1	**1.57**	1000	733	363	214
1425761_a_at	nuclear factor of activated T-cells, cytoplasmic,	Nfatc1	**1.57**	750	1250	294	359
1417520_at	nuclear factor, erythroid derived 2, like 3	Nfe2l3	**1.57**	159	100	47	39
1437760_at	UDP-N-acetyl-alpha-D-galactosamine:polypepti	Galnt12	**1.57**	516	482	143	194
1441769_at	ADP-ribosylation factor related protein 2	Arfrp2	**1.56**	10510	8762	3542	2981
1448788_at	antigen identified by monoclonal antibody MRC	Mox2	**1.56**	622	597	217	196
1457687_at	B-cell leukemia/lymphoma 2	Bcl2	**1.56**	2072	2141	723	701
1421818_at	B-cell leukemia/lymphoma 6	Bcl6	**1.56**	1436	1278	498	419
1420928_at	beta galactoside alpha 2,6 sialyltransferase 1	St6gal1	**1.55**	2503	2666	844	919
1436501_at	mitochondrial tumor suppressor 1	Mtus1	**1.55**	170	184	64	56
1445211_at	Sex comb on midleg homolog 1	Scmh1	**1.55**	2221	2021	792	660
1451359_at	cDNA sequence BC005662	BC005662	**1.54**	311	328	109	111
1419468_at	C-type lectin domain family 14, member a	Clec14a	**1.54**	39	49	15	15
1448877_at	distal-less homeobox 2	Dlx2	**1.54**	142	131	41	53
1458113_at	RIKEN cDNA 9530019H20 gene	9530019H20Rik	**1.54**	669	635	255	192
1456404_at	a disintegrin-like and metalloprotease (reprolysi	Adamts5	**1.53**	115	188	64	38
1451435_at	cut-like 1 (Drosophila)	Cutl1	**1.53**	1278	1286	418	468
1433596_at	DnaJ (Hsp40) homolog, subfamily C, member 6	Dnajc6	**1.53**	987	862	330	306
1424114_s_at	laminin B1 subunit 1	Lamb1-1	**1.53**	2068	1721	670	637
1418175_at	vitamin D receptor	Vdr	**1.53**	400	292	115	122
1457434_s_at	protein tyrosine phosphatase-like (proline instea	Ptpla	**1.52**	3249	3247	1114	1145
1460595_at	16 days embryo head cDNA, RIKEN full-length	NA	**1.51**	1269	929	422	339
1417780_at	longevity assurance homolog 4 (S. cerevisiae)	Lass4	**1.51**	232	179	84	59
1436959_x_at	nasal embryonic LHRH factor	Nelf	**1.51**	1320	1095	416	430
1426864_a_at	neural cell adhesion molecule 1	Ncam1	**1.51**	10025	9716	4194	2742
1417319_at	poliovirus receptor-related 3	Pvrl3	**1.51**	867	824	283	311
1444993_at	Ring finger protein 32	Rnf32	**1.51**	304	279	107	97
1417673_at	growth factor receptor bound protein 14	Grb14	**1.50**	556	713	246	198
1424113_at	laminin B1 subunit 1	Lamb1-1	**1.50**	144	123	47	48
1442625_at	Transcribed sequence with weak similarity to p	NA	**1.50**	116	113	44	37
1426300_at	activated leukocyte cell adhesion molecule	Alcam	**1.49**	1304	1247	499	411
1436512_at	ADP-ribosylation factor-like 7	Arl7	**1.49**	5319	4995	1950	1707
1424890_at	basonuclin 1	Bnc1	**1.49**	6659	6733	2259	2513
1455096_at	fibronectin leucine rich transmembrane protein	Flrt2	**1.49**	3069	3322	1120	1149
1441391_at	Guanine nucleotide binding protein (G protein),	Gnb1l	**1.49**	1377	1335	463	502
1428387_at	acyl-CoA synthetase long-chain family member	Acsl3	**1.48**	673	817	240	291
1448323_a_at	biglycan	Bgn	**1.48**	2110	2127	729	789
1460070_at	Carbohydrate sulfotransferase 2	Chst2	**1.48**	353	431	141	138
1430320_at	dystrophin, muscular dystrophy	Dmd	**1.48**	269	132	71	64
1450990_at	glypican 3	Gpc3	**1.48**	1034	902	380	315

1447547_at	latent transforming growth factor beta binding p	Ltbp1	**1.47**	50	37	16	15
1423331_a_at	poliovirus receptor-related 3	Pvrl3	**1.47**	468	525	171	185
1441509_at	RIKEN cDNA A130009I22 gene	A130009I22Rik	**1.47**	590	609	222	211
1439341_at	Transcribed sequences	NA	**1.47**	379	469	164	141
1459420_at	Transcribed sequences	NA	**1.47**	1611	1742	674	537
1425007_at	zinc finger protein 566	Zfp566	**1.47**	780	755	295	258
1429310_at	fibronectin leucine rich transmembrane protein	Flrt3	**1.46**	4189	4586	1658	1520
1450044_at	frizzled homolog 7 (Drosophila)	Fzd7	**1.46**	4010	3666	1445	1350
1434848_at	G protein-coupled receptor 27	Gpr27	**1.46**	273	288	106	99
1449286_at	netrin G1	Ntng1	**1.46**	240	224	84	84
1433626_at	phospholipid scramblase 4	Plscr4	**1.46**	84	93	35	29
1418835_at	pleckstrin homology-like domain, family A, mem	Phlda1	**1.46**	2031	1759	696	674
1448673_at	poliovirus receptor-related 3	Pvrl3	**1.46**	1609	1608	571	600
1440555_at	Ras-related GTP binding D	Rragd	**1.46**	308	228	97	95
1436419_a_at	RIKEN cDNA 1700097N02 gene	1700097N02Rik	**1.46**	728	451	276	140
1416405_at	biglycan	Bgn	**1.45**	2055	2057	742	760
1436917_s_at	G-protein signalling modulator 1 (AGS3-like, C.	Gpsm1	**1.45**	340	269	115	107
1440506_at	Solute carrier family 7 (cationic amino acid trans	Slc7a2	**1.45**	200	222	72	83
1451835_at	SRY-box containing gene 21	Sox21	**1.45**	969	908	375	312
1443870_at	ATP-binding cassette, sub-family C (CFTR/MRI	Abcc4	**1.44**	950	948	351	351
1456811_at	CXXC finger 4	Cxxc4	**1.44**	34	32	12	12
1455995_at	DNA segment, Chr 10, Brigham & Women's Ge	D10Bwg1379e	**1.44**	42	29	14	11
1450064_at	formin 2	Fmn2	**1.44**	135	167	53	58
1419470_at	guanine nucleotide binding protein, beta 4	Gnb4	**1.44**	495	528	191	186
1422708_at	phosphoinositide-3-kinase, catalytic, gamma po	Pik3cg	**1.44**	100	69	31	30
1447295_at	Cut-like 1 (Drosophila), transcript variant 2, mR	Cutl1	**1.44**	638	705	236	260
1446380_at	RIKEN cDNA 9430076C15 gene	9430076C15Rik	**1.44**	747	761	272	285
1439793_at	Gap junction membrane channel protein alpha	Gja3	**1.44**	108	129	42	45
1420872_at	guanylate cyclase 1, soluble, beta 3	Gucy1b3	**1.43**	49	86	22	26
1430876_at	RIKEN cDNA 2610312I10 gene	2610312I10Rik	**1.43**	148	88	46	39
1453545_at	RIKEN cDNA 5730492I20 gene	5730492I20Rik	**1.43**	724	871	297	294
1443194_at	RIKEN cDNA 5930430O07 gene	5930430O07Rik	**1.43**	816	551	276	220
1435701_at	10 days neonate medulla oblongata cDNA, RIK	NA	**1.42**	556	584	241	184
1442411_at	Glucocorticoid induced transcript 1	Glcci1	**1.42**	644	581	216	241
1454824_s_at	mitochondrial tumor suppressor 1	Mtus1	**1.42**	1208	1106	453	410
1426258_at	sortilin-related receptor, LDLR class A repeats-	Sorl1	**1.42**	1959	2057	670	828
1437122_at	B-cell leukemia/lymphoma 2	Bcl2	**1.41**	342	384	138	136
1437422_at	sema domain, seven thrombospondin repeats (	Sema5a	**1.41**	2601	2236	863	952
1454866_s_at	chloride intracellular channel 6	Clic6	**1.40**	133	109	51	40
1422851_at	high mobility group AT-hook 2	Hmga2	**1.40**	8339	8585	3150	3249
1442992_at	hypothetical LOC403343	130004C03	**1.40**	985	940	385	343
1446583_at	NA	NA	**1.40**	98	50	27	26
1444763_at	protein tyrosine phosphatase, receptor type, K	Ptprk	**1.40**	245	322	110	103
1448557_at	RIKEN cDNA 1200015N20 gene	1200015N20Rik	**1.40**	148	215	69	67
1437492_at	RIKEN cDNA 9430023B20 gene	9430023B20Rik	**1.40**	69	80	26	30
1443827_x_at	cDNA sequence BC004044	BC004044	**1.39**	196	212	80	76
1435207_at	DIX domain containing 1	Dixdc1	**1.39**	1477	1565	646	512
1437403_at	RIKEN cDNA E130306M17 gene	E130306M17Rik	**1.39**	2199	2874	939	979
1434776_at	sema domain, seven thrombospondin repeats (	Sema5a	**1.39**	2159	2086	796	819
1456315_a_at	protein tyrosine phosphatase-like (proline instea	Ptpla	**1.38**	2054	2111	781	821
1416892_s_at	RIKEN cDNA 3110001A13 gene	3110001A13Rik	**1.38**	1514	1486	594	560
1438989_s_at	RIKEN cDNA B130021B11 gene	B130021B11Rik	**1.38**	116	137	44	53
1418608_at	calmodulin-like 3	Calml3	**1.37**	311	312	148	93
1451899_a_at	general transcription factor II I repeat domain-c	Gtf2ird1	**1.37**	1724	1874	734	657
1426858_at	inhibin beta-B	Inhbb	**1.37**	357	441	172	135
1433779_at	cancer susceptibility candidate 4	Casc4	**1.37**	1122	1127	446	427
1445697_at	Similar to development- and differentiation-enha	---	**1.37**	705	717	272	279
1456095_at	Tyrosinase (Tyr), mRNA	Tyr	**1.37**	65	133	27	45
1437574_at	a disintegrin-like and metalloprotease (reprolysi	Adamts18	**1.36**	312	327	132	117
1441947_x_at	cDNA sequence BC033915	BC033915	**1.36**	1144	1115	403	476
1427579_at	rhomboid, veinlet-like 4 (Drosophila)	Rhbdl4	**1.36**	202	220	74	90
1429987_at	RIKEN cDNA 9930013L23 gene	9930013L23Rik	**1.36**	325	225	126	84
1435892_at	RIKEN cDNA D430002O22 gene	D430002O22Rik	**1.36**	191	214	92	66
1446772_at	Transcribed sequences	NA	**1.36**	954	903	388	335
1448698_at	cyclin D1	Ccnd1	**1.35**	3260	3274	1292	1277
1448665_at	dystrophin, muscular dystrophy	Dmd	**1.35**	6501	5439	2439	2226
1439795_at	G protein-coupled receptor 64	Gpr64	**1.35**	2475	2656	955	1063
1460364_at	general transcription factor II I repeat domain-c	Gtf2ird1	**1.35**	3782	3439	1508	1316
1423110_at	procollagen, type I, alpha 2	Col1a2	**1.35**	451	553	190	202
1448669_at	dickkopf homolog 3 (Xenopus laevis)	Dkk3	**1.34**	594	599	231	239
1417937_at	dapper homolog 1, antagonist of beta-catenin (x	Dact1	**1.33**	335	243	125	102
1426008_a_at	solute carrier family 7 (cationic amino acid trans	Slc7a2	**1.33**	114	113	45	45
1456515_s_at	transcription factor-like 5 (basic helix-loop-helix)	Tcfl5	**1.33**	225	218	104	72
1455436_at	DIRAS family, GTP-binding RAS-like 2	Diras2	**1.32**	203	251	94	87

1438702_at	fibronectin leucine rich transmembrane protein	Flrt2	**1.32**	5637	6152	2253	2473
1452106_at	nephronectin	Npnt	**1.32**	2856	2624	1056	1144
1436993_x_at	profilin 2	Pfn2	**1.32**	8822	9628	4227	3166
1423635_at	bone morphogenetic protein 2	Bmp2	**1.31**	3129	2528	1275	998
1448901_at	carboxypeptidase X 1 (M14 family)	Cpxm1	**1.31**	172	205	72	79
1417782_at	longevity assurance homolog 4 (S. cerevisiae)	Lass4	**1.31**	48	53	20	21
1444306_at	Musashi homolog 1(Drosophila)	Msi1h	**1.31**	213	160	79	70
1429001_at	pirin	Pir	**1.31**	115	130	54	45
1454788_at	ADP-ribosylation factor-like 7	Arl7	**1.30**	7089	5997	3031	2267
1436181_at	development and differentiation enhancing fact	Ddef2	**1.30**	760	783	326	299
1458947_at	Fanconi anemia, complementation group C	Fancc	**1.30**	6368	5673	2672	2212
1429053_at	RIKEN cDNA 1110012J17 gene	1110012J17Rik	**1.30**	1528	1542	593	652
1453595_at	RIKEN cDNA 2900064B18 gene	2900064B18Rik	**1.30**	95	85	34	39
1455325_at	RIKEN cDNA A230057G18 gene	A230057G18Rik	**1.30**	1982	1444	694	683
1434709_at	RIKEN cDNA C130076O07 gene	C130076O07Rik	**1.30**	202	203	85	80
1429285_at	serine (or cysteine) proteinase inhibitor, clade A	Serpina9	**1.30**	211	151	78	68
1437889_x_at	biglycan	Bgn	**1.29**	778	798	312	334
1434628_a_at	rhophilin, Rho GTPase binding protein 2	Rhpn2	**1.29**	326	471	162	158
1436761_s_at	RIKEN cDNA 1200015N20 gene	1200015N20Rik	**1.29**	36	39	19	12
1424625_a_at	DENN/MADD domain containing 1A	Dennd1a	**1.29**	241	258	100	105
1432103_a_at	SH3-domain GRB2-like 3	Sh3gl3	**1.29**	527	571	214	235
1431202_at	hect domain and RLD 3	Herc3	**1.28**	346	306	119	150
1452771_s_at	acyl-CoA synthetase long-chain family member	Acsl3	**1.27**	1146	1160	447	507
1451972_at	glucocorticoid induced transcript 1	Glcci1	**1.27**	2044	1653	737	791
1416842_at	glutathione S-transferase, mu 5	Gstm5	**1.27**	545	555	247	209
1423885_at	laminin, gamma 1	Lamc1	**1.27**	932	893	373	381
1429514_at	phosphatidic acid phosphatase type 2B	Ppap2b	**1.27**	553	641	249	244
1431049_at	amyotrophic lateral sclerosis 2 (juvenile) chrom	Als2cr15	**1.27**	76	43	24	24
1416257_at	calpain 2	Capn2	**1.26**	1132	1198	442	531
1421317_x_at	myeloblastosis oncogene	Myb	**1.26**	1667	1470	692	616
1450194_a_at	myeloblastosis oncogene	Myb	**1.26**	619	536	262	220
1428259_at	RIKEN cDNA 2310075M15 gene	2310075M15Rik	**1.26**	4243	4545	1776	1896
1431300_at	RIKEN cDNA 3110007P09 gene	3110007P09Rik	**1.26**	139	98	55	43
1455549_at	SEC14 and spectrin domains 1	Sestd1	**1.26**	3533	3005	1263	1450
1454764_s_at	solute carrier family 38, member 1	Slc38a1	**1.26**	67	130	29	49
1434496_at	polo-like kinase 3 (Drosophila)	Plk3	**1.25**	311	335	144	127
1452365_at	RIKEN cDNA 4732435N03 gene	4732435N03Rik	**1.25**	286	289	132	110
1417686_at	lectin, galactose binding, soluble 12	Lgals12	**1.24**	664	527	274	225
1418209_a_at	profilin 2	Pfn2	**1.24**	14379	15533	7097	5580
1441463_at	RIKEN cDNA C230079D11 gene	C230079D11Rik	**1.24**	166	212	85	73
1455250_at	SH3-domain binding protein 4	Sh3bp4	**1.24**	482	591	218	233
1434429_at	synaptotagmin 14-like	Syt14l	**1.24**	25	28	9	13
1450857_a_at	procollagen, type I, alpha 2	Col1a2	**1.23**	1099	1347	515	522
1436508_at	RIKEN cDNA 2410014A08 gene	2410014A08Rik	**1.23**	3995	4345	1820	1738
1456874_at	fibronectin leucine rich transmembrane protein	Flrt2	**1.22**	308	315	127	140
1436509_at	RIKEN cDNA 2410014A08 gene	2410014A08Rik	**1.22**	2334	2720	1055	1113
1455818_at	RIKEN cDNA 4930427A07 gene	4930427A07Rik	**1.22**	1566	2273	687	937
1454576_at	RIKEN cDNA A230102O21 gene	A230102O21Rik	**1.22**	193	227	75	105
1452214_at	SKI-like	Skil	**1.22**	4739	4351	1970	1928
1458140_at	slit homolog 2 (Drosophila)	Slit2	**1.22**	121	139	65	46
1426317_at	StAR-related lipid transfer (START) domain cor	Stard6	**1.22**	464	459	219	178
1441927_at	synaptotagmin 7	Syt7	**1.22**	199	198	79	91
1433043_at	chondroitin sulfate proteoglycan 2	Cspg2	**1.21**	140	119	58	54
1426218_at	glucocorticoid induced transcript 1	Glcci1	**1.21**	1924	1382	682	732
1459868_x_at	interleukin 11 receptor, alpha chain 1	Il11ra1	**1.21**	109	91	42	44
1450860_at	leucine aminopeptidase 3	Lap3	**1.21**	2970	3036	1417	1174
1452107_s_at	nephronectin	Npnt	**1.21**	1238	1034	446	531
1417420_at	cyclin D1	Ccnd1	**1.20**	9402	8926	3856	4102
1449630_s_at	MAP/microtubule affinity-regulating kinase 1	Mark1	**1.20**	2261	2573	958	1137
1430934_at	RIKEN cDNA 2810043G22 gene	2810043G22Rik	**1.20**	125	123	58	50
1454877_at	SERTA domain containing 4	Sertad4	**1.20**	6165	5585	2505	2587
1421052_a_at	spermine synthase	Sms	**1.20**	3674	4151	1789	1616
1445178_at	SH3 multiple domains 2	Sh3md2	**1.20**	573	574	239	261
1448569_at	CD8 antigen, beta chain	Cd8b	**1.19**	3142	3800	1489	1534
1417311_at	cysteine rich protein 2	Crip2	**1.19**	798	792	309	386
1457113_at	nuclear autoantigenic sperm protein (histone-bi	Nasp	**1.19**	1849	1314	800	563
1443589_at	DNA segment, Chr X, ERATO Doi 242, express	DXErtd242e	**1.19**	89	105	47	37
1425942_a_at	glycoprotein m6b	Gpm6b	**1.19**	291	332	144	129
1450780_s_at	high mobility group AT-hook 2	Hmga2	**1.19**	7972	8281	3444	3664
1446850_at	Phosphatidic acid phosphatase type 2B	Ppap2b	**1.19**	209	241	109	87
1442845_at	RIKEN cDNA C130075A20 gene	C130075A20Rik	**1.19**	171	130	62	69
1454268_a_at	cytochrome b-245, alpha polypeptide	Cyba	**1.18**	276	305	135	121
1455214_at	microphthalmia-associated transcription factor	Mitf	**1.18**	438	572	228	215
1416489_at	phosphatidylinositol 4-kinase type 2 beta	Pi4k2b	**1.18**	1025	1098	519	416

1435363_at	pleckstrin homology domain containing, family (	Plekhg1	**1.18**	1503	1397	733	550
1452666_a_at	transmembrane and coiled-coil domains 2	Tmcc2	**1.18**	161	172	67	80
1441038_at	Utrophin	Utrn	**1.18**	713	720	324	309
1444253_at	a disintegrin-like and metalloprotease (reprolysi	Adamts18	**1.17**	89	81	43	33
1455437_at	cDNA sequence BC033915	BC033915	**1.17**	3577	2945	1465	1430
1440952_at	MAD homolog 7 (Drosophila)	Smad7	**1.17**	368	197	133	106
1451679_at	RIKEN cDNA 6530401D17 gene	6530401D17Rik	**1.17**	707	623	344	247
1440513_at	expressed sequence C80258	C80258	**1.16**	690	698	300	319
1423680_at	fatty acid desaturase 1	Fads1	**1.16**	929	799	426	347
1449455_at	hemopoietic cell kinase	Hck	**1.16**	275	323	127	139
1460693_a_at	procollagen, type IX, alpha 3	Col9a3	**1.16**	61	60	29	25
1458942_at	RIKEN cDNA C230037E05 gene	C230037E05Rik	**1.16**	287	263	124	123
1426241_a_at	sex comb on midleg homolog 1	Scmh1	**1.16**	596	656	236	325
1445918_at	transmembrane protein 2	Tmem2	**1.16**	297	229	115	120
1416953_at	connective tissue growth factor	Ctgf	**1.15**	774	994	423	369
1433491_at	erythrocyte protein band 4.1-like 2	Epb4.1l2	**1.15**	96	116	50	45
1456072_at	protein phosphatase 1, regulatory (inhibitor) sut	Ppp1r9a	**1.15**	426	408	194	183
1452226_at	regulator of chromosome condensation 2	Rcc2	**1.15**	1072	988	488	439
1454701_at	RIKEN cDNA 4930503L19 gene	4930503L19Rik	**1.15**	643	493	333	176
1424824_at	RIKEN cDNA 9630044O09 gene	9630044O09Rik	**1.15**	47	39	19	20
1436977_at	Transcribed sequences	NA	**1.15**	376	322	153	160
1440284_at	Transcribed sequences	NA	**1.15**	26	26	13	11
1416579_a_at	tumor-associated calcium signal transducer 1	Tacstd1	**1.15**	5810	5848	2899	2340
1459144_at	Fibronectin type III domain containing 3a	Fndc3	**1.14**	692	781	328	340
1431226_a_at	fibronectin type III domain containing 4	Fndc4	**1.14**	294	271	132	124
1427028_at	leucine-rich repeat-containing G protein-couple(	Lgr6	**1.14**	397	394	181	179
1456648_at	Mannosidase 1, alpha	Man1a	**1.14**	385	521	194	212
1451516_at	Ras homolog enriched in brain like 1	Rhebl1	**1.14**	1024	1005	482	441
1419798_at	RIKEN cDNA 2610019E17 gene	2610019E17Rik	**1.14**	99	103	53	39
1434307_at	transmembrane protein 64	Tmem64	**1.14**	947	988	462	417
1442175_at	RIKEN cDNA C030027H14 gene	C030027H14Rik	**1.14**	593	538	272	243
1438783_at	Transmembrane, prostate androgen induced Rl	Tmepai	**1.14**	572	562	243	271
1447043_at	V-erb-a erythroblastic leukemia viral oncogene	Erbb4	**1.14**	214	157	77	89
1437785_at	a disintegrin-like and metalloprotease (reprolysi	Adamts9	**1.13**	5519	5115	2230	2633
1433894_at	expressed sequence AI591476	AI591476	**1.13**	119	134	54	61
1453416_at	growth arrest-specific 2 like 3	Gas2l3	**1.13**	2651	2126	1086	1087
1429896_at	RIKEN cDNA 5830408B19 gene	5830408B19Rik	**1.13**	8103	9049	4003	3817
1446461_at	SRY-box containing gene 5	Sox5	**1.13**	224	179	94	88
1437467_at	activated leukocyte cell adhesion molecule	Alcam	**1.12**	15907	14868	7572	6622
1448919_at	CD302 antigen	Cd302	**1.12**	125	132	63	55
1439568_at	gene regulated by estrogen in breast cancer pr(	Greb1	**1.12**	371	468	183	200
1424367_a_at	homer homolog 2 (Drosophila)	Homer2	**1.12**	719	817	318	386
1430033_at	RIKEN cDNA 5330431K02 gene	5330431K02Rik	**1.12**	349	269	143	138
1437059_at	SRY-box containing gene 21	Sox21	**1.12**	3230	2585	1364	1302
1423499_at	synuclein, alpha interacting protein (synphilin)	Sncaip	**1.12**	131	144	64	63
1446653_at	Transcribed sequences	NA	**1.12**	444	368	179	192
1435083_at	cortexin	Ctxn	**1.11**	547	515	220	273
1433590_at	hect domain and RLD 3	Herc3	**1.11**	1081	1043	471	516
1459493_at	SET binding protein 1 (Setbp1), mRNA	Setbp1	**1.11**	495	522	231	241
1435176_a_at	inhibitor of DNA binding 2	Idb2	**1.11**	370	437	182	189
1431402_at	kin of IRRE like 3 (Drosophila)	Kirrel3	**1.11**	439	439	205	202
1430352_at	RIKEN cDNA 8430417A20 gene	8430417A20Rik	**1.11**	3978	3771	1608	1968
1430083_at	RIKEN cDNA 2610307P16 gene	2610307P16Rik	**1.10**	125	109	58	52
1440739_at	vascular endothelial growth factor C	Vegfc	**1.10**	202	190	103	79
1438866_at	glutamate receptor ionotropic, NMDA3A	Grin3a	**1.09**	55	36	20	22
1420411_a_at	phosphatidylinositol 4-kinase type 2 beta	Pi4k2b	**1.09**	542	213	241	78
1435977_at	hepatoma-derived growth factor, related protein	Hdgfrp3	**1.09**	780	728	354	353
1434797_at	RIKEN cDNA 6720469N11 gene	6720469N11Rik	**1.09**	583	528	255	267
1458241_at	RIKEN cDNA 9230105E05 gene	9230105E05Rik	**1.09**	658	464	248	271
1448024_at	RIKEN cDNA B430320C24 gene	B430320C24Rik	**1.09**	504	618	286	237
1435050_at	RIKEN cDNA B930094H20 gene	B930094H20Rik	**1.09**	52	40	22	21
1434645_at	RIKEN cDNA C530008M17 gene	C530008M17Rik	**1.09**	56	51	26	24
1422865_at	runt related transcription factor 1	Runx1	**1.09**	74	65	30	35
1446897_at	Transcribed sequences	NA	**1.09**	256	307	137	126
1460559_at	ankyrin repeat domain 25	Ankrd25	**1.08**	1151	1377	575	612
1435387_at	expressed sequence AI505012	AI505012	**1.08**	375	433	195	187
1449058_at	GLI-Kruppel family member GLI	Gli	**1.08**	587	668	265	329
1449471_at	potassium large conductance calcium-activated	Kcnmb4	**1.08**	512	588	248	273
1447818_x_at	Ras homolog enriched in brain like 1	Rhebl1	**1.08**	1503	1344	769	576
1456377_x_at	RIKEN cDNA 0610025L06 gene	0610025L06Rik	**1.08**	2107	2327	1021	1068
1419829_a_at	Transcribed sequence with weak similarity to p	NA	**1.08**	286	248	144	107
1433531_at	acyl-CoA synthetase long-chain family member	Acsl4	**1.07**	980	887	525	364
1417312_at	dickkopf homolog 3 (Xenopus laevis)	Dkk3	**1.07**	378	388	198	168
1420342_at	ganglioside-induced differentiation-associated-p	Gdap10	**1.07**	1925	2086	958	947

1440067_at	Neural cell adhesion molecule 1	Ncam1	**1.07**	157	124	79	54
1426934_at	NHS-like 1	Nhsl1	**1.07**	1721	1737	788	865
1418711_at	platelet derived growth factor, alpha	Pdgfa	**1.07**	1668	1864	685	990
1424250_a_at	Rho guanine nucleotide exchange factor (GEF)	Arhgef3	**1.07**	559	567	283	253
1422462_at	ubiquitin-conjugating enzyme E2T (putative)	Ube2t	**1.07**	379	323	161	171
1434982_at	Transcribed sequence with weak similarity to p	NA	**1.07**	160	208	90	84
1425510_at	MAP/microtubule affinity-regulating kinase 1	Mark1	**1.06**	181	180	80	93
1452740_at	myosin heavy chain 10, non-muscle	Myh10	**1.06**	2847	2468	1344	1197
1457256_x_at	patched homolog 2	Ptch2	**1.06**	7113	6632	3415	3192
1424051_at	procollagen, type IV, alpha 2	Col4a2	**1.06**	1217	1241	600	578
1425452_s_at	protein tyrosine phosphatase, receptor type, J /.	Ptprj /// AW125753	**1.06**	3005	3130	1710	1241
1426541_a_at	RIKEN cDNA 2310067E08 gene	2310067E08Rik	**1.06**	38	39	18	19
1435184_at	RIKEN cDNA B430320C24 gene	B430320C24Rik	**1.06**	886	939	495	381
1434592_at	solute carrier family 16 (monocarboxylic acid tra	Slc16a10	**1.06**	615	517	258	283
1424950_at	SRY-box containing gene 9	Sox9	**1.06**	1393	1265	724	553
1452205_x_at	T-cell receptor beta, variable 13	Tcrb-V13	**1.06**	128	144	64	66
1418884_x_at	tubulin, alpha 1	Tuba1	**1.06**	8478	7906	4029	3798
1435913_at	cDNA sequence BC038881	BC038881	**1.05**	287	260	137	127
1427683_at	early growth response 2	Egr2	**1.05**	863	915	583	277
1417558_at	Fyn proto-oncogene	Fyn	**1.05**	153	171	65	92
1417101_at	heat shock protein 2	Hspa2	**1.05**	458	382	214	191
1454671_at	insulin induced gene 1	Insig1	**1.05**	443	596	226	269
1422771_at	MAD homolog 6 (Drosophila)	Smad6	**1.05**	57	71	30	31
1416505_at	nuclear receptor subfamily 4, group A, member	Nr4a1	**1.05**	1322	1300	675	591
1460627_at	RIKEN cDNA D130067I03 gene	D130067I03Rik	**1.05**	73	46	28	27
1429114_at	SEC14 and spectrin domains 1	Sestd1	**1.05**	393	394	182	198
1421943_at	transforming growth factor alpha	Tgfa	**1.05**	426	348	196	176
1417978_at	eukaryotic translation initiation factor 4E membe	Eif4e3	**1.04**	360	448	182	208
1435308_at	fucosyltransferase 9	Fut9	**1.04**	83	74	40	36
1444519_at	G protein-coupled receptor 49	Gpr49	**1.04**	70	184	51	59
1458575_at	SET binding protein 1 (Setbp1), mRNA	Setbp1	**1.04**	1105	1001	511	509
1417612_at	immediate early response 5	Ier5	**1.04**	1886	1662	965	753
1424594_at	lectin, galactose binding, soluble 7	Lgals7	**1.04**	426	372	172	215
1448416_at	matrix gamma-carboxyglutamate (gla) protein	Mglap	**1.04**	202	160	89	87
1434700_at	RIKEN cDNA 6030408C04 gene	6030408C04Rik	**1.04**	1446	1395	692	688
1455820_x_at	scavenger receptor class B, member 1	Scarb1	**1.04**	1084	1125	552	523
1439926_at	hypothetical protein 4632417D23	4632417D23	**1.03**	335	319	155	165
1455881_at	immediate early response 5-like	Ier5l	**1.03**	438	382	195	205
1415806_at	plasminogen activator, tissue	Plat	**1.03**	179	149	91	69
1435461_at	membrane associated guanylate kinase, WW a	Magi3	**1.03**	714	714	355	342
1434008_at	sodium channel, type IV, beta polypeptide	Scn4b	**1.03**	229	211	102	113
1436368_at	solute carrier family 16 (monocarboxylic acid tra	Slc16a10	**1.03**	2087	1700	896	943
1451152_a_at	ATPase, Na+/K+ transporting, beta 1 polypeptic	Atp1b1	**1.02**	988	1043	501	497
1417688_at	cDNA sequence BC004044	BC004044	**1.02**	329	367	157	187
1437540_at	mucolipin 3	Mcoln3	**1.02**	174	306	101	127
1444583_at	Nuclear autoantigenic sperm protein (histone-bi	Nasp	**1.02**	1249	1296	757	502
1456475_s_at	protein kinase, cAMP dependent regulatory, typ	Prkar2b	**1.02**	2551	2090	1165	1118
1448509_at	SH3-domain GRB2-like (endophilin) interacting	Sgip1	**1.02**	369	379	204	166
1432746_at	RIKEN cDNA 6030442H21 gene	6030442H21Rik	**1.02**	266	219	129	109
1455149_at	SH3 multiple domains 2	Sh3md2	**1.02**	641	596	288	322
1415964_at	stearoyl-Coenzyme A desaturase 1	Scd1	**1.02**	2508	3322	1443	1395
1417749_a_at	tight junction protein 1	Tjp1	**1.02**	8251	7217	4086	3533
1459054_at	cDNA sequence BC035954	BC035954	**1.01**	146	129	58	78
1416326_at	cysteine-rich protein 1 (intestinal)	Crip1	**1.01**	803	813	389	411
1433770_at	dihydropyrimidinase-like 2	Dpysl2	**1.01**	2010	2294	1045	1091
1419593_at	gene regulated by estrogen in breast cancer pro	Greb1	**1.01**	169	201	92	91
1457229_at	G-protein coupled receptor 173	Gpr173	**1.01**	337	346	164	175
1455687_at	intestinal cell kinase	Ick	**1.01**	2803	2305	1193	1331
1441995_at	Neural cell adhesion molecule 1	Ncam1	**1.01**	571	420	272	212
1417928_at	PDZ and LIM domain 4	Pdlim4	**1.01**	371	285	197	127
1448908_at	phosphatidic acid phosphatase type 2B	Ppap2b	**1.01**	377	410	201	190
1455980_a_at	PREDICTED: similar to growth arrest-specific 2	Gas2l3	**1.01**	449	292	174	186
1433571_at	serine incorporator 5	Serinc5	**1.01**	728	553	350	278
1446326_at	procollagen, type I, alpha 2	Col1a2	**1.00**	61	68	31	33
1437894_at	prospero-related homeobox 1	Prox1	**1.00**	57	41	23	25
1438664_at	protein kinase, cAMP dependent regulatory, typ	Prkar2b	**1.00**	1136	1010	565	506
1428749_at	Dmx-like 2	Dmxl2	**1.00**	572	598	296	290
1453523_at	RIKEN cDNA A030006P16 gene	A030006P16Rik	**1.00**	185	158	79	91
1449198_a_at	sialyltransferase 9 (CMP-NeuAc:lactosylcerami	Siat9	**1.00**	456	569	261	247
1426712_at	solute carrier family 6 (neurotransmitter transpo	Slc6a15	**1.00**	58	50	29	25
1429581_at	acyl-Coenzyme A dehydrogenase family, memt	Acad9	**-1.00**	1908	1711	3811	3429
1451243_at	arginyl aminopeptidase (aminopeptidase B)	Rnpep	**-1.00**	252	183	454	407
1428549_at	coiled-coil domain containing 3	Ccdc3	**-1.00**	565	599	1084	1241

1429021_at	Eph receptor A4	Epha4	**-1.00**	925	798	1904	1535
1419309_at	glycoprotein 38	Gp38	**-1.00**	197	200	345	450
1445897_s_at	interferon-induced protein 35	Ifi35	**-1.00**	190	192	410	354
1419161_a_at	NADPH oxidase 4	Nox4	**-1.00**	43	47	99	80
1430191_at	RIKEN cDNA 9130004J05 gene	9130004J05Rik	**-1.00**	524	498	1052	988
1439731_at	RIKEN cDNA E130309F12 gene	E130309F12Rik	**-1.00**	64	42	102	105
1426584_a_at	sorbitol dehydrogenase 1	Sdh1	**-1.00**	188	160	343	353
1416137_at	annexin A7	Anxa7	**-1.01**	193	197	413	374
1422470_at	BCL2/adenovirus E1B 19kDa-interacting protei	Bnip3	**-1.01**	2059	1348	4148	2581
1452434_s_at	DiGeorge syndrome critical region gene 6	Dgcr6	**-1.01**	260	253	565	471
1427510_at	guanine nucleotide binding protein, alpha inhibi	Gnai1	**-1.01**	101	91	168	216
1424172_at	hydroxyacyl glutathione hydrolase	Hagh	**-1.01**	445	394	856	825
1416401_at	kangai 1 (suppression of tumorigenicity 6, prost	Kai1	**-1.01**	259	231	513	474
1417701_at	protein phosphatase 1, regulatory (inhibitor) sut	Ppp1r14c	**-1.01**	1841	2267	4441	3780
1430286_s_at	protein phosphatase 1, regulatory (inhibitor) sut	Ppp1r14c	**-1.01**	221	230	483	427
1449256_a_at	RAB11a, member RAS oncogene family	Rab11a	**-1.01**	1041	1168	2267	2184
1453261_at	RIKEN cDNA 2610035D17 gene	2610035D17Rik	**-1.01**	151	101	252	246
1452519_a_at	zinc finger protein 36	Zfp36	**-1.01**	821	944	2074	1484
1423420_at	adrenergic receptor, beta 1	Adrb1	**-1.02**	43	54	109	87
1438764_at	annexin A7	Anxa7	**-1.02**	370	376	837	672
1417649_at	cyclin-dependent kinase inhibitor 1C (P57)	Cdkn1c	**-1.02**	131	161	291	299
1417195_at	DNA segment, Chr 8, ERATO Doi 594, express	D8Ertd594e	**-1.02**	191	204	368	435
1416021_a_at	fatty acid binding protein 5, epidermal	Fabp5	**-1.02**	7649	6955	15545	14020
1426873_s_at	junction plakoglobin	Jup	**-1.02**	242	237	479	492
1422743_at	phosphorylase kinase alpha 1	Phka1	**-1.02**	97	99	184	213
1423909_at	RIKEN cDNA 0610011I04 gene	0610011I04Rik	**-1.02**	313	324	618	669
1420150_at	splA/ryanodine receptor domain and SOCS box	Spsb1	**-1.02**	165	159	284	373
1457883_at	Adult male aorta and vein cDNA, RIKEN full-len	NA	**-1.03**	215	247	431	512
1438093_x_at	diazepam binding inhibitor	Dbi	**-1.03**	3129	2925	6563	5766
1442606_at	dynamin binding protein	Dnmbp	**-1.03**	116	106	242	211
1455994_x_at	elongation of very long chain fatty acids (FEN1/	Elovl1	**-1.03**	598	668	1295	1294
1459948_at	Growth hormone receptor	Ghr	**-1.03**	70	65	136	138
1419052_at	OVO homolog-like 1 (Drosophila)	Ovol1	**-1.03**	70	62	152	117
1435571_at	RIKEN cDNA A530065I17 gene	A530065I17Rik	**-1.03**	175	210	412	372
1435205_at	transcription factor AP-2, epsilon	Tcfap2e	**-1.03**	822	903	1612	1909
1425645_s_at	cytochrome P450, family 2, subfamily b, polype	Cyp2b20	**-1.04**	64	74	160	123
1449852_a_at	EH-domain containing 4	Ehd4	**-1.04**	387	287	837	532
1418517_at	Iroquois related homeobox 3 (Drosophila)	Irx3	**-1.04**	122	126	264	243
1421106_at	jagged 1	Jag1	**-1.04**	288	176	616	313
1441547_at	Nuclear factor I/A	Nfia	**-1.04**	1102	1117	2179	2389
1430483_a_at	RIKEN cDNA 2310042N02 gene	2310042N02Rik	**-1.04**	99	100	203	207
1430655_at	RIKEN cDNA 4631405K08 gene	4631405K08Rik	**-1.04**	496	421	843	1029
1446281_at	RIKEN cDNA C530008M07 gene	C530008M07Rik	**-1.04**	134	111	291	211
1424530_at	SEC14-like 2 (S. cerevisiae)	Sec14l2	**-1.04**	130	139	288	265
1430724_at	abhydrolase domain containing 9	Abhd9	**-1.05**	138	106	256	247
1432018_at	achaete-scute complex homolog-like 2 (Drosop	Ascl2	**-1.05**	15	13	30	28
1451210_at	phosphatidic acid phosphatase type 2c	Ppap2c	**-1.05**	842	1019	1931	1909
1428400_at	RIKEN cDNA 2200002K05 gene	2200002K05Rik	**-1.05**	83	90	202	154
1423494_at	RIKEN cDNA 2310042E22 gene	2310042E22Rik	**-1.05**	90	108	207	203
1433943_at	RIKEN cDNA 4930463G05 gene	4930463G05Rik	**-1.05**	97	94	200	195
1450034_at	signal transducer and activator of transcription 1	Stat1	**-1.05**	310	340	688	656
1448529_at	thrombomodulin	Thbd	**-1.05**	28	39	90	47
1417196_s_at	DNA segment, Chr 8, ERATO Doi 594, express	D8Ertd594e	**-1.06**	604	544	1160	1237
1448194_a_at	H19 fetal liver mRNA	H19	**-1.06**	14012	11770	27644	25780
1417047_at	prominin 2	Prom2	**-1.06**	194	184	462	329
1425603_at	RIKEN cDNA 0610011I04 gene	0610011I04Rik	**-1.06**	381	416	787	877
1453511_at	RIKEN cDNA 2310007B03 gene	2310007B03Rik	**-1.06**	52	51	116	98
1458578_at	RNA binding motif, single stranded interacting p	Rbms1	**-1.06**	274	258	503	606
1438937_x_at	angiogenin, ribonuclease A family, member 1	Ang1	**-1.07**	61	38	101	101
1448985_at	dual specificity phosphatase 22	Dusp22	**-1.07**	687	706	1523	1412
1425918_at	EGL nine homolog 3 (C. elegans)	Egln3	**-1.07**	678	715	1592	1338
1417301_at	frizzled homolog 6 (Drosophila)	Fzd6	**-1.07**	1540	1441	3208	3058
1422784_at	keratin complex 2, basic, gene 6a	Krt2-6a	**-1.07**	123	144	312	245
1450626_at	mannosidase, beta A, lysosomal	Manba	**-1.07**	255	297	511	648
1453593_at	RIKEN cDNA 1700110N18 gene	1700110N18Rik	**-1.07**	434	394	851	880
1424308_at	solute carrier family 24 (sodium/potassium/calci	Slc24a3	**-1.07**	193	245	407	506
1443720_s_at	bone morphogenetic protein receptor, type 1B	Bmpr1b	**-1.08**	17	14	31	34
1437057_at	EGF-like-domain, multiple 3	Egfl3	**-1.08**	444	487	937	1026
1439757_s_at	Eph receptor A4	Epha4	**-1.08**	246	212	475	493
1424400_a_at	formyltetrahydrofolate dehydrogenase	Fthfd	**-1.08**	78	123	174	241
1417395_at	Kruppel-like factor 4 (gut)	Klf4	**-1.08**	586	590	1223	1270
1445929_at	Potassium channel, subfamily K, member 2	Kcnk2	**-1.08**	68	62	137	139
1440693_at	RIKEN cDNA 2410003B16 gene	2410003B16Rik	**-1.08**	94	86	194	188
1428450_at	RIKEN cDNA 2610034B18 gene	2610034B18Rik	**-1.08**	196	243	477	446

1437245_at	RIKEN cDNA 9930117H01 gene	9930117H01Rik	**-1.08**	22	22	58	35
1420614_at	t-complex-associated-testis-expressed 1-like	Tcte1l	**-1.08**	628	733	1465	1401
1416431_at	tubulin, beta 6	Tubb6	**-1.08**	164	171	374	335
1423126_at	ATPase, Na+/K+ transporting, beta 3 polypeptic	Atp1b3	**-1.09**	4489	4920	10040	9992
1436346_at	CD109 antigen	Cd109	**-1.09**	1370	1430	3341	2638
1420498_a_at	disabled homolog 2 (Drosophila)	Dab2	**-1.09**	109	66	142	219
1418648_at	EGL nine homolog 3 (C. elegans)	Egln3	**-1.09**	269	216	578	445
1418483_a_at	glycoprotein galactosyltransferase alpha 1, 3	Ggta1	**-1.09**	450	473	946	1014
1434440_at	guanine nucleotide binding protein, alpha inhibi	Gnai1	**-1.09**	4199	4308	8972	9096
1417777_at	leukotriene B4 12-hydroxydehydrogenase	Ltb4dh	**-1.09**	742	923	1850	1666
1441163_at	mediator of RNA polymerase II transcription, su	Med12l	**-1.09**	35	46	76	94
1448954_at	nuclear receptor interacting protein 3	Nrip3	**-1.09**	180	206	331	487
1422293_a_at	potassium channel tetramerisation domain cont	Kctd1	**-1.09**	143	152	317	310
1424507_at	Ras and Rab interactor 1	Rin1	**-1.09**	26	18	39	53
1415850_at	RAS p21 protein activator 3	Rasa3	**-1.09**	362	397	791	819
1440283_at	RIKEN cDNA 1810059H22 gene	1810059H22Rik	**-1.09**	126	99	239	236
1450947_at	RIKEN cDNA 2610528J11 gene	2610528J11Rik	**-1.09**	123	95	234	226
1434725_at	RIKEN cDNA 4921521N14 gene	4921521N14Rik	**-1.09**	239	303	561	585
1447655_x_at	SRY-box containing gene 6	Sox6	**-1.09**	798	744	1639	1646
1449929_at	t-complex-associated-testis-expressed 1-like	Tcte1l	**-1.09**	2975	2957	6576	6068
1444974_at	expressed sequence AU023617	AU023617	**-1.10**	257	266	493	626
1437874_s_at	hexosaminidase B	Hexb	**-1.10**	202	141	415	308
1424942_a_at	myelocytomatosis oncogene	Myc	**-1.10**	63	73	172	118
1434534_at	NA	NA	**-1.10**	5518	4035	11594	8601
1429284_at	RIKEN cDNA 8430436F23 gene	8430436F23Rik	**-1.10**	725	744	1737	1419
1451594_s_at	serine (or cysteine) proteinase inhibitor, clade E	Serpinb6c	**-1.10**	55	66	137	121
1416528_at	SH3 domain binding glutamic acid-rich protein-l	Sh3bgrl3	**-1.10**	533	551	1084	1247
1424030_at	grainyhead-like 1 (Drosophila)	Grhl1	**-1.10**	690	780	1811	1324
1454862_at	pleckstrin homology-like domain, family B, mem	Phldb2	**-1.11**	934	1036	1988	2245
1438882_at	Rho GTPase activating protein 18	Arhgap18	**-1.11**	424	308	871	694
1427677_a_at	SRY-box containing gene 6	Sox6	**-1.11**	1167	1221	2598	2555
1416564_at	SRY-box containing gene 7	Sox7	**-1.11**	85	70	190	143
1436651_at	Transcribed sequences	NA	**-1.11**	257	218	498	522
1439352_at	tripartite motif protein 7	Trim7	**-1.11**	51	52	111	110
1419572_a_at	ATP-binding cassette, sub-family D (ALD), men	Abcd4	**-1.12**	143	118	326	238
1425108_a_at	cDNA sequence BC004728	BC004728	**-1.12**	72	65	162	135
1424303_at	expressed sequence AV216087	AV216087	**-1.12**	371	420	843	878
1443997_at	RIKEN cDNA C130040D06 gene	C130040D06Rik	**-1.12**	129	92	292	180
1426908_at	UDP-N-acetyl-alpha-D-galactosamine: polypept	Galnt7	**-1.12**	168	184	410	352
1441153_at	Utrophin	Utrn	**-1.12**	619	540	1369	1145
1417122_at	vav 3 oncogene	Vav3	**-1.12**	925	1131	2282	2169
1437302_at	adrenergic receptor, beta 2	Adrb2	**-1.13**	51	53	126	101
1451446_at	anthrax toxin receptor 1	Antxr1	**-1.13**	1492	1509	3214	3363
1448359_a_at	hypoxia induced gene 1	Hig1	**-1.13**	272	284	683	535
1417813_at	inhibitor of kappaB kinase epsilon	Ikbke	**-1.13**	142	134	313	290
1451775_s_at	interleukin 13 receptor, alpha 1	Il13ra1	**-1.13**	171	184	394	385
1434070_at	jagged 1	Jag1	**-1.13**	1758	1383	3955	2887
1421163_a_at	nuclear factor I/A	Nfia	**-1.13**	557	490	1078	1203
1440491_at	solute carrier family 1 (glial high affinity glutama	Slc1a3	**-1.13**	34	25	69	57
1438183_x_at	sorbitol dehydrogenase 1	Sdh1	**-1.13**	72	63	145	148
1416008_at	special AT-rich sequence binding protein 1	Satb1	**-1.13**	3483	3307	7376	7483
1433819_s_at	1-acylglycerol-3-phosphate O-acyltransferase 3	Agpat3	**-1.14**	156	155	380	307
1417566_at	abhydrolase domain containing 5	Abhd5	**-1.14**	203	233	543	415
1422678_at	diacylglycerol O-acyltransferase 2	Dgat2	**-1.14**	219	223	604	374
1416855_at	growth arrest specific 1	Gas1	**-1.14**	6714	5863	14228	13385
1447173_at	NA	NA	**-1.14**	25	26	60	53
1426952_at	Rho GTPase activating protein 18	Arhgap18	**-1.14**	140	138	320	293
1423824_at	RIKEN cDNA 5031439A09 gene	5031439A09Rik	**-1.14**	1106	1177	2475	2560
1420915_at	signal transducer and activator of transcription 1	Stat1	**-1.14**	177	162	411	333
1450618_a_at	small proline-rich protein 2A	Sprr2a	**-1.14**	649	777	1707	1419
1417639_at	solute carrier family 22 (organic cation transport	Slc22a4	**-1.14**	238	222	540	474
1444479_at	Transcribed sequences	NA	**-1.14**	2794	3662	6420	7713
1434486_x_at	UDP-glucose pyrophosphorylase 2	Ugp2	**-1.14**	579	616	1374	1257
1437932_a_at	claudin 1	Cldn1	**-1.15**	1061	947	2637	1810
1437458_x_at	clusterin	Clu	**-1.15**	329	313	773	655
1453072_at	G protein-coupled receptor 160	Gpr160	**-1.15**	177	225	490	396
1423062_at	insulin-like growth factor binding protein 3	Igfbp3	**-1.15**	94	75	190	184
1451690_a_at	poliovirus receptor-related 4	Pvrl4	**-1.15**	137	73	277	166
1448312_at	proprotein convertase subtilisin/kexin type 2	Pcsk2	**-1.15**	150	191	307	446
1435842_at	RIKEN cDNA 1110038O08 gene	1110038O08Rik	**-1.15**	111	130	226	306
1456321_at	RIKEN cDNA 3830408G10 gene	3830408G10Rik	**-1.15**	28	26	77	45
1423844_s_at	cystathionine beta-synthase	Cbs	**-1.16**	94	81	168	221
1421365_at	follistatin	Fst	**-1.16**	1925	1790	3610	4709
1455872_at	hypothetical protein A030013D21	A030013D21	**-1.16**	95	114	230	235

1416481_s_at	hypoxia induced gene 1	Hig1	**-1.16**	1348	1560	3770	2729
1460236_at	kallikrein 10	Klk10	**-1.16**	52	57	128	115
1439847_s_at	Kruppel-like factor 12	Klf12	**-1.16**	122	117	290	241
1421217_a_at	lectin, galactose binding, soluble 9	Lgals9	**-1.16**	91	100	193	235
1450976_at	N-myc downstream regulated gene 1	Ndrg1	**-1.16**	237	172	606	299
1439148_a_at	phosphofructokinase, liver, B-type	Pfkl	**-1.16**	940	734	2055	1648
1415943_at	syndecan 1	Sdc1	**-1.16**	2465	3026	6493	5739
1437279_x_at	syndecan 1	Sdc1	**-1.16**	1817	1817	4034	4073
1444274_at	Transcribed sequence with moderate similarity	NA	**-1.16**	116	102	214	270
1451546_s_at	transmembrane protein 40	Tmem40	**-1.16**	131	115	290	259
1426911_at	desmocollin 2	Dsc2	**-1.17**	437	355	1102	677
1431777_a_at	high mobility group nucleosomal binding domai	Hmgn3	**-1.17**	867	987	2091	2062
1426604_at	ribonuclease L (2', 5'-oligoisoadenylate synthet	Rnasel	**-1.17**	53	54	148	94
1433266_at	RIKEN cDNA 2810416A17 gene	2810416A17Rik	**-1.17**	170	202	490	345
1452092_at	RIKEN cDNA 4631426J05 gene	4631426J05Rik	**-1.17**	1797	2081	4056	4623
1441971_at	Transcribed sequences	NA	**-1.17**	721	691	1796	1379
1451742_a_at	UDP-glucose pyrophosphorylase 2	Ugp2	**-1.17**	949	995	2305	2069
1459009_at	Utrophin	Utrn	**-1.17**	255	236	613	488
1422941_at	wingless-related MMTV integration site 16	Wnt16	**-1.17**	101	101	214	240
1442348_at	2 days pregnant adult female oviduct cDNA, RI	NA	**-1.18**	125	96	251	247
1441242_at	Dipeptidylpeptidase 4	Dpp4	**-1.18**	256	252	638	513
1417143_at	endothelial differentiation, lysophosphatidic acic	Edg2	**-1.18**	157	166	341	389
1438251_x_at	protease, serine, 11 (Igf binding)	Prss11	**-1.18**	1231	1020	2442	2636
1445710_x_at	RIKEN cDNA 1110051B16 gene	1110051B16Rik	**-1.18**	413	253	793	669
1455915_at	UDP-N-acetyl-alpha-D-galactosamine:polypepti	Galnt4	**-1.18**	304	343	738	723
1446480_at	Adult male corpora quadrigemina cDNA, RIKEI	NA	**-1.19**	44	55	116	108
1416455_a_at	crystallin, alpha B	Cryab	**-1.19**	33	29	65	78
1418497_at	fibroblast growth factor 13	Fgf13	**-1.19**	340	368	698	920
1418135_at	homolog of human MLLT2 unidentified gene	Mllt2h	**-1.19**	813	880	1808	2064
1434059_at	RIKEN cDNA B230312A22 gene	B230312A22Rik	**-1.19**	457	425	1074	939
1425560_a_at	S100 calcium binding protein A16	S100a16	**-1.19**	2352	2726	5872	5718
1420822_s_at	sphingosine-1-phosphate phosphatase 1	Sgpp1	**-1.19**	1212	1001	2971	2058
1452138_a_at	angiotensin I converting enzyme (peptidyl-dipep	Ace2	**-1.20**	59	85	187	137
1429582_at	BTB (POZ) domain containing 14A	Btbd14a	**-1.20**	88	124	261	220
1435059_at	development and differentiation enhancing	Ddef1	**-1.20**	556	515	1186	1267
1435283_s_at	expressed sequence AI414343	AI414343	**-1.20**	122	108	240	288
1452388_at	heat shock protein 1A	Hspa1a	**-1.20**	436	937	1141	1800
1436994_a_at	histone 1, H1c	Hist1h1c	**-1.20**	568	508	1603	866
1421045_at	mannose receptor, C type 2	Mrc2	**-1.20**	101	104	209	262
1419663_at	osteoglycin	Ogn	**-1.20**	24	22	54	51
1430114_at	RIKEN cDNA 5430420C16 gene	5430420C16Rik	**-1.20**	58	43	146	83
1447676_x_at	S100 calcium binding protein A16	S100a16	**-1.20**	4183	4279	9787	9710
1415906_at	thymosin, beta 4, X chromosome	Tmsb4x	**-1.20**	4175	4965	10107	10783
1445421_at	Transcribed sequences	NA	**-1.20**	90	84	216	186
1437868_at	cDNA sequence BC023892	BC023892	**-1.21**	229	251	603	508
1417795_at	cell adhesion molecule with homology to L1CAI	Chl1	**-1.21**	164	204	378	467
1443906_at	decay accelerating factor 1	Daf1	**-1.21**	61	66	142	152
1448499_a_at	epoxide hydrolase 2, cytoplasmic	Ephx2	**-1.21**	89	80	190	199
1416101_a_at	histone 1, H1c	Hist1h1c	**-1.21**	827	866	2301	1599
1458127_at	NA	NA	**-1.21**	295	220	631	549
1425284_a_at	RAB27A, member RAS oncogene family	Rab27a	**-1.21**	12	14	35	24
1439184_s_at	thioredoxin-like 5	Txnl5	**-1.21**	1718	1693	3802	4074
1419239_at	zinc finger protein 54	Zfp54	**-1.21**	104	102	287	189
1433971_at	calmodulin binding transcription activator 1	Camta1	**-1.22**	181	170	389	427
1439203_at	Special AT-rich sequence binding protein 1	Satb1	**-1.22**	117	95	247	245
1424359_at	5-oxoprolinase (ATP-hydrolysing)	Oplah	**-1.23**	83	76	197	175
1432418_a_at	creatine kinase, mitochondrial 1, ubiquitous	Ckmt1	**-1.23**	60	58	144	135
1447299_at	NA	NA	**-1.23**	65	32	146	70
1452160_at	TCDD-inducible poly(ADP-ribose) polymerase	Tiparp	**-1.23**	909	813	2105	1933
1434485_a_at	UDP-glucose pyrophosphorylase 2	Ugp2	**-1.23**	535	567	1377	1209
1418073_at	acyl-Coenzyme A thioesterase 2, mitochondrial	Acate2	**-1.24**	2208	2195	5417	4991
1455372_at	cytoplasmic polyadenylation element binding pr	Cpeb3	**-1.24**	97	102	251	218
1449773_s_at	growth arrest and DNA-damage-inducible 45 be	Gadd45b	**-1.24**	95	81	212	201
1436633_at	LOC380741 (LOC380741), mRNA	NA	**-1.24**	83	75	184	188
1416749_at	protease, serine, 11 (Igf binding)	Prss11	**-1.24**	1487	1133	2924	3208
1437869_at	RIKEN cDNA 3222402P14 gene	3222402P14Rik	**-1.24**	1196	961	2670	2404
1436183_at	RIKEN cDNA 9830115L13 gene	9830115L13Rik	**-1.24**	1010	1040	2335	2521
1456891_at	DENN/MADD domain containing 2C	Dennd2c	**-1.24**	627	713	1614	1551
1438115_a_at	solute carrier family 9 (sodium/hydrogen exchar	Slc9a3r1	**-1.24**	396	362	866	923
1427477_at	transmembrane protease, serine 13	Tmprss13	**-1.24**	243	271	664	545
1449968_s_at	acyl-Coenzyme A thioesterase 2, mitochondrial	Acate2	**-1.25**	1362	1593	3655	3360
1459823_at	EH-domain containing 2	Ehd2	**-1.25**	363	377	917	844
1434575_at	erythrocyte protein band 4.1-like 1	Epb4.1l1	**-1.25**	217	221	484	560
1434802_s_at	neurotrophin 3	Ntf3	**-1.25**	520	427	1065	1169

1438588_at	pleiomorphic adenoma gene-like 1	Plagl1	**-1.25**	104	118	276	249
1435354_at	potassium inwardly-rectifying channel, subfamil	Kcnj15	**-1.25**	419	395	1017	925
1455786_at	RIKEN cDNA 2610036F08 gene	2610036F08Rik	**-1.25**	114	118	295	256
1437434_a_at	RIKEN cDNA 5031439A09 gene	5031439A09Rik	**-1.25**	978	955	2352	2243
1437469_at	RIKEN cDNA A030007D23 gene	A030007D23Rik	**-1.25**	148	131	370	292
1430567_at	serine protease inhibitor, Kazal type 5	Spink5	**-1.25**	35	31	88	68
1453377_at	SH2 domain containing 4A	Sh2d4a	**-1.25**	136	100	333	224
1456003_a_at	solute carrier family 1 (glutamate/neutral amino	Slc1a4	**-1.25**	394	420	843	1086
1420821_at	sphingosine-1-phosphate phosphatase 1	Sgpp1	**-1.25**	427	377	1127	783
1434738_at	threonyl-tRNA synthetase-like 2	Tarsl2	**-1.25**	145	155	385	327
1436293_x_at	DNA segment, Chr 1, ERATO Doi 471, express	D1Ertd471e	**-1.26**	242	205	494	576
1419133_at	envoplakin	Evpl	**-1.26**	174	161	400	405
1416343_a_at	lysosomal membrane glycoprotein 2	Lamp2	**-1.26**	210	240	578	492
1448233_at	prion protein	Prnp	**-1.26**	1734	1515	4009	3736
1418890_a_at	RAB3D, member RAS oncogene family	Rab3d	**-1.26**	170	208	505	398
1451201_s_at	ribonuclease/angiogenin inhibitor 1	Rnh1	**-1.26**	728	815	2042	1649
1429637_at	RIKEN cDNA 2210419I08 gene	2210419I08Rik	**-1.26**	186	202	546	385
1436122_at	Zinc finger protein 667 (Zfp667), mRNA	A830025F02Rik	**-1.26**	276	270	716	590
1460351_at	S100 calcium binding protein A11 (calizzarin)	S100a11	**-1.26**	2296	2561	5515	6105
1455304_at	Similar to Munc13-3 (LOC235480), mRNA	NA	**-1.26**	68	64	122	195
1416921_x_at	aldolase 1, A isoform	Aldo1	**-1.27**	3017	2143	6834	5430
1424877_a_at	aminolevulinate, delta-, dehydratase	Alad	**-1.27**	244	240	619	549
1437058_at	EGF-like-domain, multiple 3	Egfl3	**-1.27**	324	292	705	777
1433481_at	FK506 binding protein 14	Fkbp14	**-1.27**	194	231	539	480
1434815_a_at	mitogen-activated protein kinase-activated prote	Mapkapk3	**-1.27**	467	422	1108	1028
1443122_at	NA	NA	**-1.27**	59	49	155	104
1451508_at	RIKEN cDNA 1700108L22 gene	1700108L22Rik	**-1.27**	145	158	349	383
1417580_s_at	selenium binding protein 1	Selenbp1	**-1.27**	98	96	234	234
1438116_x_at	solute carrier family 9 (sodium/hydrogen exchar	Slc9a3r1	**-1.27**	262	273	589	706
1444441_at	Transcribed sequences	NA	**-1.27**	246	231	589	561
1449131_s_at	CD1d1 antigen	Cd1d1	**-1.28**	397	534	1141	1101
1418267_at	macrophage stimulating 1 (hepatocyte growth fa	Mst1	**-1.28**	91	88	221	213
1457358_at	Myeloid ecotropic viral integration site-related g	Mrg1	**-1.28**	66	77	157	189
1441793_at	Protein phosphatase 1, regulatory (inhibitor) sul	Ppp1r11	**-1.28**	414	327	766	1018
1448786_at	RIKEN cDNA 1100001H23 gene	1100001H23Rik	**-1.28**	726	626	1811	1472
1439375_x_at	aldolase 1, A isoform	Aldo1	**-1.29**	2011	1447	4330	4032
1416138_at	annexin A7	Anxa7	**-1.29**	358	386	944	868
1416194_at	cytochrome P450, family 4, subfamily b, polype	Cyp4b1	**-1.29**	689	627	1529	1675
1448606_at	endothelial differentiation, lysophosphatidic acic	Edg2	**-1.29**	287	305	710	734
1424096_at	keratin complex 2, basic, gene 5	Krt2-5	**-1.29**	8392	8994	21358	21270
1455521_at	Kruppel-like factor 12	Klf12	**-1.29**	277	269	743	595
1428922_at	RIKEN cDNA 1200009O22 gene	1200009O22Rik	**-1.29**	192	214	540	455
1460407_at	Spi-B transcription factor (Spi-1/PU.1 related)	Spib	**-1.29**	120	124	304	293
1422822_at	StAR-related lipid transfer (START) domain cor	Stard5	**-1.29**	381	370	1045	793
1437665_at	Transcribed sequences	NA	**-1.29**	98	92	259	205
1427553_at	Clone IMAGE:4190185, mRNA, partial cds	NA	**-1.30**	120	81	253	232
1438407_at	RIKEN cDNA 9330132E09 gene	9330132E09Rik	**-1.30**	2138	2354	5406	5666
1417335_at	sulfotransferase family, cytosolic, 2B, member 1	Sult2b1	**-1.30**	526	400	1606	649
1423035_s_at	thioredoxin-like 5	Txnl5	**-1.30**	1691	1992	4117	4950
1445701_at	ATPase, Ca++ transporting, plasma membrane	Atp2b4	**-1.30**	252	212	620	515
1460657_at	wingless related MMTV integration site 10a	Wnt10a	**-1.30**	414	343	803	1049
1419401_at	ankyrin repeat and SOCS box-containing protei	Asb13	**-1.31**	295	281	783	647
1449130_at	CD1d1 antigen	Cd1d1	**-1.31**	460	520	1226	1202
1437689_x_at	clusterin	Clu	**-1.31**	248	256	633	618
1435435_at	cortactin binding protein 2	Cortbp2	**-1.31**	57	73	198	121
1448491_at	enoyl coenzyme A hydratase 1, peroxisoma	Ech1	**-1.31**	366	453	982	1041
1416554_at	PDZ and LIM domain 1 (elfin)	Pdlim1	**-1.31**	1349	1547	3382	3790
1452714_at	RIKEN cDNA 1200003E16 gene	1200003E16Rik	**-1.31**	806	834	2220	1847
1420191_s_at	DNA segment, Chr 16, Brigham & Women's Ge	D16Bwg1494e	**-1.32**	185	194	471	475
1449770_x_at	DNA segment, Chr 16, Brigham & Women's Ge	D16Bwg1494e	**-1.32**	374	384	908	982
1451177_at	DnaJ (Hsp40) homolog, subfamily B, member 4	Dnajb4	**-1.32**	1742	2005	5109	4211
1449036_at	ring finger protein 128	Rnf128	**-1.32**	48	47	100	139
1452246_at	osteoclast stimulating factor 1	Ostf1	**-1.33**	164	187	515	363
1447992_s_at	proprotein convertase subtilisin/kexin type 2	Pcsk2	**-1.33**	31	28	69	80
1459749_s_at	FAT tumor suppressor homolog 4 (Drosophila)	Fat4	**-1.33**	50	52	114	141
1425248_a_at	TYRO3 protein tyrosine kinase 3	Tyro3	**-1.33**	38	49	91	125
1455101_at	Clone IMAGE:2647821, mRNA	NA	**-1.34**	116	132	308	317
1439860_at	eukaryotic elongation factor-2 kinase	Eef2k	**-1.34**	294	316	799	745
1420565_at	homeo box A1	Hoxa1	**-1.34**	1356	960	3163	2634
1450726_at	N-acylsphingosine amidohydrolase 2	Asah2	**-1.34**	141	114	325	319
1441774_at	Rab38, member of RAS oncogene family	Rab38	**-1.34**	184	178	508	405
1416805_at	RIKEN cDNA 1110032E23 gene	1110032E23Rik	**-1.34**	67	64	180	149
1433582_at	RIKEN cDNA 1190002N15 gene	1190002N15Rik	**-1.34**	703	804	2032	1766
1418951_at	taxilin beta	Txlnb	**-1.34**	9	14	24	33

1430396_at	RIKEN cDNA 5730403I07 gene	5730403I07Rik	**-1.34**	61	56	155	142
1426721_s_at	TCDD-inducible poly(ADP-ribose) polymerase	Tiparp	**-1.34**	795	899	2030	2258
1445574_at	Transcribed sequences	NA	**-1.34**	255	290	666	714
1457533_at	Transcribed sequences	NA	**-1.34**	67	72	200	150
1439429_x_at	deltex 2 homolog (Drosophila)	Dtx2	**-1.35**	482	547	1117	1498
1450724_at	down-regulated by Ctnnb1, a	Drctnnb1a	**-1.35**	1167	1099	2908	2876
1445558_at	NA	NA	**-1.35**	169	199	512	427
1417738_at	RAB25, member RAS oncogene family	Rab25	**-1.35**	325	314	881	745
1420583_a_at	RAR-related orphan receptor alpha	Rora	**-1.35**	152	111	383	277
1431057_a_at	protease, serine, 23	Prss23	**-1.35**	1091	920	2702	2419
1427228_at	RIKEN cDNA 2410003B16 gene	2410003B16Rik	**-1.35**	211	223	553	553
1442791_x_at	RIKEN cDNA 6720407P12 gene	6720407P12Rik	**-1.35**	83	71	195	194
1423135_at	thymus cell antigen 1, theta	Thy1	**-1.35**	71	90	187	219
1438057_at	Transcribed sequence with moderate similarity	NA	**-1.35**	36	33	99	77
1442074_at	Transcribed sequences	NA	**-1.35**	34	38	103	79
1434799_x_at	aldolase 1, A isoform	Aldo1	**-1.36**	2521	1837	5999	5047
1422631_at	aryl-hydrocarbon receptor	Ahr	**-1.36**	2410	2470	6475	6073
1425658_at	CD109 antigen	Cd109	**-1.36**	166	155	444	379
1426276_at	interferon induced with helicase C domain 1	Ifih1	**-1.36**	141	159	377	393
1436475_at	nuclear receptor subfamily 2, group F, member	Nr2f2	**-1.36**	54	38	123	112
1422637_at	Ras association (RalGDS/AF-6) domain family	Rassf5	**-1.36**	69	57	144	178
1422638_s_at	Ras association (RalGDS/AF-6) domain family	Rassf5	**-1.36**	333	290	715	885
1432739_at	RIKEN cDNA 2900060K15 gene	2900060K15Rik	**-1.36**	55	57	133	153
1415944_at	syndecan 1	Sdc1	**-1.36**	1038	1251	2708	3131
1458706_at	Transcribed sequences	NA	**-1.36**	387	316	959	830
1419738_a_at	tropomyosin 2, beta	Tpm2	**-1.36**	375	426	910	1142
1452411_at	leucine rich repeat containing 1	Lrrc1	**-1.37**	440	467	1247	1099
1418601_at	aldehyde dehydrogenase family 1, subfamily A7	Aldh1a7	**-1.38**	54	46	156	104
1433604_x_at	aldolase 1, A isoform	Aldo1	**-1.38**	1462	1046	3570	2877
1425002_at	cDNA sequence BC010462	BC010462	**-1.38**	24	29	87	52
1417823_at	glycine C-acetyltransferase (2-amino-3-ketobuty	Gcat	**-1.38**	517	469	1364	1199
1422667_at	keratin complex 1, acidic, gene 15	Krt1-15	**-1.38**	8112	10073	24844	22319
1455091_at	male-specific lethal-2 homolog (Drosophila)	Msl2	**-1.38**	262	251	712	625
1442560_at	Monoglyceride lipase	Mgll	**-1.38**	113	104	255	308
1449459_s_at	ankyrin repeat and SOCS box-containing protei	Asb13	**-1.39**	340	334	954	807
1419091_a_at	annexin A2	Anxa2	**-1.39**	3973	3719	10655	9485
1459301_at	Myeloid ecotropic viral integration site-related g	Mrg1	**-1.39**	246	236	550	716
1435342_at	potassium inwardly-rectifying channel, subfamil	Kcnk6	**-1.39**	380	340	960	928
1418799_a_at	procollagen, type XVII, alpha 1	Col17a1	**-1.39**	1273	1547	3098	4265
1460459_at	progestin and adipoQ receptor family member \	Paqr5	**-1.39**	162	164	493	362
1433581_at	RIKEN cDNA 1190002N15 gene	1190002N15Rik	**-1.39**	733	824	2024	2057
1456317_at	RIKEN cDNA 1700055N04 gene	1700055N04Rik	**-1.39**	109	147	348	317
1458055_at	Desmocollin 3	Dsc3	**-1.40**	30	21	82	49
1427318_s_at	dysferlin /// fer-1-like 3, myoferlin (C. elegans)	Dysf /// Fer1l3	**-1.40**	76	86	250	177
1418925_at	cadherin EGF LAG seven-pass G-type receptor	Celsr1	**-1.41**	466	423	1154	1201
1448792_a_at	cytochrome P450, family 2, subfamily f, polypep	Cyp2f2	**-1.41**	69	59	182	157
1422662_at	lectin, galactose binding, soluble 8	Lgals8	**-1.41**	557	542	1536	1384
1426941_at	mucin 15	Muc15	**-1.41**	657	590	2163	1145
1423034_at	thioredoxin-like 5	Txnl5	**-1.41**	450	533	1272	1326
1425801_x_at	coactosin-like 1 (Dictyostelium)	Cotl1	**-1.42**	760	723	1849	2123
1449013_at	eukaryotic elongation factor-2 kinase	Eef2k	**-1.42**	294	307	796	808
1449259_at	RAB3D, member RAS oncogene family	Rab3d	**-1.42**	217	323	750	665
1436733_at	RIKEN cDNA E130309F12 gene	E130309F12Rik	**-1.42**	60	59	160	157
1437258_at	Small proline-rich protein 2B	Sprr2a	**-1.42**	13	9	27	30
1448612_at	stratifin	Sfn	**-1.42**	121	162	368	381
1437927_at	discs, large homolog 2 (Drosophila)	Dlgh2	**-1.43**	61	48	143	149
1429779_at	eukaryotic translation initiation factor 2C, 4	Eif2c4	**-1.43**	257	192	614	581
1435551_at	formin-family protein FHOS2	FHOS2	**-1.43**	235	194	530	618
1428083_at	RIKEN cDNA 2310043N10 gene	2310043N10Rik	**-1.43**	1158	987	3241	2541
1450699_at	selenium binding protein 1	Selenbp1	**-1.43**	120	150	358	362
1443749_x_at	solute carrier family 1 (glial high affinity glutama	Slc1a3	**-1.43**	471	447	1131	1338
1451413_at	calpastatin	Cast	**-1.44**	542	596	1561	1521
1418944_at	cysteinyl leukotriene receptor 1	Cysltr1	**-1.44**	40	56	118	141
1427183_at	epidermal growth factor-containing fibulin-like e	Efemp1	**-1.44**	880	889	2209	2603
1427165_at	interleukin 13 receptor, alpha 1	Il13ra1	**-1.44**	575	634	1746	1522
1437303_at	interleukin 6 signal transducer	Il6st	**-1.44**	542	504	1336	1509
1457413_at	Receptor tyrosine kinase-like orphan receptor 1	Ror1	**-1.44**	129	103	320	306
1428891_at	RIKEN cDNA 9130213B05 gene	9130213B05Rik	**-1.44**	1361	1263	3634	3468
1428145_at	acetyl-Coenzyme A acyltransferase 2 (mitochor	Acaa2	**-1.45**	1229	1415	3882	3336
1435972_at	calpastatin	Cast	**-1.45**	391	527	1220	1264
1427912_at	carbonyl reductase 3	Cbr3	**-1.45**	204	247	583	645
1460732_a_at	periplakin	Ppl	**-1.45**	1017	913	2719	2541
1422603_at	ribonuclease, RNase A family 4	Rnase4	**-1.45**	2128	2268	5996	5975
1424214_at	RIKEN cDNA 9130213B05 gene	9130213B05Rik	**-1.45**	418	398	992	1236

1436092_at	Transcribed sequence with weak similarity to p	NA	**-1.45**	410	456	990	1370
1418091_at	transcription factor CP2-like 1	Tcfcp2l1	**-1.45**	187	159	483	459
1418762_at	decay accelerating factor 1	Daf1	**-1.46**	34	32	103	79
1419086_at	fibroblast growth factor binding protein 1	Fgfbp1	**-1.46**	758	788	2063	2192
1430843_at	glutamate decarboxylase-like 1	Gadl1	**-1.46**	79	85	271	180
1434051_s_at	heat shock 70kDa protein 12A	Hspa12a	**-1.46**	90	72	243	200
1439153_at	IBR domain containing 2	Ibrdc2	**-1.46**	832	834	2516	2062
1425028_a_at	tropomyosin 2, beta	Tpm2	**-1.46**	108	109	263	335
1448213_at	annexin A1	Anxa1	**-1.47**	3908	3893	12052	9581
1436932_at	similar to sister-of-mammalian grainyhead prote	LOC230824	**-1.47**	190	141	498	410
1433610_at	expressed sequence AA986860	AA986860	**-1.48**	26	21	72	57
1421492_at	prostaglandin D2 synthase 2, hematopoietic	Ptgds2	**-1.48**	115	127	367	306
1423771_at	protein kinase C, delta binding protein	Prkcdbp	**-1.48**	78	101	241	257
1428146_s_at	acetyl-Coenzyme A acyltransferase 2 (mitochor	Acaa2	**-1.49**	1649	1689	4732	4630
1453289_at	eukaryotic translation initiation factor 2C, 4	Eif2c4	**-1.49**	917	1000	2760	2635
1416531_at	glutathione S-transferase omega 1	Gsto1	**-1.49**	994	970	2797	2731
1419027_s_at	glycolipid transfer protein	Gltp	**-1.49**	4227	3880	11776	10898
1450971_at	growth arrest and DNA-damage-inducible 45 be	Gadd45b	**-1.49**	149	146	440	386
1417962_s_at	growth hormone receptor	Ghr	**-1.49**	1525	1663	4426	4504
1457044_at	RIKEN cDNA 4732474O15 gene	4732474O15Rik	**-1.49**	131	172	450	395
1452059_at	solute carrier family 35, member F5	Slc35f5	**-1.49**	315	365	1042	867
1422906_at	ATP-binding cassette, sub-family G (WHITE), m	Abcg2	**-1.50**	1048	1082	2849	3184
1437312_at	bone morphogenetic protein receptor, type 1B	Bmpr1b	**-1.50**	638	644	1839	1791
1448494_at	growth arrest specific 1	Gas1	**-1.50**	2558	2259	7153	6410
1451385_at	RIKEN cDNA 2310056P07 gene	2310056P07Rik	**-1.50**	2407	2246	6901	6232
1431248_at	RIKEN cDNA 5031426D15 gene	5031426D15Rik	**-1.50**	98	75	260	225
1449577_x_at	tropomyosin 2, beta	Tpm2	**-1.50**	32	34	90	99
1423606_at	periostin, osteoblast specific factor	Postn	**-1.51**	4069	3972	11291	11576
1453286_at	plexin A2	Plxna2	**-1.51**	352	277	900	876
1421456_at	purinergic receptor P2Y, G-protein coupled 1	P2ry1	**-1.51**	140	152	403	426
1424239_at	RIKEN cDNA 2310066E14 gene	2310066E14Rik	**-1.51**	92	90	238	283
1444740_at	Transcribed sequences	NA	**-1.51**	298	275	871	757
1436702_at	cDNA sequence BC034068	BC034068	**-1.52**	66	51	159	170
1454783_at	interleukin 13 receptor, alpha 1	Il13ra1	**-1.52**	796	795	2373	2188
1425506_at	myosin, light polypeptide kinase	Mylk	**-1.52**	99	112	284	320
1419201_at	RIKEN cDNA 2310015I08 gene	2310015I08Rik	**-1.52**	169	132	431	425
1424612_at	NIPA-like domain containing 2	Npal2	**-1.52**	695	640	2095	1741
1438125_at	RIKEN cDNA C230085N15 gene	C230085N15Rik	**-1.52**	125	118	344	351
1436365_at	zinc finger and BTB domain containing 36	Zbtb36	**-1.52**	112	108	319	308
1455238_at	melanoma associated antigen (mutated) 1-like 1	Mum1l1	**-1.53**	55	68	182	172
1440635_at	Transcribed sequences	NA	**-1.53**	155	155	442	454
1451739_at	Kruppel-like factor 5	Klf5	**-1.54**	814	660	2708	1560
1426221_at	loss of heterozygosity, 11, chromosomal region	Loh11cr2a	**-1.54**	301	522	705	1595
1429274_at	RIKEN cDNA 2310010M24 gene	2310010M24Rik	**-1.54**	1049	928	2956	2796
1433719_at	solute carrier family 9 (sodium/hydrogen exchar	Slc9a9	**-1.54**	60	51	148	171
1450633_at	calmodulin 4	Calm4	**-1.55**	1623	1997	6095	4421
1452843_at	interleukin 6 signal transducer	Il6st	**-1.55**	260	307	831	822
1435973_at	Transcribed sequences	NA	**-1.55**	161	120	498	313
1441342_at	dipeptidylpeptidase 4	Dpp4	**-1.56**	44	53	170	115
1456036_x_at	glutathione S-transferase omega 1	Gsto1	**-1.56**	2440	1916	6087	6642
1428680_at	CDP-diacylglycerol synthase 1	Cds1	**-1.57**	207	218	632	632
1435785_at	EH-domain containing 2	Ehd2	**-1.57**	306	318	842	1005
1455140_at	expressed sequence AI848332	AI848332	**-1.57**	395	404	1145	1223
1450769_s_at	StAR-related lipid transfer (START) domain cor	Stard5	**-1.57**	474	442	1547	1174
1450391_a_at	monoglyceride lipase	Mgll	**-1.59**	46	45	130	144
1444937_at	NA	NA	**-1.59**	238	133	600	472
1424130_a_at	polymerase I and transcript release factor	Ptrf	**-1.59**	1106	891	2929	3043
1450435_at	solute carrier family 7 (cationic amino acid trans	Slc7a2	**-1.59**	325	296	942	929
1421844_at	interleukin 1 receptor accessory protein	Il1rap	**-1.60**	412	397	1244	1202
1442920_at	Kruppel-like factor 3 (basic)	Klf3	**-1.60**	77	73	240	214
1426245_s_at	microtubule-associated protein, RP/EB family, r	Mapre2	**-1.60**	121	110	311	388
1424842_a_at	Rho GTPase activating protein 24	Arhgap24	**-1.60**	398	482	1504	1147
1426397_at	transforming growth factor, beta receptor I	Tgfbr2	**-1.60**	830	730	2283	2444
1434957_at	cell adhesion molecule-related/down-regulated	Cdon	**-1.61**	1615	1699	4426	5656
1427011_a_at	LanC (bacterial lantibiotic synthetase componer	Lancl1	**-1.61**	1710	1684	5489	4886
1421690_s_at	agouti related protein	Agrp	**-1.62**	32	38	101	115
1450981_at	calponin 2	Cnn2	**-1.62**	1235	1216	3736	3815
1434866_x_at	carnitine palmitoyltransferase 1a, liver	Cpt1a	**-1.62**	83	62	203	237
1416527_at	RAB32, member RAS oncogene family	Rab32	**-1.62**	66	98	231	264
1431110_at	RIKEN cDNA 5430431D22 gene	5430431D22Rik	**-1.62**	107	95	323	297
1416589_at	secreted acidic cysteine rich glycoprotein	Sparc	**-1.62**	771	722	2151	2436
1416002_x_at	coactosin-like 1 (Dictyostelium)	Cotl1	**-1.63**	232	207	629	727
1451451_at	grancalcin	Gca	**-1.63**	34	29	123	68
1452614_at	hypothetical gene supported by AF014453	LOC229672	**-1.63**	101	143	352	390

1439628_x_at	Rab38, member of RAS oncogene family	Rab38	**-1.63**	1633	1705	5175	5142
1422573_at	AMP deaminase 3	Ampd3	**-1.64**	403	571	1336	1657
1460406_at	expressed sequence AI427122	AI427122	**-1.64**	224	225	719	681
1456084_x_at	fibromodulin	Fmod	**-1.64**	15	18	44	59
1427012_at	LanC (bacterial lantibiotic synthetase componer	Lancl1	**-1.64**	623	614	1837	2028
1419051_at	OVO homolog-like 1 (Drosophila)	Ovol1	**-1.64**	107	82	308	277
1444147_at	proprotein convertase subtilisin/kexin type 2	Pcsk2	**-1.64**	42	23	108	87
1449848_at	guanine nucleotide binding protein, alpha 14	Gna14	**-1.65**	134	132	369	465
1449586_at	plakophilin 1	Pkp1	**-1.65**	4162	3627	13242	11215
1416007_at	special AT-rich sequence binding protein 1	Satb1	**-1.65**	1071	943	2921	3380
1454867_at	meningioma 1	Mn1	**-1.65**	63	95	236	249
1438156_x_at	carnitine palmitoyltransferase 1a, liver	Cpt1a	**-1.66**	33	22	78	92
1451989_a_at	microtubule-associated protein, RP/EB family, r	Mapre2	**-1.66**	412	469	1229	1549
1455037_at	plexin A2	Plxna2	**-1.66**	191	161	574	532
1459529_at	RIKEN cDNA E230016K23 gene	E230016K23Rik	**-1.66**	21	15	49	62
1437231_at	SLIT and NTRK-like family, member 6	Slitrk6	**-1.66**	119	159	408	462
1428650_at	tensin	Tns	**-1.66**	336	258	813	1045
1435693_at	mal, T-cell differentiation protein-like	Mall	**-1.67**	622	583	1974	1870
1456114_at	CDP-diacylglycerol synthase 1	Cds1	**-1.67**	259	271	863	820
1420461_at	macrophage stimulating 1 receptor (c-met-relate	Mst1r	**-1.67**	70	59	200	208
1418318_at	ring finger protein 128	Rnf128	**-1.67**	85	75	252	258
1455061_a_at	acetyl-Coenzyme A acyltransferase 2 (mitochor	Acaa2	**-1.68**	101	111	375	303
1433509_s_at	DNA segment, Chr 6, ERATO Doi 253, express	D6Ertd253e	**-1.68**	246	203	784	645
1427164_at	interleukin 13 receptor, alpha 1	Il13ra1	**-1.68**	266	263	832	866
1424034_at	RAR-related orphan receptor alpha	Rora	**-1.68**	457	315	1440	997
1441214_at	synaptotagmin-like homologue lacking C2 doma	MGI:2443248	**-1.68**	314	261	958	873
1450005_x_at	EGF-like-domain, multiple 9	Egfl9	**-1.69**	125	126	381	430
1437829_s_at	eukaryotic elongation factor-2 kinase	Eef2k	**-1.69**	1416	1360	4574	4380
1417394_at	Kruppel-like factor 4 (gut)	Klf4	**-1.69**	2460	2128	7689	7115
1455627_at	procollagen, type VIII, alpha 1	Col8a1	**-1.69**	524	399	1528	1433
1434146_at	Glutamate receptor, ionotropic, AMPA2 (alpha 2	Gria2	**-1.70**	11	11	41	32
1436236_x_at	coactosin-like 1 (Dictyostelium)	Cotl1	**-1.70**	494	393	1480	1382
1421970_a_at	glutamate receptor, ionotropic, AMPA2 (alpha 2	Gria2	**-1.70**	52	29	152	100
1427537_at	epiplakin 1	Eppk1	**-1.71**	1293	963	3848	3465
1424638_at	cyclin-dependent kinase inhibitor 1A (P21)	Cdkn1a	**-1.72**	387	369	1558	931
1453345_at	RIKEN cDNA 3830408G10 gene	3830408G10Rik	**-1.72**	60	79	296	159
1439675_at	RIKEN cDNA 4933429D07 gene	4933429D07Rik	**-1.72**	72	59	200	232
1436119_at	aldehyde dehydrogenase 1 family, member L2	Aldh1l2	**-1.73**	236	271	893	783
1416592_at	glutaredoxin 1 (thioltransferase)	Glrx1	**-1.73**	149	130	444	481
1436182_at	special AT-rich sequence binding protein 1	Satb1	**-1.73**	1460	1472	5196	4547
1456741_s_at	glycoprotein m6a	Gpm6a	**-1.75**	28	26	88	94
1445626_at	Lectin, galactose binding, soluble 3	Lgals3	**-1.75**	67	70	311	150
1420760_s_at	N-myc downstream regulated gene 1	Ndrg1	**-1.75**	1203	740	4082	2280
1436590_at	protein phosphatase 1, regulatory (inhibitor) sub	Ppp1r3b	**-1.75**	594	582	2169	1790
1434773_a_at	solute carrier family 2 (facilitated glucose transp	Slc2a1	**-1.75**	1693	959	4707	3889
1442434_at	DNA segment, Chr 8, ERATO Doi 82, expresse	D8Ertd82e	**-1.76**	293	270	907	994
1427019_at	protein tyrosine phosphatase, receptor type Z, p	Ptprz1	**-1.76**	176	197	631	626
1416200_at	RIKEN cDNA 9230117N10 gene	9230117N10Rik	**-1.76**	59	58	227	167
1418891_a_at	RAB3D, member RAS oncogene family	Rab3d	**-1.77**	251	368	1016	1057
1455377_at	RIKEN cDNA 4921517B04 gene /// similar to FL	17B04Rik /// LOC3	**-1.77**	65	57	246	170
1439449_at	special AT-rich sequence binding protein 1	Satb1	**-1.77**	665	755	2154	2679
1418086_at	protein phosphatase 1, regulatory (inhibitor) sub	Ppp1r14a	**-1.78**	35	34	118	119
1424701_at	protocadherin 20	Pcdh20	**-1.78**	338	311	1067	1161
1455288_at	RIKEN cDNA 1110036O03 gene	1110036O03Rik	**-1.78**	107	88	362	304
1457656_s_at	RIKEN cDNA C230085N15 gene	C230085N15Rik	**-1.78**	557	498	1695	1922
1448392_at	secreted acidic cysteine rich glycoprotein	Sparc	**-1.78**	1084	1030	3542	3740
1426600_at	solute carrier family 2 (facilitated glucose transp	Slc2a1	**-1.79**	812	592	2622	2164
1443284_at	Special AT-rich sequence binding protein 1	Satb1	**-1.79**	143	135	470	489
1424698_s_at	grancalcin	Gca	**-1.80**	42	47	189	122
1422308_a_at	lectin, galactose binding, soluble 7	Lgals7	**-1.80**	2769	3095	11282	9116
1432976_at	RIKEN cDNA 2310038E17 gene	2310038E17Rik	**-1.80**	41	37	138	133
1460003_at	expressed sequence AI956758	AI956758	**-1.81**	262	264	1035	812
1458738_at	Guanine nucleotide binding protein, alpha 14	Gna14	**-1.82**	225	192	663	801
1425213_at	RIKEN cDNA 6430514L14 gene	6430514L14Rik	**-1.82**	246	249	818	926
1444392_at	Leprecan-like 1	Leprel1	**-1.83**	374	352	1395	1182
1439794_at	Netrin 4 (Ntn4), mRNA	Ntn4	**-1.83**	287	236	857	986
1421679_a_at	cyclin-dependent kinase inhibitor 1A (P21)	Cdkn1a	**-1.84**	1077	948	4377	2845
1429808_at	RIKEN cDNA 1110020C03 gene	1110020C03Rik	**-1.84**	65	66	208	260
1420468_at	ankyrin repeat and SOCS box-containing protei	Asb17	**-1.85**	31	33	130	101
1417700_at	Rab38, member of RAS oncogene family	Rab38	**-1.85**	1158	1182	4230	4223
1426599_a_at	solute carrier family 2 (facilitated glucose transp	Slc2a1	**-1.85**	933	604	2948	2460
1437813_at	absent in melanoma 1-like	Aim1l	**-1.86**	50	57	227	161
1426243_at	cystathionase (cystathionine gamma-lyase)	Cth	**-1.86**	372	365	1236	1431
1420807_a_at	EGF-like-domain, multiple 9	Egfl9	**-1.86**	142	147	490	554

1460463_at	RIKEN cDNA 4632413I24 gene	4632413I24Rik	**-1.86**	945	781	3408	2839
1450782_at	wingless-related MMTV integration site 4	Wnt4	**-1.86**	639	676	2281	2474
1420312_s_at	NA	NA	**-1.87**	77	73	292	254
1441687_at	wingless-related MMTV integration site 4	Wnt4	**-1.87**	149	149	585	501
1417089_a_at	creatine kinase, mitochondrial 1, ubiquitous	Ckmt1	**-1.88**	755	825	2828	2989
1449994_at	epithelial mitogen	Epgn	**-1.88**	134	160	468	612
1452284_at	protein tyrosine phosphatase, receptor type Z, p	Ptprz1	**-1.89**	598	612	2274	2205
1431775_at	RIKEN cDNA 3100002H09 gene	3100002H09Rik	**-1.89**	91	96	357	335
1455165_at	RAR-related orphan receptor alpha, mRNA (cD	Rora	**-1.89**	157	115	606	392
1418912_at	plexin domain containing 2	Plxdc2	**-1.90**	97	87	356	331
1449158_at	potassium channel, subfamily K, member 2	Kcnk2	**-1.90**	416	350	1419	1421
1441917_s_at	transmembrane protein 40	Tmem40	**-1.90**	177	231	743	763
1419204_at	delta-like 1 (Drosophila)	Dll1	**-1.91**	335	328	1138	1355
1428622_at	DEP domain containing 6	Depdc6	**-1.91**	155	186	730	547
1445638_at	Myeloid ecotropic viral integration site-related g	Mrg1	**-1.91**	19	20	77	68
1437019_at	RIKEN cDNA 2200001I15 gene	2200001I15Rik	**-1.91**	120	120	482	418
1449816_at	sulfotransferase family 5A, member 1	Sult5a1	**-1.91**	396	336	1356	1380
1429067_at	calpain, small subunit 2	Capns2	**-1.92**	811	869	3616	2754
1456174_x_at	N-myc downstream regulated gene 1	Ndrg1	**-1.92**	923	508	3358	1826
1438570_at	Transcribed sequences	NA	**-1.92**	681	523	2302	2228
1416022_at	fatty acid binding protein 5, epidermal	Fabp5	**-1.93**	2096	2157	9802	6350
1417129_a_at	myeloid ecotropic viral integration site-related g	Mrg1	**-1.94**	202	235	730	947
1455200_at	p21 (CDKN1A)-activated kinase 6	Pak6	**-1.94**	394	420	1346	1774
1435595_at	RIKEN cDNA 1810011O10 gene	1810011O10Rik	**-1.94**	346	286	1457	951
1433203_at	RIKEN cDNA 6030400A10 gene	6030400A10Rik	**-1.94**	506	487	1894	1911
1448987_at	acetyl-Coenzyme A dehydrogenase, long-chair	Acadl	**-1.95**	351	315	1266	1307
1417346_at	apoptosis-associated speck-like protein contain	Asc	**-1.95**	404	486	1877	1538
1430550_at	lipase-like, ab-hydrolase domain containing 3	Lipl3	**-1.95**	174	238	988	581
1417185_at	lymphocyte antigen 6 complex, locus A	Ly6a	**-1.95**	236	163	764	757
1460038_at	POU domain, class 3, transcription factor 1	Pou3f1	**-1.95**	1245	1326	5105	4847
1436325_at	RAR-related orphan receptor alpha	Rora	**-1.95**	94	74	400	245
1455408_at	RIKEN cDNA 4732472I07 gene	4732472I07Rik	**-1.95**	20	18	66	79
1455794_at	RIKEN cDNA D130058I21 gene	D130058I21Rik	**-1.95**	114	112	532	343
1447791_s_at	guanine nucleotide binding protein, alpha 14	Gna14	**-1.98**	43	54	163	216
1418084_at	neuropilin	Nrp	**-1.98**	181	184	677	762
1442936_at	NA	NA	**-1.99**	751	681	2903	2790
1440842_at	RIKEN cDNA C230085N15 gene	C230085N15Rik	**-1.99**	271	272	1089	1062
1451021_a_at	Kruppel-like factor 5	Klf5	**-2.00**	1244	1077	4930	4322
1416318_at	serine (or cysteine) proteinase inhibitor, clade E	Serpinb1a	**-2.01**	26	37	117	133
1440091_at	myeloid ecotropic viral integration site-related g	Mrg1	**-2.02**	182	188	730	773
1434425_at	expressed sequence AI597080	AI597080	**-2.05**	66	66	315	234
1439819_at	expressed sequence AU015263	AU015263	**-2.05**	124	136	677	396
1419905_s_at	hydroxyprostaglandin dehydrogenase 15 (NAD)	Hpgd	**-2.05**	17	21	77	82
1436178_at	leprecan-like 1	Leprel1	**-2.05**	248	239	969	1053
1426785_s_at	monoglyceride lipase	Mgll	**-2.05**	117	109	402	533
1437699_at	RIKEN cDNA E430014B02 gene	E430014B02Rik	**-2.05**	330	356	1485	1357
1452031_at	solute carrier family 1 (glial high affinity glutama	Slc1a3	**-2.05**	178	151	647	713
1434025_at	Kruppel-like factor 5	Klf5	**-2.06**	2268	2027	9682	8207
1421964_at	Notch gene homolog 3 (Drosophila)	Notch3	**-2.06**	68	81	354	265
1433768_at	RIKEN cDNA 2410003B16 gene	2410003B16Rik	**-2.06**	1281	1203	5286	5072
1424852_at	myocyte enhancer factor 2C	Mef2c	**-2.07**	98	123	544	376
1452232_at	UDP-N-acetyl-alpha-D-galactosamine: polypept	Galnt7	**-2.07**	277	342	1512	1073
1418365_at	cathepsin H	Ctsh	**-2.08**	242	203	997	878
1451308_at	elongation of very long chain fatty acids (FEN1/	Elovl4	**-2.08**	44	37	218	125
1417214_at	RAB27b, member RAS oncogene family	Rab27b	**-2.08**	129	104	522	457
1424976_at	ras homolog gene family, member V	Rhov	**-2.08**	76	67	349	254
1451415_at	RIKEN cDNA 1810011O10 gene	1810011O10Rik	**-2.08**	167	207	979	585
1447861_x_at	myeloid ecotropic viral integration site-related g	Mrg1	**-2.09**	44	49	194	198
1448943_at	neuropilin	Nrp	**-2.09**	211	243	930	999
1424208_at	prostaglandin E receptor 4 (subtype EP4)	Ptger4	**-2.11**	286	332	1154	1512
1455186_a_at	RIKEN cDNA 1190003J15 gene	1190003J15Rik	**-2.11**	429	466	2029	1841
1436838_x_at	coactosin-like 1 (Dictyostelium)	Cotl1	**-2.12**	928	628	3383	3263
1437811_x_at	Coactosin-like 1 (Dictyostelium)	Cotl1	**-2.13**	627	427	2289	2227
1415897_a_at	microsomal glutathione S-transferase 1	Mgst1	**-2.13**	218	260	1093	991
1448873_at	occludin	Ocln	**-2.14**	65	65	336	238
1449938_at	placental protein 11 related	Pp11r	**-2.16**	300	346	1705	1184
1443579_s_at	DEP domain containing 6	Depdc6	**-2.17**	29	25	161	80
1454666_at	Kruppel-like factor 3 (basic)	Klf3	**-2.17**	2420	2262	10926	10119
1426340_at	solute carrier family 1 (glial high affinity glutama	Slc1a3	**-2.17**	60	56	255	269
1424966_at	transmembrane protein 40	Tmem40	**-2.17**	311	345	1561	1382
1455573_at	keratin complex 1, acidic, gene 14	Krt1-14	**-2.18**	712	405	2558	2307
1439915_at	Myeloid ecotropic viral integration site-related g	Mrg1	**-2.18**	110	114	508	509
1459713_s_at	transmembrane protein 16A	Tmem16a	**-2.18**	319	341	1689	1308
1419082_at	serine (or cysteine) proteinase inhibitor, clade E	Serpinb2	**-2.19**	21	18	103	74

1450643_s_at	acyl-CoA synthetase long-chain family member	Acsl1	**-2.20**	55	53	303	193
1437232_at	bactericidal/permeability-increasing protein-like	Bpil2	**-2.20**	20	19	130	50
1443814_x_at	cathepsin H	Ctsh	**-2.20**	235	202	1086	910
1451348_at	DEP domain containing 6	Depdc6	**-2.21**	75	60	328	292
1417429_at	flavin containing monooxygenase 1	Fmo1	**-2.21**	363	285	1339	1641
1456815_at	forkhead box N1	Foxn1	**-2.21**	84	83	414	361
1439492_at	RIKEN cDNA C130053K05 gene	C130053K05Rik	**-2.21**	134	186	834	626
1446764_at	Wingless-related MMTV integration site 3A	Wnt3a	**-2.21**	217	196	870	1038
1426914_at	MARVEL (membrane-associating) domain cont	Mrvldc2	**-2.22**	158	153	800	652
1429503_at	RIKEN cDNA 2900024C23 gene	2900024C23Rik	**-2.22**	239	232	1251	950
1450744_at	elongation factor RNA polymerase II 2	Ell2	**-2.23**	1120	1056	5629	4596
1420385_at	guanine nucleotide binding protein, alpha 14	Gna14	**-2.23**	154	150	726	694
1429123_at	RAB27A, member RAS oncogene family	Rab27a	**-2.23**	131	147	686	616
1418649_at	EGL nine homolog 3 (C. elegans)	Egln3	**-2.24**	344	208	1594	930
1448852_at	regucalcin	Rgn	**-2.24**	72	63	305	333
1443138_at	Sulfotransferase family 5A, member 1	Sult5a1	**-2.24**	231	159	958	853
1439610_at	Transcribed sequences	NA	**-2.24**	119	92	508	478
1431786_s_at	RIKEN cDNA 1190003J15 gene	1190003J15Rik	**-2.25**	230	255	1197	1112
1417942_at	Ly6/Plaur domain containing 3	Lypd3	**-2.25**	129	141	637	647
1419215_at	aldehyde oxidase 4	Aox4	**-2.26**	97	102	507	446
1435076_at	RIKEN cDNA 2310047D13 gene	2310047D13Rik	**-2.26**	176	216	1010	861
1434369_a_at	crystallin, alpha B	Cryab	**-2.27**	33	22	121	137
1419709_at	stefin A3	Stfa3	**-2.28**	2049	2878	11649	11900
1460302_at	thrombospondin 1	Thbs1	**-2.29**	112	109	461	624
1420944_at	zinc finger protein 185	Zfp185	**-2.29**	376	308	2034	1296
1452114_s_at	insulin-like growth factor binding protein 5	Igfbp5	**-2.31**	175	128	760	721
1448944_at	neuropilin	Nrp	**-2.31**	150	145	794	661
1451716_at	v-maf musculoaponeurotic fibrosarcoma oncog	Mafb	**-2.31**	417	368	2247	1655
1434272_at	cytoplasmic polyadenylation element binding pr	Cpeb2	**-2.33**	333	343	1791	1611
1423856_at	popeye domain containing 3	Popdc3	**-2.33**	297	360	1192	2101
1430551_s_at	lipase-like, ab-hydrolase domain containing 3	Lipl3	**-2.34**	219	235	1552	740
1419591_at	melanoma-derived leucine zipper, extra-nuclea	Mlze	**-2.36**	202	296	1538	975
1434411_at	expressed sequence AW743884	AW743884	**-2.37**	123	117	537	706
1421811_at	thrombospondin 1	Thbs1	**-2.37**	767	586	3014	3901
1457632_s_at	myeloid ecotropic viral integration site-related g	Mrg1	**-2.38**	207	223	1029	1215
1425103_at	angiotensin I converting enzyme (peptidyl-dipep	Ace2	**-2.41**	206	205	1312	873
1451798_at	interleukin 1 receptor antagonist	Il1rn	**-2.42**	95	67	567	287
1435639_at	RIKEN cDNA 2610528A11 gene	2610528A11Rik	**-2.42**	36	31	157	198
1439630_x_at	suprabasin	Sbsn	**-2.44**	638	745	4205	3283
1420364_at	G protein-coupled receptor 87	Gpr87	**-2.45**	158	157	908	813
1449064_at	L-threonine dehydrogenase	Tdh	**-2.45**	97	107	699	413
1437517_x_at	serine (or cysteine) proteinase inhibitor, clade B	Serpinb3a	**-2.45**	126	131	798	606
1437463_x_at	transforming growth factor, beta induced	Tgfbi	**-2.45**	270	197	1242	1268
1421604_a_at	Kruppel-like factor 3 (basic)	Klf3	**-2.46**	133	136	751	731
1434150_a_at	RIKEN cDNA 3300001H21 gene	3300001H21Rik	**-2.46**	107	85	601	446
1453239_a_at	ankyrin repeat domain 22	Ankrd22	**-2.48**	33	47	259	181
1437876_at	Hypothetical gene supported by BC030430 (LO	NA	**-2.48**	76	86	456	447
1449937_at	placental protein 11 related	Pp11r	**-2.48**	1106	1309	7863	5584
1451006_at	xanthine dehydrogenase	Xdh	**-2.48**	46	32	260	164
1416697_at	dipeptidylpeptidase 4	Dpp4	**-2.49**	192	176	1178	890
1422588_at	keratin complex 2, basic, gene 6b	Krt2-6b	**-2.49**	88	106	577	507
1429360_at	Kruppel-like factor 3 (basic)	Klf3	**-2.49**	540	476	2769	2935
1442067_at	Receptor tyrosine kinase-like orphan receptor 1	Ror1	**-2.49**	662	425	3277	2673
1448123_s_at	transforming growth factor, beta induced	Tgfbi	**-2.49**	664	543	3308	3455
1452766_at	RIKEN cDNA 2900041A09 gene	2900041A09Rik	**-2.51**	69	74	377	436
1423883_at	acyl-CoA synthetase long-chain family member	Acsl1	**-2.52**	495	493	3261	2427
1425789_s_at	annexin A8	Anxa8	**-2.52**	94	93	605	466
1429313_at	receptor tyrosine kinase-like orphan receptor 1	Ror1	**-2.52**	166	136	970	751
1415871_at	transforming growth factor, beta induced	Tgfbi	**-2.52**	176	159	938	990
1446834_at	Cathepsin C	Ctsc	**-2.54**	60	77	479	309
1443017_at	cytoplasmic polyadenylation element binding pr	Cpeb2	**-2.54**	50	81	399	346
1424356_a_at	meteorin, glial cell differentiation regulator-like	Metrnl	**-2.54**	78	75	538	347
1421965_s_at	Notch gene homolog 3 (Drosophila)	Notch3	**-2.56**	308	302	1937	1648
1459897_a_at	suprabasin	Sbsn	**-2.56**	631	697	4636	3173
1421040_a_at	glutathione S-transferase, alpha 2 (Yc2)	Gsta2	**-2.57**	31	45	273	171
1460330_at	annexin A3	Anxa3	**-2.59**	79	74	421	506
1421308_at	carbonic anhydrase 13	Car13	**-2.59**	80	90	609	412
1434295_at	RAS guanyl releasing protein 1	Rasgrp1	**-2.61**	322	224	1870	1404
1454858_x_at	RIKEN cDNA 3300001H21 gene	3300001H21Rik	**-2.62**	125	98	785	581
1427957_at	RIKEN cDNA 9530008L14 gene	9530008L14Rik	**-2.65**	115	172	929	828
1420955_at	visinin-like 1	Vsnl1	**-2.65**	261	225	1506	1545
1456250_x_at	transforming growth factor, beta induced	Tgfbi	**-2.66**	871	663	4574	5016
1429076_a_at	glycerophosphodiester phosphodiesterase dom	Gdpd2	**-2.68**	108	121	753	718
1423414_at	prostaglandin-endoperoxide synthase 1	Ptgs1	**-2.69**	139	135	1001	767

1416382_at	cathepsin C	Ctsc	**-2.70**	847	870	6502	4688
1441094_at	alcohol dehydrogenase 6B (class V)	Adh6b	**-2.70**	174	180	1354	955
1452166_a_at	keratin complex 1, acidic, gene 10	Krt1-10	**-2.73**	3442	3963	25956	23170
1454159_a_at	insulin-like growth factor binding protein 2	Igfbp2	**-2.74**	73	55	407	441
1443926_at	Myeloid ecotropic viral integration site-related g	Mrg1	**-2.74**	49	40	271	323
1426208_x_at	pleiomorphic adenoma gene-like 1	Plagl1	**-2.74**	1668	1643	10892	11189
1423323_at	tumor-associated calcium signal transducer 2	Tacstd2	**-2.76**	260	222	1740	1520
1417852_x_at	chloride channel calcium activated 1	Clca1	**-2.79**	524	416	3711	2732
1459973_x_at	dipeptidylpeptidase 4	Dpp4	**-2.80**	42	35	322	211
1460591_at	estrogen receptor 1 (alpha)	Esr1	**-2.80**	56	66	366	484
1438109_at	chloride channel calcium activated 5	Clca5	**-2.81**	92	67	656	446
1447891_at	NA	NA	**-2.81**	311	190	1939	1471
1434151_at	RIKEN cDNA 3300001H21 gene	3300001H21Rik	**-2.82**	145	168	1166	1044
1421307_at	carbonic anhydrase 13	Car13	**-2.83**	100	107	745	722
1419492_s_at	defensin beta 1	Defb1	**-2.83**	156	116	761	1146
1417702_a_at	histamine N-methyltransferase	Hnmt	**-2.83**	22	24	169	159
1435761_at	stefin A1	Stfa1	**-2.83**	1452	1288	10084	9335
1425102_a_at	angiotensin I converting enzyme (peptidyl-dipep	Ace2	**-2.87**	34	36	313	201
1439528_at	RIKEN cDNA 4833423E24 gene	4833423E24Rik	**-2.88**	148	134	1408	658
1426708_at	anthrax toxin receptor 2	Antxr2	**-2.92**	137	203	966	1560
1435436_at	Transcribed sequences	NA	**-2.92**	133	156	1387	788
1416225_at	alcohol dehydrogenase 1 (class I)	Adh1	**-2.93**	191	174	1790	991
1450460_at	aquaporin 3	Aqp3	**-2.95**	193	189	1456	1497
1449500_at	serine (or cysteine) proteinase inhibitor, clade B	Serpinb7	**-2.96**	434	414	3210	3392
1431211_s_at	thioesterase superfamily member 5	Them5	**-2.99**	64	60	675	309
1424968_at	RIKEN cDNA 2210023G05 gene	2210023G05Rik	**-2.99**	112	105	853	867
1456539_at	Transcribed sequence with strong similarity to p	NA	**-3.02**	244	213	2121	1590
1422587_at	transmembrane protein 45a	Tmem45a	**-3.09**	291	342	3426	1965
1438474_at	ankyrin repeat domain 35	Ankrd35	**-3.12**	26	28	310	162
1419491_at	defensin beta 1	Defb1	**-3.12**	230	177	1662	1852
1434227_at	keratinocyte differentiation associated protein	Krtdap	**-3.16**	722	673	6328	6098
1436520_at	expressed sequence AI450948	AI450948	**-3.18**	286	196	2525	1767
1441909_s_at	RIKEN cDNA 9530066K23 gene	9530066K23Rik	**-3.20**	27	21	252	177
1417853_at	chloride channel calcium activated 2	Clca2	**-3.26**	256	199	2582	1742
1459898_at	suprabasin	Sbsn	**-3.31**	55	87	885	482
1441341_at	Transcribed sequences	NA	**-3.32**	109	105	1065	1080
1437939_s_at	Cathepsin C	Ctsc	**-3.34**	61	56	701	479
1424713_at	calmodulin-like 4	Calml4	**-3.36**	66	63	612	703
1422008_a_at	aquaporin 3	Aqp3	**-3.38**	12	12	136	118
1435760_at	cystatin A	MGI:3524930	**-3.43**	168	177	1842	1875
1448932_at	keratin complex 1, acidic, gene 16	Krt1-16	**-3.44**	81	88	1101	735
1417732_at	annexin A8	Anxa8	**-3.45**	243	203	2780	2085
1457025_at	RIKEN cDNA 4833413O15 gene	4833413O15Rik	**-3.46**	81	50	998	405
1440523_at	retinal short chain dehydrogenase reductase	Rdhe2	**-3.53**	289	260	3978	2367
1441384_at	Transcribed sequences	NA	**-3.55**	87	101	1318	885
1417408_at	coagulation factor III	F3	**-3.63**	44	33	574	376
1448152_at	insulin-like growth factor 2	Igf2	**-3.64**	650	540	7115	7633
1458000_at	desmoglein 1 alpha	Dsg1a	**-3.70**	317	263	4344	3172
1426808_at	lectin, galactose binding, soluble 3	Lgals3	**-3.74**	312	260	4311	3269
1416930_at	lymphocyte antigen 6 complex, locus D	Ly6d	**-3.80**	495	434	7376	5495
1419463_at	chloride channel calcium activated 1	Clca1	**-3.86**	592	614	9974	7551
1455519_at	desmoglein 1 alpha	Dsg1a	**-3.90**	46	44	853	494
1460259_s_at	chloride channel calcium activated 1	Clca1	**-3.92**	351	362	6390	4408
1439620_at	carbonic anhydrase 13	Car13	**-3.93**	19	16	272	266
1422481_at	keratin complex 2, basic, gene 1	Krt2-1	**-4.06**	998	995	18569	14590
1456203_at	RIKEN cDNA 1110020A10 gene	1110020A10Rik	**-4.35**	108	75	2497	1172
1424306_at	elongation of very long chain fatty acids (FEN1/	Elovl4	**-4.40**	50	42	1254	686
1439183_at	N-acylsphingosine amidohydrolase (alkaline ce	Asah3	**-4.57**	16	23	570	323
1424265_at	N-acetylneuraminate pyruvate lyase	Npl	**-4.60**	260	308	7595	6168
1453801_at	thioesterase superfamily member 5	Them5	**-4.68**	31	25	915	511
1437578_at	chloride channel calcium activated 2	Clca2	**-4.86**	29	20	932	483
1429297_at	serine (or cysteine) proteinase inhibitor, clade B	Serpinb12	**-4.97**	19	21	815	422
1422939_at	serine (or cysteine) proteinase inhibitor, clade B	Serpinb3b	**-5.05**	74	97	3139	2491
1422940_x_at	serine (or cysteine) proteinase inhibitor, clade B	Serpinb3b	**-5.07**	124	143	4887	4052
1436448_a_at	prostaglandin-endoperoxide synthase 1	Ptgs1	**-5.11**	68	93	3215	2265

REFERENCES

Aho S., Li K., Ryoo Y., McGee C., Ishida-Yamamoto A., Uitto J., and Klement J.F. 2004. Periplakin gene targeting reveals a constituent of the cornified cell envelope dispensable for normal mouse development. *Molecular and Cellular Biology* 24: 6410-6418.

Alonso L. and Fuchs E. 2003. Stem cells in the skin: waste not, wnt not. *Genes & Development* 17: 1189-1200.

Alonso L., Okada H., Pasolli H.A., Wakeham A., You-Ten A.I., Mak T.W., and Fuchs E. 2005. Sgk3 links growth factor signaling to maintenance of progenitor cells in the hair follicle. *Journal of Cell Biology* 170: 559-570.

Andersen B., Weinberg W.C., Rennekampff O., McEvilly R.J., Bermingham J.R., Hooshmand F., Vasilyev V., Hansbrough J.F., Pittelkow M.R., Yuspa S.H., and Rosenfeld M.G. 1997. Functions of the POU domain genes Skn-1a/i and Tst-1/Oct-6/SCIP in epidermal differentiation. *Genes & Development* 11: 1873-1884.

Andl T., Ahn K., Kairo A., Chu E.Y., Wine-Lee L., Reddy S.T., Croft N.J., Cebra-Thomas J.A., Metzger D., Chambon P., Lyons K.M., Mishina Y., Seykora J.T., Crenshaw E.B., and Millar S.E. 2004. Epithelial Bmpr1a regulates differentiation and proliferation in postnatal hair follicles and is essential for tooth development. *Development* 131: 2257-2268.

Andl T., Reddy S.T., Gaddapara T., and Millar, S.E. 2002. WNT signals are required for the initiation of hair follicle development. *Developmental Cell* 2: 643-653.

Arnold I. and Watt F.M. 2001. c-Myc activation in transgenic mouse epidermis results in mobilization of stem cells and differentiation of their progeny. *Current Biology* 11: 558-568.

Bach I. 2000. The LIM domain: regulation by association. *Mechanisms of Development* 91: 5-17.

Baker C.V.H. and Bronner-Fraser M. 2001. Vertebrate cranial placodes: I. Embryonic induction. *Developmental Biology* 232: 1-61.

Baxter R.M. and Brissette J.L. 2002. Role of the nude gene in epithelial terminal differentiation. *Journal of Investigative Dermatology* 118: 303-309.

Bhattacharyya S. and Bronner-Fraser M. 2004. Hierarchy of regulatory events in sensory placode development. *Current Opinion in Genetics & Development* 14: 520-526.

Bierkamp C., Mclaughlin K.J., Schwarz H., Huber O., and Kemler R. 1996. Embryonic heart and skin defects in mice lacking plakoglobin. *Developmental Biology* 180: 780-785.

Blanpain C., Lowry W.E., Geoghegan A., Polak L., and Fuchs E. 2004. Self-renewal, multipotency, and the existence of two cell populations within an epithelial stem cell niche. *Cell* 118: 635-648.

Botchkarev V.A. 2003. Bone morphogenetic proteins and their antagonists in skin and hair follicle biology. *Journal of Investigative Dermatology* 120: 36-47.

Botchkarev V.A., Botchkareva N.V., Nakamura M., Huber O., Funa K., Lauster R., Paus R., and Gilchrest B.A. 2001. Noggin is required for induction of the hair follicle growth phase in postnatal skin. *FASEB Journal* 15: 2205-2214.

Botchkarev V.A., Botchkareva N.V., Roth W., Nakamura M., Chen L.H., Herzog W., Lindner G., McMahon J.A., Peter C., Lauster R., McMahon A.P., and Paus R. 1999. Noggin is a mesenchymally derived stimulator of hair-follicle induction. *Nature Cell Biology* 1: 158-164.

Botchkarev V.A. and Fessing M.Y. 2005. Edar signaling in the control of hair follicle development. *Journal of Investigative Dermatology Symposium Proceedings* 10: 247-251.

Botchkarev V.A. and Paus R. 2003. Molecular biology of hair morphogenesis: development and cycling. *Journal of Experimental Zoology* 298B: 164-180.

Botchkarev V.A. and Sharov A.A. 2004. BMP signaling in the control of skin development and hair follicle growth. *Differentiation* 72: 512-526.

Brissette J.L., Li J., Kamimura J., Lee D., and Dotto G.P. 1996. The product of the mouse nude locus, Whn, regulates the balance between epithelial cell growth and differentiation. *Genes & Development* 10: 2212-2221.

Bulchand S., Grove E.A., Porter F.D., and Tole S. 2001. LIM-homeodomain gene Lhx2 regulates the formation of the cortical hem. *Mechanisms of Development* 100: 165-175.

Byrne C., Tainsky M., and Fuchs E. 1994. Programming gene expression in developing epidermis. *Development* 120: 2369-2383.

Cabral A., Voskamp P., Cleton-Jansen A.M., South A., Nizetic D., and Backendorf C. 2001. Structural organization and regulation of the small proline-rich family of cornified envelope precursors suggest a role in adaptive barrier function. *Journal of Biological Chemistry* 276: 19231-19237.

Callahan C.A. and Oro A.E. 2001. Monstrous attempts at adnexogenesis: regulating hair follicle progenitors through sonic hedgehog signaling. *Current Opinion in Genetics & Development* 11: 541-546.

Chan E.F., Gat U., McNiff J.M., and Fuchs E. 1999. A common human skin tumour is caused by activating mutations in β-catenin. *Nature Genetics* 21: 410-413.

Chang D.H., Cattoretti G., and Calame K.L. 2002. The dynamic expression pattern of B lymphocyte induced maturation protein-1 (Blimp-1) during mouse embryonic development. *Mechanisms of Development* 117: 305-309.

Cheng J., Syder A.J., Yu Q.C., Letai A., Paller A.S., and Fuchs E. 1992. The genetic basis of epidermolytic hyperkeratosis: a disorder of differentiation-specific epidermal keratin genes. *Cell* 70: 811-819.

Chiang C., Swan R.Z., Grachtchouk M., Bolinger M., Litingtung Y., Robertson E.K., Cooper M.K., Gaffield W., Westphal H., Beachy P.A., and Dlugosz A.A. 1999. Essential role for sonic hedgehog during hair follicle morphogenesis. *Developmental Biology* 205: 1-9.

Chipev C.C., Korge B.P., Markova N., Bale S.J., DiGiovanna J.J., Compton J.G., and Steinert P.M. 1992. A leucine→proline mutation in the H1 subdomain of keratin 1 causes epidermolytic hyperkeratosis. *Cell* 70: 821-828.

Claudinot S., Nicolas M., Oshima H., Rochat A., and Barrandon Y. 2005. Long-term renewal of hair follicles from clonogenic multipotent stem cells. *Proc Natl Acad Sci USA* 102: 14677-14682.

Cohen B., McGuffin M.E., Pfeifle C., Segal D., and Cohen S.M. 1992. apterous, a gene required for imaginal disc development in Drosophila encodes a member of the LIM family of developmental regulatory proteins. *Genes & Development* 6: 715-729.

Cotsarelis G. 2006. Epithelial stem cells: a folliculocentric view. *Journal of Investigative Dermatology* 126: 1459-1468.

Cotsarelis G., Sun T.T., and Lavker R.M. 1990. Label-retaining cells reside in the bulge area of pilosebasceous unit: implications for follicular stem cells, hair cycle, and skin carcinogenesis. *Cell* 61: 1329-1337.

Coulombe P.A., Hutton M.E., Letai A., Hebert A., Paller A.S., and Fuchs E. 1991. Point mutations in human keratin 14 genes of epidermolysis bullosa simplex patients: genetic and functional analyses. *Cell* 66: 1301-1311.

Curtiss J. and Heilig J.S. 1998. DeLIMiting development. *Bioessays* 20: 58-69.

Dai X. and Segre J.A. 2004. Transcriptional control of epidermal specification and differentiation. *Current Opinion in Genetics & Development* 14: 485-491.

DasGupta R. and Fuchs E. 1999. Multiple roles for activated LEF/TCF transcription complexes during hair follicle development and differentiation. *Development* 126: 4557-4568.

Daya-Grosjean L. and Couve-Privat S. 2005. Sonic hedgehog signaling in basal cell carcinomas. *Cancer Letters* 225: 181-192.

Ellis T., Gambardella L., Horcher M., Tschanz S., Capol J., Bertram P., Jochum W., Barrandon Y., and Busslinger M. 2001. The transcriptional repressor CDP (Cutl1) is essential for epithelial cell differentiation of the lung and the hair follicle. *Genes & Development* 15: 2307-2319.

Ess K.C., Witte D.P., Bascomb C.P., and Aronow B.J. 1999. Diverse developing mouse lineages exhibit high-level c-Myb expression in immature cells and loss of expression upon differentiation. *Oncogene* 18: 1103-1111.

Fan H., Oro A.E., Scott M.P., and Khavari P.A. 1997. Induction of basal cell carcinoma features in transgenic human skin expressing sonic hedgehog. *Nature Medicine* 3: 788-792.

Foitzik K., Paus R., Doetschman T., and Dotto G.P. 1999. The TGF-β2 isoform is both a required and sufficient inducer of murine hair follicle morphogenesis. *Developmental Biology* 212: 278-289.

Fuchs E., Merrill B.J., Jamora C., and DasGupta R. 2001. At the roots of a never-ending cycle. *Developmental Cell* 1: 13-25.

Fuchs E. and Raghavan S. 2002. Getting under the skin of epidermal morphogenesis. *Nature Reviews Genetics* 3: 199-209.

Fuchs E., Tumbar T., and Guasch G. 2004. Socializing with the neighbors: stem cells and their niche. *Cell* 116: 769-778.

Fujiwara S., Takeo N., Otani Y., Parry D.A., Kunimatsu M., Lu R., Sasaki M., Matsuo N., Khaleduzzaman M., and Yoshioka H. 2001. Epiplakin, a novel member of the plakin family originally identified as a 450-kDa human epidermal autoantigen. Structure and tissue localization. *Journal of Biological Chemistry* 276: 13340-13347.

Furuse M., Hata M., Furuse K., Yoshida Y., Haratake A., Sugitani Y., Noda T., Kubo A., and Tsukita S. 2002. Claudin-based tight junctions are crucial for the mammalian epidermal barrier: a lesson from claudin-1-deficient mice. *Journal of Cell Biology* 156: 1099-1111.

Gailani M.R., Stahle-Backdahl M., Leffell D.J., Glynn M., Zaphiropoulos P.G., Pressman C., Unden A.B., Dean M., Brash D.E., Bale A.E., and Toftgard R. 1996. The role of the human homologue of Drosophila patched in sporadic basal cell carcinomas. *Nature Genetics* 14: 78-81.

Gambardella L. and Barrandon Y. 2003. The multifaceted adult epidermal stem cell. *Current Opinion in Cell Biology* 15: 771-777.

Gambardella L., Schneider-Maunoury S., Voiculescu O., Charnay P., and Barrandon Y. 2000. Pattern of expression of the transcription factor Krox-20 in mouse hair follicle. *Mechanisms of Development* 96: 215-218.

Garrod D.R., Merritt A.J., and Nie Z. 2002. Desmosomal cadherins. *Current Opinion in Cell Biology* 14: 537-545.

Gat U., DasGupta R., Degenstein L., and Fuchs E. 1998. De novo hair follicle morphogenesis and hair tumors in mice expressing a truncated β-catenin in skin. *Cell* 95: 605-614.

Godwin A.R. and Capecchi MR. 1998. Hoxc13 mutant mice lack external hair. *Genes & Development* 12: 11-20.

Grachtchouk M., Mo R., Yu S., Zhang X., Sasaki H., Hui C.C., and Dlugosz A.A. 2000. Basal cell carcinomas in mice overexpressing Gli2 in skin. *Nature Genetics* 24: 216-217.

Hahn H., Wicking C., Zaphiropoulous P.G., Gailani M.R., Shanley S, Chidambaram A., Vorechovsky I., Holmberg E., Unden A.B., Gillies S., Negus K., Smyth I., Pressman C., Leffell D.J., Gerrard B., Goldstein A.M., Dean M., Toftgard R., Chenevix-Trench G., Wainwright B., and Bale A.E. 1996. Mutations of the human homolog of Drosophila patched in the nevoid basal cell carcinoma syndrome. *Cell* 85: 841-851.

Hardy M.H. 1992. The secret life of the hair follicle. *Trends in Genetics* 8: 55-61.

Hardy M.H. and Vielkind U. 1996. Changing patterns of cell adhesion molecules during mouse pelage hair follicle development. 1. Follicle morphogenesis in wild-type mice. *Acta Anatomica* 157: 169-182.

Headon D.J. and Overbeek P.A. 1999. Involvement of a novel Tnf receptor homologue in hair follicle induction. *Nature Genetics* 22: 370-374.

Hemmati-Brivanlou A. and Melton D. 1997. Vertebrate embryonic cells will become nerve cells unless told otherwise. *Cell* 88: 13-17.

Herron B.J., Liddell R.A., Parker A., Grant S., Kinne J., Fisher J.K., and Siracusa L.D. 2005. A mutation in stratifin is responsible for the repeated epilation (Er) phenotype in mice. *Nature Genetics* 37: 1210-1212.

Hirota J. and Mombaerts P. 2004. The LIM-homeodomain protein Lhx2 is required for complete development of mouse olfactory sensory neurons. *Proc Natl Acad Sci USA* 101: 8751-8755.

Hobert O. and Westphal H. 2000. Functions of LIM-homeobox genes. *Trends in Genetics* 16: 75-83.

Hogan B.L.M. 1999. Morphogenesis. *Cell* 96: 225-233.

Horsley V., O'Carroll D., Tooze R., Ohinata Y., Saitou M., Obukhanych T., Nussenzweig M., Tarakhovsky A., and Fuchs E. 2006. Blimp1 defines a progenitor population that governs cellular input to the sebaceous gland. *Cell* 126: 597-609.

Hsieh J.C., Sisk J.M., Jurutka P.W., Haussler C.A., Slater S.A., Haussler M.R., and Thompson C.C. 2003. Physical and functional interaction between the vitamin D receptor and hairless corepressor, two proteins required for hair cycling. *Journal of Biological Chemistry* 278: 38665-38674.

Huelsken J., Vogel R., Erdmann B., Cotsarelis G., and Birchmeier W. 2001. β-catenin controls hair follicle morphogenesis and stem cell differentiation in the skin. *Cell* 105: 533-545.

Hunter C.S. and Rhodes S.J. 2005. LIM-homeodomain genes in mammalian development and human disease. *Molecular Biology Reports* 32: 67-77.

Hutchin M.E., Kariapper M.S., Grachtchouk M., Wang A., Wei L., Cummings D., Liu J., Michael L.E., Glick A., and Dlugosz A.A. 2005. Sustained hedgehog signaling is required for basal cell carcinoma proliferation and survival: conditional skin tumorigenesis recapitulates the hair growth cycle. *Genes & Development* 19: 214-223.

Ito M., Liu Y., Yang Z., Nguyen J., Liang F., Morris R.J., and Cotsarelis G. 2005. Stem cells in the hair follicle bulge contribute to wound repair but not to homeostasis of the epidermis. *Nature Medicine* 11: 1351-1354.

Jamora C., DasGupta R., Kocieniewski P., and Fuchs E. 2003. Links between signal transduction, transcription and adhesion in epithelial bud development. *Nature* 422: 317-322.

Jamora C. and Fuchs E. 2002. Intercellular adhesion, signalling and the cytoskeleton. *Nature Cell Biology* 4: E101-108.

Jamora C., Lee P., Kocieniewski P., Azhar M., Hosokawa R., Chai Y., and Fuchs E. 2005. A signaling pathway involving TGF-β2 and snail in hair follicle morphogenesis. *PLoS Biology* 3: e11.

Jerome L.A. and Papaioannou V.E. 2001. DiGeorge syndrome phenotype in mice mutant for the T-box gene, Tbx1. *Nature Genetics* 27: 286-291.

Jih D.M., Lyle S., Elenitsas R., Elder D.E., and Cotsarelis G. 1999. Cytokeratin 15 expression in trichoepitheliomas and a subset of basal cell carcinomas suggests they originate from hair follicle stem cells. *Journal of Cutaneous Pathology* 26: 113-118.

Johnson R.L., Rothman A.L., Xie J., Goodrich L.V., Bare J.W., Bonifas J.M., Quinn A.G., Myers R.M., Cox D.R., Epstein E.H., and Scott M.P. 1996. Human homolog of patched, a candidate gene for the basal cell nevus syndrome. *Science* 272: 1668-1671.

Jung H.S., Francis-West P.H., Widelitz R.B., Jiang T.X., Ting-Berreth S., Tickle C., Wolpert L., and Chuong C.M. 1998. Local inhibitory action of BMPs and their relationships with activators in feather formation: implications for periodic patterning. *Developmental Biology* 196: 11-23.

Karlsson L., Bondjers C., and Betsholtz C. 1999. Roles for PDGF-A and sonic hedgehog in development of mesenchymal components of the hair follicle. *Development* 126: 2611-2621.

Kobayashi K., Rochat A., and Barrandon Y. 1993. Segregation of keratinocyte colony-forming cells in the bulge of the rat vibrissa. *Proc Natl Acad Sci USA* 90: 7391-7395.

Kobielak K., Pasolli H.A., Alonso L., Polak L., and Fuchs E. 2003. Defining BMP functions in the hair follicle by conditional ablation of BMP receptor IA. *Journal of Cell Biology* 163: 609-623.

Kolterud A., Alenius M., Carlsson L., and Bohm S. 2004. The Lim homeobox gene Lhx2 is required for olfactory sensory neuron identity. *Development* 131: 5319-53126.

Kottke M.D., Delva E., and Kowalczyk A.P. 2006. The desmosome: cell science lessons from human diseases.*Journal of Cell Science* 119: 797-806.

Kratochwil K., Dull M., Farinas I., Galceran J., and Grosschedl R. 1996. Lef1 expression is activated by BMP-4 and regulates inductive tissue interactions in tooth and hair development. *Genes & Development* 10: 1382-1394.

Kulessa H., Turk G., and Hogan B.L. 2000. Inhibition of BMP signaling affects growth and differentiation in the anagen hair follicle. *EMBO Journal* 19: 6664-6674.

Lane E.B. and McLean W.H. 2004. Keratins and skin disorders. *Journal of Pathology* 204: 355-366.

Lane E.B., Rugg E.L., Navsaria H., Leigh I.M., Heagerty A.H., Ishida-Yamamoto A., and Eady R.A. 1992. A mutation in the conserved helix termination peptide of keratin 5 in hereditary skin blistering. *Nature* 356: 244-246.

Laurikkala J., Pispa J., Jung H.S., Nieminen P., Mikkola M., Wang X., Saarialho-Kere U., Galceran J., Grosschedl R., and Thesleff I. 2002. Regulation of hair follicle development by the TNF signal ectodysplasin and its receptor Edar. *Development* 129: 2541-2553.

Lechler T. and Fuchs E. 2005. Asymmetric cell divisions promote stratification and differentiation of mammalian skin. *Nature* 437: 275-280.

Leung C.L., Green K.J., and Liem R.K. 2002. Plakins: a family of versatile cytolinker proteins. *Trends in Cell Biology* 12: 37-45.

Levy V., Lindon C., Harfe B.D., and Morgan BA. 2005. Distinct stem cell populations regenerate the follicle and interfollicular epidermis. *Developmental Cell* 9: 855-861.

Li C., Guo H., Xu X., Weinberg W., and Deng C.X. 2001. Fibroblast growth factor receptor 2 (Fgfr2) plays an important role in eyelid and skin formation and patterning. *Developmental Dynamics* 222: 471-483.

Li L. and Xie T. 2005. Stem cell niche: structure and function. *Annual Review of Cell and Developmental Biology* 21: 605-631.

Li M., Chiba H., Warot X., Messaddeq N., Gerard C., Chambon P., and Metzger D. 2001. RXR-alpha ablation in skin keratinocytes results in alopecia and epidermal alterations. *Development* 128: 675-688.

Li Q., Lu Q., Estepa G., and Verma I.M. 2005. Identification of 14-3-3σ mutation causing cutaneous abnormality in repeated-epilation mutant mouse. *Proc Natl Acad Sci USA* 102: 15977-15982.

Li Y.C., Pirro A.E., Amling M., Delling G., Baron R., Bronson R., and Demay M.B. 1997. Targeted ablation of the vitamin D receptor: an animal model of vitamin D-dependent rickets type II with alopecia. *Proc Natl Acad Sci USA* 94: 9831-9835.

Lindsay E.A., Vitelli F., Su H., Morishima M., Huynh T., Pramparo T., Jurecic V., Ogunrinu G., Sutherland H.F., Scambler P.J., Bradley A., and Baldini A. 2001. Tbx1 haploinsufficieny in the DiGeorge syndrome region causes aortic arch defects in mice. *Nature* 410: 97-101.

Lloyd C., Yu Q.C., Cheng J., Turksen K., Degenstein L., Hutton E., and Fuchs E. 1995. The basal keratin network of stratified squamous epithelia: defining K15 function in the absence of K14. *Journal of Cell Biology* 129: 1329-1344.

Lo Celso C., Prowse D.M., and Watt F.M. 2004. Transient activation of β-catenin signalling in adult mouse epidermis is sufficient to induce new hair follicles but continuous activation is required to maintain hair follicle tumours. *Development* 131: 1787-1799.

Logan C.Y. and Nusse R. 2004. The Wnt signaling pathway in development and disease. *Annual Review of Cell and Developmental Biology* 20: 781-810.

Lowell S., Jones P., Le Roux I., Dunne J., and Watt F.M. 2000. Stimulation of human epidermal differentiation by delta-notch signalling at the boundaries of stem-cell clusters. *Current Biology* 10: 491-500.

Lowry W.E., Blanpain C., Nowak J.A., Guasch G., Lewis L., and Fuchs E. 2005. Defining the impact of β-catenin/Tcf transactivation on epithelial stem cells. *Genes & Development* 19: 1596-1611.

Luetteke N.C., Qiu T.H., Peiffer R.L., Oliver P., Smithies O., and Lee D.C. 1993. TGF alpha deficiency results in hair follicle and eye abnormalities in targeted and waved-1 mice. *Cell* 73: 263-278.

Lum L. and Beachy P.A. 2004. The hedgehog response network: sensors, switches, and routers. *Science* 304: 1755-1759.

Maatta A., DiColandrea T., Groot K., and Watt FM. 2001. Gene targeting of envoplakin, a cytoskeletal linker protein and precursor of the epidermal cornified envelope. *Molecular and Cellular Biology* 21: 7047-7053.

Malik T.H., Von Stechow D., Bronson R.T., and Shivdasani R.A. 2002. Deletion of the GATA domain of TRPS1 causes an absence of facial hair and provides new insights into the bone disorder in inherited tricho-rhino-phalangeal syndromes. *Molecular and Cellular Biology* 22: 8592-8600.

Mann G.B., Fowler K.J., Gabriel A., Nice E.C., Williams R.L., and Dunn A.R. 1993. Mice with a null mutation of the TGF alpha gene have abnormal skin architecture, wavy hair, and curly whiskers and often develop corneal inflammation. *Cell* 73: 249-261.

Mann S.J. 1962. Prenatal formation of hair follicle types. *The Anatomical Record* 144: 135-142.

Mao B., Wu W., Davidson G., Marhold J., Li M., Mechler B.M., Delius H., Hoppe D., Stannek P., Walter C., Glinka A., and Niehrs C. 2002. Kremen proteins are dickkopf receptors that regulate Wnt/β-catenin signalling. *Nature* 417: 664-667.

Matter K., Aijaz S., Tsapara A., and Balda M.S. 2005. Mammalian tight junctions in the regulation of epithelial differentiation and proliferation. *Current Opinion in Cell Biology* 17: 453-458.

Matzuk M.M., Kumar T.R., Vassalli A., Bickenbach J.R., Roop D.R., Jaenisch R., and Bradley A. 1995. Functional analysis of activins during mammalian development. *Nature* 374: 354-356.

McGrath J.A., Gatalica B., Christiano A.M., Li K., Owaribe K., McMillan J.R., Eady R.A., and Uitto J. 1995. Mutations in the 180-kD bullous pemphigoid antigen (BPAG2), a hemidesmosomal transmembrane collagen (COL17A1), in generalized atrophic benign epidermolysis bullosa. *Nature Genetics* 11: 83-86.

McGrath J.A., McMillan J.R., Shemanko C.S., Runswick S.K., Leigh I.M., Lane E.B., Garrod D.R., and Eady R.A. 1997. Mutations in the plakophilin 1 gene result in ectodermal dysplasia/skin fragility syndrome. *Nature Genetics* 17: 240-244.

McLean W.H., Rugg E.L., Lunny D.P., Morley S.M., Lane E.B., Swensson O., Dopping-Hepenstal P.J., Griffiths W.A., Eady R.A., Higgins C., Navsaria H.A., Leigh I.M., Strachan T., Kunkeler L., and Munro C.S. 1995. Keratin 16 and keratin 17 mutations cause pachyonychia congenita. *Nature Genetics* 9: 273-278.

Merrill B.J., Gat U., DasGupta R., and Fuchs E. 2001. Tcf3 and Lef1 regulate lineage differentiation of multipotent stem cells in skin. *Genes & Development* 15: 1688-1705.

Merscher S., Funke B., Epstein J.A., Heyer J., Puech A., Lu M.M., Xavier R.J., Demay M.B., Russell R.G., Factor S., Tokooya K., Jore B.S., Lopez M., Pandita R.K., Lia M., Carrion D., Xu H., Schorle H., Kobler J.B., Scambler P., Wynshaw-Boris A., Skoultchi A.I., Morrow B.E., and Kucherlapati R. 2001. TBX1 is responsible for cardiovascular defects in velo-cardio-facial/DiGeorge syndrome. *Cell* 104: 619-629.

Mill P., Mo R., Fu H., Grachtchouk M., Kim P.C., Dlugosz A.A., and Hui C.C. 2003. Sonic hedgehog-dependent activation of Gli2 is essential for embryonic hair follicle development. *Genes & Development* 17: 282-294.

Mill P., Mo R., Hu M.C., Dagnino L., Rosenblum N.D., and Hui C.C. 2005. Shh controls epithelial proliferation via independent pathways that converge on N-Myc. *Developmental Cell* 9: 293-303.

Millar S.E. 2002. Molecular mechanisms regulating hair follicle development. *Journal of Investigative Dermatology* 118: 216-225.

Momeni P., Glockner G., Schmidt O., von Holtum D., Albrecht B., Gillessen-Kaesbach G., Hennekam R., Meinecke P., Zabel B., Rosenthal A., Horsthemke. B., and Ludecke H.J. 2000. Mutations in a new gene, encoding a zinc-finger protein, cause tricho-rhino-phalangeal syndrome type I. *Nature Genetics* 24: 71-74.

Monuki E.S., Porter F.D., and Walsh C.A. 2001. Patterning of the dorsal telencephalon and cerebral cortex by a roof plate-Lhx2 pathway. *Neuron* 32: 591-604.

Moore K.A. and Lemischka I.R. 2006. Stem cells and their niches. *Science* 311: 1880-1885.

Morris R.J., Liu Y., Marles L., Yang Z., Trempus C., Li S., Lin J.S., Sawicki J.A., and Cotsarelis G. 2004. Capturing and profiling adult hair follicle stem cells. *Nature Biotechnology* 4: 411-417.

Morris R.J. and Potten C.S. 1999. Highly persistent label-retaining cells in the hair follicles of mice and their fate following induction of anagen. *Journal of Investigative Dermatology* 1999 112: 470-475.

Mucenski M.L., McLain K., Kier A.B., Swerdlow S.H., Schreiner C.M., Miller T.A., Pietryga D.W., Scott W.J., and Potter S.S. 1991. A functional c-myb gene is required for normal murine fetal hepatic hematopoiesis.
Cell 65: 677-689.

Muller-Rover S., Handjiski B., van der Veen C., Eichmuller S., Foitzik K., McKay I.A., Stenn K.S., and Paus R. 2001. A comprehensive guide for the accurate classification of murine hair follicles in distinct hair cycle stages. *Journal of Investigative Dermatology* 117: 3-15.

Nair M., Teng A., Bilanchone V., Agrawal A., Li B., and Dai X. 2006. Ovol1 regulates the growth arrest of embryonic epidermal progenitor cells and represses c-myc transcription. *Journal of Cell Biology* 173: 253-264.

Nakamura M., Sundberg J.P., and Paus R. 2001. Mutant laboratory mice with abnormalities in hair follicle morphogenesis, cycling, and/or structure: annotated tables. *Experimental Dermatology* 10: 369-390.

Nguyen H., Rendl M., and Fuchs E. 2006. Tcf3 governs stem cell features and represses cell fate determination in skin. *Cell* in press.

Nicolas M., Wolfer A., Raj K., Kummer J.A., Mill P., van Noort M., Hui C.C., Clevers H., Dotto G.P., and Radtke F. 2003. Notch1 functions as a tumor suppressor in mouse skin. *Nature Genetics* 33: 416-421.

Niemann C. and Watt F.M. 2002. Designer skin: lineage commitment in postnatal epidermis. *Trends in Cell Biology* 12: 185-192.

Nilsson M., Unden A.B., Krause D., Malmqwist U., Raza K., Zaphiropoulos P.G., and Toftgard R. 2000. Induction of basal cell carcinomas and trichoepitheliomas in mice overexpressing GLI-1. *Proc Natl Acad Sci USA* 97: 3438-3443.

Noramly S. and Morgan B.A. 1998. BMPs mediate lateral inhibition at successive stages in feather tract development. *Development* 125: 3775-3787.

Ohnishi S., Laub F., Matsumoto N., Asaka M., Ramirez F., Yoshida T., and Terada M. 2000. Developmental expression of the mouse gene coding for the kruppel-like transcription factor KLF5. *Developmental Dynamics* 217: 421-429.

Oomizu S., Sahuc F., Asahina K., Inamatsu M., Matsuzaki T., Sasaki M., Obara M., and Yoshizato K. 2000. Kdap, a novel gene associated with the stratification of the epithelium. *Gene* 256: 19-27.

Oro A.E. and Higgins K. 2003. Hair cycle regulation of hedgehog signal reception. *Developmental Biology* 255: 238-248.

Oro A.E., Higgins K.M., Hu Z., Bonifas J.M., Epstein E.H., and Scott M.P. 1997. Basal cell carcinomas in mice overexpressing sonic hedgehog. *Science* 276: 817-821.

Oshima H., Rochat R., Kedzia C., Kobayashi K., and Barrandon Y. 2001. Morphogenesis and renewal of hair follicles from adult multipotent stem cells. *Cell* 104: 233-245.

Paladini R.D., Saleh J., Qian C., Xu G.X., and Rubin L.L. 2005. Modulation of hair growth with small molecule agonists of the hedgehog signaling pathway. *Journal of Investigative Dermatology* 125: 638-646.

Park G.T., Lim S.E., Jang S.I., and Morasso M.I. 2002. Suprabasin, a novel epidermal differentiation marker and potential cornified envelope precursor. *Journal of Biological Chemistry* 277: 45195-202.

Paus R., Muller-Rover S., van der Veen C., Maurer M., Eichmuller S., Ling G., Hofmann U., Foitzik K., Mechlenburg L., and Handjiski B. 1999. A comprehensive guide for the recognition and classification of distinct stages of hair follicle morphogenesis. *Journal of Investigative Dermatology* 113: 523-532.

Peng G. and Westerfield M. 2006. Lhx5 promotes forebrain development and activates transcription of secreted Wnt antagonists. *Development* 133: 3191-3200.

Peters K.G., Werner S., Chen G., and Williams L.T. 1992. Two FGF receptor genes are differentially expressed in epithelial and mesenchymal tissues during limb formation and organogenesis in the mouse. *Development* 114: 233-243.

Petiot A., Conti F.J.A., Grose R., Revest J.M., Hodivala-Dilke K.M., and Dickson C. 2003. A crucial role for Fgfr2-IIIb signaling in epidermal development and hair follicle patterning. *Development* 130: 5493-5501.

Pinto do O P., Kolterud A., and Carlsson L. 1998. Expression of the LIM-homeobox gene LH2 generates immortalized steel factor-dependent multipotent hematopoietic precursors. *EMBO Journal* 17: 5744-5756.

Pinto do O P., Richter K., and Carlsson L. 2002. Hematopoietic progenitor/stem cells immortalized by Lhx2 generate functional hematopoietic cells in vivo. *Blood* 99: 3939-3946.

Pinto do O P., Wandzioch E., Kolterud A., and Carlsson L. 2001. Multipotent hematopoietic progenitor cells immortalized by Lhx2 self-renew by a cell nonautonomous mechanism. *Experimental Hematology* 29: 1019-1028.

Pispa J. and Thesleff I. 2003. Mechanisms of ectodermal organogenesis. *Developmental Biology* 262: 195-205.

Plikus M., Wang W.P., Liu J., Wang X., Jiang T.X., and Chuong C.M. 2004. Morpho-regulation of ectodermal organs: integument pathology and phenotypic variations in K14-Noggin engineered mice through modulation of bone morphogenic protein pathway. *American Journal of Pathology* 164: 1099-1114.

Polakis P. 2000. Wnt signaling and cancer. *Genes & Development* 14: 1837-1851.

Porter F.D., Drago J., Xu Y., Cheema S.S., Wassif C., Huang S.P., Lee E., Grinberg A., Massalas J.S., Bodine D., Alt F., and Westphal H. 1997. Lhx2, a LIM homeobox gene, is required for eye, forebrain, and definitive erythrocyte development. *Development* 124: 2935-2944.

Rangarajan A., Talora C., Okuyama R., Nicolas M., Mammucari C., Oh H., Aster J.C., Krishna S., Metzger D., Chambon P., Miele L., Aguet M., Radtke F., and

Dotto G.P. 2001. Notch signaling is a direct determinant of keratinocyte growth arrest and entry into differentiation. *EMBO Journal* 20: 3427-3436.

Reddy S., Andl T., Bagasra A., Lu M.M., Epstein D.J., Morrisey E.E., and Millar S.E. 2001. Characterization of Wnt gene expression in developing and postnatal hair follicles and identification of Wnt5a as a target of Sonic hedgehog in hair follicle morphogenesis. *Mechanisms of Development* 107: 69-82.

Reddy S.T., Andl T., Lu M.M., Morrisey E.E., and Millar S.E. 2004. Expression of frizzled genes in developing and postnatal hair follicles. *Journal of Investigative Dermatology* 123: 275-282.

Rendl M., Lewis L., and Fuchs E. 2005. Molecular dissection of mesenchymal-epithelial interactions in the hair follicle. *PLoS Biology* 3: e331.

Reya T., Morrison S.J., Clarke M.F., and Weissman I.L. 2001. Stem cells, cancer, and cancer stem cells. *Nature* 414: 105-111.

Richter K., Pinto do O P., Hagglund A.C., Wahlin A., and Carlsson L. 2003. Lhx2 expression in hematopoietic progenitor/stem cells in vivo causes a chronic myeloproliferative disorder and altered globin expression. *Haematologica* 88: 1336-1347.

Rincon-Limas D.E., Lu C.H., Canal I., Calleja M., Rodriguez-Esteban C., Izpisua-Belmonte J.C., and Botas J. 1999. Conservation of the expression and function of apterous orthologs in Drosophila and mammals. *Proc Natl Acad Sci USA* 96: 2165-2170.

Rochat A., Kobayashi K., and Barrandon Y. 1994. Location of stem cells of human hair follicles by clonal analysis. *Cell* 76: 1063-1073.

Romano R.A., Li H., Tummala R., Maul R., and Sinha S. 2004. Identification of basonuclin2, a DNA-binding zinc-finger protein expressed in germ tissues and skin keratinocytes. *Genomics* 83: 821-833.

Roose J., Korver W., Oving E., Wilson A., Wagenaar G., Markman M., Lamers W., and Clevers H. 1998. High expression of the HMG box factor Sox-13 in arterial walls during embryonic development. *Nucleic Acids Research* 26: 469-476.

Rugg E.L. and Leigh I.M. 2004. The keratins and their disorders. *American Journal of Medical Genetics* 131C: 4-11.

Saitou M., Furuse M., Sasaki H., Schulzke J.D., Fromm M., Takano H., Noda T., and Tsukita S. 2000. Complex phenotype of mice lacking occludin, a component of tight junction strands. *Molecular Biology of the Cell* 11: 4131-4142.

Sakai Y., Kishimoto J., and Demay M.B. 2001. Metabolic and cellular analysis of alopecia in vitamin D receptor knockout mice. *Journal of Clinical Investigation* 107: 961-966.

Sato N., Leopold P.L., and Crystal R.G. 1999. Induction of the hair growth phase in postnatal mice by localized transient expression of sonic hedgehog. *Journal of Clinical Investigation* 104: 855-864.

Satokata I., Ma L., Ohshima H., Bei M., Woo I., Nishizawa K., Maeda T., Takano Y., Uchiyama M., Heaney S., Peters H., Tang Z., Maxson R., and Maas R. 2000. Msx2 deficiency in mice causes pleiotropic defects in bone growth and ectodermal organ formation. *Nature Genetics* 24: 391-395.

Schmidt-Ullrich R. and Paus R. 2005. Molecular principles of hair follicle induction and morphogenesis. *Bioessays* 27: 247-261.

Schmidt-Ullrich R., Tobin D.J., Lenhard D., Schneider P., Paus R., and Scheidereit C. 2006. NF-ϰB transmits Eda A1/EdaR signalling to activate Shh and cyclin D1 expression, and controls post-initiation hair placode down growth. *Development* 133: 1045-1057.

Schneider-Maunoury S., Topilko P., Seitandou T., Levi G., Cohen-Tannoudji M., Pournin S., Babinet C., and Charnay P. 1993. Disruption of Krox-20 results in alteration of rhombomeres 3 and 5 in the developing hindbrain. *Cell* 75: 1199-1214.

Schrewe H., Gendron-Maguire M., Harbison M.L., and Gridley T. 1994. Mice homozygous for a null mutation of activin beta B are viable and fertile. *Mechanisms of Development* 47: 43-51.

Segre J.A., Bauer C., and Fuchs E. 1999. Klf4 is a transcription factor required for establishing the barrier function of the skin. *Nature Genetics* 22: 356-360.

Shi Y. and Massague J. 2003. Mechanisms of TGF-β signaling from cell membrane to the nucleus. *Cell* 113: 685-700.

Silva-Vargas V., Lo Celso C., Giangreco A., Ofstad T., Prowse D.M., Braun K.M., and Watt F.M. 2005. β-catenin and hedgehog signal strength can specify number and location of hair follicles in adult epidermis without recruitment of bulge stem cells. *Developmental Cell* 9: 121-131.

Skorija K., Cox M., Sisk J.M., Dowd D.R., MacDonald P.N., Thompson C.C., and Demay M.B. 2005. Ligand-independent actions of the vitamin D receptor maintain hair follicle homeostasis. *Molecular Endocrinology* 19: 855-862.

St-Jacques B., Dassule H.R., Karavanova I., Botchkarev V.A., Li J., Danielian P.S., McMahon J.A., Lewis P.M., Paus R., and McMahon A.P. 1998. Sonic hedgehog signaling is essential for hair development. *Current Biology* 8: 1058-1068.

Stenn K.S. and Paus R. 2001. Controls of hair follicle cycling. *Physiological Reviews* 81: 449-494.

Swiatek P.J. and Gridley T. 1993. Perinatal lethality and defects in hindbrain development in mice homozygous for a targeted mutation of the zinc finger gene Krox20. *Genes & Development* 7: 2071-2084.

Tao J., Kuliyev E., Wang X., Li X., Wilanowski T., Jane S.M., Mead P.E., and Cunningham J.M. 2005. BMP4-dependent expression of Xenopus grainyhead-like 1 is essential for epidermal differentiation. *Development* 132: 1021-1034.

Tasanen K., Tunggal L., Chometon G., Bruckner-Tuderman L., and Aumailley M. 2004. Keratinocytes from patients lacking collagen XVII display a migratory phenotype. *American Journal of Pathology* 164: 2027-2038.

Taylor G., Lehrer M.S., Jensen P.J., Sun T.T., and Lavker R.M. 2000. Involvement of follicular stem cells in forming not only the follicle but also the epidermis. *Cell* 102: 451-461.

Thelu J., Rossio P., and Favier B. 2002. Notch signalling is linked to epidermal cell differentiation level in basal cell carcinoma, psoriasis and wound healing. *BMC Dermatology* 2: 7.

Thornton M.J. 2002. The biological actions of estrogens on skin. *Experimental Dermatology* 11: 487-502.

Ting S.B., Caddy J., Hislop N., Wilanowski T., Auden A., Zhao L.L., Ellis S., Kaur P., Uchida Y., Holleran W.M., Elias P.M., Cunningham J.M., and Jane S.M. 2005. A homolog of Drosophila grainy head is essential for epidermal integrity in mice. *Science* 308: 411-413.

Ting-Berreth S.A. and Chuong C.M. 1996. Local delivery of TGF β2 can substitute for placode epithelium to induce mesenchymal condensation during skin appendage morphogenesis. *Developmental Biology* 179: 347-359.

Trempus C.S., Morris R.J., Bortner C.D., Cotsarelis G., Faircloth R.S., Reece J.M., and Tennant R.W. 2003. Enrichment for living murine keratinocytes from the hair follicle bulge with the cell surface marker CD34. *Journal of Investigative Dermatology* 120: 501-511.

Tumbar T., Guasch G., Greco V., Blanpain C., Lowry W.E., Rendl M., and Fuchs E. 2004. Defining the epithelial stem cell niche in skin. *Science* 303: 359-363.

Tummala R., Romano R.A., Fuchs E., and Sinha S. 2003. Molecular cloning and characterization of AP-2ε, a fifth member of the AP-2 family. *Gene* 321: 93-102.

Vaezi A., Bauer C., Vasioukhin V., and Fuchs E. 2002. Actin cable dynamics and Rho/Rock orchestrate a polarized cytoskeletal architecture in the early steps of assembling a stratified epithelium. *Developmental Cell* 3: 367-381.

van Genderen C., Okamura R.M., Farinas I., Quo R.G., Parslow T.G., Bruhn L., and Grosschedl R. 1994. Development of several organs that require inductive epithelial-mesenchymal interactions is impaired in LEF-1 deficient mice. *Genes & Development* 8: 2691-2703.

van Mater D., Kolligs F.T., Dlugosz A.A., and Fearon E.R. 2003. Transient activation of β-catenin signaling in cutaneous keratinocytes is sufficient to trigger the active growth phase of the hair cycle in mice. *Genes & Development* 17: 1219-1224.

Vasioukhin V., Bauer C., Degenstein L., Wise B., and Fuchs E. 2001. Hyperproliferation and defects in epithelial polarity upon conditional ablation of α-catenin in skin. *Cell* 104: 605-617.

Vasioukhin V., Degenstein L., Wise B., and Fuchs E. 1999. The magical touch: genome targeting in epidermal stem cells induced by tamoxifen application to mouse skin. *Proc Natl Acad Sci USA* 96: 8551-8556.

Vassar R., Rosenberg M., Ross S., Tyner A., and Fuchs E. 1989. Tissue-specific and differentiation-specific expression of a human K14 keratin gene in transgenic mice. *Proc Natl Acad Sci USA* 86: 1563-1567.

Vidal V.P., Chaboissier M.C., Lutzkendorf S., Cotsarelis G., Mill P., Hui C.C., Ortonne N., Ortonne J.P., and Schedl A. 2005. Sox9 is essential for outer root sheath differentiation and the formation of the hair stem cell compartment. *Current Biology* 15: 1340-1351.

Vincent S.D., Dunn N.R., Sciammas R., Shapiro-Shalef M., Davis M.M., Calame K., Bikoff E.K., and Robertson E.J. 2005. The zinc finger transcriptional repressor Blimp1/Prdm1 is dispensable for early axis formation but is required for specification of primordial germ cells in the mouse. *Development* 132: 1315-1325.

Waikel R.L., Kawachi Y., Waikel P.A., Wang X.J., and Roop D.R. 2001. Deregulated expression of c-Myc depletes epidermal stem cells. *Nature Genetics* 28: 165-168.

Wandzioch E., Kolterud A., Jacobsson M., Friedman S.L., and Carlsson L. 2004. Lhx2-/- mice develop liver fibrosis. *Proc Natl Acad Sci USA* 101: 16549-16554.

Wang L.C., Liu Z.Y., Gambardella L., Delacour A., Shapiro R., Yang J., Sizing I., Rayhorn P., Garber E.A., Benjamin C.D., Williams K.P., Taylor F.R., Barrandon Y., Ling L., and Burkly L.C. 2000. Regular articles: conditional disruption of hedgehog signaling pathway defines its critical role in hair development and regeneration. *Journal of Investigative Dermatology* 114: 901-908.

Weiner L. and Green H. 1998. Basonuclin as a cell marker in the formation and cycling of the murine hair follicle. *Differentiation* 63: 263-272.

Wong P., Colucci-Guyon E., Takahashi K., Gu C., Babinet C., and Coulombe P.A. 2000. Introducing a null mutation in the mouse K6α and K6β genes reveals their essential structural role in the oral mucosa. *Journal of Cell Biology* 150: 921-928.

Wu H.K., Heng H.H., Siderovski D.P., Dong W.F., Okuno Y., Shi X.M., Tsui L.C., and Minden M.D. 1996. Identification of a human LIM-Hox gene, hLH-2, aberrantly expressed in chronic myelogenous leukaemia and located on 9q33-34.1. *Oncogene* 12: 1205-1212.

Xie J., Murone M., Luoh S.M., Ryan A., Gu Q., Zhang C., Bonifas J.M., Lam C.W., Hynes M., Goddard A., Rosenthal A., Epstein E.H., and de Sauvage F.J. 1998. Activating smoothened mutations in sporadic basal-cell carcinoma. *Nature* 391: 90-92.

Xu Y., Baldassare M., Fisher P., Rathbun G., Oltz E.M., Yancopoulos G.D., Jessell T.M., and Alt F.W. 1993. LH-2: a LIM/homeodomain gene expressed in developing lymphocytes and neural cells. *Proc Natl Acad Sci USA* 90: 227-231.

Yin T., Getsios S., Caldelari R., Kowalczyk A.P., Muller E.J., Jones J.C., and Green K.J. 2005. Plakoglobin suppresses keratinocyte motility through both cell-cell adhesion-dependent and -independent mechanisms. *Proc Natl Acad Sci USA* 102: 5420-5425.

Yoshizawa T., Handa Y., Uematsu Y., Takeda S., Sekine K., Yoshihara Y., Kawakami T., Arioka K., Sato H., Uchiyama Y., Masushige S., Fukamizu A., Matsumoto T., and Kato S. 1997. Mice lacking the vitamin D receptor exhibit impaired bone formation, uterine hypoplasia and growth retardation after weaning. *Nature Genetics* 16: 391-396.

Yuhki M., Yamada M., Kawano M., Iwasato T., Itohara S., Yoshida H., Ogawa M., and Mishina Y. 2004. BMPR1A signaling is necessary for hair follicle cycling and hair shaft differentiation in mice. *Development* 131: 1825-1833.

Zarach J.M., Beaudoin G.M., Coulombe P.A., and Thompson C.C. 2004. The co-repressor hairless has a role in epithelial cell differentiation in the skin. *Development* 131: 4189-4200.

Zhou P., Byrne C., Jacobs J., and Fuchs E. 1995. Lymphoid enhancer factor 1 directs hair follicle patterning and epithelial cell fate. *Genes & Development* 9: 700-713.

Zoupa M., Seppala M., Mitsiadis T., and Cobourne M.T. 2006. Tbx1 is expressed at multiple sites of epithelial-mesenchymal interaction during early development

of the facial complex. *International Journal of Developmental Biology* 50: 504-510.